

# **Role Of Astrocytes On Neuronal Health In Models Of Alzheimer's Disease**

**Thesis submitted for the degree of  
Doctor of Philosophy (Science)  
In Biochemistry**

**By**

**SUBHALAKSHMI GUHA**

**Regn no: 07791/Ph.D.(Sc.)Proceed/2017**

**DEPARTMENT OF BIOCHEMISTRY  
UNIVERSITY OF CALCUTTA**

**2021**

No words are enough to  
describe your support and  
kindness in my path towards goal.

I dedicate my thesis to  
**“Ma, Baba & Dipayan”**

# Acknowledgement

Submitting the thesis which has been the journey and motive since the last 6 years of my life feels extremely satisfying today. However crossing this great mountain would be impossible without the contribution of those near and dear ones who not only made this huge attempt successful but comfortable too.

The dream of completing my Ph.D. would be so incomplete without the immense sacrifice made by my parents **Mr Gautam K. Guha** and **Mrs Sumita Guha**. Never have I come across a more critical and strict person than my ma who has groomed me so much to be me today. My baba has taught me the biggest lesson in life which states to tackle all the little disappointments in a good humor. It is only because of their encouragement and constant inspiration that I stand here today. Thanking you would never be enough but I can only pledge to be a better person each day and make a single person happy everyday as I promised you both.

I am so grateful to my parents-in-law **Mr D. N. De** and **Lt. Mrs Minati De** for believing in me and always treating me as a daughter. Uncle, with you beside me life become so much simpler and easier. Thank you for everything.

My doctoral study would have been extremely different if I had not been mentored by my guide **Dr. Subhas C Biswas**. The best thing about Sir is his incessant belief in me that I would succeed well one day in my goal. His constant support and words of wisdom has not only improved me professionally but also made my personal niche successful in last few years. The best lesson he has taught me is that “patience and hardwork is the only key towards success”. He has supported me on those days when I needed mentoring the most and gave me enough independence to choose what is best for me. Sir, I heartily thank you for all the little and big things you offered.

When I first joined CSIR-IICB, I used to sit in room 247 which then belonged to **Dr Sumantra Das** and he was designated my co-guide for the first two years. In course of time I have realized how much I have learnt from him in all fronts possible. His outlook and perspective towards science, life and knowledge has really groomed me well. Pursuing science requires an immense conviction and determination. I have

known these words to be true by meeting **Dr. P.K.Sarkar**. I have been fortunate enough to have been guided by him and seen him visiting lab even at 80 years of his age with equal enthusiasm and zeal.

Joining my lab in 2014 was an event in itself and the stay became memorable truly due to a bunch of friends, seniors and later juniors who made this tedious hard tenure quite bearable at all times. My first mention would of my "**Pet Akash**". He is never a colleague or a friends but he is family to me. Not a single day has passed when we didn't share our views on "we know what". **Anoy** is that friend which everyone craves for. Whenever I have been in a fix in lab, he has always been my go to person. Defining **Pallabi** is so difficult. I have seldom come across a person so elegant and diligent in all her ways. All four of us joined lab together and I am so lucky to be friends with them. My Ph.D. work would have never been possible without **Ramesh**. I will be forever indebted to you for all your help and at times I feel I have troubled you too much.. but again partner, who else if not you ??

Next I would like to thank my seniors **Rebeccadi, Pampadi, Maitreyee di, Kusumikadi** without whom my knowledge of astrocyte culture would be so incomplete. I would also like to mention **Nandinidi, Priyankarda, Suraiyadi** and **Hrishita** for all their encouragement and help. Coming to my wonderful juniors. **Sukanya, Soumita, Naquia, Diptesh** it has been wonderful teaching and learning from you guys. I shall always cherish all the happy moments I have spent with all of you.

Here in IICB I have been so blessed with a wonderful group of friends who subsequently became my family and therapy at all times. I have felt an emotional roller coaster with **Avijit** and **Bartika** and their friendship has been truly unparallel. **Satarupa**, thank you for being my go to person at all those stressful times and I will never forget our continuous laughter sessions. **YC** and **MB** has been the elder brothers, always making me smile no matter what. I would never leave behind **Kumar** in the list of my priority friends. Thank you for bringing smile to my face at all those difficult times and I am so glad "Gwalior" happened. I was blessed with a wonderful group of kiddos in this tenure. **Diptankar**, a gem of a person and a beautiful soul in and out, it was never a dull moment with you around. I want to heartily thank **Sourav, Shyamantak, Ishani, Shreya**.. I wish I had words to express my love and gratitude

towards you guys...thank you for keeping your “ Subhodi” sane for all these years.. I was blessed to have been friends with **Anand, Sambit, Debojyoti** and **Namrata** without whom I am sure my publications would have been impossible. Thank you guys for everything. I want to thank **Gobindada** for all his contributions in this tenure.

I would like to take the opportunity to thank the directors of CSIR-IICB, **Prof. Siddhartha Roy, Prof. Samit Chattopadhyay, Prof. Arun Bandhopadhyay** who has been there during my tenure. I want to thank **Dr. Aditya Konar, Dr Suvendra N. Bhattacharya, Dr Nahid Ali** and her lab members. I also want to thank **Laluda, Sambhuda** and other animal house staff for their immense help in providing us with animals. A special mention would be for **Tapasda and Sounakda** for all their help in imaging purposes.

I would like to thank all my teachers and professors of Carmel High School, St Xavier’s College and Dept. of Biochemistry, University of Calcutta for teaching me and making me dream bigger each day. I want to thank **Vidyadi, Sandip Sir, Madhumita Aunty, Bubaidada** for believing in me. My journey would have been so impossible without my best friend “**Shreya Sikdar**”. I take this opportunity to actually thank you for every nonsense and horrible things I have done to you in name of frustration.. Be there always.

This journey would be so incomplete without my family at **1, Park Side Road**. Born to the Guhas, I have always learnt to hold myself strong even in the darkest hour and keep my head high no matter what. My life is very incomplete without my sister **Meghna** (Guria). Every day when I wake up I pray to the Almighty such that we both may always be together till the last breath. **Amma, Mejudida, Nadida, Chhotodida** really took care of every little requirement I had. **Nadadu, bhalodadu, cchotodadu** actually made sure I reached school in time every day. **Pishi** taught me “ Read every word you see even if it is written in the tiniest of the scrap”. **Kaku** held me so strongly at all times and **No** taught me to say “no” which I think is the biggest lesson of my life. Contribution of **Miradida** and **Borojethi** in my daily life can never be said in few words. They are two of the biggest pillars I have. I sincerely want to thank **Rajakaku, Kishore kaku, Sampadi, Debamitra kaki, Sudeshna kaki, Boropishi, pishai** and **Toradi** for all their motivational thoughts and support since my childhood. Finally to sum it

my brothers “**Rahul and Rakesh**” ..thank you for everything...and I mean everything....and my dear “**Yashodhara**” thank you for being you and making my life better with your wishes and songs.

Coming next to the person without whom my life would really never be what it is.. my favourite “**Mistudi**” ....I can’t describe in words what you have done for me. I can only thank you and promise to be with you at all times and continue to love you as dearly as I can. My sweetheart **Hridhaan (Gultu)**... you make me so complete.. and I am indebted for all the love you shower on me. I want to thank **Dadu-Dida, chhotomama...mejomashi-mesho...tukumashi...jyotimesho...mejomama-mami... boromama-monima** and all my cousins (**Tantudi, Rahul, Bubun, Rupun, Tuli**) for all your prayers and support.

Finally acknowledging that individual whose exceptional guidance and daily contribution in science and life defines me today... “**Dipayan**”... this journey together was never easy but you made it possible in all your little ways...holding me thoroughly in those terrible days... assuring me that every problem can be solved in a very simple way and making me so comforted when the world turned treacherous at times. I remember starting our journey together as classmates since our college days...being best of friends during our post-graduation days. I often feel an awe thinking how far we have come together both professionally and in personal front. You make the best husband, friend and colleague. Keep guiding me and making each day worth living as you do. Thanking you is actually impossible but I can only promise to complete this marvelous journey we have started together, making each day worth celebrating over and over again. Wishing both of us the best luck ever...

I want to finally thank the Almighty for giving me the courage to fight those long battles and helping me shape my life to be the individual I am today.

**Subhalakshmi**

# CONTENTS

List of Abbreviation	3
Abstract	10
Introductory Review	12
Objective of the thesis	68
Methodology	71
Chapter I	91
Chapter II	113
Chapter III	131
Summary	155
Conclusive Discussion	157
References	162
Certificates and Publications	189

## List of Abbreviations

- A $\beta$  : Amyloid Beta
- AD : Alzheimer's Disease
- ACM : Astrocyte Conditioned Medium
- GFAP : Glial Fibrillary Acidic protein
- ICAM-1: Intercellular adhesion molecule-1
- PARP : Poly(ADP-ribose) polymerase
- CSF :Cerebro Spinal Fluid
- APP : Amyloid Precursor protein
- NFT : Neurofibrillary Tangle
- ILs : Interleukins
- TNF- $\alpha$  : Tumour Necrosis Factor- $\alpha$
- IFN- $\gamma$  : Interferon-  $\gamma$
- Bim : Bcl-2 interacting mediator of cell death
- IDE : Insulin Degrading Enzyme
- BSA : Bovine serum albumin
- DIV : Days *in vitro*
- DMEM : Dulbecco's modified Eagle medium
- DMSO : Dimethyl Sulphoxide
- E18 : Embryonic day 18
- GFP : Green fluorescent protein
- HFIP : 1,1,1,3,3,3-hexafluoro-2-propanol
- HRP : Horse radish peroxidase
- NF- $\kappa$ B: nuclear factor kappa light chain enhancer of activated B cells



NFDM : Non Fat Dry Milk

PBS : Phosphate Buffer saline

PDL : Poly D-Lysine

PFA : Paraformaldehyde

## Abstract

Alzheimer's disease (AD), one of the major forms of dementia in elderly population, is characterized by amyloid beta ( $A\beta$ ) plaque along with commonly procured tau hyperphosphorylation. Here, we set to recognize the molecules which are secreted by  $A\beta_{1-42}$  treated astrocytes at very early stage and their probable role in conferring neuroprotection along with improvement in cognitive behavior and pathogenesis of AD. Astrocyte activation has been marked by various specific marker proteins like GFAP, Vimentin, S100 $\beta$ . The conditioned medium obtained from the astrocytes cultured from neonatal pups has been used to check the differential expression of various cytokines in  $A\beta_{42}$  treated astrocytes as compared to control cells. From there soluble intercellular adhesion molecule-1 (sICAM-1) has been noted as a potential candidate. We observed that sICAM-1 protects the cortical neurons from death influenced by  $A\beta_{42}$  oligomers. It attenuates the PARP cleavage caused by  $A\beta_{42}$  and increases the amount of anti-apoptotic proteins such as Bcl-2 and Bcl-xL, along with decrease in the amount of pro-apoptotic protein Bim. TUNEL assay performed both in cortex and hippocampus of  $A\beta_{42}$  infused rat brain and 5xFAD mice brain showed that rICAM-1 treatment reduced the number of TUNEL positive cells in vivo. Several behavioral experiments namely open field test, contextual and cue dependent fear conditioning, passive avoidance tests, novel object recognition and elevated plus maze that can be related to multiple kinds of memory and learning have displayed that rat recombinant ICAM-1 on being injected within the system intraperitoneally, restored the malfunctioning in the rat behavior caused due to bilateral  $A\beta_{42}$  infusion. We took further interest in checking the underlying disease modifying mechanism rendered by ICAM-1 both in vitro and in vivo systems which might be considered being a therapeutic target for neuroprotection. Mechanistically we observed that

ICAM-1 administration decreases NF- $\kappa$ B protein level in AD pathology suggesting that ICAM-1 might play a crucial role in manipulating the stability of NF- $\kappa$ B through multiple degradation process. Also PDTC mediated inhibition of NF- $\kappa$ B protein in 5xFAD transgenic mice brain showed an improvement in cognitive behaviors including learning and memory in mice. Therapeutic approach towards prevalent neurodegenerative diseases like AD is one of the major concerns in the scientific world. Our work suggests that ICAM-1 protein could be said as a potential therapeutic agent that promotes neuronal protection along with recovery in cognitive functioning complemented with clearance of A $\beta$  in A $\beta$ <sub>42</sub> infused rats and 5xFAD mice model of AD.



**INTRODUCTORY  
REVIEW**

*“We are all the pieces of what we remember. As long as there is love and memory, there is no true loss.”— Cassandra Clare, City of Heavenly Fire*

## **General Introduction**

Alzheimer’s disease (AD), one of the most widespread neurodegenerative diseases was discovered by Dr. Alois Alzheimer’s in early 1900s. Worldwide more than 44 million people are affected by this disease causing impairment of synaptic plasticity followed by neuronal death and severe reduction in cognitive abilities. The major characterisation of pathological AD includes two core lesions: extracellular amyloid- $\beta$  ( $A\beta$ ) plaques and intracellular neurofibrillary tangles (NFTs) (Serrano-Pozo et al., 2011). An estimated survey of world health statistics by World Alzheimer Report 2020 shows that more than 55million peoples across the globe suffer the wrath of dementia, and latest as of 2020 the average annual expenses indulged in this diseases has surpassed \$1.3 trillion. AD constitutes among 60 to 80% of the dementia cases, less than half being pure AD and the majority expected to be mixed dementias (Barker et al., 2002), others including mostly vascular dementia, Lewy body dementia and frontotemporal lobe degeneration. The inevitable process of aging is the utmost risk factor associated with AD, with a probable incidence for all forms of dementia (Qiu et al., 2009).

Scrutinising the cognitive decline in patients and learning their underlying brain pathology, has become one of the great challenges faced by neuroscientists and neuropsychologists over several decades. This challenge has not only increased substantially over the past years with the elderly population, but also has been entangled in the age-related nature of major dementia-causing neurodegenerative

diseases. Although the concept of dementia has existed for thousands of years (Yang et al., 2016), the thorough knowledge about the disease has been seeing its light of investigation since a century only. In 1907 Mrs. Auguste Deter, a 51 year aged patient staying under Dr. Alois Alzheimer's supervision at state mental asylum, Frankfurt, Germany, caught his interest in the pathophysiological and medical perspective. Upon her unfortunate death, her post mortem brain studied by Sir Alzheimer's by silver staining microscopically revealed the detailed neuritic plaques, neurofibrillary tangles, and amyloid angiopathy, which in modern day are known to be the major pathological hallmarks of this disease. The term "Alzheimer's Disease" was coined by Sir Eric Kraepelin at the Munich Medical School in his book Handbook of Psychiatry in 1910, as a recognition to his student Dr. Alois Alzheimer.

The earliest and the most salient symptom of AD include the loss of episodic memory, also known as amnesia, which may also coincide with an elaborate underlying neuropathological lesions occurring in the medial temporal lobe structures like the hippocampus and the entorhinal cortex (Hyman et al., 1984). Since last two decades, breakthrough advances have been made in identifying genetic risk factors for AD. Three separate genes were recognised in large families whose mutations showed an autosomal dominant inheritance pattern in an early-onset form of AD, generally before 60 years of age. They are namely the amyloid precursor protein (APP) gene on chromosome 21, the presenilin 1 gene (PSN1) on chromosome 14, and the presenilin 2 (PSN2) gene on chromosome 1 (Saunders A.M., 2001). These are noted as the familial forms of AD and account for approximately 1 to 2% of cumulative cases of AD. However type  $\epsilon$ 4 allele apolipoprotein E (APOE) gene, a low density lipoprotein cholesterol carrier has been identified as a far more common and graver genetic risk factor for sporadic, late-onset AD (Strittmatter et al., 1993).

In the last 20 years, a biomarker era has ushered in which it has been complemented with several of the advanced neuroimaging methodologies like functional MRI, diffuse tensor imaging and these has been used for developing several algorithmic patterns to classify AD and mild cognitive impairment (MCI). By combining forces among all disciplines and assembling the vivid and intricate facts, new initiatives may be evolved which may not have been imagined previously. Complex brain diseases like AD could only succumb to such integrated efforts. Each effective pre-clinical diagnosis and treatments including exploding personal and financial costs may help to attenuate the disease progression even before the symptomatic onset.

## Review of literature:

### 1. Alzheimer's Disease

*“Be kind to your father, even if his mind fail him.” – Old Testament: Sirach 3:12*

Though the concept of dementia has been written over long ages past, yet the deep knowledge behind the cause underlying the phenomenon is nothing less than a century old. Sir Alois Alzheimer may have published his famous case study concerning the memory loss of Mrs. Auguste Deter a century ago, yet our modern understanding and outlook accelerated only in the 1980s, witnessing an extreme enthusiasm in the origin, characterization and every possible treatment of this deadly neurodegenerative disease. The most prevalent form of dementia is AD, others being Lewy body dementia, frontotemporal lobar degeneration, Parkinson's disease associated dementia, which are mostly associated with mixed pathology (Karantzoulis et al., 2011).

#### 1.1 Symptoms of AD

The major symptomatic hallmark of AD is neuro-psychiatric symptoms (NPS) causing notable distress for both the patient and the caregiver. The major concern of the disease lies in the fact that the initiation of the process may occur quite superficially, showing majorly the under-recognized symptoms. According to the recent reports of Alzheimer's Association, the stages of AD, categorized on the basis of symptoms and onset, are as follows:

**A. Preclinical Stage:** This is the earliest stage when the brain of an AD affiliated patient starts showing initial changes without any real clinical symptom visible in the patients. Much later the apparent symptoms become visible in the patients (Caselli and Reiman, 2013).



**B. Early mild stage of AD (mild):** The initial stages of AD show trivial alarms, for the person may be competently functioning in daily household chores, like driving and taking part in social activities. With progression, some discrepancy follows in initial lapse and subtle memory details. Certain biochemical markers may show an alteration but since no apparent changes in behaviour are observed in patients here, most of the cases are left undiagnosed. Some common difficulties have been located in some patients like their inability to come up with the right word, forgetting the names of newly introduced people, having trouble in planning or executing a pre-planned notion etc (Morris et al., 2001).

**C. Middle-stage Alzheimer's (moderate):** The middle stage of AD shows more conspicuous features and displays a much prolonged duration among the patients requiring extreme care and compassion from the caregiver towards the patient here. At this stage, the affected person usually shows confusion in framing words and expressing their ideals and thought. The defiling of the neuronal cells in brain makes it extremely difficult for them to express themselves and performing daily chores like bathing, cleansing etc without proper assistance. The manifestation may alter from person to person but the basic forgetfulness of events and history, mood fluctuations and social withdrawal is mostly common among all. Relentless change in the sleep pattern is another noticeable change observed in these middle stages AD patients. However still with proper encouragement and support these patients may be able to participate in normal daily life and get involved in social life too (Boller et al., 2002).

**D. Late-stage Alzheimer's (severe):** The final stage of AD is the most dangerous of all where the patient is absolutely unable to recollect and respond to the surrounding. Their inability to communicate and identify people become prominent as the disease progresses to an extreme level. Most importantly, even with a few imparting words of

thought, yet the feelings of pain remain mostly non-communicated. With decline in cognitive functioning and memory, remarkable personality changes may be observed in the patients. At this phase of disease, a daily personal assistance is mandatory for the patient as they lose their environmental awareness and confront alteration in physical abilities like sitting, standing, and finally swallowing. At the final stages of AD, the patient becomes more prone towards infections like pneumonia and may breathe their last in the process (Voisin et al., 2009). Though AD mediated death is not much heard of, yet a life so mundane might not be less than an afterlife.

## **1.2 Global Impact of AD**

The impact of this exponential growth should be observed more in low- and middle-income countries which centers around two-thirds of affected people, though the overall impact will be felt almost around the world. Scientists have pointed out that the ultimate reason behind this global explosion of dementia is primarily due to the aging. In 2006, 500 million people above 65 years, which is about 8% of the world population have been said to be affected under the curse of dementia; yet by 2030, those above 65 years are expected to be among the affected 13% of the total population. These statistics reflect that people, in the developing countries are living longer and healthier due to medical advances with a significant reduction in malnutrition and the incidence of communicable diseases (National Institute on Aging: Why Population Aging Matters: a Global Perspective., 2007; United Nations: World Population Prospects. The 2004 Revision). However, collaterally, chronic age-related diseases including AD are rising (*Barker* et al., 2002; Fratiglioni et al., 2000). The astronomical numbers of AD affected people exerts an immense strain on the concerned governments public health systems across the world. In the year 2010, total estimated worldwide cost of dementia was around USD 1.3 trillion, exceeding

annual revenue of world's top most companies (Alzheimer's Disease International: World Alzheimer Report, 2020). The major cost of dementia care is inclusive of medical care, social care, and informal costs. About 70% of the dementia caring expenses is common in Western Europe and North America including nursing home care and professional care for the welfare of the community. However in the lower income countries, predominance lies in the care provided by family. As the prevalence of dementia increases worldwide, the costs of caring for people with dementia should be increasing likewise. The responsibility of AD care falls on families and caregivers, mainly in low and middle-income countries where patients prefer home supervision rather than long-term residential facilities. Unfortunately, with little or no research and awareness being seen about the caregiver's burden, the resource utilization process in the developing world makes it a very difficult and underappreciated life for the caregivers. The major concern today still lies in the low level awareness about the disease, with special emphasis on the lacking of appropriate and affordable healthcare services, causing a heavy reliance on family (Prince et al., 2009). NIA-Alzheimer's Association has published a revised guideline which identifies people having predisposition to AD later in life, even during the asymptomatic phase of the disease (Sperling et al., 2011; McKhann et al., 2011; Albert et al., 2011). Even though all seems better to be further investigated, yet the proposed framework directs towards a hopeful stage for future therapeutic trials among asymptomatic populations.

### **1.3 Causes and Risk Factors of AD**

AD has been long considered a composite disease having many facets to its cause having associated with several risk factors like age, genetic predisposition,

environmental factor, lifestyle manifestations etc. Over long periods, researchers have proposed several theories which encapsulate the underlying causing pathology, yet the probable cause has been narrowed down to two main hypotheses:

### A. Cholinergic Hypothesis:

In the early 1970s, choline acetyltransferase (ChAT) enzyme was identified that helps in the synthesis of acetylcholine along with other critical functions. This theory involves around the faulty cholinergic neurotransmission caused by  $A\beta$  along with a reduced choline uptake and Acetyl Choline release.

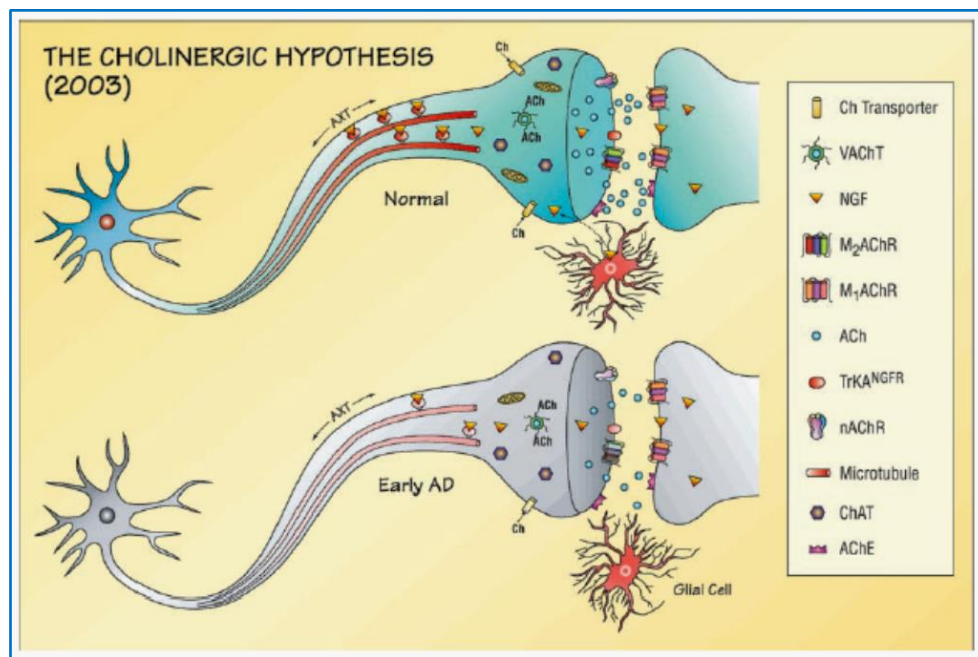


**Figure 1:** Cholinergic Hypothesis in Alzheimer's Disease (Terry and Buccafusco, 2003)

$A\beta$  brings about cholinergic neuronal degeneration causing serious alteration in the cognitive functioning and memory loss. Studies have elucidated that a sound relation exists between neurotoxicity caused by  $A\beta$  and cholinergic synaptic loss. Additional factors like nicotinic and muscarinic (M2) ACh receptor reduction, and deficiency in excitatory amino acid (EAA) neurotransmission, may be common in AD in which the

glutamate concentration and D-aspartate uptake are extremely reduced in many cortical areas of AD brain. Among AD patients, an uniform reduction in the presynaptic markers of the cholinergic system was apparent. Also a significant drop in ChAT activity and ACh synthesis was observed among patients with enhanced degree of cognition among them (Francis et al., 1993; Wilcock et al., 1982; Sims et al., 1983). Thus clinicians have been trying to reverse the effects by using acetylcholine activators which may influence their formation within the milieu (Babic et al., 1999; Ferreira-Vieira et al., 2016; Breijyeh et al., 2020).

### **B. The Amyloid Cascade Hypothesis**

The concept of the amyloid hypothesis has been in strong discussion for decades among scientists and clinicians. With aging, amyloid plaques (AP) have been found to be deposited in healthy brains, which affirms the probability of AP deposition being responsible for AD onset. The amyloid hypothesis holds true as the most accepted pathological mechanism for inherited AD (IAD).

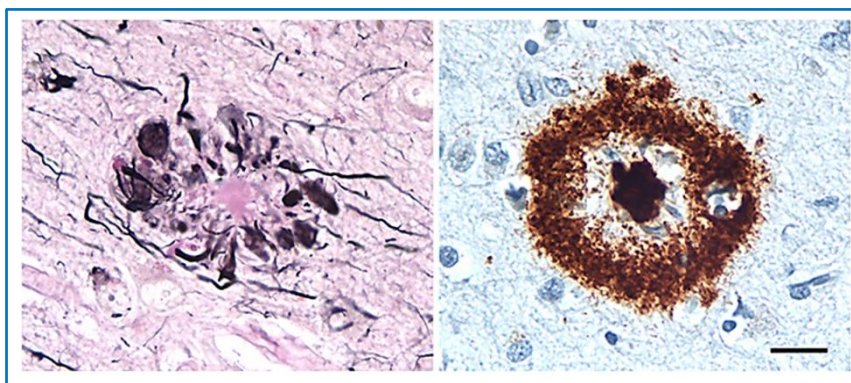


**Figure 2:** Left panel: AD post mortem brain showing 'Classical' A $\beta$  (senile) plaques in the cortex of stained with the Naoumenko-Feigin silver method and periodic acid-Schiff (PAS) counterstain. Right panel: plaque stained with antibody 4G8 to the A $\beta$  protein (brown) along with a Nissl counterstain (blue) Bar = 20 $\mu$ m for both panels (Walker L.C., 2020).

The amyloid hypothesis suggests that the accumulation of A $\beta$  peptides (A $\beta$ <sub>40</sub> and A $\beta$ <sub>42</sub>) is accelerated by the inability of  $\beta$ - and  $\gamma$ -secretase to degrade APP derived A $\beta$ , due to aging or other pathological conditions (Scheuner et al., 1996). The major imbalance in the A $\beta$ <sub>42</sub>/A $\beta$ <sub>40</sub> causes the formation of amyloid fibril, followed by tau formation and neurodegeneration. Several AD risk factors and mutations of genes namely APP, PSEN1, and PSEN2 results in faulty A $\beta$  metabolism amplifying its accumulation along with progression of the disease (Paroni et al., 2019; Kametani and Hasegawa, 2018; Ricciarelli and Fedele, 2017). Initiation of this hypothesis dates back to 1984, when the proposal given by George Glenner (Glenner and Wong, 1984) met with superb skepticism but eventual steady accumulation of evidence among the researchers led to strengthening of the theory (Beyreuther & Masters, 1991; Hardy & Allsop, 1991; Selkoe D.J., 1991; Hardy and Higgins, 1992). The underlying mechanism unfolded over years explained that the presenilin genes are responsible for encoding the active site of the intra-membranal cleaving  $\gamma$ -secretase (De Strooper et al., 1998; Wolfe et al., 1999) and when in the transmembrane/cytoplasmic interface of APP an initial endopeptidase cleavage occurs, multiple carboxypeptidase cleavages follows, sequentially removing 3 or 4 C-terminal amino acids (Qi-Takahara et al., 2005; Takami et al., 2009; Chavez-Gutierrez et al., 2012; Okochi et al., 2013; Fernandez et al., 2014). The initial indication of the amyloid hypothesis was implied on the basis of a discovery of APP gene residing on chromosome 21, suggesting that Down's syndrome individuals have a tendency of developing typical Alzheimer pathology producing too much A $\beta$  throughout their life (Prasher et al., 1998). Another research group has imposed that this mechanism is a representation a functional loss of presenilin causing the neural

phenotype of AD patients, independent to the effects of only A $\beta$  accumulation (Shen & Kelleher, 2007; Xia et al., 2015)

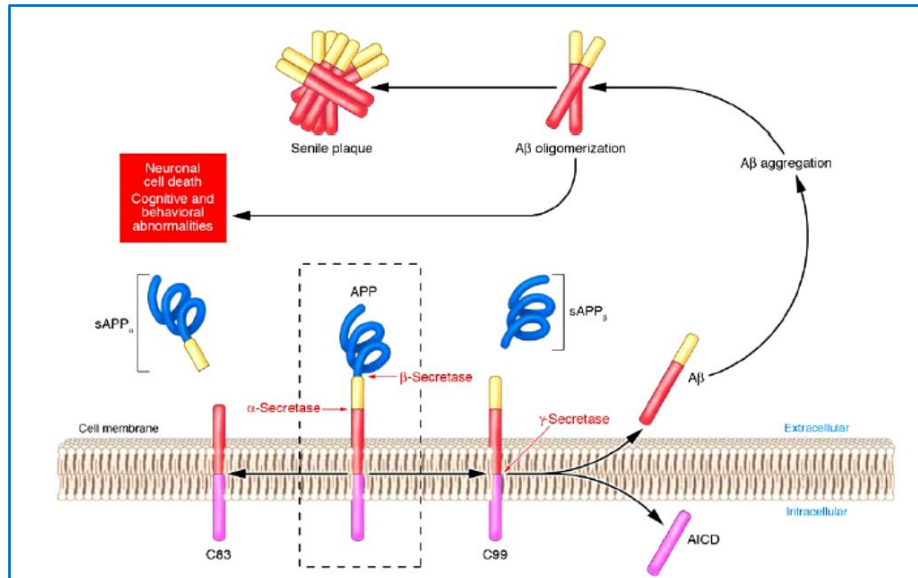


**Figure 3:**The method of APP processing in amyloidogenic pathway (Imbimbo and Lombard, 2005)

Recently a remarkable identification of missense mutation in APP (A673T) has taken place, which may result in a permanent decrease in APP cleavage by  $\beta$ -secretase (Jonsson et al., 2012) making the resultant mutant A $\beta$  peptide having altered aggregation properties (Benilova et al., 2014; Maloney et al., 2014; Zheng et al., 2015). The patients carrying the A673T gene have shown a reduction in clinical AD along with improved cognitive functions (Guyon et al., 2020), and surprisingly they have been devoid of plaque deposition even at a very old age as 100 years (Kero et al., 2013). These finds have strengthened the amyloid hypothesis strongly and paved the path for a better researching therapeutic ground.

### C.THE TAU HYPOTHESIS

Recent advances in imaging have shown that A $\beta$  accumulation may sometimes be sparse in the patient's brain whereas, several among the normal patients have displayed amyloid deposits too (Edison et al., 2007; Li et al., 2008) along with a comparable amount of senile plaques distribution as in the dementia aided patients (Davis et al., 1999; Fagan et al., 2009; Price et al., 2009; Chetelat et al., 2013). Recently, a new school of thought known as the Tau hypothesis has recently come up drawing much attention to several clinicians and scientists across the world.

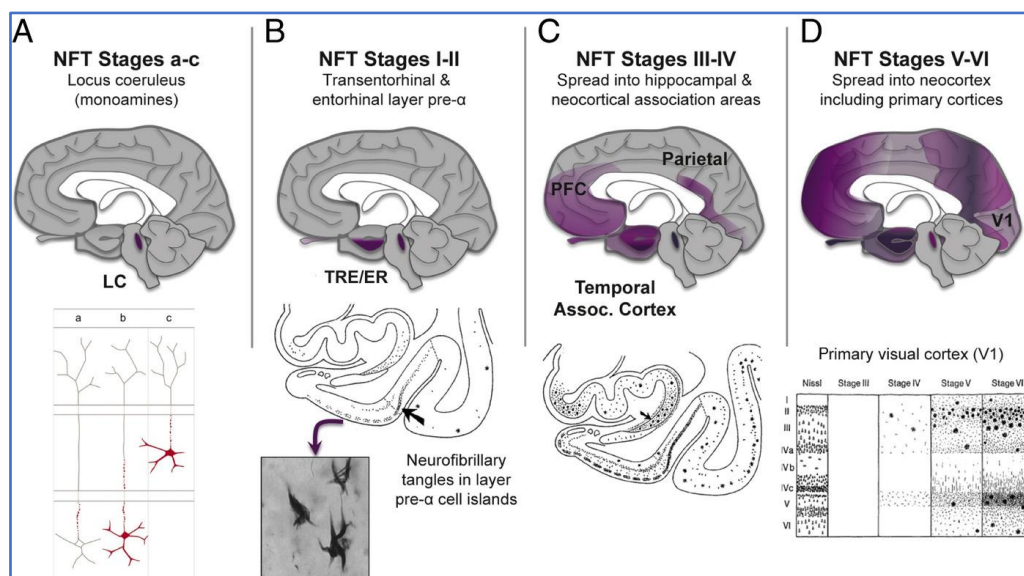


**Figure 4:** The sequence of tau pathology in the human brain (Arnsten et al., 2021)

A deep relation has been established between the AD and expression of Tau which finds an appearance in the trans-entorhinal region spreading to the limbic region and neocortical areas of the brain in the various stages (Braak and Braak, 1991). Recent PET studies showing spatial patterns of tau by tracer binding have been closely linked to cognitive decline in AD patients (Okamura and Yanai, 2017). In fact, it is believed that the indication of early tauopathy in the medial temporal lobe, proves to be a better marker for declined brain functioning than an elevated global increase of



A $\beta$  (Schöll et al., 2016; Hanseeuw et al., 2019; Schwarz et al., 2016; Buckley et al., 2017). Furthermore, tau lesions in many cases have been noted to appear before A $\beta$  accumulation (Braak and Del Tredici, 2014). Thus, in view of some researchers and clinicians, progression of AD has been markedly associated with tau pathology, more than A $\beta$  amyloid accumulation.

#### **1.4 Alzheimer's Disease Risk Factors**

Multiple risk factors associated with Alzheimer's Disease have been identified over the time. They may be as follows :

**A. Aging :** Aging, known to be the complex and irreversible change of the body and organs, has often been declared the primary risk factor of AD. This aging process allows the reduction in brain volume which encourages the deposition of Neuro Fibrillary Tangles (NFT) and Senile Plaque in brain reducing the synaptic connections. Depending on the time of initiation of the disease, it can be classified as Early-onset AD (EOAD) and Late-onset AD (LOAD), both being evitable in people having an AD familial history in previous generations (Guerreiro and Bras, 2015; Riedel et al., 2016)

**B. Genetic risk factors :** Over long years genetic factors have been known to play a vital role in AD. One among the many important ones is APP, a type I transmembrane protein, situated on chromosome 21. It requires the cleavage of  $\beta$ -, and  $\gamma$ -secretase to release A $\beta$ . Although a single protective mutation, A673T has been identified to be helpful (Li et al., 2019, Tcw and Goate, 2017), yet mutations like KM670/671NL and D678H, E682K have been established to cause A $\beta$  accumulation along with cortical and hippocampal atrophy (Bi et al., 2019). Several other mutations such as T714I, V715A, L723P, K724N, and I716V have affected the

$\gamma$ -secretase cleavage resulting in a  $A\beta_{42}/A\beta_{40}$  ratio imbalance. Also E693G and A692G cause mutations in the  $\alpha$ -secretase cleavage site forming polymorphic aggregates which disrupts the bilayer integrity. Other deletion mutation like E693 delta has shown to enhance the formation of synaptotoxic  $A\beta$  (Dai et al., 2018; Zhao et al., 2020).

The second most important genes responsible for AD are PSEN1 and PSEN2, which are the autosomal dominant form of EOAD. They are located on chromosomes 14 and 1 respectively, homology being around 67% between the two. Mutation in PSEN1 is reportedly more common, compared to PSEN2 gene (Cai et al., 2015, Lanoiselee et al., 2017). Extensive research showed that PSEN1 knock-in mice having C410Y or L435F mutations enhanced the  $A\beta_{42}/A\beta_{40}$  ratio, reducing the  $A\beta_{40}$  amount (De Strooper, 2007). However PSEN-2 mutations are rare and are not found to play any major role in  $A\beta$  production. Another well-known gene, ApoE, with three isoforms ApoE2, ApoE3, and ApoE4, is a strong risk factor for AD. The ApoE $\epsilon$ 4 allele is more vital for both EOAD and LOAD in comparison to ApoE $\epsilon$ 2 and ApoE $\epsilon$ 3 alleles which are known to have lower risk and protective effect, respectively (Kim et al., 2009). ApoE $\epsilon$ 4 has not only been called another responsible candidate for causing  $A\beta$  deposition as senile plaque and cerebral amyloid angiopathy (CAA), marking AD symptom (Liu et al., 2013), but also has been associated with brain vascular damage, leading to AD pathogenesis (Giau et al., 2015).

In 2009, two other genes clusterin (CLU), located on chromosome 8 and Bridging Integrator 1 (BIN1) has been identified by Genome-Wide Association Studies (GWAS) as novel risk factors for LOAD. Clusterin showed upregulation in the cortex and hippocampus of AD brains, along with cerebrospinal fluid (CSF) and plasma, making it a promising biomarker for this disease. Researches have also shown that

CLU may play a dual beneficial or detrimental role by either promoting A $\beta$  clearance, or by reducing A $\beta$  clearance respectively (Foster et al., 2019). BIN1 is an adaptor protein which interact with different proteins like clathrin, synaptojanin, and amphiphysin 1 in brain, regulating the endocytosis of the synaptic vesicle. Recently, seeing its role in A $\beta$  production and tau and NFT pathology modulation, BIN1 has been recognized as the second most important risk factor for LOAD after ApoE (Holler et al., 2014; Andrew et al., 2019). Other genes like Evolutionarily Conserved Signaling Intermediate in Toll pathway (ECSIT) stabilizing the mitochondrial respiratory complex along with NF- $\kappa$ B, IRFs, and AP-1 activation and Estrogen Receptor Gene (ESR), have recently been identified as a contributor to the genetic risk factors associated with AD (Liu et al., 2018).

**C. Environmental risk factors:** In spite of the genetic predisposition and the age, many AD cases are incomplete without the influence of serious environmental and lifestyle issues, which we often take for granted. On exposure to high levels of air pollution, several in vivo and in vitro models have shown damage to the olfactory mucosa and bulb, along with frontal cortex region, similar to that observed in AD. Individuals exposed to air pollutants have displayed clinical symptoms of oxidative stress, neuroinflammation and neuronal degeneration, along with hyperphosphorylated tau and A $\beta$  plaque deposition in the frontal cortex (Moulton and Yang, 2012; Croze and Zimmer, 2018). Some of the metals like aluminium and lead can be harmful for brain. Recent Studies demonstrated that too much of Aluminium exposure may enhance the chance of its deposition in brain, causing protein misfolding, aggregation, and phosphorylation of tau protein (Akiyama and Bush, 2006; Colomina and Peris-Sampedro, 2017). Lead has been reported to modify neural differentiation and synaptogenesis competing with the binding site of bio-

metals like calcium and can crossing the BBB rapidly. Also an acute exposure to lead has been associated with increase of  $\beta$ -secretase expression and A $\beta$  accumulation (Huat et al., 2019).

In recent past, role of nutrition on AD have been of real interest to the scientists and healthcare personnel. The processed food being deficient of vitamin C and folates, along with reduced water content has resulted in formation of toxic secondary products like advanced glycation end products, AGEs. The AGE receptor (RAGE), being a primary receptor of microglia and astrocytes, has been well established to be overexpressed in AD patients serving as a cell surface receptor for A $\beta$  transporting the same (Abate et al., 2017). Elevation in AGEs serum level has also been associated with cognitive decline and AD progression. Malnutrition, causing deficiency in folate, vitamin B12, and vitamin D is said to be another risk factor for AD (Koyama et al., 2016).

Medical risk factors like cardiovascular disease (CVD), obesity, diabetes, and others has been long associated with increased risk of AD (Stampfer M.J., 2006; Santos et al., 2017). Chronic infections like herpes simplex virus (HSV-1) and syphilitic dementia caused by spirochete bacteria (*Treponema pallidum*) may be responsible for producing lesions similar to neurofibrillary tangles within the central nervous system (CNS). Bacteria like *Chlamydia pneumonia* has also been reported to activate astrocyte triggering LOAD, disrupting calcium regulation and apoptosis, resulting in decline of cognitive function, increasing the risk of AD (Sochocka et al., 2017; Fülöp et al., 2018; Muzambi et al., 2019). Obesity and uncontrolled diabetes, often caused by unhealthy diet and erroneous lifestyle has found an intricate association with decreased brain blood supply causing brain ischemia, memory loss and vascular dementia. These diseases are often responsible for increased pro-

inflammatory cytokines secretions causing systemic inflammation, ultimately leading to increased A $\beta$  accumulation, mitochondrial dysfunction and neuroinflammation (Alford et al., 2018; Pegueroles et al., 2018; Anjum et al., 2018; Lee et al., 2018).

### **1.5 Pathophysiology of AD**

The pathological diagnosis of AD remains to be of gold standard with cumulation of both several macroscopic and microscopic traits. The macroscopic analysis of post mortem AD brain often shows cortical atrophy in moderation that marks its multimodal association with cortices and limbic lobe areas. The frontal and temporal cortices often show enlarged sulcal and gyrus region, while primary motor and somatosensory cortices most often appearing unperturbed (Perl D.P., 2010). The brain regions of amygdala and hippocampus often find medial temporal atrophy along with temporal horn enlargement marking a typical feature in AD (Apostolova et al., 2012). All these may accompany loss of neuromelanin pigmentation in the region of locus coeruleus (*Serrano-Pozo et al., 2011*). The microscopic examination of overall brain region is extremely essential for the conclusive diagnosis of AD, employing various staining and scanning methods indicating much of the neuropathological change (Montine et al., 2012), emphasising also on the diagnosis depending upon the lesion morphology and density and partly also on their topographic distribution.

Several of the brain regions vulnerable to AD type pathology has been found to be predisposed to other disease processes too, like the  $\alpha$ -synucleinopathy and TDP-43 proteinopathy. With observation aging over 100 years, localization of extracellular amyloid plaques along with intracellular neurofibrillary tangles has been quintessential for diagnosing the disease. The senile amyloid plaques or “miliary

foci”, first elaborated by Oskar Fischer, results due to accumulation of extracellular nonvascular A $\beta$ <sub>40</sub> and A $\beta$ <sub>42</sub> peptides, caused due to alteration of amyloid precursor protein by the  $\beta$ - and  $\gamma$ -secretases accompanied by imbalance in the production and clearance pathway of the same (Alzheimer et al., 1907; Kumar et al., 2015; Goedert M., 2009; Thal et al., 2006).

The amyloid plaques may have a subset of dense rigid core plaques called **neuritic plaques (NPs)** which may be associated to tau-positive or dystrophic neurites, which has been well defined by synaptic markers and APP staining (Dickson D.W., 1997). These dense cored NPs are marked by synaptic loss, activated microglia and reactive astrocytes (Yasuhara et al., 1994). However the other type of diffused plaques containing filamentous A $\beta$  often lack these specific neuritic components and can be observed in later stages of AD (DeTure and Dickson, 2019). Detailed clinical observations also suggest that A $\beta$  peptides may be deposited in parts of the cerebral blood vessels too, estimating that gross 85–95% of AD cases constitute certain degree of **cerebral amyloid angiopathy (CAA)**. CAA have been known to affect small arteries and arterioles along with the capillaries in leptomeningeal vessels and in the gray matter of the cerebral cortices. They are also extremely like to be associated to APOE4 and APOE2 depending on CAA type-1 or type 2-AD respectively (Thal et al., 2002 ; Attems et al., 2010).

Another renowned pathological hallmark of AD include the **Neurofibrillary tangles (NFTs)** which were first explained in Alzheimer’s seminal paper as “neurofibrils,” forming thick bundles near affected neurons (Ryan et al., 2015). These were well visible when stained with Bielschowsky silver stain and is often associated with neuronal cell death and adjournment resulting in extracellular neurofibrillary tangles or “ghost tangles”. They are primarily composed of filamentous tau proteins and are

known to find a better co-relation with cognitive impairment as compared to amyloid deposits (Dickson et al., 1992). In AD brain, the tau filaments hold a nomenclature of “paired helical filaments” (PHFs) (KIDD M., 1963), exhibiting marked periodicity in electron microscopy and are composed of two small filaments of size about 10 nm diameter twisting around leading to a periodic structure having 65–80 nm crossover distance. Tau proteins in AD show hyperphosphorylation along with abnormal folding having lost their normal nature of binding and stabilizing microtubules in the axon. AD finds the dual property of lost functionality in tau along with enhanced aggregation property in abnormal Tau (Alonso et al.,1994; Alonso et al.,1996).

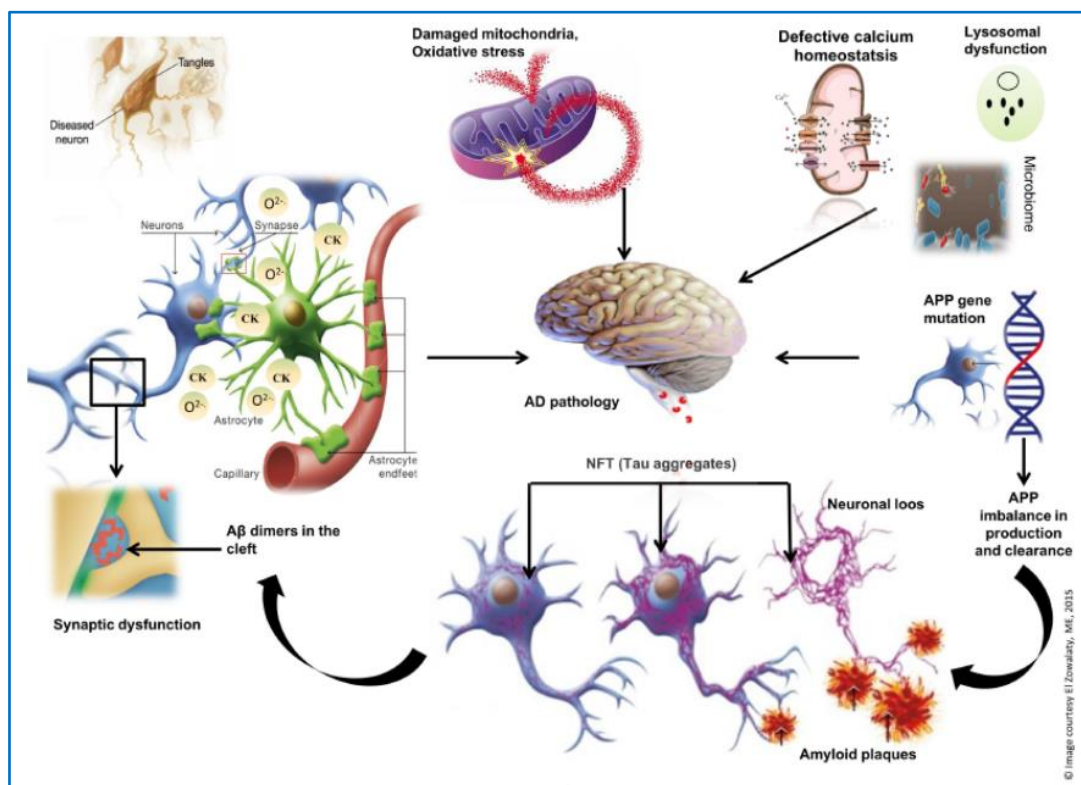


**Figure 5 :** Pathophysiology of AD (El Zowalaty, ME, 2015) .

There are some other pathological alterations like **Granulovacuolar degeneration**, which has shown an inevitability in display but requires detailed characterisation (Köhler C., 2016; Woodard J.S., 1962). These autophagic granules, which can be labelled with lysosomal markers like acid phosphatase (Hirano et al., 1968; Funk et al., 2011) are most frequently found in the pyramidal neurons of the hippocampus. Various stage analysis has shown that hippocampus shows its first accumulation followed by the entorhinal and temporal neocortex. The parts affected at last are amygdala, thalamus, cingulate gyrus along with the associated cortices (Thal et al., 2011). Another rod-like eosinophilic intracytoplasmic inclusion bodies, also called **Hirano bodies**, have been located in neuronal dendrites (Hirano A., 1994). They are commonly observed in the CA1 region of the hippocampus in middle age and elderly individuals suffering from AD (Gibson and Tomlinson, 1977). Hirano bodies have also been associated with reduced synaptic responses and impaired spatial working memory (Furgerson et al., 2014).

**Inflammatory response** caused by the phagocytic microglia and the astrocytes are also among the essential pathological hallmarks pointing the disease. Microglial activation during A $\beta$  fibril and tau accumulation are common near senile plaques which often increase in numbers due to neuronal damage associated with NFTs and NT (Serrano-Pozo et al., 2011; Wake et al., 2009). Receptors on microglia like TREM2, shows a tendency towards binding A $\beta$  fibrils, driving an inflammatory response similar to the M1 phenotype, claiming it to be a source of inflammatory cause (Heneka et al., 2015). Reactive astrocytes are another set of inflammatory response in the AD brain which are initially thought to serve protection towards the damaged neurons trying to restore the initial homeostasis. Like microglia in AD, they are often found grown around senile plaques (Steele and Robinson, 2012; Liddelov



et al., 2017). Reactive astrocyte at later stages in AD, are known to be detrimental with increased dementia and is often correlated with tau burden (Vehmas et al., 2003). Numerous researches including electron microscopy of synaptic protein markers have hinted that synaptic loss can be better correlated to cognitive decline than tau burden (Gomez-Isla et al., 1997; Overk et al., 2014). Synaptic loss and reduced density of hippocampus and medial temporal lobe appears to be in strong association with cognitive decline in AD over neuronal loss and tau burden (Terry et al., 1991). Earliest study demonstrating synaptic decline resulting due to axonal dysfunction, along with transporter damage have been validated in AD (Scheff S.W., 2006, Masliah E., 1991 Scheff S.W., 2011). These pathogenic alterations have shown a direct relation to Alzheimer's pathology, along with an association with clinical symptoms.

## **2. Glia : General overview**

Despite the fundamental significance held by neuron, functioning of CNS seems inadequate without the non-neuronal cells like the glial cells (Barres B.A., 2008). In spite of glia being traditionally recognised distinctively from neurons in their morphology, lacking axons and dendrites and having separate synaptic junctions (Morest and Silver, 2003), yet the specialised morphology and indispensable functioning of the same has been unravelled with decades of detailed research equipped by advanced RNA sequencing and high-dimensional, single-cell analysis with regards to the system (Saunders et al., 2018; Böttcher et al., 2019 ; Masuda et al., 2019). Cells like astrocytes along with oligodendrocytes and microglia comprise the main subtypes of the CNS glia.

**Astrocytes:** They are cells containing multiple stellate shaped dendritic processes constituting a widely depicted territory, located mostly throughout the central nervous

system (Zhou et al., 2019 ). Other than forming widely intimate contact with synapse, blood vesicular bodies and other glial cells, astrocytes perform multiple other functions like metabolic modulation (Allen et al., 2012) while controlling the neuronal excitement and plasticity by immediately uptaking various neurotransmitters (Bergles and Jahr, 1997). Along with having wide functional domains including memory accumulation and maintaining the circadian clock (Santello et al., 2019), astrocytes have established their capacity to generate inflammation, subsequently resulting in disease onset and progression (Heneka et al., 2018). In response to an acute injury within the CNS caused by trauma or any specific disease, several astrocytes form barriers which ensure proper restriction for the inflammatory cells to enter the CNS (Anderson et al., 2016 ). Due to these vital functions performed by astrocytes in maintaining health and adding resistance in a disease state and injury, detailed study on astrocytes has been of utmost interest to scientists across the world since a long time.

**Oligodendrocytes:** Oligodendrocytes primarily originate from their progenitor cells called OPCs and are located across the Central Nervous System (Zhu et al., 2008) overlapping the axons of neurons. They majorly help in myelin production enhancing the axonal conductivity (Boulanger and Messier, 2014) and ensures advanced network activity across the neuronal soma forming vascular structures (Battefeld et al., 2016; Niu et al., 2019). In this way, oligodendrocytes are known to play a wide range of functionality in maintaining health and disease holistically.

**Microglia:** Microglia which can be categorized as both glia and immune activating cells, are myeloid cells often considered also as macrophages (Greter et al., 2015). It has been shown that they are derived from yolk sac of the embryo, which clearly suggest them being diverted from the postnatal blood vesicular system leading to

intrinsic developmental and functional adaptation to the brain environment (Ginhoux et al., 2010; Schulz et al., 2010). In spite of the reliability in the morphology based study about the astrocytes activation (Kreutzberg G.W., 1996), microglial morphology owing to its high dynamicity, has depicted the use of modern technologies revealing that the genetic or translational signature of the same could be a potent venture to describe the multiple microglial states (Beccari et al., 2018 ). They are involved in producing a compulsive response to the brain when encountered with an injury (Perry et al., 1998) and the multiple genetic mutations also contribute in selective gene expressions during neurodegeneration (Jansen et al., 2019 ; Villegas-Llerena et al., 2016). Also, microglia are known to develop strong neuronal connections maintaining their plasticity within a system (Schafer et al., 2012; Stevens et al., 2007). Although many more stories need to unveil, yet microglia can be regarded a bit more than latent sentinels which are optimally reactive to brain homeostasis alteration activating signalling system and facilitating homeostasis to the milieu (Herz et al., 2017 ).

## 2.1 Astrocyte in AD

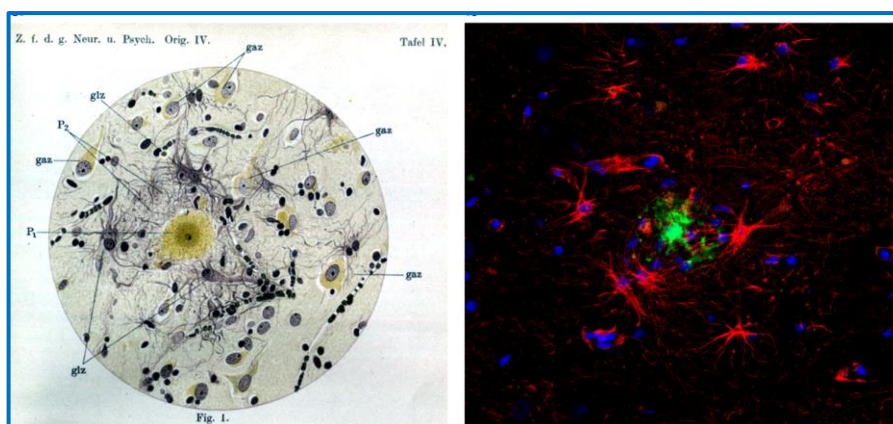


**Figure 6** : Left panel: Glia around A $\beta$  plaque and neighboring neurons drawn by Alois Alzheimer. Right panel: AD Post mortem hippocampal section showing reactive astroglia stained with GFAP-DAKO (red), DAPI (blue) and 6E10 (green) surrounding an amyloid plaque. (Osborn, Lana M et al. 2016)

Astrocytes are exclusive glial cells, scaffolding the entire CNS in their protoplasmic or fibrous form, which contribute to the BBB in collaboration with the endothelial cells and deeply encased synapses (Sofroniew and Vinters, 2010). In consistence to their phenotypic niche, the functionality of astroglia mainly includes cerebral blood flow maintaining the homeostasis between the fluid and neurotransmitters. It also initiates synapse formation providing them with suitable neurotrophic support (Rouach et al., 2008; Eroglu and Barres, 2010). Astrocytes also form the glymphatic system ensuring the removal of neurotoxic waste products like amyloid and tau proteins (Jessen et al., 2015; Tarasoff-Conway et al., 2015). Given their multiple housekeeping properties, it would be expected that astrocytes might attempt in regaining homeostasis at early stages of AD. Most often astrocytes near the formed plaques have been found to contain granules possessing A $\beta$  protein which has left scientists in suggesting that astrocytes make an ardent attempt in removing amyloid deposition in course of the disease process (Thal et al., 200 ; Funato et al., 1998). Further experiments have also revealed that a steady migration of astrocytes are observed towards the formed plaque resulting in A $\beta$  degradation both in vitro and in vivo (Wyss-Coray et al., 2003). In AD animal model, reactive astrocytes often release GABA and glutamate in excess, causing memory impairment and synaptic loss (Jo et al., 2014, Chang et al., 2013). Moreover, these cells cause dysfunctional microcirculation and BBB disturbance, causing sufficient progression of the disease (Kisler et al., 2017).

Extensive studies have shown that many AD associated factors in elderly patients, revolve around the glial genes like APOE, APOJ and SORL. This has readily moved the central feature of research away from neurons encouraging study of glia and neuroinflammation. Ageing rodent models elucidating the molecular signaling mechanism occurring within glia are quite insufficient for their mimic towards the human system. So recently in-vivo models depicting astrocytic stem cell implantation bringing insight into disease pathogenesis has been in vogue and is resulting in developing specific astrocyte based biomarkers to stall the neurodegenerative diseases like AD. 3xTg-AD animals having mutation for APPSwe and PS1M146V mice have been found to undergo several phenotypic alterations resulting in altered functions and morphology (Liddelow and Barres, 2017; Verkhratsky et al., 2016; Rodríguez-Arellano et al., 2016). Reactive astrocytes stay at a separate niche producing functionally different chemical oscillation and unprecedented calcium waves (Zorec et al., 2017). Several inflammatory genes like CST-7, CCL-4, IL-1 $\beta$  and CLEC-7A are found to be upregulated in astrocytes (Orre et al., 2014). The dual role played by astrocytes in AD raises an essential question of whether they being innocent or playing a pivotal role in neurodegenerative process. Researchers have shown that microglia secrete several cytokines like interleukin-1 $\alpha$  (IL-1 $\alpha$ ), tumour necrosis factor- $\alpha$  (TNF- $\alpha$ ) and complement component 1q (C1q), which influence A1 neurotoxic astrocytes (Liddelow et al., 2017). These A1 astrocytes upregulate complement component 3 (C3) genes, releasing neurotoxin, which along with reducing the synaptic ability and function, contribute widely in neuronal death (Liddelow et al., 2017; Sekar et al., 2016; Hong et al., 2016). Prefrontal cortical region of post-mortem brain of patients with AD show almost 60% of A1 astrocytes and further studies are currently being conducted about them.

Astrocytes have been found to be involved in amyloid- $\beta$  generation by upregulating the amyloid precursor protein and  $\beta$ -secretase1 (Frost et al., 2017). However, more likeliness of astrocytes lie in being associated to amyloid- $\beta$  clearance, with the help of degrading enzymes proteins like ApoE, ApoJ,  $\alpha$ 1-antichymotrypsin, and  $\alpha$ 2-macroglobulin which regulate A $\beta$  transport across the blood–brain barrier (Ries et al., 2016). Amyloid- $\beta$  activates the NF- $\kappa$ B pathway in astrocytes which instigates C3 to be released into the extracellular matrix and binding to the C3A-receptor on neurons causing disruption in dendritic network and morphology (Lian et al., 2015).

While neuroinflammation causes the rise in toxic A1 astrocyte, neuroprotective A2 astrocytes, characterized by upregulated neurotrophic genes such as cardiotrophin-like cytokine factor 1, transglutaminase 1, pentraxin 3, or sphingosine kinase 1 are often common in certain stages of AD. These A2 astrocytes produce several neurotrophic factors which ensure survival and growth, along with synapse repair (Liddelow et al., 2017). In fact, TGF- $\beta$  secreted by activated astrocytes and microglia increases A $\beta$  uptake by microglia helping in neurons against the toxicity of the same (Lian et al., 2016; Diniz et al., 2017). Also morphological analysis displaying the phagocytosis of dystrophic neurites performed by reactive astrocytes add as a further evidence towards reactive astroglia A2 being a protective component in Alzheimer's disease (Gomez-Arboledas et al., 2018). Current studies often tend to stress on the dual role played by astrocytes in the neurodegenerative disease like AD.

## **2.2. Microglia in AD**

Pio del Rio-Hortega in 1919 first described the microglial phenotypic diversity in human brain (Sierra et al., 2016) along with the altered morphology and state of the same in neurodegenerative diseases indicating that these cells have a common nature

of being adaptable. Recently further studies introduced by detailed networking and multi-functional high throughput tools showed the varied functional divergence of microglial phenotype in pathological conditions (Hanisch and Kettenmann, 2007; Ransohoff and Perry, 2009; Kierdorf and Prinz, 2017). Microglia are known to be the major immunocompetent cells colonizing within an early prenatal period (*Ginhoux et al., 2010*). The entire CNS microenvironment holds the major responsibility in shaping the functionality of the microglia, providing them with capability to maintain and support the brain homeostasis (*Kierdorf and Prinz, 2017*). Thus with an altered brain homeostasis, microglia tend to switch their phenotype initiating a defense program by undergoing multiple morphological and functional changes resulting in various reactive states enabling receptor expression and cytokine secretion along with other inflammatory molecules (Wolf et al., 2017). The main cause of the trigger is found to be associated with danger or pathogen associated molecular patterns (DAMPs/PAMPs) which results in activation of several receptor.

The functioning of microglia may be mainly characterized as the gain or loss of function. Gaining of function is possible in the cases where the complement proteins like CR3 and C1q present in microglia contribute in synaptic pruning (Veerhuis et al., 2011 ; Schafer et al., 2012).

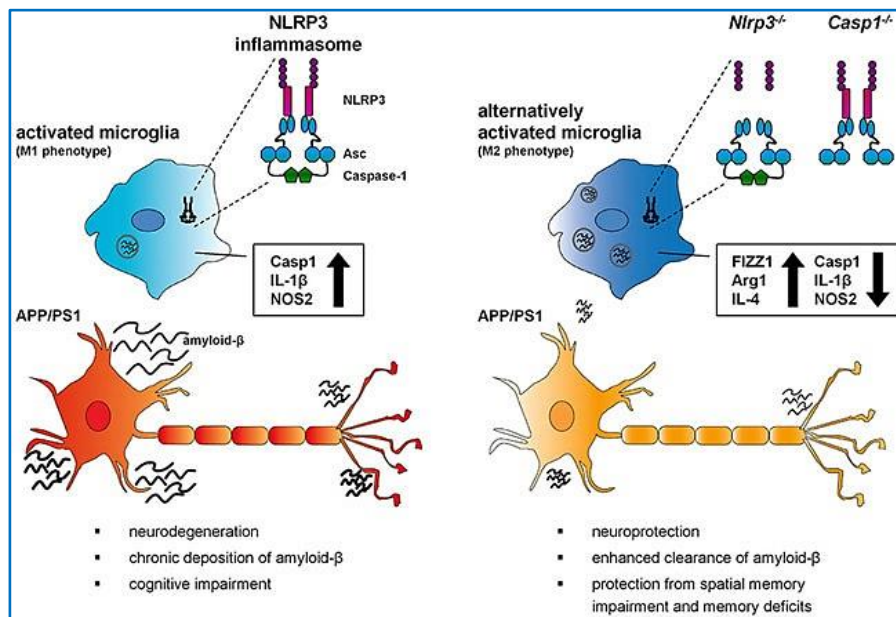


**Figure 7:** Role of microglia in coordination with inflammasomes in AD (Goldmann et al., 2013)

Also another instance of gaining in function occurs with major inflammasomes composed of the NLRP3 and ASC also known as apoptosis associated Speck-like protein, containing caspase recruitment domain, which contribute to the pathology in microglia (Martinon et al., 2002). Numerous studies have shown that all of these eventually lead to failure in vital mechanism of autophagy and results in formation of autophagosome (Nixon et al., 2005; Halle et al., 2008). Although majority of the clinical studies revolve around the reactivity-acquired functions of the microglia, yet the neuronal misfunctioning may be brought about by loss of homeostasis contributing massively to the detrimental role played by microglia. For instance glutamatergic synaptic maturation is caused by CX3CR1 which is present in microglia and binds to Fractalkine maintaining the synaptic homeostasis (Paolicelli et al., 2011; Hoshiko et al., 2012). However in AD, this CX3CR1 may decrease, causing a major disruption in signaling and communication, resulted due to aggravated pathophysiology of microglia (Keren-Shaulet et al., 2017). Also P2y12 gene



for a membrane receptor is normally present in microglia (Butovsky et al., 2014) but in reactive microglia this particular receptor reduces resulting in changed microglial migration and polarization (Haynes et al., 2006).

Apolipoprotein E (APOE) is known to be a very common risk factor associated with Late Onset Alzheimer's Disease. Early post-mortem studies in patients have revealed a much greater number of reactive microglia in APOE- $\epsilon$ 4 carriers compared to APOE $\epsilon$ 3 (Egensperger et al., 1998), and recently researchers (Minett et al., 2016) found that APOE $\epsilon$ 4 allele was strongly associated with reactive microglia. One of the other primary genes expressing specific surface receptor in microglia associated with AD is TREM2 (Schmid et al., 2002). Among several rare genetic variants of this protein, the rs75932628 causing the loss-of-function by R47H mutation, is known to provide significantly protective role for TREM2 activation in AD (Guerreiro et al., 2013; Jonsson et al., 2013). This protein modulates inflammatory reaction (Piccio et al., 2007) and chemokine secretion (Bouchon et al., 2002; Sieber et al., 2013). Even though TREM2 is enhanced in plaque-associated microglia (Frank et al., 2008) of hippocampus and cortices in APP/PS1transgenic mice, yet much detailed study of its role in AD is still to be understood (Jiang et al., 2014). Several other microglial genes, like Cd33, Cr1, or Abca7 helping in phagocytosis, has been identified by genetic sequencing and regarded as a potential risk factor in AD (Villegas-Llerena et al., 2016). Additionally, CD33 in conjugation with CR1 helps in A $\beta$  clearance (McQuade and Blurton-Jones, 2019).

Other than these, many other signaling cascades of microglia like the purinergic signaling and calcium signaling quite useful and emerging in the field. Inculcating these aspects into further details could help in improving the therapeutic role played by microglia in AD.

### 3. Neuroinflammation in AD

#### 3.1. Components of neuroinflammation

Neuroinflammation may be defined as an acute or sustained response to a trauma or insult causing inflammation in central nervous system. It often results in production of proinflammatory cytokines, e.g. IL-1 $\beta$ , IL-6, IL-18 and TNF, leading to synaptic malfunctioning and neuronal distress with reduced neurogenesis (Lyman et al., 2014). The resultant products also include chemokines like CCL1, CCL5 and CXCL1. Several small-molecule messengers, like the prostaglandins and nitric oxide (NO), along with the reactive oxygen species (ROS) are produced by the innate immune cells (Di Sabato et al., 2016). The major cells taking part in neuroinflammation include microglia and astrocytes. However the endothelial cells within the minor capillaries and the infiltrating blood corpuscles are also found to contribute to the neuroinflammation, particularly when mechanical damage in the blood–brain barrier (BBB) takes place (Heneka et al., 2014). IL-1 $\beta$  helps in upregulating the prostaglandin E2 secretion NMDA receptor activation resulting in synaptic loss (Mishra et al., 2012). On the other hand TNF activated TNFR1 along with recruitment of caspase 8 leading to NF- $\kappa$ B pathway inhibition causing an inappropriate demise of the neurons (Micheau and Tschopp, 2003). Additionally activation of the complement system during neuroinflammation causing increased phagocytosis in microglia can lead to its activation promoting the phagocytic function of microglia, which might finally result in untimely synaptic pruning (Hong et al., 2016). Neuroinflammation often results in secretion of several anti-inflammatory cytokines too. Some of them are namely IL-4, IL-10 and IL-11, which take part in preventing the excessive inflammatory process (Calsolaro and Edison, 2016). However, in global neurodegenerative diseases, neuroinflammation remains a

chronic process most of the time and its failure to resolve its condition acts as a vital reason for the disease progression (*Heneka et al., 2015*).

Reactive astrogliosis is common neuroinflammatory response to varied mechanical injury and ischemia along with abnormal protein assimilation through reactive gliosis (*Pekny et al., 2014*). Inflammatory insults are suggested to result in A1 astrocyte formation with the help of the NF- $\kappa$ B pathway, whereas with assistance of STAT-3 pathway, ischemia often induces A2 phenotype. Reportedly the major characteristic of A1 astrocyte lies in over-expressive inflammation along with induction of neuronal and glial death destabilizing the homeostasis of the milieu and the neuro-protective A2 cells are often marked by neurotrophic factors release (*Liddelow et al., 2014; Liddelow et al., 2017*). Complementing the astrocytes, microglia behaves as an ardent player in the trajectory of AD progression. Traditionally, function of microglia has been defined exclusively by immune markers like CD68, HLADR along with the altered morphology (*Hopperton et al., 2018*). The method of M1–M2 activation, is often defined by M1 and M2 being the pro-inflammatory and anti-inflammatory phenotype respectively (*Varnum and Ikezu, 2012*). However, several school of thoughts challenge this simple model suggesting the failure of microglia in maintaining the M1–M2 dichotomy (*Ransohoff R.M., 2016*). Also the recognized immunochemical markers of microglial like HLA-DR and CD68, do not specifically identify the pro-inflammatory and anti-inflammatory phenotypes (*Walker and Lue, 2015; Kim et al., 2016*). However the classification still holds true widely for a sorted idea of M2 and M1 being the protective and detrimental under various circumstances.

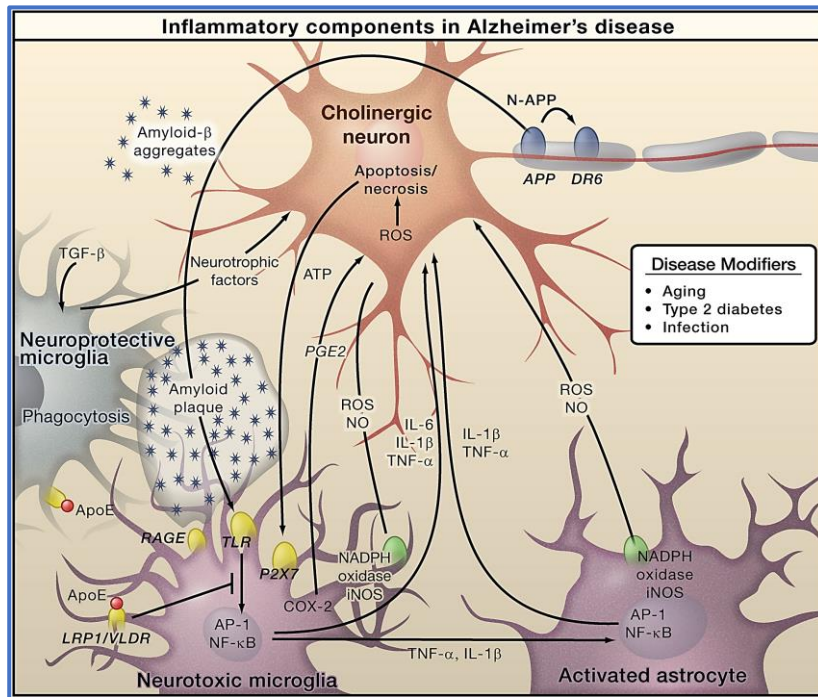


**Figure 8 :** Inflammatory components of Alzheimer's Disease (Glass et al., 2010).

Studies delving into the depth of neuroinflammation has shown a well-defined synchronization taking place between microglia, astrocytes and neurons to bring about neurodegeneration. It was shown in astrocytes that Aβ causes activation of the NF-κB pathway increasing the complement C3 release. Microglia and neurons having the C3a receptors on them causing microglial activation followed by the neuronal demise (Lian et al., 2015; Lian et al., 2016). Conversely, activated microglia release IL-1α, C1q and TNF-38 inducing the A1 neurotoxic astrocytes. This cellular cross regulation among the glia could contribute towards forming a positive feedback loop within the neuroinflammatory milieu in AD, causing damaged and self-amplifying inflammatory response. Since long time, AD subjects have displayed a chronic underlying malfunctioning in the neuron–glial crosstalk which is often caused due to dysregulated CD200–CD200R and CX3CL1–CX3CR1 signaling pathways present in microglia (Simon et al., 2019 ; Walker et al., 2014; Holtman et al., 2015).

Given the importance of microglial physiological changes, targeting the dysregulated inter-cellular communication could be a viable method for therapeutic intervention.

To unravel the basic feature of neuroinflammation in AD, several approaches both clinical and preclinical have been embraced. It includes histopathological examination along with detailed neuroimaging studies and evaluation of the proteomic signatures of fluid biomarkers. In context to the biomarkers, various studies involving the blood and CSF examination has revealed presence of several cytokines among which upregulation was common in IL-1 $\beta$ , IL-6, IL-12, IL-18, TNF- $\gamma$  and TGF- $\beta$  levels in AD patients as compared to the healthy controls (Swardfager et al., 2010). The latest research focuses primarily on the new glial activation markers, like chitinase 3-like protein 1, also known as YKL40, MCP1, VILIP1 and GFAP. A meta-analysis result showed that amount of YKL40 and VILIP1 in the CSF was significantly increased in AD, though the change in GFAP as a biomarker in CSF was not sufficient (El Kadmiri et al., 2018). Detailed multifaceted studies showed that amount of YKL40 was already upregulated in the preclinical stage and finds a better correlation to the disease depicting it to be a potent biomarker (Sutphen et al., 2015, Alcolea et al., 2015). The other essential method of detecting the neuroinflammation in AD is the neuroimaging studies often performed with PET involving the radioactive ligands which target translocator protein (TSPO). This protein, previously called the PBR, is found to be expressed primarily in activated glial cells within the CNS. TSPO is known as a constituent of the mitochondrial permeability transition pore and it casts itself as an important player in synthesizing steroid, regulating the permeability of mitochondria along with inflammatory modulation in glial cells (Edison et al., 2018). Autoradiography studies of stroke and AD has revealed the attachment of

elevated tracer binding to TSPO in the brain (Venneti et al., 2006 ; Diorio et al., 1991).

The sequential procurance of A $\beta$  plaques, activation of microglia and formation of neurofibrillary tangles led to the extremely interesting hypothesis behind the amyloid cascade–inflammation which propose the conjunction between pathological phosphorylation and tau aggregation relies on the microglial activation primarily (Hayes et al., 2002 ; Kitazawa et al., 2004; McGeer and McGeer, 2013). Previous studies showed that varied isoforms of A $\beta$  aggregates was able to cause glial activation along with differential expression of several pro-inflammatory cytokines like IL-1 $\beta$ , IL-6, IL-8, anti-inflammatory cytokine like TGF- $\beta$ , chemokines namely MCP-1 and MIP-1, several cell adhesion molecules, Nitric Oxide and ROS, all of which helped in bringing about neuronal dysfunction and death (Del Bo et al., 1995 ; Hanisch U.K., 2002) . The Toll-like receptors on microglia recognize A $\beta$  species activating molecular pathways inducing IL-8 and TNF expression along with IL-1 $\beta$  and NO production through NF- $\kappa$ B, c-JNK and MAPK pathways ultimately causing its phenotypic alteration (Venegas and Heneka, 2017 ; Liu et al., 2012 ; Murgas et al., 2012 ; Husemann et al., 2001). One molecule that marks the A $\beta$ -induced inflammatory response in microglia is TRPM2 channel which is primarily induced as a result of oxidative stress (Malko et al., 2019). A $\beta$ <sub>42</sub> induces oxidative stress through the activation of PKC and NADPH oxidase, which results in activating poly (ADP-ribose) polymerase-1, ADP-ribose and TRPM2. This causes an influx of calcium which initiates a series of cytokine production and the MAPK positive feedback pathway (Mortadza et al., 2017).

### 3.2. Neuroinflammation and AD trajectory

Neuroinflammation is vital component to the initiation of AD pathology process in its true sense (Dunn et al., 2005). Researchers have often debated that non-steroidal anti-inflammatory drugs or NSAIDs often play a protective role against AD onset and progression (t' Veld et al., 2001; Etminan et al., 2003), though the efficacy of them are quite often questioned in inflammation. Epidemiological studies have shown that systemic inflammation caused by risk factors like smoking, unhealthy lifestyle and diabetes, can cause neuroinflammation in CNS through circumventricular organs, along with active transport or disruption of the BBB (*Calsolaro and Edison, 2016*). Microglial activation has been found to be common at the pre-plaque stage in animal models of AD (Hanzel et al., 2014). Also detailed studies showed that infusing A $\beta$  into the brain could induce amyloid causing chronic systemic inflammation within the system (Philippens et al., 2017). More-compelling evidence was revealed from a human post-mortem study, which failed to show the relevant changes in microglia in asymptomatic individuals having increased amyloid plaque burden at various ages (Streit et al., 2009), strongly suggesting that both neuroinflammation and A $\beta$  deposition together is essential for AD pathogenesis. Genome wide analysis shows that mutation in glial genes like CD33, TREM2 cause neuroinflammation and could increase AD occurrence (Hollingworth et al., 2011; Lambert et al., 2013). The accumulating evidence show that systemic inflammation and consistent ageing in AD cause priming of microglia which results in quite an exaggerative inflammatory response when manifested to multiple pathological stimuli (Perry et al., 2014).

The effect of neuroinflammation on the varied phases of AD has been concluded from imaging studies that showed an inverse relation between microglial activation

and morphological or functional activity of the brain as assessed by volume of hippocampus and glucose metabolism respectively (Femminella et al., 2016 ; Fan et al., 2015.). The clinical imaging data braced with preclinical studies, showed that A $\beta$  activated microglia produced neurotoxic cytokines like TNF, IL-6, IL-1 $\beta$  and CCL2, causing subsequent neuronal malfunction and death (Spangenberg and Green, 2017; , Combs et al., 2001 ; Floden et al., 2005; Martin et al., 2017). Moreover, microglia activated due to the complement pathway can engulf synapses, causing an early synaptic loss and defecting the long-term potentiation (Neniskyte et al., 2011 ). Also it has been shown that, the knocking out the complement C3 in APP/PS1 hippocampus in mice, resulted in increased A $\beta$  deposition but levels of IBA1, CD68 immunoreactivity and pro-inflammatory cytokine production was found to be reduced (Shi et al., 2017). . Maintaining an accordance with imaging analysis, a study suggested that A $\beta$  plaques increased local toxicity with disease progression (Serrano-Pozo et al., 2016). A substantial increase in CD68+ microglial activation but not amyloid deposition throughout clinical stages of AD was observed, suggesting that a major mediator of amyloid toxicity could be microglia. These findings have navigated the further studies about the dynamic changes surrounding neuroinflammation from the early to late stage of AD.

A meta-analysis of various accumulated evidences from neuroimaging aspects provided assuring insights about the spatiao-temporal evolution of neuroinflammation in AD subjects (*Hardy and Higgins, 1992*). MCI displayed lower neuroinflammation than AD which corelated to the increased microglial activation parallel to the AD trajectory. The study also explained the spatial pattern of neuroinflammation in disease, with an initiation of microglial activation in neocortex at the early stage accompanied by further spreading of the same throughout the



cerebellum and temporal regions where tau pathology is found to be present majorly in the late stage of AD (Bradburn et al., 2016).

Three major intervention in the role of microglia played in the AD trajectory profile are firstly the suppression of microglial pro-inflammatory properties limiting the detrimental effect of microglia; secondly, modulation of the microglial phenotypic alteration to encourage the anti-inflammatory properties; and thirdly, ensuring that the priming of microglia may take place earlier. Though ineffective in several individuals yet usage of NSAIDs to suppress the inflammation was extremely common among all the early approaches taken by clinicians towards AD treatment (Miguel-Álvarez et al., 2015). Also an antibiotic called the minocycline, often used to inhibit the NO synthase IL-1 $\beta$  converting enzyme, and MMPs are common tool for suppressing the microglial activation (Elewa et al., 2006). Attempts have also been made targeting the NF- $\kappa$ B, NLPR3-caspase 1 and p38 MAPK pathways, causing massive suppression of the pro-inflammatory microglial phenotype (Munoz and Ammit, 2010; Thawkar et al., 2019; Mandrekar-Colucci et al., 2012). However, compounds helpful in clinical applications are yet being developed which require further testing and conformations. A preliminary clinical study involving subcutaneous administration of IFN $\beta$ -1a has displayed a slowing down of the disease progression in early AD patients (Grimaldi et al., 2014). Also sirtuin -1 which acts against resveratrol, enabled a reduction in inflammation in CSF activating the caloric restriction mechanisms. This lowering of markers like MMP-9 and IL-4, displayed a marked potential towards attenuating the cognitive decline in early AD (Moussa et al., 2017). According to several clinical trials, dietary discipline has also been considered for the management of neuroinflammation as research suggested of folic acid and omega-3 fatty acid supplementation being an inhibitory agent for the

inflammatory markers within CSF and plasma of patients AD (Chen et al., 2016 ; Vedin et al., 2008)

#### 4. Role of Cognition and memory in AD

If ever asked to find and name a disease that concerns “memory,” most of the clinicians and scientists would probably choose AD over all others. Consensus studies reveal that the primary symptom of AD as assessed clinically gets initiated with episodic memory loss along with various speech production or semantic problems. Memory is often defined as a procedure involving the encoding, storage and information retrieval concerning both external and inner stimuli, along with representing the information to neuronal system such that the organism may conduct a suitable reaction to the nascent stimuli.

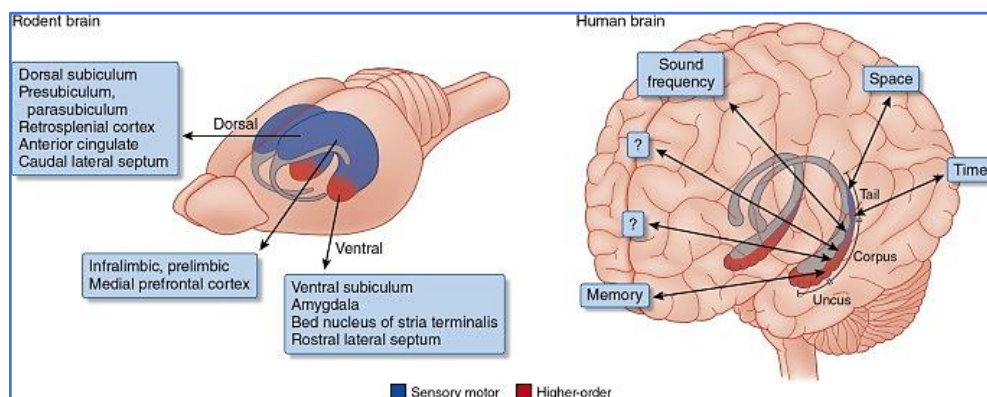


**Figure 9:** Parts of hippocampus influencing the memory as other cognitive abilities (Lisman et al., 2017)

On the basis of neuroanatomical and neurophysiological states, memory has often been categorized as short-term or long-term memory. Short-term memory is

dependent on the frontal and parietal lobe of the brain lasting from few seconds to minutes (Miller G.A., 1956). On the other hand, long-term memory quite unlimited in its storage capacities, owes much to the de novo protein synthesis and altered molecular components of the widely dispersed neuronal networks present within certain cortical areas which attribute to varied memory types.

Memory can also be categorized into declarative or imperative on the basis of the brain capacity of an individual to remember the facts and events in daily life. Declarative memory further can be subdivided into semantic and episodic memory, where context independent or dependent memory is stored respectively. Semantic memory which occur at much earlier stages or prior to AD shows the first sign of impaired language with faltered verbal fluency and naming (Verma et al., 2012). Hippocampus contributes primarily to the major consolidation of essential information to establish long-term memory from short-term making the storage of new memories impossible without it. Clinically neuropsychological testing batteries like the CERAD examination, the Mini-Mental State examination, and various other test constructs the clinical dementia rating scale, which asserts different aspects of memory over a wide range of multiple cognitive domains in comparison to healthy control individuals (Morris J.C., 1997; Morris et al., 1989). AD patients typically show multiple impaired cognitive profile coupled with a progressive decay in the working memory. Interestingly, nowadays memantine and other acetylcholinesterase inhibitors are prescribed to the patients with mild symptomatic AD enabling them to procure an increased attention and concentration (Parsons et al., 2013). The attention and working memory deficiency along with frontal subcortical circuits impairment also bring an impact on the functional execution in patients. AD subjects failed adequately in tests like Wisconsin Card Sorting Test, the Stroop test, that required organization,

problem management, or maintaining cognitive flexibility. Another analysis namely the Boston Naming test which assessed the potential to identify and name objects through spontaneous recognition to cue related response, was also verified as a test for AD (Jahn H., 2013). Other simple tests like the Clock Drawing test and Trail Making Test helps in checking the visuospatial and mental processing along with differential work switching among the AD patients.

Subjective cognitive misfunctioning devoid of any detectable memory deficit are no more regarded as “normal aging” because this underlying symptom could be a major risk factor for upcoming dementia in a subject (Jessen et al., 2010). Subjective cognitive impairment is a mild feeling of an individual of something not being in order, and may be regarded as a preclinical stage of AD (Jessen et al., 2006). Individuals having subjective memory problem showed similar AD gray matter pattern, and the degenerative decline in episodic memory was strongly associated with AD gray matter pattern with subjective memory impairment (Peter et al., 2014). Another major cognitive functioning occurring in early stages of AD apart from PD is losing the sense of smell or hyposmia (Peters et al., 2002). This phenomenon can be linked to the fact that entorhinal cortex is the first location where plaque formation starts and also the centre for smell processing lies here. A recent study involving the meta-analysis of multiple studies showed that AD and PD patients are far more faulty on odor identification and recognition tasks as compared to the odor detection threshold tasks. AD patients suffered impairment on higher order olfactory work involving certain cognitive processes (Rahayel et al., 2012). The degenerative neural network of the entorhinal cortex results in an impairment in the capacity of brain to store and recover different representations of smell.

Sporadic AD patients have been observed to show quite high impulse of seizures as compared to the control patients.<sup>1</sup> among 5 sporadic AD candidates displays minimum single apparent seizure during their condition, treatment being recommended on a mandatory basis. Since several mutations in the presenilin-1 gene are related with epilepsy, hence the occurrence of epileptic activity is suspected to be higher in the early-onset AD. Often AD patients display an oscillation in cognitive tasks such as disoriented episodic features of amnesic wandering which may primarily be caused due to undesired alteration in the epileptic activity of neuronal works. A possibility may be there of extreme  $\beta$ -amyloid deposition inducing the epileptiform activity, which in turn stimulates the compensatory inhibitory reaction to counteract the hyper excitability leading to an alteration in synaptic circuit in the temporal cortex (Palop and Mucke, 2009; Palop and Mucke, 2010). These progressive toxicity of the trans-synaptic network due to  $\beta$ -amyloid plaque burden causing the epileptic activity across entorhinal cortex to various brain regions may help in explaining the mechanism or feature of cognitive dysfunctions in AD (Harris et al., 2010).

## 4.1 Animal models in AD

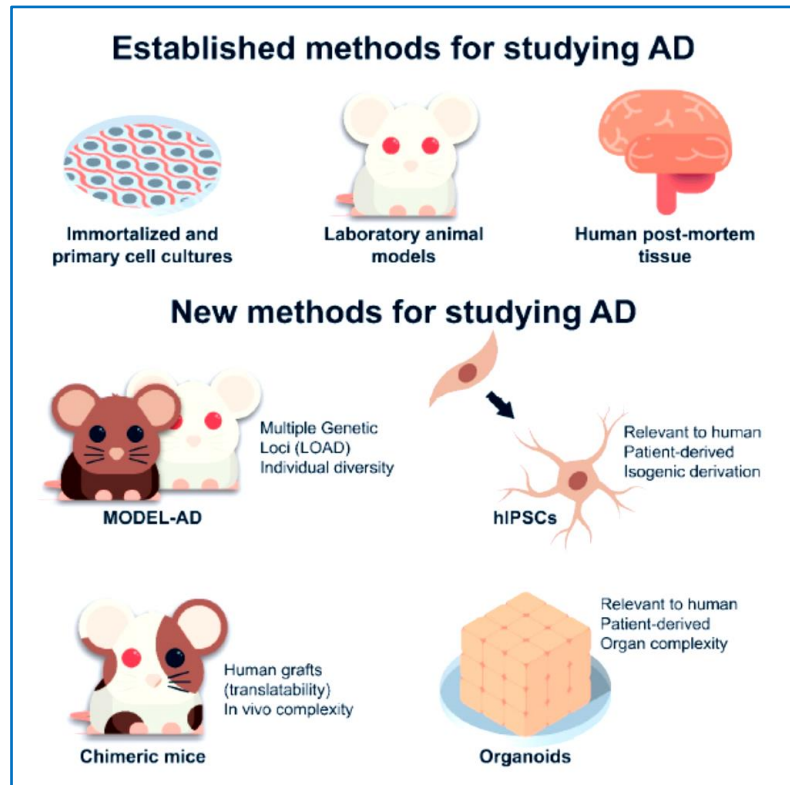


**Figure 10** : Various animal models to study the disease pathology in Alzheimer’s Disease (Spanos and Liddelw, 2020).

To find a therapeutic intervention and also with a sole purpose to mimic the AD system, animal models are often selected by the scientists and the clinicians, representing features of human mild cognitive impairment (MCI). Animals cannot complain about memory loss or how their daily life is difficult owing to dementia. Hence these models serve two essential purposes: (a) unraveling the underlying pathogenic mechanisms of a disease and (b) testing the possible new drugs to determine their therapeutic potential after which clinical trials may be performed. The ideal features of these animal subjects are primarily minute memory impairment owing to age along with light underlying neuropathological changes with altered

cholinergic system and may vary within the species used (DeCarli et al., 2001). Since AD is majorly characterized by cholinergic neuronal death of the forebrain, early experimental strategies were planned with animal models obtained the nucleus basalis destruction of the forebrain using neurotoxins (Pepeu G., 2001 ). However this resulted in establishing the MCI model of AD rat only. Later extensive studies showed that animals with lesion in the medial septal of brain exhibited better behavioral deficits similar to the earliest stages of AD (McDonald and Overmier, 1998). Finally, transgenic mice with excessively expressing  $\beta$ -amyloid ( $A\beta$ ) and presenilin 1, and aged monkeys are often used as models in AD research. The rats used in modelling the neurodegenerative disease may vary in species essentially like the Wistar rats, Sprague Dawley rats, Dark Agouti rats etc. Detailed research has been performed among the age group of all these young to adult group of rats to check their onset of disease.

The earliest and the most essential symptoms of MCI expressing the cognitive damage is the phenotypic memory loss (Petersen et al., 2001). To create such a model, initially anticholinergic agents like scopolamine was introduced into the animal subjects. But this essentially resulted in an “indiscriminate model” and further analysis failed utterly (Sarter et al.,1992). Also other pharmacological models of memory impairment obtained by blocking the NMDA–type receptors (Paoli et al.,1990) or administration of benzodiazepines (McNamara and Skelton,1992) were refrained from being entitled as an AD model for the features of MCI other than memory impairment were lacking here. Recently transgenic mice, overexpressing various genes like APP, presenilin etc. and having extensive amyloid- $\beta$  plaque burden have been engineered which has contributed essentially to the forthcoming research in AD. Passive avoidance study showed that 9 months old C57BL/6 were

more responsive to the study and memory loss as compared to the 3 months old mice (Dean et al.,1981). Similar case was reported when 10 months aged mice needed a higher number of trials to excel the T-maze task as compared to the 3-month-old mice. The cognitive impairment obtained by the tests revealed that ageing and inefficiency became progressively severe at 23 and 31 months of age (Sauer et al., 1999). Since transgenic mice with A $\beta$  deposits represent an AD model, it should also indicate a prodromal phase of the disease having MCI features. Investigation involving the loss in learning and memory correlated with aging and subsequent A $\beta$  plaque formation in PDAPP transgenic and control mice of varied ages showed that object recognition test in transgenic or wild-type mice was independent of its age (Chen et al., 2000). However, Morris maze test, explained that transgenic mice showed higher impairment of spatial memory linking a relationship between the A $\beta$  plaque burden and memory loss. Also in Transgenic model of Tg2576 mice which overexpressed human APP695 along with “Swedish” mutation, spatial memory faltering was observed by Morris water maze from 6 to 11 months age and it matched with the appearance of A $\beta$  (Westerman et al., 2002). Transgenic mice overexpressing mutant form of the human APP showed an initial cognitive impairment, along with A $\beta$  deposits, and cholinergic misfunctioning enabling it to be considered as a model of MCI. These have been the therapeutic model using vaccination, with a vision to reduce A $\beta$  deposition and retrieving subsequent memory loss (Janus et al., 2000; Morgan et al., 2000). All these work along with many others helped in demonstrating the potential role of transgenic mice in testing drugs as AD animal model.



## 5. Neuroprotection

### 5.1. Neuroprotection targeting signaling pathways

The main concept of neuroprotection in AD revolve around strategies to delay the onset or slowing down the progression of the same, primarily by trial to reduce the A $\beta$  plaque burden (Golde T., 2003 ; Selkoe and Schenk, 2003) or to bring down the overtly expressed neuroinflammatory reaction in system (Golde T., 2003; McGeer et al., 2002). Owing to the sufficient evidence indicating amyloid- $\beta$  accumulation to be a major cause for AD progression (Hardy & Selkoe, 2002), the primary strategies involving inhibition of the A $\beta$  generation, along with its clearance has been the promising steps taken by the scientists (Holtzman et al., 2002). However certain drawbacks escalate the therapeutic struggle. For instance, with A $\beta$  burden being several-fold above than those sufficient to cause maximum neural degeneration, heavy proportionate reduction in its level by any agent might never be sufficient to stall the degeneration. Secondly, the normal physiological role like that of anti-oxidation played by A $\beta$  (Smith et al., 2002) may be disrupted proving fatal to the system. Also only A $\beta$ -based therapies would definitely not be suffice to recover the damaged but still surviving neurons. Finally, even though massive evidence points to A $\beta$  accumulation as a primary player of sporadic AD, several other potential mechanisms might include important causative factors which may be synergistic towards disease degeneration (Yankner B.A., 2000 ).

Evidence show that A $\beta$  binding to multiple neuronal target receptors of neurotrophin p75, APP, RAGE and BBP-1 with higher affinity (Niikura et al., 2006) finally results in neuronal demise. Formation of Ca<sup>2+</sup>-permeable channels or modulation of K<sup>+</sup> channels are other receptor independent methods which can be modulated by A $\beta$  leading to degeneration of neurons (Tran et al., 2002). In these cases, using

compounds which inhibit the A $\beta$  binding procedure are being considered as a potent neuroprotective agent because they help in stopping the proximal stages of the detrimental signaling. However these approaches are sometimes limited owing to the fact that multiple targets of functional disruption might be active with the A $\beta$  introduction to a system. The ability of a selected small molecule to be able to apply neuroprotection by inhibiting such interactions solely depends on the depth of interaction between A $\beta$  and its target. So an alternative approach often taken here is to modulate the primary signaling pathways mediated by A $\beta$ .

Interestingly, studies of all AD models including the human, mice and in vitro systems emphasize on the stimulation of stress-influenced protein kinases, like c-JNK, MAPK, as critical players in the early onset of AD (Bozyczko-Coyne et al., 2001). JNK activation in cortical neuron often results in subsequent downstream activation of caspases followed by expression of several proapoptotic genes such as bax (Morishima et al., 2001; Fogarty et al., 2003). This has been validated in post mortem brain of AD patients (Shoji et al., 2000) also showing intraneuronal A $\beta$  congregation with tangle inclusions in entorhinal cortex (Pei et al., 2002; Savage et al., 2002). CEP-1347 is a compound that successfully inhibits stress kinase signaling resulting in partial blockage of neuronal degeneration (Harris et al., 2002).

Another neuroprotective target occurs with inhibiting GSK-3 $\beta$  which stimulates the accumulation of phosphorylated tau forming the neurofibrillary tangles causing disrupted microtubules and subsequent neuronal dysfunction (Trojanowski and Lee, 2002 ; Gozes I., 2002). It has been found that valproate and lithium often inhibit GSK-3 $\beta$  stabilizing and improving the mood of the subject (Loy and Tariot, 2002). Evidence that JNK contributes to tau phosphorylation suggests that inhibition of JNK activation might promote the parallel beneficial effects of inhibiting tau

phosphorylation along with cell death signaling (Yarza et al., 2016). The large number of kinases found to be capable of phosphorylating tau, including extracellular signal-regulated kinase (ERK) and cyclin-dependent kinase 5 (Cdk5), among others (Mazanetz et al., 2007) introduce a number of potential small molecule targets. The presence of multiple candidate targets raises the important questions of which kinases play a critical pathophysiological role in AD, and if more than one is involved, how many would have to be targeted to prevent pathological tau phosphorylation. Another neuroprotective approach considered in the aspect of microtubular study is the introduction of small molecules which could stabilize microtubules along with preventing the disruption of the cytoskeletal accompanied by toxicity (Michaelis et al., 2002)

## **5.2. Neuroprotection via inhibition of caspase activation**

Several observations have established the possibility of neurofibrillary tangles (NFT) associated caspases (Avila J., 2010 ) activated by upstream players like JNK, NF- $\kappa$ B, contributing widely to the resultant neurodegeneration in AD (Tare et al., 2011; Roth K.A., 2001 ). In vitro studies have shown that caspase inhibitors have helped in blocking A $\beta$ -induced cell death compromising the metabolism along with reduced glucose uptake and mitochondrial functioning (Fricker et al., 2013; D'Amelio et al., 2010). Also finding an association between the senile plaque formation and caspase activation during early onset of AD led the scientists to suggest that caspase contributes well to early along with the terminal steps of neuronal apoptosis (Cribbs et al., 2004 ). Minocycline which is a tetracycline-type antibiotic inhibiting caspases, is currently undergoing trials in AD (Metz et al., 2017).

### **5.3. Neuroprotection via activation of growth factor signaling**

In recent past multiple contributions of the growth factors and various ligands and peptides working in coordination with the receptors have been found to be neuroprotective against A $\beta$  toxicity. Neurotrophins like IGF-1 (Chen et al., 2019), FGF (Dordoe et al., 2021) and Humanin (Yen et al., 2018) regulate several extensive network of signaling which along with their receptors while undergoing degradation or malfunctioning contribute to the basic cause of neurodegenerative diseases. Neurotrophins like NGF and BDNF help in synaptic stabilization and functioning (Miranda et al., 2019; Latina et al., 2017). Neurotrophin signaling relates directly to the anomaly in core signaling, causing neuronal degeneration in AD. Neurotrophins like NGF and BDNF bind to TrkA and TrkB receptor expressed in hippocampal pyramidal neurons and layer V cortical neurons respectively (Pradhan et al., 2019), resulting in fundamental pathways, including PI3K/Akt kinase, MAPK and phospholipase C signaling (Matsumoto and Shimizu, 2013; Licznerski and Jonas, 2018). On activation, PI3K/Akt pathway downregulates two important players of JNK activation SEK1 and ASK1, which results in JNK suppression, finally inhibiting pro-apoptotic genes of Bcl-2 group. This as a result, activates CREB and I- $\kappa$ B kinase/NF- $\kappa$ B signaling which helps in neuronal survival and protection of the same against A $\beta$  toxicity (Snow and Albenzi, 2016; Ortega-Martínez S., 2015). NGF-induced MAP kinase activation prevents formation of multiple reaction oxygen species ROS (McCubrey et al., 2006). Multiple neurotrophins like “pro-NGF,” a precursor form of NGF, bind to p75NTR regulating the cell death and trophic status (De Nadai et al., 2016). The major pathways which are activated during the ligand-induced activation of p75NTR preventing neuronal death, are either PI3K/Akt pathway and/or NF- $\kappa$ B activation (Massa et al., 2006). Studies have shown that NGF

along with A $\beta$  up-regulates p75<sup>NTR</sup> expression in cultured E18 rat hippocampal neurons causing neurotoxicity (Culmsee et al., 2002). An early pathological event occurring in AD is most commonly the degeneration of the cholinergic neurons present in the basal forebrain along with other brain areas like the hippocampus, cortex and limbic region (Teipel et al., 2020 ). Strategies revolving around using acetylcholinesterase inhibitors (ACIs) and cholinergic agonists have often remained in focus to improve the cognitive and behavioral symptoms in AD. Recent clinical observations, complemented with apparent insight into reciprocal interactions between A $\beta$  generation and cholinergic neuronal functioning, imply that therapies depending on the cholinergic neurons might help in neuroprotection (Hempel et al., 2018; Maurer and Williams, 2017) . Current trials of ACIs are being performed on patients with mild cognitive impairment (MCI) which would help in determining their effort in delaying the disease progression. Several potential mechanisms which might take place with application of ACIs or cholinergic agonists have been found which by all means helps in reducing the disease progression (Colović et al., 2013). M1 muscarinic acetylcholine receptors otherwise known as mAChR are mainly found post-synaptically within the terminals of the cortical cholinergic neurons. This receptor activates protein kinase C (PKC) signaling, which results in increasing APP processing finally down-regulating A $\beta$  production (Kim et al., 2011; Talman et al., 2016). Besides reducing tau phosphorylation (Du et al., 2018), this signaling also confers neuroprotection by releasing neurotrophin (Hongpaisan et al., 2011). Since clinical trials by using M1 agonist have shown a significant reduction in A $\beta$  levels in CSF of AD patients (Hong-Qi et al., 2012), hence they have been included among the primary methods for the development of therapeutics with sufficient potency and receptor selectivity.

#### **5.4. Oxidative stress and antioxidant neuroprotective strategies**

An extensive search still continues about the massive role played by oxidative stress causing imbalance between the procurement and detoxification of products formed due to oxidative reaction (Pizzino et al., 2017). While limited accumulation of oxidation products is known in normal brain, yet with aging and progression of AD their levels increase substantially (Liguori et al., 2018). Enhanced levels of hydrogen peroxide and ROS like hydroxyl free radical and superoxide results in formation of lipid peroxides, advanced glycosylation end products (AGEs), and other oxidized proteins. All these cause anomaly in glutamate transport regulation leading to loss of critical enzyme functions, resulting in accumulation of toxic extracellular glutamate and loss of ion-transporting ATPases. These agents of neuroinflammation not only brings about disrupted calcium homeostasis but also provokes impaired mitochondrial function (de Oliveira et al., 2021). Neuroinflammation often causes oxidative stress which subsequently activates JNK caspases and other stress molecules (Mittal et al., 2014). However adding vitamin E to neuronal in vitro system attenuates protein oxidation, and JNK and p38 MAPK activation followed by the reduction in A $\beta$  toxicity (Gu et al., 2018). Studies using AD transgenic mice like Tg2576 revealed an enhanced peroxidation occurring much before the presence of detectable accumulated A $\beta$  and amyloid plaque formation (Boonruamkaew et al., 2017). Also, administration of well-known antioxidant curcumin to these subjects improved oxidative stress and amyloid pathology (Askarizadeh et al., 2020). Clioquinol (CQ), containing Cu/Zn-chelating properties, as shown in Tg2576 transgenic mice, is also considered a potent agent for obstructing the A $\beta$  accumulation causing decreased ROS production and improved cognitive score

(Grossi et al., 2009). Clinical trials are also being conducted though the results are yet to be published.

### **5.5. Modulation of NMDA receptor function**

Persistent depolarization caused due to the oxidative stress by A $\beta$  accumulation leads to NMDA receptor activation deleteriously increasing the intracellular Ca<sup>2+</sup> concentration (Danysz and Parsons, 2012). Reports have suggested that increased sensitivity to glutamate-induced excitotoxicity are visible in early stages of AD pathophysiology where glutamate uptake gets reduced in synaptosomes and glia (Sheldon and Robinson, 2007). These effects like increased glutamate release but lowered uptake, followed by neuronal vulnerability, along with derogatory feedback loop of excessive glutamate, causing enhanced depolarization indicates the role of A $\beta$  in neuroinflammation followed by excitotoxicity in AD (Harris et al., 1995). This led the scientists to suggest that modulating the glutamate receptors could be a potential neuroprotective strategy in AD. Memantine is an NMDA channel antagonist which blocks channel opening and neuronal death caused owing to the enhanced exposure to glutamate (Liu et al., 2019). Treatment of the same in A $\beta$  infused rats has shown an improvement in neuronal decay raising the possibility that memantine could be protective against A $\beta$ -induced degeneration (Martinez-Coria et al., 2010). Recently a clinical trial among AD and the control patients have also shown that after 26 weeks of memantine administration, an overall improvement in the daily living among the AD patients were evident (Reisberg et al., 2003 ).

Owing to various potential limitations of exclusive A $\beta$ -based therapies, neuroprotection via targeting multiple events occurring widely during the process, has been an essential parallel strategy against degenerative diseases like AD. Given the multiple layers of potential integration and the synaptic reinforcement conferred

by the nature of these processes, indispensability of the phenomenon assuring the clinical achievement owing to the modulation of the same could help in improving the onset or progression of the Alzheimer's Disease.

## **5.6 Therapeutic approach in AD**

Neurodegenerative diseases like AD require therapy not only for cure but also holistic management. AD being a multifactorial disease has directed a shift in the drug designing paradigms from single target approach (primarily amyloid-centric) to drug development targeting multiple aspects. In modern world with greater awareness and concern, preventive strategies at early onset of disease are prioritized from treating AD at later stages with advanced progression.

The primary concern of AD is often the accumulation of A $\beta$  across the hippocampus and cortical regions (Morris J.C., 2005), caused primarily due to APP cleavage by  $\beta$ -secretase and  $\gamma$ -secretase complex. So, modulating these enzymes to minimize A $\beta$  production has been a major focus for AD therapies. The development of  $\beta$ -site APP cleaving enzyme 1 (BACE1) inhibitors has shown promising efficacy at A $\beta$  reduction in animal models (May et al., 2015; May et al., 2011), clinical trial however being quite unsuccessful beyond phase II/III. Non-steroidal anti-inflammatory drugs or NSAIDs like R-flurbiprofen were the first among the  $\gamma$ -secretase modulators which showed a shift in A $\beta$  production from the aggregable form (A $\beta_{42}$ ) to a more soluble form (A $\beta_{38}$ ) (Weggen et al., 2001) in vitro and in vivo models, but in Phase III trial of mild AD subjects, they seemed to be a failure (Green et al., 2009).

Scientists across the globe have used several other non-selective  $\gamma$ -secretase inhibitors like Semagacestat, Gleevec, Avagacestat and Notch-sparing  $\gamma$ -secretase inhibitor pinitol (NIC5-15)(Lanz et al., 2010 ; Albright et al., 2013), which have been well appreciated in several animal and primary culture models. But unfortunately



they found an end to their fate over stage 2 clinical trials. Another method of drug targeting could be by accelerating the A $\beta$  clearance. Crenezumab, Gantenerumab, and Aducanumab targeted both soluble and aggregated A $\beta$  species (both oligomeric and fibrillar A $\beta$ ), are currently in Phase III trials in patients with prodromal, mild, and early AD, respectively (Sevigny et al., 2016).

Tau when hyperphosphorylated contributes to AD pathogenesis (Buée et al., 2000, Drechsel et al., 1992). Currently multiple Tau stabilizing and aggregation inhibitors are being developed and undergoing phase trials but the success seems quite far ahead till now (Bakota and Brandt, 2016). Inhibiting the action of GSK3 and CDK5 like kinases which cause hyper-phosphorylation of tau are also targeted to check the aggregation but not much advancement has been yet seen in the trials (Pei et al., 2008). Other approaches towards formation of a therapeutic model regarding the Tau based AD has been by limiting the tau acetylation in K280/K281 (Trzeciakiewicz et al., 2017) or by using the protein deacetylase SIRT1 (Min et al., 2018) to reduce the same. Immunotherapy has been studied worldwide contributing globally to prevent several diseases known. Several of such studies done by the clinicians have involved the use of vaccines like AADvac1 and ACI-35 in creating a phase such that active immunization may be checked against phospho-tau peptides which has proved to alter the tau pathology showing positive results in tauopathy or in AD mouse model and patients (Chukwu et al., 2018 ; Rajamohamedsait et al., 2017).

Malfunctioning of the synaptic machinery caused due to aging, toxic product accumulation resulting into neuroinflammation is extremely common in AD. Hence in addition to the extensive efforts given towards clinical trials involving amyloid and tau protein, several other strategies to ensure neuroprotection has also been under the scrutiny recently. Even though in AD therapeutics neurotrophins and several

other receptors have been a target for trials since long time (Malcangio and Lessmann, 2003 ; Sah et al., 2003), yet their inability to cross BBB and restrained ability to diffuse within the brain tissue has given rise to the need of exploring other methods like the gene transfer technology (Pardridge W.M., 2002). The pivotal strategy of therapies involving gene transfer mainly include developing small molecules which can inhibit the p75 and Tropomyosin Receptor Kinase A (TrkA) (Longo and Massa, 2013; *Massa et al., 2006*).

Wide number of studies complemented by extensive genetic study and network analysis has directed towards neuroinflammation which is a major event involving the glial activation occurring in degenerative diseases is neuroinflammation (Prokop et al., 2013; Zhang et al., 2013). Multiple strategies including reduction in cytokine production manipulating their respective genes such that their binding to the receptors may also be prevented, has often been designed with the help of molecules like minocycline (Garwood et al., 2010 ; Parachikova et al., 2010). In AD models, passive immunization by the usage of anti-A $\beta$  antibody (Wang et al., 2011), or anti-ApoE antibody (Kim et al., 2012) have also shown an increase in microglia recruitment near the plaque burden in the system. Also CX3CR1 receptor has contributed in forming the microglial barrier bear amyloid plaques (Condello et al., 2015). All these have contributed in reducing plaque load to further regulate neuroinflammation in the disease (Lee et al., 2010 ; Liu et al., 2010).

Many a times improving the declining cognitive symptoms has been attempted by using drug like memantine which inhibits the overtly excited NMDA receptors preventing the glutamate release, causing a reduction in neurotoxicity (Johnson and Kotermanski, 2010). Also Acetyl cholinesterase inhibitors namely Namzaric have also known to decrease the acetylcholine degeneration which are produced by the

cholinergic neurons, resulting in an excessive synaptic transmission bringing a major alteration in the synaptic signaling functioning (Buckley and Salpeter, 2015). Therapies involving the synaptic function modulators like protein kinase C (PKC- $\xi$ ) activators, inhibitors of Fyn kinase and phosphodiesterase (PDE) inhibitors have been common recently. Bryostatin has been found to reduce PKC- $\xi$  activity improving impaired synaptic and cognitive functioning in AD models (*Hongpaisan et al., 2011*). Moreover, Fyn kinase has often been correlated to synaptic functioning by regulating trafficking of the NMDA glutamate receptor subunits NR2A and NR2B (Prybylowski et al., 2005) and AD pathogenesis. Transgenic mice developed with Fyn deficiency showed blunt long-term potentiation (LTP) and damaged contextual fear memory functioning (Nakazawa et al., 2001). A preclinical study suggested that saracatinib (AZD0530), which is a Src family kinase inhibitor, having substantial potency for Fyn and Src kinase, prevented synaptic dysfunction along with impaired spatial memory AD transgenic mice (Kaufman et al., 2015).

With advancement in AD research, the deep knowledge of underlying mechanism of AD pathogenesis will guide the drug development effort for the cause in future. Since a couple of decades, it has been seen that amyloid is definitely not the sole agent to be targeted for therapeutic purpose. Combination therapy is also essential in neurodegenerative disease like AD. Biomarkers have been established increasingly to diagnose the preclinical AD (Bateman et al., 2012). Recent failures of multiple AD clinical trials have indicate that after AD progressing to a certain level, neurodegeneration takes an irreversible path and the aberrant neuronal network fails to be repaired by reduction of amyloid burden or oxidative stress only. Currently efforts are being made to prevent AD at an early onset (Hsu and Marshall., 2017; Panza et al., 2014).

**OBJECTIVE**

Alzheimer's Disease is arguably one of the most fearsome neurodegenerative diseases affecting people all over the world. Not only the main hallmark of the disease pathology concerns around the inevitable neuronal degeneration but also glial activation is another key symphony which synchronizes the whole disease physiology. Astrocytes are known to modulate various chemical transmissions causing interaction with the neurons , along with formation of various tripartite synapses in the process affecting global synaptic plasticity. The ability of glial cells to respond actively to A $\beta$  has been well established since long, however its beneficial and detrimental role has been a topic of debate ever since.

Astrocytes are known to perform a number of functions like restricting glutamic uptake, synaptogenesis, release of various neurotransmitters and antioxidants. Several recent investigations have disclosed the fact that a wide intercellular communication between astroglia and neurons contribute to the homeostatic maintenance of the milieu. Also, various proteins and chemokines travel across these cells resulting in various pro- and anti-inflammatory signaling process. Reports also suggest that an initial protective role is played by astrocytes towards neuronal rescue from death upon A $\beta$  exposure with the help of several secretary agents. Searching for a wide perspective in role of astrocyte being neuroprotective in AD and to assess the specific role of certain cytokines secreted from the same in restoring homeostasis even in presence of A $\beta$ , the major objectives of our work include :

## **Chapter 1:**

- ✓ Identifying certain signaling pathways involved in astrocyte activation

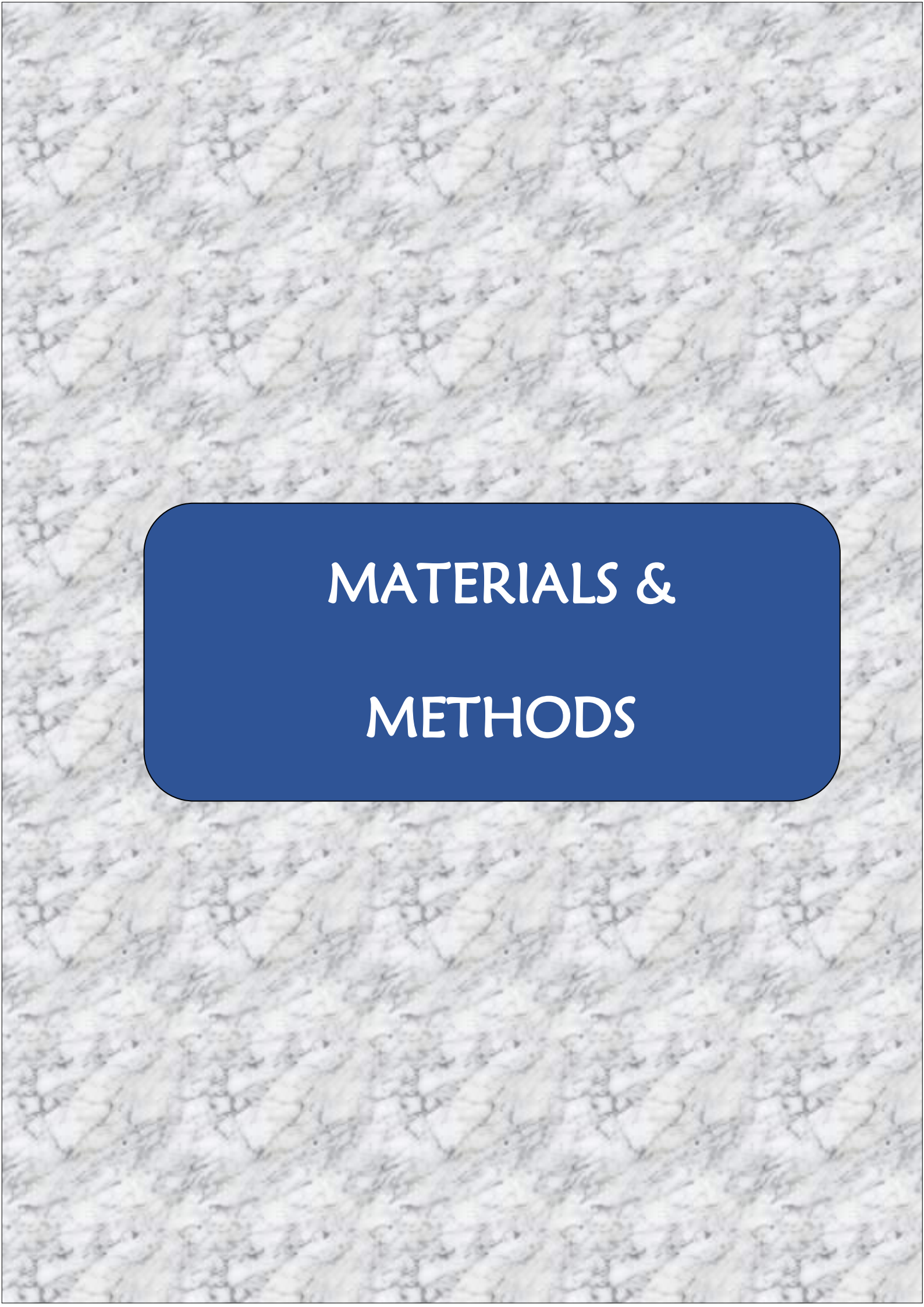
- ✓ Profiling of cytokines and identification of neuroprotective secretory proteins in primary astrocytes upon A $\beta$  treatment
- ✓ Neuroprotection offered by Astrocyte Conditioned Medium while in exposure to A $\beta$
- ✓ Translational and secretory status of sICAM-1 and its role played in neuroprotection in in vitro.

## **Chapter 2:**

- ✓ Investigating the importance of ICAM-1 in improving cellular health and A $\beta$  plaque load reduction in A $\beta$  infused models of AD.
- ✓ Unraveling the role of ICAM-1 in improving cognitive functioning in cortical and hippocampus infused A $\beta$  rat model.

## **Chapter 3:**

- ✓ To determine the role of ICAM-1 in reducing A $\beta$  plaque load and cell death in 5xFAD transgenic AD model.
- ✓ To recognize the role of ICAM-1 in improving cognitive and memory functioning in 5xFAD mice.
- ✓ Deciphering the underlying mechanism involved in neuronal protection rendered by ICAM-1 both in vitro and in vivo.
- ✓ To determine the effect of NF- $\kappa$ B inhibition on cognition and memory in 5xFAD mice.



**MATERIALS &  
METHODS**

## **2. Materials and methods**

Cell culture medium Dulbecco's modified Eagle's medium (DMEM), DMEM-F12, Foetal Bovine Serum (FBS), Penicillin-Streptomycin, Neurobasal medium (GIBCO) which was supplemented with B27 purchased from Thermo Fisher Scientific (Waltham, MA, USA). Essentials for neuronal culture, like Poly-D-lysine, apo-transferrin, insulin, progesterone, putrescine, selenium were purchased from Sigma-Aldrich (St.Louis, MO,USA). Hoechst stain was provided by Invitrogen. A $\beta_{1-42}$  was purchased from American Peptide (Sunnyvale, CA, USA) and Alexotech (Umea, Vasterbotten County, Sweden). DMSO, paraformaldehyde (PFA), 1,1,1,3,3,3 hexafluoro-2-propanol (HFIP), GFAP & Actin antibodies and NF- $\kappa$ B inhibitor PDTC were supplied by Sigma-Aldric (St.Louis, MO, USA). Rat recombinant ICAM-1 were purchased from Novus Biologicals (CO, USA). MAP2 and neprilysin antibodies were supplied by SantaCruz Biotechnology (Santa Cruz, CA, USA). NF- $\kappa$ B, Bcl-2, Bcl-xL and PARP antibodies were purchased from Cell Signaling Technology (Danvers, MA, USA). Bim and A $\beta_{1-42}$  antibodies were purchased from Abcam (Cambridge, UK). ECL reagent and polyvinylidenedifluoride (PVDF) membrane were purchased from GE Healthcare (Buckinghamshire, UK). Sodium dodecyl sulphate (SDS) was purchased from Merck (Darmstadt, Germany). Trypsin and Bovine Serum Albumin (BSA) were purchased from Sisco Research Laboratories Pvt. Ltd (Mumbai, India). All other fine chemicals were procured from standard local suppliers

### **2.1. Primary astrocyte culture**

Primary astrocytes were cultured following the protocol that has been described earlier (Garwood et al., 2011; Saha & Biswas, 2015). Briefly, whole brain from 0-1 day aged Sprague Dawley rat pups were extracted followed by removing the



meninges carefully. Cortical area of the brain was subjected to trypsinization at 37°C for 30 min after which a careful trituration of the trypsinized brain tissue was performed in DMEM+10%FBS. It was then passed through fine nylon mesh to avoid tissue clumps and the single cell suspension was plated on a poly-D-lysine (PDL) (0.1mg/ml) coated plate allowing it to be in plate for 2–3 min such that the preferential sticking of neurons may occur. Next the astrocyte enriched cell suspension was harvested by centrifugation for 5 min at 1200 rpm. Resuspension of the cells was done in fresh medium and seeded at a density of 1.3 million/35 mm or 0.45 million/well of a 24-well PDL coated plates. Cells were maintained for 14 days at 37°C in 5% CO<sub>2</sub> incubator for maturation with occasional change to medium until the treatment which was given on 13DIV.

## **2.2. Primary neuron culture**

Primary neuron culture was followed from the method described earlier (Park et al.,1998). Briefly, neocortical tissues from E18 rodent embryos were dissected and triturated aseptically with Pasteur pipette. Triturated cell suspension was centrifuged for 5 min at 1200 rpm and the harvested cells were resuspended in fresh complete neuronal medium. The cells were plated at a seeding density of 1 million/well of 24 well and 3 million/35mm PDL coated plates and maintained in DMEM/F12 medium supplemented with insulin (25µg/ml), glucose (6mg/ml), apo-transferrin (100µg/ml), progesterone (20nM), putrescine (60µM) and selenium (30nM), 1% pen-strep. The cells were provided with neurobasal medium supplemented with B-27 for 4 days before the treatment. The neurons were treated with oligomeric A $\beta$ <sub>1–42</sub> on 5 DIV

### **2.3 Astrocyte-neuron coculture**

Astrocyte-neuron coculture was done by transferring astrocyte conditioned medium (ACM) from multiple treated conditions to primary cultured neurons (Nagai et al., 2007).

### **2.4. Preparation of A $\beta$ <sub>1-42</sub> oligomers**

100% HFIP was used as a solvent to reconstitute the lyophilized A $\beta$ <sub>1-42</sub> peptide to a final concentration of 1mM. This was followed by a vacuum centrifugation in a speed vac (Eppendorf, Hamburg, Germany). The A $\beta$ <sub>1-42</sub> pellet was resuspended in DMSO to obtain a 5mM solution after which sonication was done for 10min at 37°C. It was then diluted in sterile phosphate-buffered saline (PBS: NaCl-137mmole/L, KCL-2.7mmole/L, Na<sub>2</sub>HPO<sub>4</sub>-10mmole/L, KH<sub>2</sub>PO<sub>4</sub>-2mmole/L, pH7.2) and SDS (0.2%) to a concentration of 400 $\mu$ M. This solution was incubated for 6h-18 h at 37°C and a final concentration of 100  $\mu$ M was achieved by adding PBS to it followed by incubation for 18–24h at 37 °C prior to treatment. SDS–polyacrylamide gel electrophoresis (SDS-PAGE) followed by Sypro Ruby stain was done to confirm the oligomeric conformation of A $\beta$ <sub>1-42</sub> which was described before (*Saha & Biswas, 2015*).

### **2.5. Treatments on cells**

Mature astrocyte was maintained in DMEM-FBS for 13 days and treated with sera free DMEM/F-12 overnight. To remove the previous FBS including cytokine and growth factors multiple washes was given before the treatment with same medium. 14DIV mature astrocytes were treated with 41.5 $\mu$ M A $\beta$ <sub>1-42</sub> at various time points. Matured cultures were treated with ICAM-1 neutralizing antibody (Novus Biochemicals, USA) at 4 $\mu$ g/ml concentration. Cortical neurons were treated with

1.5 $\mu$ M A $\beta$  for 24h, both in presence and absence of rat recombinant ICAM-1 protein (rrICAM-1)(R&D systems, USA) at 50 ng/ml for 24h. Neurons were further treated with astrocyte conditioned medium (ACM) as indicated in the result sections.

### **2.6. Cytokine array**

sICAM-1 level within the ACM was analyzed by cytokine array kit (R&D systems) maintaining the manufacturer's instructions. In short, array membranes were incubated for 1h at RT in blocking buffer provided. After mixing with reconstituted detection antibody cocktails, samples were then incubated on the membranes overnight at 4°C on platform shaker. All of the following steps were performed at RT, and all wash procedures involved three washes with 1x wash buffer for 10 min. After incubation with detection antibody, membranes were washed and incubated with streptavidin-conjugated horseradish peroxidase (1:2000) for 30min. Unbound reagents were removed by washing and the membranes were incubated in chemiluminescent detection reagents for 1 min. The chemiluminescent signal on each membrane was captured in UVP Bio-Imager 600, system equipped with Vision Works Life Science software (UVP) V6.80. The intensity (pixel density) of each spot on membrane was quantified using NIH-Image J software (National Institutes of Health, Bethesda, MD, USA) and normalized to the membrane's positive control.

### **2.7. Cell viability assay**

Trypan blue was used as the counting method. After being washed with PBS twice, the cells, with or without treatment, were collected and centrifuged at 1900xg for 5 min and resuspended in PBS. 10  $\mu$ l of cell suspension was mixed with equal volume of 0.4% Trypan blue solution and the mix was checked in hemocytometer under light

microscope. The live cells which did not take up the dye were counted and the percentage (%) of live cells in the experimental samples was obtained as compared to the control cell number.

## **2.8. ELISA**

Quantitative Sandwich Enzyme Linked Immunosorbent Assay (ELISA) was performed to quantify the amount of sICAM-1 secreted from A $\beta$ <sub>1-42</sub> treated astrocyte in ACM using a kit (R&D systems, Minneapolis, USA). As per manufacturers protocol, collected ACM from treated and control astrocytes were centrifuged at 900xg for 5 minutes to remove the debris and they were added to the microplate which was precoated with rat sICAM-1 specific antibody. Several washing was done by the buffer provided in the kit to remove the excess unattached substances, after which the enzyme-linked polyclonal antibody specific for rat sICAM-1 was added. This was followed by washing to ensure the removal of excess free antibody-enzyme complex. In the next step the substrate solution was added to the wells and kept in the dark. This incubation was followed by the addition of stop solution that turns the blue solution into yellow. The colour intensity was measured spectrophotometrically at 450 nm, and the amount of sICAM-1 in the medium was determined from standard curve.

## **2.9. Western blot**

Western blotting was done with lysed cells. After treatment, PBS was used to wash the cells thoroughly, further collecting them post centrifugation at 900g at 4°C for 5min. Protein was extracted by Lysis buffer (10 mM Tris pH 7.4, 150 mM NaCl, 1% Triton X-100, 0.5% NP-40, 1mM EDTA, 1mM EGTA, 20mM NaF, 0.2mM

Orthovanadate, Protease Inhibitors) after centrifugation at 14000g for 15min and quantification was done by Bradford method.

Regarding preparation of the brain samples, RIPA also known as the radioimmunoprecipitation assay buffer (50 mM Tris- HCl, 1 mM EDTA, 150 mM NaCl, 1% Nonidet P-40, 0.25% sodium deoxycholate, protease inhibitor) was used to extract protein from brain following the similar protocol as mentioned above. 40µg protein was loaded in SDS–PAGE gel and after separation they were transferred onto PVDF membrane. Probing was done with the desired primary antibodies overnight at 4°C, after the membrane being blocked with 5% BSA for 1h at RT. The primary antibodies used are as follows: GFAP (1:2000, Sigma-Aldrich), ICAM-1 (1:500,Novus), Actin (1:20000, Sigma-Aldrich), NF-κB (1:1000), Bim (1:1000), Bcl-2 (1:1000), Bcl-xL (1:1000), PARP (1:1000), for overnight at 4°C. Next, HRP-conjugated secondary antibodies were used with respect to the corresponding primary antibody. Repeated washing was done by the Tris Buffer Saline-T (TBST) buffer after which detection was done by Amersham ECL detection reagent. The protein band was detected with UVP BiImager 600, system equipped with Vision Works Life Science software (UVP) V6.80. The intensity (pixel density) of each band on membrane was quantified using NIH-Image J software, and corrected for background intensity and normalized to the loading control band intensity.

### **2.10. Immunocytochemistry**

Immunocytochemistry was performed following the methods described previously (Biswas et al., 2005). 4% Paraformaldehyde (PFA) was used to fix the primary neurons for 10 min at RT following which a couple of thorough PBS washes was done for removing the excess PFA. To ensure proper permeabilization and blocking

of the cells, samples were incubated in 3% goat serum, 0.3% Triton X-100 in PBS for almost about 1hr. After this the cells were incubated with MAP2 (1:50) antibodies overnight at 4°C and species specific secondary antibodies Alexafluor 546 was used for 45min at RT. Nucleus was stained by Hoechst 33342 solution (Molecular Probes, Invitrogen, MA, USA), concentration being used 1µg/ml in PBS solution for 30min at RT. Images were captured in LeicaCTR4000 Fluorescence Microscope (Wetzlar, Germany) at 20x or higher magnification.

### **2.11. Sholl Analysis**

The dendritic arborization of the primary neurons post treatment was measured by Sholl analysis with NIH-ImageJ software (Sholl D.A., 1953; Cuesto et al., 2011; Sanphui and Biswas, 2013). Control and treated primary cortical neurons were immuno-stained with MAP2 antibody and images were taken at low magnification. With Image J, magnification of selected images were done followed by tracing the processes. Several concentric circles were drawn from the cell body with increase in radius by 10µm. A 2-D analysis was done where the number of intersecting points was calculated at each concentric circle. Data have been represented as the mean  $\pm$  S.E.M. of five neurons from three independent experiments.

### **2.12. Animal housing and care**

Equal population of adult male and female Sprague Dawley rats weighing on average between 270-330 g and 5xFAD transgenic mice (purchased from Jackson Laboratory), both male and female with an average body weight between 25 g and 30 g were kept in maximum three per cage in a room providing food and water to ad-libitum and temperature being controlled around 25°C and humidity 65%. A 12h light-

dark cycle was ensured in the animal house of CSIR-Indian Institute of Chemical Biology, Kolkata. Those littermates which are non-transgenic in nature were marked as “WT” and housed similarly as 5xFAD mice. All studies were conducted in accordance with the guidelines formulated by the Committee for the Purpose of Control and Supervision of Experiments on Animals (Animal Welfare Divisions, Ministry of Environments and Forests, Govt. of India) with approval from the Institutional Animal Ethics Committee (IAEC).

### **2.13. Brain stereotaxic surgery**

Before performing the surgery, Sprague-Dawley rats (300–380g) were anesthetized with 50mg/kg sodium thiopentone (Thiosol, Neon laboratories, Mumbai, India) intraperitoneally (I.P.) in 0.9% normal saline (Paidy et al., 2015). The animals were then kept on the stereotaxic frame (Stoelting, MO, USA) and infusion was done with Hamilton syringe positioned on the frame after placing of the incision bar precisely at the Bregma point. To manage the post-operative trauma, homeothermic blanket was applied to maintain the body temperature at 37°C (Harvard apparatus, U.K.). The infusion in the brain cortex and hippocampus was performed bilaterally with oligomeric A $\beta$ <sub>1-42</sub> at an amount of 2.25  $\mu$ g in 5  $\mu$ l in each hemisphere. Cortical infusion was done with the bregma co-ordinates being AP:4.1, L:2.5, DV:1.3mm on both sides of brain. For hippocampus at CA1 region, the stereotaxic co-ordinates from bregma were : AP: 3.6, L: 2.1, DV: 2.8 mm, according to the rat brain atlas. The flow rate of the working syringe pump was 0.5  $\mu$ l/min (BAS, West Lafayette, USA) and diffusion of A $\beta$  was allowed for an excess 5 min post- delivery. PBS was infused bilaterally in the control animals in similar way. Furthermore, among them a cohort of rats, PBS and A $\beta$  infused were treated with rrlCAM-1 at 0.25 $\mu$ g/kg b.w. and 0.5 $\mu$ g/kg

b.w after 11 days (5 doses alternately on each day) until sacrifice after 21 days. The brain tissues of the respective animals were taken and processed for protein preparation. To perform immunohistochemistry studies, the brains were collected after cardiac perfusion, and fixed in 4% PFA for 24h. They were then incubated in a 30% sucrose solution for another 24h before proceeding for cryo-sectioning. 20µm sections of the brain were taken in cryotome (Thermo, West Palm Beach, FL, USA).

#### **2.14. Congo Red Staining**

21 days post infusion (DPI), the control and the treated animals were subjected to anesthesia with Urethane (1g/kg b.w.) followed by transcardial perfusion with 50 mL of cold 100 mM potassium phosphate buffer at pH 7.4 followed by 50 mL of 4% (w/v) PFA. The brains were dissected out and kept in 4% PFA overnight for fixation after which they were kept in 30% (w/v) sucrose, at 4°C for cryoprotection. 20µm thick hippocampal sections were cut using cryotome (Thermo Shandon, Pittsburgh, PA, USA), and collected on gelatin-coated slides for histological staining. Congo red staining was performed with Accustain® amyloid stain-Congo red kit (Sigma-Aldrich). Initially sections were stained with haematoxylin dye for 60-90 seconds, followed by a rinsing process of slides in slow running tap water. Then the sections were covered with alkaline NaCl solution for 20 min after which the Congo red stain was applied for 20 min. Finally sections were washed with absolute ethanol thrice, followed by xylene and individual sections were mounted on coverslips with Dibutylphthalate Polyesterene Xylene (DPX).



## **2.15. Immunohistochemistry**

21 days post A $\beta$  infusion, animals were anesthetized with urethane and perfused with 4% (w/v) PFA. The brain was dissected out and fixed in 4% PFA overnight at 4°C. This was followed by immersion of the same in 30% (w/v) sucrose solution in PBS at 4°C. 20  $\mu$ m thick sections were obtained using cryotome (Thermo Shandon, Pittsburgh, PA, USA), and collected on gelatin-coated slides. The process of immunofluorescence involved three rounds of initial washing with PBS after which permeabilization was done with PBS + 0.4% Triton-X for 40 min. Then repeated washing of the sections with PBS + 0.1% Triton-X was done for 5 min each. After that, the samples were blocked using 4% BSA in 0.1% PBST for 1 h. Primary antibodies used include A $\beta$ <sub>1-42</sub> (1:100), ICAM-1 (1:100), GFAP (1:50), Neprilysin (1:50), NF- $\kappa$ B(1:100). The sections were subjected to primary antibody solution diluted in blocking solution, for 48h at 4°C. The sections were washed with PBST (0.1%) thrice to remove the excess unbound antibody. The secondary antibodies, Alexafluor-tagged were used to incubate the sections at RT for further 2hr. Finally Hoechst 33342 was used to stain the nuclei for 30min at 37°C, followed by three times rinsing with PBS and mounting them with Prolong Gold Antifade with DAPI (Thermo Fisher Scientific, Waltham, MA, USA) for further microscopic analysis. 5x and 20x magnification images were captured through Leica CTR4000 Fluorescence Microscope (Wetzlar, Germany). Leica DMI6000 B inverted microscope equipped with Plan Apo100x/1.40 oil objective (Leica TCS SP8 confocal system) was used for 40x magnification images. A $\beta$ <sub>1-42</sub> labeled plaques were analyzed quantitatively by calculating a percentage of plaque area or number of plaques by NIH-ImageJ software. The corrected total cell fluorescence (CTCF) was calculated by including integrated density of staining, area of the cell, and the background fluorescence of

different experimental conditions by ImageJ software. CTCF = Integrated density-(area of selected cell × mean fluorescence of background value).

For DAB (Diamino benzidine) staining, tissue sections were subjected to quenching by the quenching buffer (methanol and H<sub>2</sub>O<sub>2</sub>), followed by washing with phosphate buffer saline. Then the tissues were blocked with 4% BSA, followed by an overnight incubation of the same in primary antibody at 4°C. Next day, the tissues were washed and incubated with HRP-conjugated secondary antibodies against the primary antibodies for 1.30 h. Counter staining was done with 0.1% cresyl violet followed by washing process of the tissue. After drying the tissue overnight, it was dehydrated in gradients of ethanol and finally mounted with DPX. The images were taken in light microscope (Leica DM2500, Wetzler, Germany)

### ***2.16. Terminal deoxynucleotidyl transferase dUTP nick end labeling (TUNEL) staining***

Apoptotic cell death in the PFA perfused brain sections were evaluated with terminal deoxynucleotidyl transferase-mediated dUTP nick end-labeling (TUNEL) staining using a TMR red *in situ* cell death detection kit (Roche, Indianapolis, IN) and Clontech Apo Alert DNA Fragmentation kit (Takara, Kusatsu, Shiga, Japan) according to the manufacturer's protocol. Firstly, washing of the sections were done with Phosphate Buffer Saline after which the sections were subjected to digestion by Proteinase K solution (20 µg/ml) for around 20 min. 4% PFA was given on them to bring about stoppage to the reaction. The tissues were rewashed in PBS and equilibrated in buffer at RT for 10 min. The experimental samples were then incubated in the nucleotide mix and Tdt enzyme solution in equilibration buffer for 1h at 37°C in absence of light. 2x SSC buffer was used to bring halt to the tailing

reaction at RT for 15 min and PBS washing was done to the samples. Following this, nuclei were stained with Hoechst 33342 for 30 min at 37°C and finally washed twice with PBS before mounting with Prolong Gold Antifade with DAPI for microscopy analysis. TUNEL images were captured through Leica CTR4000 Fluorescence Microscope. The percentage of apoptotic cells were calculated by dividing the number of TUNEL-positive cells with the total number of cells (Hoechst stained nuclei) multiplied by 100. Negative controls were evaluated by using all reagents except terminal transferase.

### 2.17. Behavioral Studies in AD model

To evaluate the cognitive deficits and their recovery with ICAM-1, A $\beta$ -infused rats and 5xFAD mice from various groups (Table 1, Table 2 ) were assessed sequentially by open-field or locomotion test, novel object recognition test, elevated plus maze test, passive avoidance test and fear conditioning tests as per the schedule indicated below:

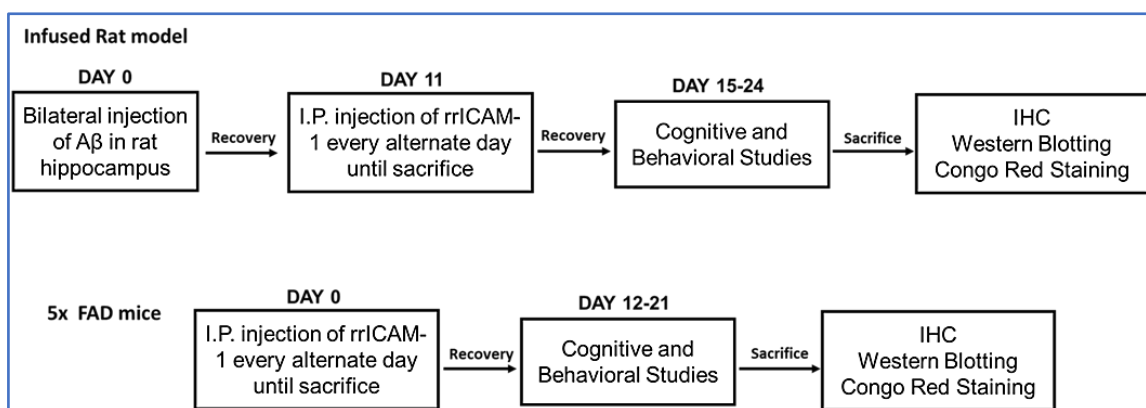


**Table 1A: Total number of rats involved in cognitive experiments**

Cognitive tests	Experimental Animal Groups				
	PBS	ICAM-1	A $\beta$	A $\beta$ +ICAM-1(0.25 $\mu$ g)	A $\beta$ +ICAM-1(0.5 $\mu$ g)
Open Field Test	4	4	6	6	4
Elevated plus maze(Cognition)	6	4	6	6	6
Novel object recognition	4	4	6	6	4
Passive Avoidance	6	4	4	6	6
Contextual Fear conditioning	6	4	6	6	6

**Table 1B: Total number of mice involved in cognitive experiments**

Cognitive tests	Experimental Animal Groups				
	WT	ICAM-1	5xFAD	5xFAD+ICAM-1(0.5 $\mu$ g)	5xFAD+ICAM-1(1 $\mu$ g)
Open Field Test	8	6	8	8	6
Elevated plus maze(Cognition)	8	6	10	8	10
Elevated plus maze(Anxiety)	4	4	4	4	6
Novel object recognition	6	6	8	6	8
Contextual Fear conditioning	10	4	8	8	10
Cue dependent fear conditioning (Single trial)	6	6	10	10	8
Cue dependent fear conditioning (multi trial trial)	6	6	8	8	8

**Table 1C: Total number of mice involved in cognitive experiments**

<b>Experimental Animal Groups</b>				
<b>Cognitive tests</b>	<b>WT</b>	<b>PDTC</b>	<b>5xFAD</b>	<b>5xFAD+PDTC</b>
<b>Open Field Test</b>	4	8	8	8
<b>Elevated plus maze(Cognition)</b>	8	12	12	12
<b>Novel object recognition</b>	8	6	10	8
<b>Cue dependent fear conditioning (Single trial)</b>	6	6	10	10
<b>Cue dependent fear conditioning (multi trial trial)</b>	6	6	8	8

### **2.17a. Open Field Test (OFT)**

The open field test involves the understanding of the general activity and exploratory behavior in rodents (Crusio W.E., 2001). On the first day each of the subjects i.e. A $\beta$ -infused rats or 5xFAD mice were placed on an empty plexiglass arena sized 40cm x 40cm x 40cm (IR Actimeter Panlab, Barcelona, Spain). They consisted of the photocell emitters and receptors equally placed along the perimeter which builds a grid of invisible infrared rays. Animals placed here while moving caused beam breaks and subsequently data were recorded and analyzed by the analyzer. The rodents were allowed to explore the arena for 10 min under dim lighting and the distances travelled by rats were determined. The %centre distance covered depicts the % of area travelled by subjects in the central grid of the arena, keeping the total distance covered within the arena as 100%. The positions of the rodents were tracked using custom PANLAB scripts (ActiTrack Software). A portion of videos were generated by the machine to verify accuracy.

### **2.17b. Elevated plus maze (EPM) test**

Another essential tool used to assess the cognitive capability and memory in experimental subjects was elevated plus-maze. The maze consists of an apparatus with two open arms each measuring 50 x 10 cm, with a very small, 1 cm-wall in between, and 60 cm high from the floor. To prevent the rodents from falling off the edge during the experiment, the whole apparatus is provided with a 1 cm high plywood edge surrounding the open arms. Perpendicular to the open arms, closed arms of similar dimensions but with tall walls, 50 cm each are also found. On the acquisition day, the subject was placed on the open arm facing away from the center and the initial transfer latency (ITL) i.e time taken by subject to move from the open to the closed arm was recorded. The time taken by the same animal, on the following probe day to move from open to the closed arm is noted as retention transfer latency (RTL). The maximum duration for which the trial took place was 300 sec.

### **2.17c. Novel object recognition (NOR) test**

The Novel object recognition test is a primary task to decide the innovative exploration and memory formation in rodents assessed by the index of differentiation and preference. The basic principle here involves the subjects preferring a novel object in comparison to a familiar one within an arena (Ennaceur A., 2010). Habituation, familiarization, and test phase are the major determining steps of this protocol. Firstly rodents are placed in the open field for 5 minutes. Next in familiarization phase, the subject kept in front of two objects which have the same diameter, color and length such that they could explore both within an arena (50 cm

x 35 cm x 40 cm for rats and 40 cm x 30 cm x 40 cm for mice) for 10 min. On probing day, one of the objects were replaced by another object different in shape and color and the animals were exposed it (Hammond et al., 2004) for 5min. The time duration employed by the animals in exploring each of the objects on test day or second day was calculated and designated as TN and TF for the novel and familiar objects respectively. Discrimination index (DI) and preference index (PI) were derived according to the formulas:  $DI = (TN - TF)/(TN + TF)$ ,  $PI = TN/(TN + TF) \times 100$  (Janus et al., 2000; Antunes & Biala, 2012).

#### **2.17d. Passive avoidance test**

The Passive avoidance test recognizes the short term fear learning and memory by exploiting natural trait of rats to prefer darker venue over lit up one. The system consists of two identical chambers one having light and another being dark (25 x 25 x 20 cm), which are compartmentalized by a guillotine door (SHUTTLEBOX, Panlab, Barcelona, Spain). The acclimatization of the individual animal was done for 5 min in closed door condition. On the acquisition day, the animals were kept in light chamber so that it would enter dark chamber by its innate nature. On entering the room, 0.8mA of foot shock was applied to them which compelled them to come back to the other room. To verify their potential learning memory, during the probe test next these were kept in the light chamber in the same condition. Those showing maximum response latency while remembering not enter the dark chamber were marked to be well trained for passive avoidance test. The wait latency was recorded in the SHUTAVOID software. Threshold time of 300 seconds on the acquisition phase for entering of the animals in to the dark chamber determined their efficiency

on training. The animals taking less than 5 min to enter the dark chamber were considered efficient as test subjects (Mc Gaugh et al., 1996).

### **2.17e. Fear conditioning tests**

Fear conditioning tests has been a popular devise which enables us to rightly determine the efficacy of the subjects in hippocampal dependent associative cognitive learning and amygdala based memory and recognition (Fanselow and Tighe, 1980).The study involves experimental subjects being held within a soundproof dark chamber which has steel grids having controlled shock mechanism. In response to the experimental input, %freezing is recorded in the machine as an output reading of the same which is noted as the parameter of rodent fear defense index. To create a virtual odor cue 1ml of 10% vanilla extract was provided to the chamber. The tests were performed as described as follows:

#### **A. Contextual fear conditioning test**

Following a compulsory habituation time of 2 min, the contextual fear conditioning test was performed where four consecutive unconditioned stimulus (89sec pre-shock interval, 0.8 mA 1-s foot shock for rats and 0.4 mA 1-s foot shock for mice) were delivered followed by 2min rest devoid of any stimuli. On the following probe day, subjects were exposed to the same conditioning context (identical conditioning chamber and odor cue) under shock free conditions. Freezing behavior, defined by stillness of the animal, excluding the noted respiratory movements, was measured in the absence of any shock stimuli for 8 min by PACKWIN 2.0 software (Panlab, Barcelona, Spain).

#### **B. Cue-Dependent Fear Conditioning test**

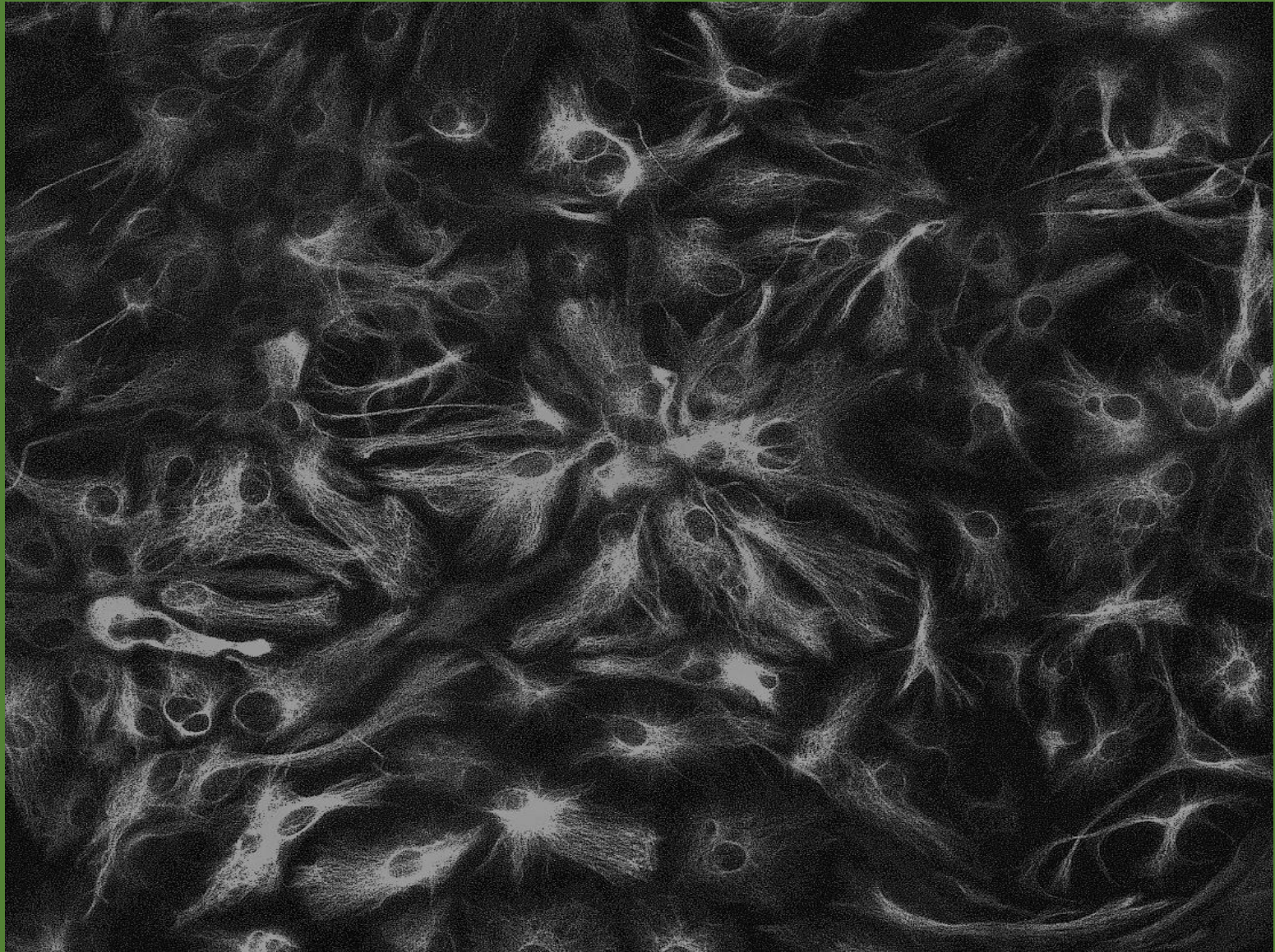


During this test, in addition to the previous context an extra cue of light and sound was provided to the subjects. On the first day i.e. the day of acquisition the rodents were kept in the chamber as described above and allowed a mandatory habituation for 2 min. This was additionally followed by four consecutive sessions of 29 seconds of light and sound exposure (85dB, 4000Hz for rat and 85dB, 2500 Hz for mice) co-terminating with a foot shock (0.8 mA, 1-s for rat and 0.4 mA, 1-s for mice) with an inter-trial interval of 60s, followed by a 2min rest without stimuli. For 1-trial experiment, the practice was provided for a single day and for multi-trial cue dependent test, the training was performed for consecutive four days. During the probe stage the context of the chamber was altered with the addition of a white plexiglass floor on top of the shock grid, a black teepee to alter the shape/size of the chamber, and a 0.5mL 10% Eucalyptus oil odor cue. On the probing day, rodents were exposed to the identical testing paradigm as on conditioning day but without the shock stimuli. Again, freezing behavior was measured in the absence of any shock stimuli by PACKWIN 2.0 software (Panlab, Barcelona, Spain).

### **2.18. Statistical Analysis**

All of the experimental data were analyzed with the help of one way ANOVA which was followed by Bonferroni's test and Tukey's multiple comparison of means post hoc test by using Graphpad software for comparing more than two experimental groups. Student's t-test was used to compare the significant difference among two groups,. Data are presented as mean  $\pm$  standard error of mean, and  $p < 0.05$  was considered to be statistically significant.

# RESULTS



# Chapter:1

Profiling of cytokines in A $\beta$ -mediated astrocytes activation and its protection in-vitro

## **Introduction**

One of the major forms of dementia in elderly patients is the Alzheimer's disease (AD) chiefly beginning with an elusive decline in episodic memory, followed by a devaluation in cognition and functioning in daily life. Although the exact underlying mechanism triggering this course of event is yet to be unfolded, yet the involvement of astrocytes and its reactivity due to Amyloid- $\beta$  ( $A\beta$ ) is undeniable from the neuropathological point of view. It was long proposed by Sir Santiago Ramón Y Cajal and Camillo Golgi, that astrocytes hold a much integral role in functionality than only in its simple structural support (García-Marín et al., 2007; Kettenmann and Verkhratsky, 2008). There are molecular mechanisms triggered during astrogliosis both in prenatal and postnatal phase, which are determined by the expression of mainly two proteins: Glial Acidic Fibrillary protein (GFAP) and calcium binding protein S100 $\beta$  (Guillemot F., 2007; He et al., 2005). The embryonic development of astrocytes is determined by Notch, JAK-STAT signalling working in a synergistic fashion (Kanski et al., 2013) whereas the initiation of glial differentiation is decided by the family of IL-6 cytokines namely CNTF etc (Nakashima et al., 1999). In the postnatal astrogenesis, predominance of BMP-SMAD pathway is extremely well documented, for its inactivation causes an evident reduction in GFAP and S100 $\beta$  activation (Qin et al., 2014).

Multiple research findings have explained the beneficial protection offered by reactive astrocytes on neighbouring neurons. The majority of reactive astrocytes help to restrict the damage by tissue repairing, integrating the blood brain barrier (BBB), and providing nutrients to substantiate energy supply when the requirement is high (Buffo et al., 2010). Many instances have shown that disruption in astrogliosis

initiation by attenuation of the signal transducer and activator of transcription-3 (STAT3) pathway, a key molecule in causing gliosis, has caused an increased oxidative stress, where the effect has been sufficiently detrimental for the system (Sarafian et al., 2010). The success of the homeostatic maintenance offered by astroglia lies in its immensely varied secretory ability. The secreted agents derived from astrocytes include various classical neurotransmitters like Glutamate, GABA, Glycine and their precursors (Malarkey and Parpura, 2008 ; Unichenko et al., 2013; Eulenburg and Gomez, 2010) neuromodulators like D-Serine, Taurine, L-aspartate (Martineau et al., 2014; Kimelberg et al., 1990), hormones, peptides, various metabolic substrates and several relevant inflammatory factors like IL-1, IL-6 and other complementary factors, eg. C3a (Choi et al., 2014; Erta et al., 2015; Lafon-Cazal et al., 2003).

A sufficient amount of recent work establishes the fact that astrocytes play a pivotal role in maintaining a balance between neuronal health and homeostasis. Our work tries to initially identify the major pathway which holds the responsibility in glial differentiation, followed by an investigation of the neuroprotection offered by A $\beta$ -treated astrocyte conditioned medium. As discussed earlier, astrocytes are known to secrete several cytokines which provide a beneficial role in neuronal survival and health improvement (Saha et al., 2020). In our study, we have tried to identify an array of cytokines secreted from astrocytes in treatment to A $\beta$ . Among them, we identified a single cytokine sICAM-1 which previously has been shown to have a beneficial role over neuronal health (Kim et al., 2000). In our findings, we have shown that A $\beta$  treatment increases ICAM-1 both at translational and secretory level in astrocytes. Besides, we observed that ICAM-1 treatment in vitro provided neuroprotection by reducing the neuronal death and improving the neuronal

connectivity. Neuronal death is often measured by cleaved PARP (Chaitanya et al., 2010), which showed a significant reduction with ICAM-1 administration in A $\beta$  treated neuronal cells. In this study, we explored whether ICAM-1 can be a therapeutic target in models of AD.

## **Results**

### **Exposure to A $\beta$ leads to activation and proliferation in astrocytes**

Activation of astrocytes are an integral part and pathological hallmark of several neurodegenerative disease, especially in AD. The initial assessment of the activation of astrocytes, also known as astrogliosis were performed both in vitro and in vivo. Firstly primary cultured astrocytes isolated from 0-1 day rat pups were treated with oligomeric amyloid- $\beta$  in a dose of 1.5 $\mu$ m which is pathologically commemorative to the milieu (Saha et al., 2013). Immunocytochemistry performed in the cultured cells against GFAP when seen microscopically revealed a significant increase in activation of astrocyte along with increased proliferation (Fig.1A). Immunohistochemistry of A $\beta$ -infused rat brain also showed an increase in glial fibrillary acidic protein in astrocytes as compared to the PBS-infused rats. Also protein isolated from the primary cultured astrocytes both in presence and absence of oligomeric A $\beta$ <sub>1-42</sub>, was subjected to western blotting and a significant increase in GFAP was observed at increasing timepoints (Fig. 1B,C).

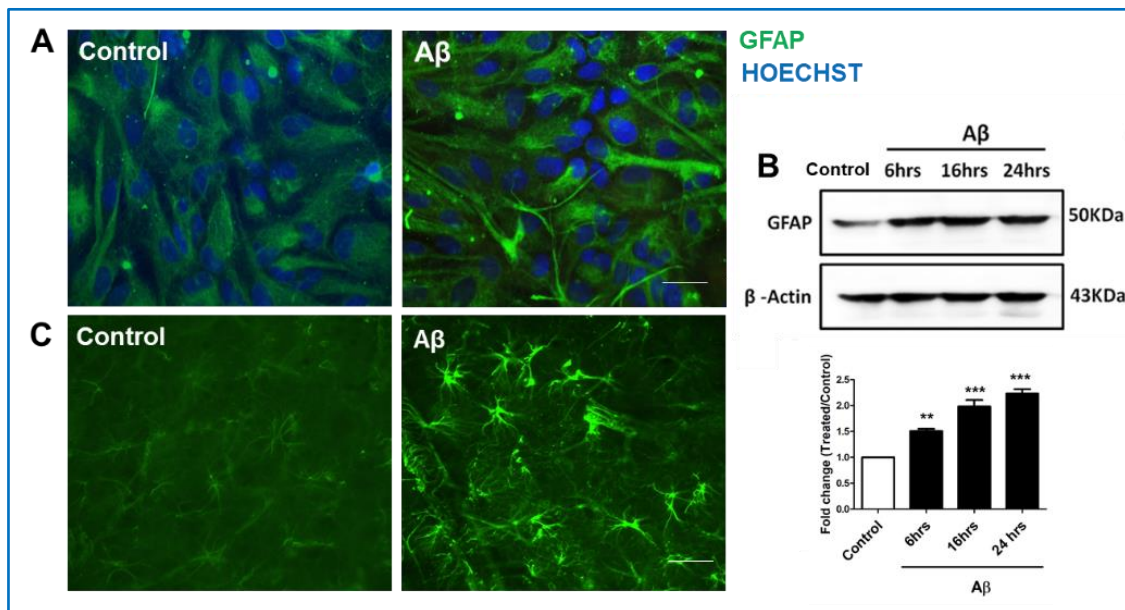


**Figure 1: Amyloid- $\beta$  leads to activation of astrocytes both in-vitro and in-vivo.** Astrocyte developed from brain of 0-1 days rat pups were kept for maturation for 14 days and treated with 1.5 $\mu$ M A $\beta_{1-42}$  at various time points. **(A)** Fluorescence microscopic image taken at 40x magnification shows glial activation with A $\beta_{1-42}$  treatment as compared to control marked by GFAP. scale bar:20 $\mu$ m **(B)** Western blot showing significant increase in GFAP at various time points 6h, 16h, 24h with A $\beta$  treatment. Experiments performed in triplicates. Bar diagram showing the increased fold change in GFAP at selected time points \*\*\*p<0.0001, \*\*p<0.001. **(C)** Adult Sprague Dawley rats were infused with oligomeric A $\beta_{1-42}$  in cortical region of brain following perfusion and isolation of the same. Fluorescence images of immunohistochemical staining of brain cryo-sections taken at 20x magnification showed an enhanced GFAP in A $\beta$  infused rats as compared to the PBS infused group of animals in vivo. Scale bar :50 $\mu$ m.

To further validate the increase in astrocyte activation and proliferation in vitro, cultured primary astrocytes were subjected to 1.5 $\mu$ M A $\beta$  and immunocytochemistry was performed against the astrocyte proliferative markers S100 $\beta$  and vimentin. Microscopic images taken at 40x magnification showed astrocyte activation with increase in proliferation of the same as indicated by markers S100 $\beta$  and Vimentin (Fig. 2A, B).

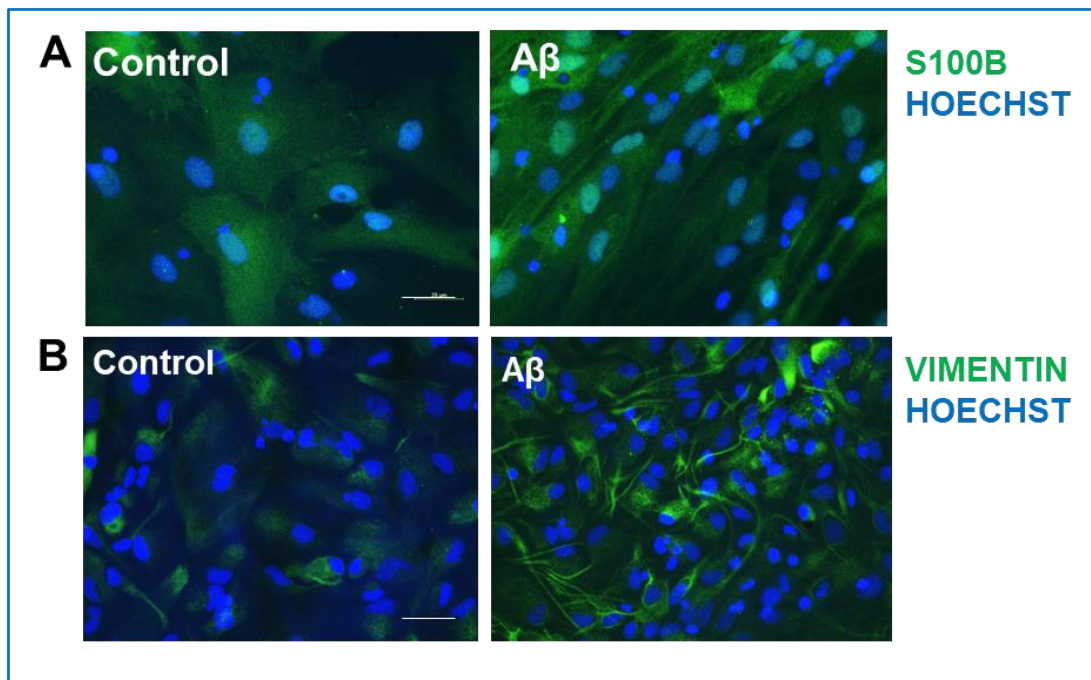


**Figure 2:** Validation of astrocyte proliferation and activation in vitro. (**A, B**) Primary cultured astrocytes (14DIV) were subjected to 1.5 $\mu$ M A $\beta$  treatment. After 24h, immunocytochemistry was done in both control and treated cells against S100 $\beta$  and Vimentin. The nuclei were stained with Hoechst and images were taken at 40x magnification using fluorescence microscopy. Scale bar: 50 $\mu$ m.

### **Astrocyte activation involves mainly MAPK pathways activation**

Since long time multiple signaling cascades including JNK pathway has been reported to be activated with astrocyte activation (Gadea et al., 2008; Li et al., 2017). Also the involvement of JNK along with its notable downstream target c-Jun has been known to play a role in neuronal apoptosis brought about by A $\beta$  (Morishima et al., 2001; Troy et al., 2001; Yao et al., 2005). However, the role played by the same in A $\beta$  induced astrocyte activation is yet to be investigated. Astrogliosis shows an alteration in several metabolic aspects which leads to multiple changes in various pathways and molecules, one of the essential being MAPK. MAPK may include an involvement of mainly three molecules namely, ERK, p38, JNK (Plotnikov et al.,



2018; Raman et al., 2007) and in our study a differential expression in essentially most of the molecules involved in MAPK signaling i.e. p-JNK, p-p38, although no change in ERK has been observed (Saha et al., 2020). With treatment of 1.5  $\mu$ M A $\beta$ , astrocyte cells, p38K and JNK phosphorylation showed a significant increase in 16h and 24h time point of A $\beta$  treatment. However the corresponding total p38 and total JNK showed an unaltered levels at all the time points (Fig. 3A, B).

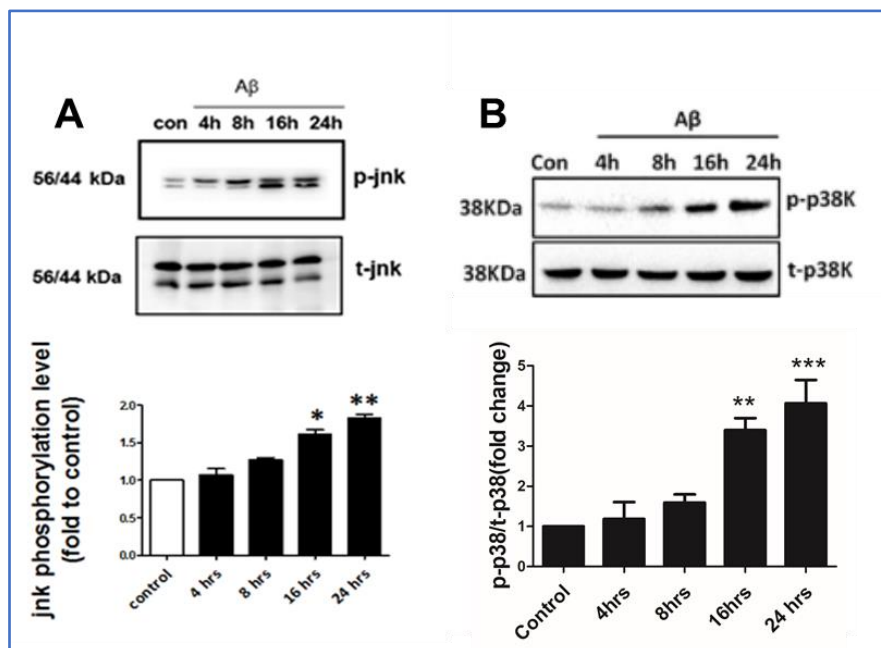


**Figure 3 : MAPK shows an significant upregulation with Amyloid  $\beta$  treatment in-vitro.** Primary astrocytes cultured from 0-1 day were treated with A $\beta_{1-42}$  14DIV. The cell lysates were collected followed by western blotting with antibodies against JNK and p38 (both phospho and total forms were considered). (A,B) Representative western blot showing p-JNK and p-p38 in the upper panel with the corresponding total forms of each below. Lower panel indicates the densitometric representation of the corresponding blot. Values expressed as mean $\pm$ SEM. n=3, \*\*\*p<0.0001, \*\*p<0.001, \*p<0.01.

Also the molecules downstream to MAP kinases signaling namely c-JUN and p-ATF-2 had been checked in primary astrocytes both in presence and absence of A $\beta$ . The

results showed a consistent increase in each of the molecules corresponding to the increasing time point of 4h,8h,16h and 24h (Fig. 4 A,B).

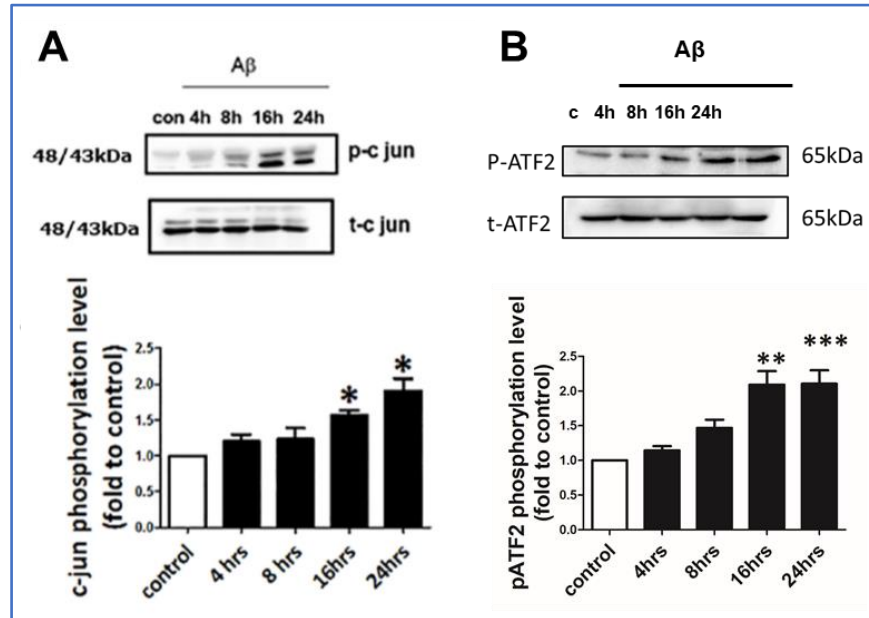


**Figure 4: Amyloid- $\beta$  contributes significantly in upregulating p-c-jun and p-ATF-2 in-vitro. (A,B)** Upper panel shows representative western blot of p-c-Jun and p-ATF-2 along with their corresponding total forms. Lower panel indicates the graphical representation of the densitometry of the corresponding blot. Values expressed as mean $\pm$ SEM: n=3, \*\*\*p<0.0001, \*\*p<0.001, \*p<0.01.

### **p38 plays an essential role in astrocyte activation**

Activation of p38 MAPK pathway has been long known to play a pivotal role in several pro-inflammatory cytokine production, which often takes place during astrocyte activation (Smith et al., 2006). So to check whether they are involved in A $\beta$  mediated astrocyte activation, primary astrocytes were treated with A $\beta$  in 1.5 $\mu$ M at 16hrs time point. It was observed that a significant upregulation was present in p-p38 in the glial cells upon A $\beta$  treatment, with no alteration being observed in the total form of p-p38 (Fig. 5).

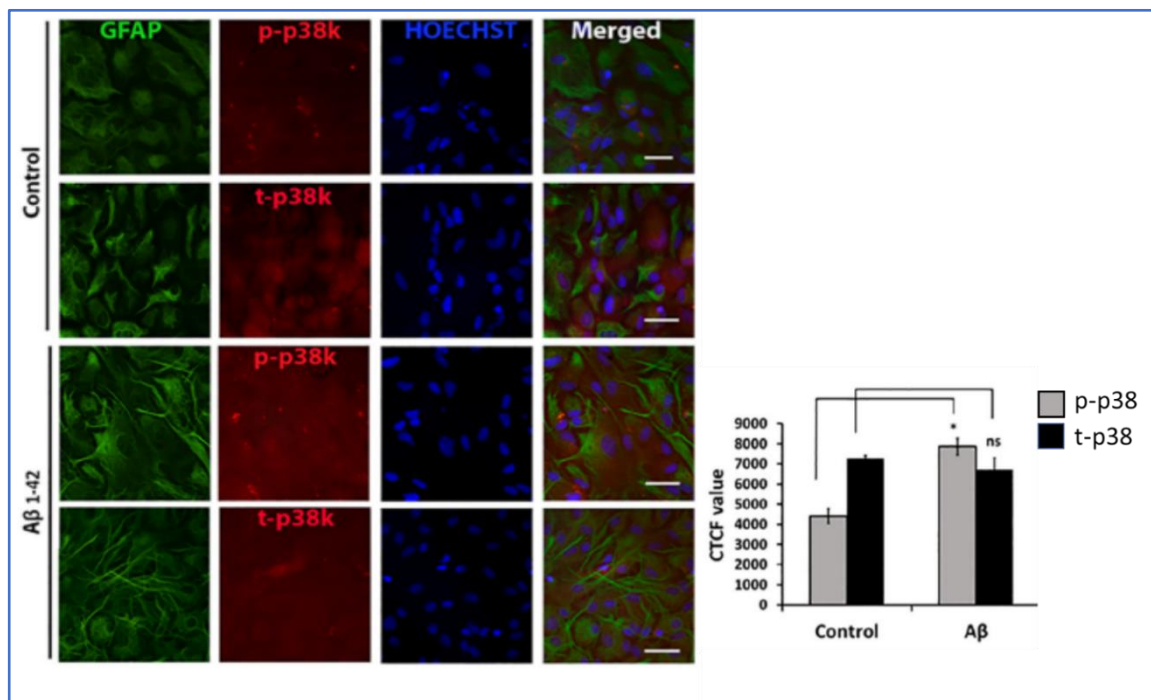


**Figure 5: Astrocytes show an increased P38 MAPK with treatment to A $\beta$  in vitro.** Primary astrocytes were treated with A $\beta$  for 16h and immunocytochemistry was done with antibody against phospho and total p38K along with GFAP. Nuclei was stained with Hoechst. Fluorescence microscopic images showing the panels representing GFAP, p38K, Hoechst and merged (from left). Top two panels show control phospho-p38K and total-p38K and lower two panels indicate A $\beta$  treated sections. Images were taken at 40X magnification. scale bar:30 $\mu$ m. Right panel indicates the graphical representation of the corresponding fluorescence images. \* $p < 0.01$ .

To validate the previous observation in an in-vivo model of AD, A $\beta$ -infused rat brain slices were subjected to immunohistochemistry against p-p38 and t-p38 proteins. The treated rat brain sections showed around 2 fold elevation in p-p38K level which colocalized with the GFAP+ve cells. This was in comparison to A $\beta_{42-1}$  infused brain sections. The level of total p38K in both A $\beta_{42-1}$  and A $\beta_{1-42}$  infused brain cortex was observed to remain same. The microscopic image was analysed by Image J software and graphically represented to show the CTCF value (Fig. 6).

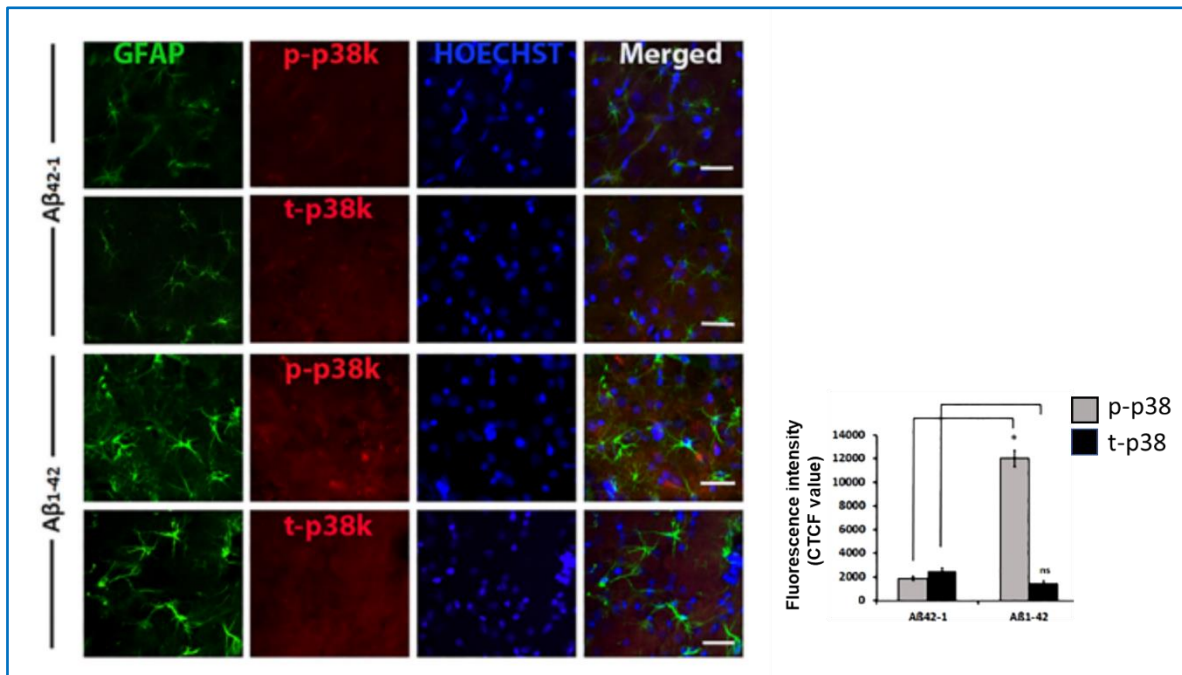


**Figure 6:** Amyloid- $\beta_{1-42}$  and its reverse peptide was infused in rat cortex and cryo-sections were used for immunohistochemistry against phospho and total p38K along with GFAP. Nuclei were stained with Hoechst. From left, panels reveal GFAP, p38K, Hoechst and merged images. From top, first two panels indicate reverse peptide infused within phospho and total p38K staining posed as control and the lower two panels are showing A $\beta$  induced phospho and total p38K level respective. Right panel indicates the bar diagram indicating the graphical representation of the corresponding fluorescence images. \* $p < 0.01$ .

To finally check whether the p-p38 MAPK is essential for GFAP enhancement during A $\beta$  mediated astrocyte activation, primary astrocytes were exposed to p38 inhibitor (SB239063), both in presence and absence of A $\beta$  for 24 hrs. By western blotting analysis, it was observed that GFAP increased almost 2 fold in only A $\beta$  treated astrocytes, whereas after co-treating the same with p38 inhibitor, a significant drop was found in GFAP (Fig.7). This indicated that p38 pathway is extremely vital for astrocyte differentiation and activation.

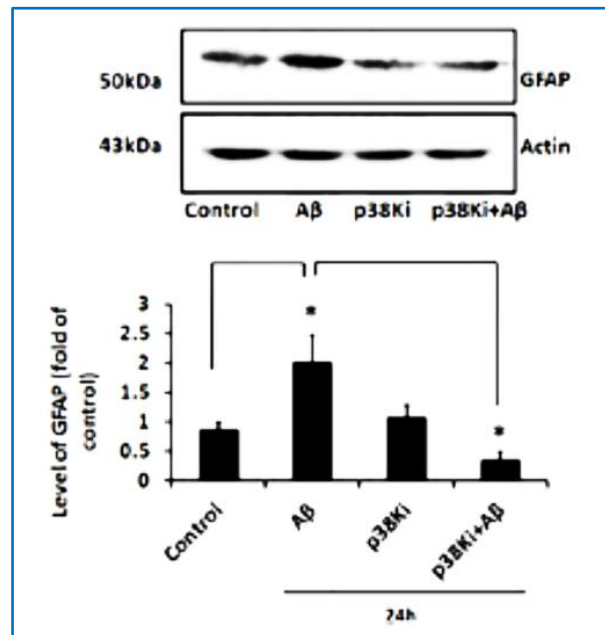


**Figure 7:** SB239063, an inhibitor of p38K was co-treated along with A $\beta$  for 24h on astrocytes. Upper panel shows western blotting against GFAP done with the cell lysates. Lower panel depicts the graphical representation of the GFAP level quantitation among various treated and untreated samples. Densitometric analysis expressed as mean  $\pm$ SEM. n=3.\*p<0.05.

### Primary rat astrocytes secrete sICAM-1 in response to A $\beta$

Astrocyte secretion and its useful properties has been well documented since a long time, the concept being as old as the discovery of the glial cell itself. A wide amount of work all over the world is currently dedicated to determine the molecules and factors secreted by astrocytes which contribute in improving the neuronal health and mortality. Human astrocytes are known to secrete wide array of cytokines specifically including the interleukins (Choi et al., 2014), with a possibility that several of them may be transported by extracellular vesicles, for the defined mechanism is yet to be elucidated well. Since it was seen in our previous experiments that A $\beta$  treated astrocyte conditioned medium (A $\beta$ -ACM) contributed in improving the A $\beta$  mediated

degenerating neurons to a high extent, we decided to unravel the specific cytokines which may contribute in doing so (Fig. 8).

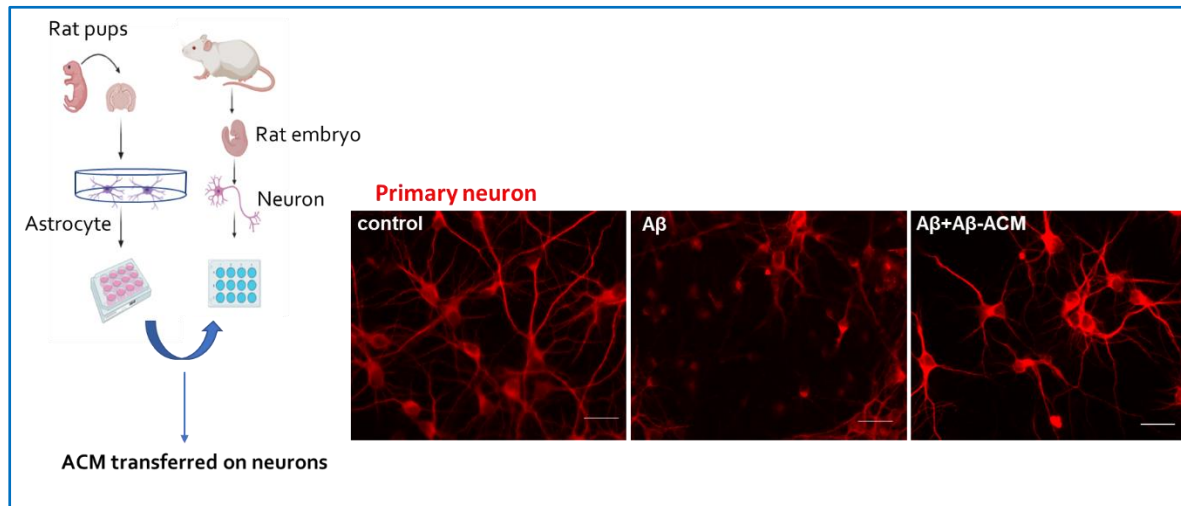


**Figure 8:** Left panel indicates the experimental plan of applying astrocyte conditioned medium on primary cultured neurons to check the cytokine secretion and further possibilities of neuroprotection. Right panel shows the improvement in neuronal morphology with application of A $\beta$ -astrocyte conditioned medium (A $\beta$ -ACM) on A $\beta$  treatment.

Having seen previously, the beneficial contribution of 6h A $\beta$ -ACM on neuronal health, the same was selected to determine the various cytokines secreted from primary astrocyte culture by performing the cytokine array. Several differentially expressed cytokines were identified, from which a subset of adhesion molecules, sICAM-1 showed a 2-fold increase in A $\beta$ -treated astrocytes as compared to the control (Fig. 9A). The molecule was selected on the basis of a very interesting finding established by Kim et al. in 2014, which stated that sICAM-1 influenced microglia to produce neprilysin which helped in reducing A $\beta$  plaque load in neuron. Also serum processed from human blood of normal and AD patients (Male, aged 65years) were subjected to cytokine profiling where an increase in sICAM-1 was observed in AD patients as compared to the normal patients (Fig. 9B).

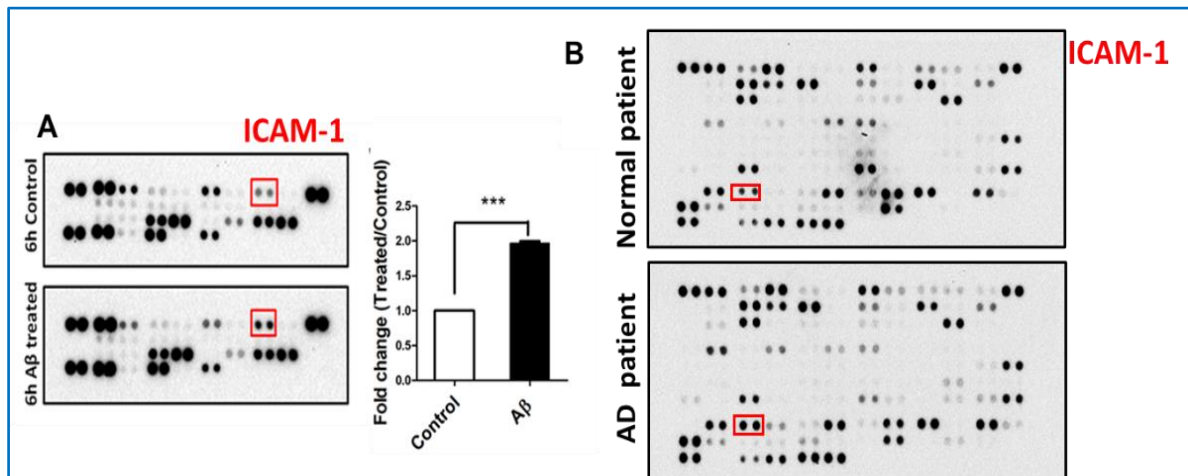


**Figure 9:** Differential release of sICAM-1 cytokine in response to A $\beta$  treatment. Brain obtained from 0-1 day rat pups yielded astrocytes, along with neuron cultured from E16-18 rat embryo. Astrocyte conditioned medium was applied to A $\beta$  treated degrading neurons to check their phenotypic betterment. **(A)** In order to check the differential secretary status of various astrocyte originated cytokines, ACM of the control and treated cells subjected to cytokines array. Red Box shows the sICAM-1 dot blot. Densitometric analysis of sICAM-1 indicates the relative fold change of sICAM-1 represented as mean  $\pm$  SEM, n=3, \*\*\*p< 0.0001. **(B)** Cytokine array of control and AD patient showing differential expression of cytokines emphasizing increase in sICAM-1.

### ICAM-1 level increases with A $\beta$ treatment in vitro and in vivo

In order to check the abundance of intracellular protein levels of ICAM-1, western blotting of primary cultured rat astrocytes were done which showed a significant 2.5 fold increase in 6h, 16h, 24h time point with treatment of 1.5 $\mu$ M A $\beta$ <sub>1-42</sub> (Fig. 10 A,B). Furthermore, to gain insight into the detailed secretary status of the molecule sICAM-1, Enzyme-linked immune assay (ELISA) was performed with the treated and untreated astrocyte conditioned medium which showed that sICAM-1 in A $\beta$ -treated ACM was significantly increased by 2 folds, 2.5 folds and 3folds in 6h, 16h and 24h A $\beta$ -treated ACM respectively in a time dependent manner (Fig.10C).

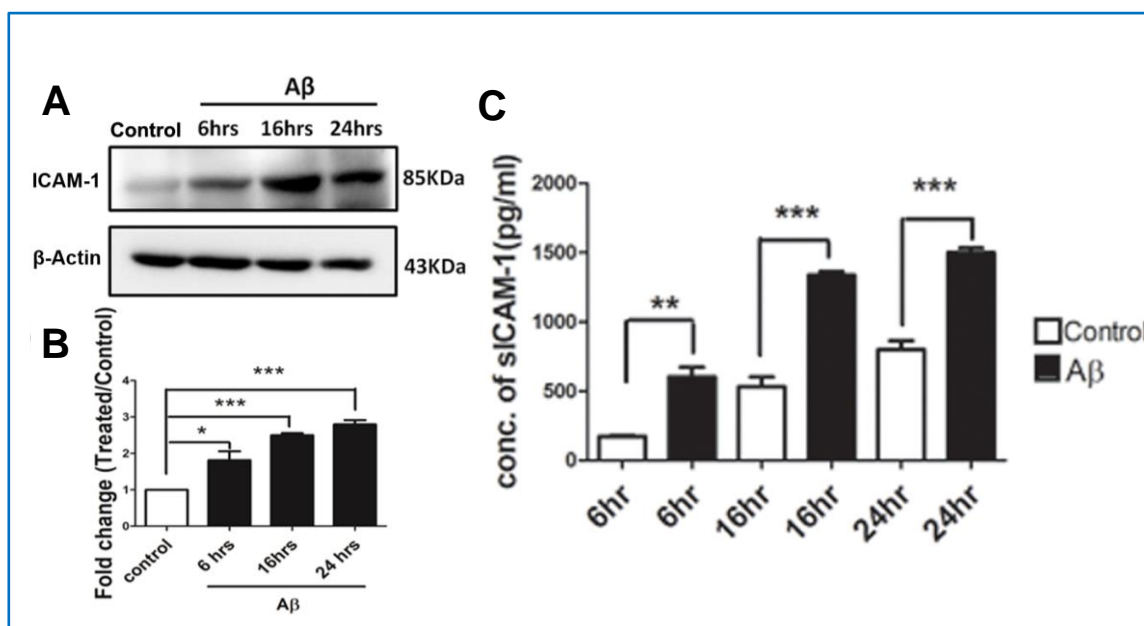


**Figure 10:** (A) Expression of ICAM-1 in primary astrocytes with or without treatment of A $\beta$  was checked by western blotting with antibody against ICAM-1. (B) The data was represented as mean  $\pm$  SEM of three independent experiments, n=3,\*\*\*p<0.0001, \*p<0.01. (C) Conditioned medium collected from primary astrocytes treated with 1.5 $\mu$ M A $\beta$  were subjected to ELISA. Graph showing the quantitation of sICAM-1 in ACM of the control and treated cells. The data represented as mean  $\pm$  SEM of three independent experiments; n=6,\*\*\*p<0.0001, \*\*p<0.001.

Finally, the differential expression of ICAM-1 in A $\beta$  treated astrocytes was validated in-vivo using infusion model performed in Sprague Dawley rat and 5xFAD transgenic mouse model. First, a specific animal model where A $\beta$ <sub>1-42</sub> peptide was stereotactically infused in the hippocampus of Sprague Dawley rat brain (Sanphui & Biswas, 2013). In corroboration with the in vitro data, in A $\beta$ -infused rat brain cortex area, a significant increase of about 3-4 folds in immunoreactivity of ICAM-1 and GFAP was found, and ICAM-1 immunoreactivity was mostly present in the GFAP-positive astrocytes (Fig. 11A-D).



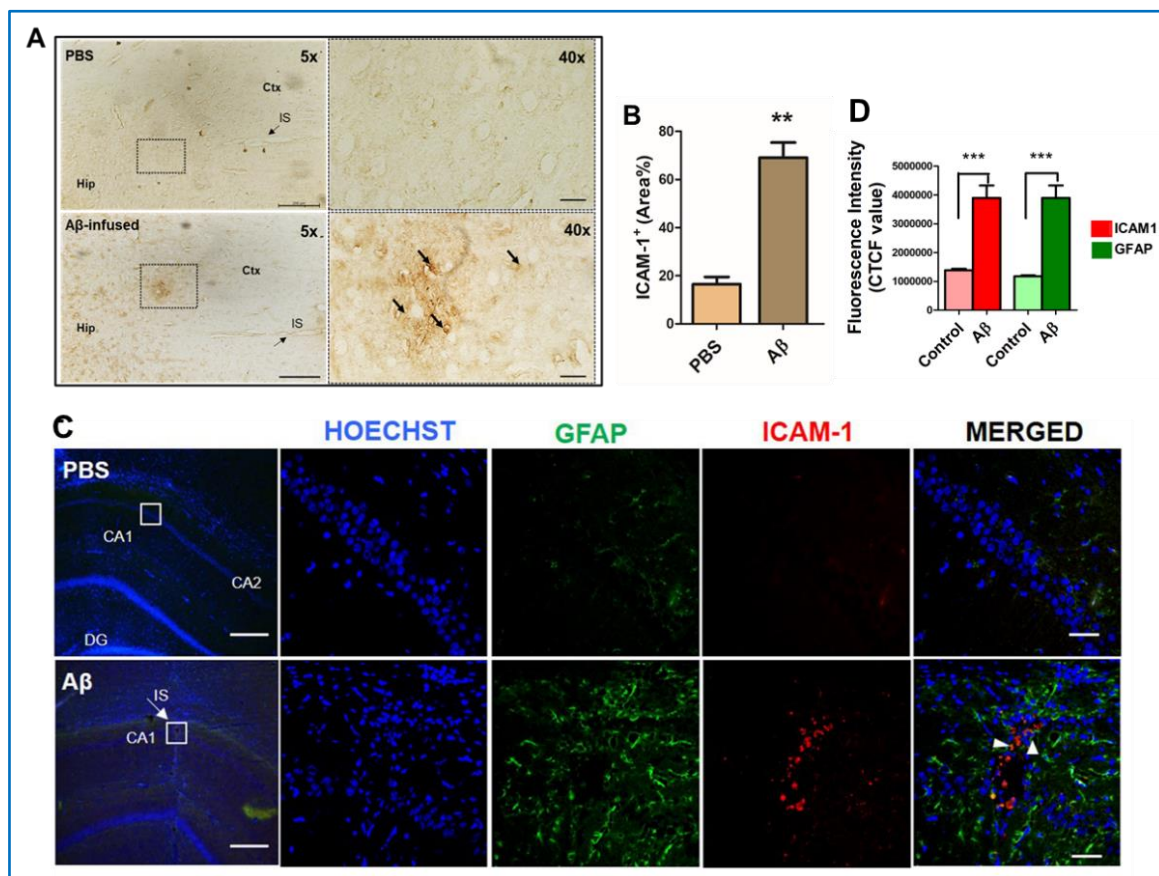


**Figure 11:** ICAM-1 expression in response to A $\beta$  infused Sprague Dawley rat. A $\beta$  was stereotactically infused in the rat brain cortex and sacrificed at day 24. **(A)** Immunohistochemistry in 20 $\mu$ m brain tissue sections of PBS infused and A $\beta$  -infused rats was performed with antibody against ICAM-1 protein and was checked by DAB. Left panel shows a 5x magnification of the same with an inset; scale bar: 200  $\mu$ m. Right panel depicts the 40x image of the inset, arrows indicate higher expression of ICAM-1 protein in A $\beta$ -infused rat brain; scale bar: 20 $\mu$ m. The infusion site (IS) of the protein and sham has been indicated in arrow in the left panel. **(B)** Bar diagram shows the differential expression of the protein within two experimental groups. n=3 for each group, 3 slices of each rat brain (\*\*p<.001). **(C)** 20 $\mu$ m cortical slices were co-immunostained with ICAM-1 and GFAP antibodies. Fluorescence images were taken at 5x (scale bar: 100  $\mu$ m) and 40x (scale bar: 12.5 $\mu$ m) magnifications. **(D)** Bar diagram represents the intracellular intensity of the same. Values are expressed as Mean  $\pm$  SEM from three independent experiments: \*\*\*p < 0.0001 (n=3).

In cumulation, these observations led us to conclude that A $\beta$  induces intracellular ICAM-1 level in astrocytes both in vitro and in vivo and thereby an increased secretion of its soluble form, sICAM-1 in ACM of activated astrocytes.

## ICAM-1 improves neuronal health and viability in vitro

Our initial hypothesis was to check whether ICAM-1 offers any protection on A $\beta$  treated neurons in vitro. So to check the part played by secreted sICAM-1 against A $\beta$ , the activity of sICAM-1 was halted by adding neutralizing antibody (4 $\mu$ g/ml) in ACM and transferring it to the primary cortical neuron culture in presence and absence of A $\beta$ . Neurons were treated with control, ACM, 6h A $\beta$ -ACM or only A $\beta$ . 24h following the treatment, trypan blue assay was done to count the number of viable cells. A significant cellular death of 40% were observed in those which were treated only with A $\beta$  as compared to the untreated ones, whereas A $\beta$ -ACM treatment significantly recovered cell viability. However, by neutralizing sICAM-1 in A $\beta$ -ACM milieu neuroprotection against A $\beta$  toxicity was found to reduce significantly (Fig. 12A). To further strengthen these observations, rat recombinant ICAM-1 (rrICAM-1) was added to the cortical neurons both in presence and absence of A $\beta$  and checked for cell viability with trypan blue assay. A significant recovery in cell viability was with rrICAM-1 treatment even in the presence of A $\beta$  (Fig. 12B).

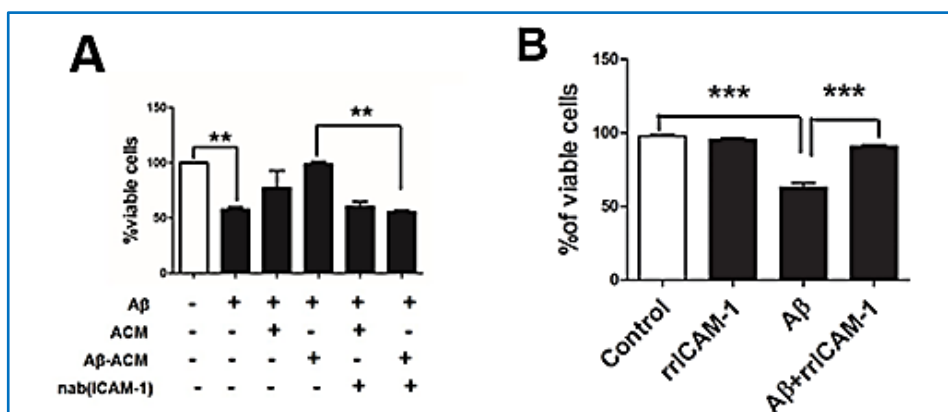


**Figure 12:** (A) 6h ACM with and without 1.5  $\mu$ M A $\beta$  treatment was transferred to the cultured neurons exposed to 1.5 $\mu$ M A $\beta$  for 24h and cell viability was checked both in presence and absence of neutralizing antibody against ICAM-1(4 $\mu$ g/ml). Trypan Blue test was performed to check the cell viability. Graphical data represents the %viable cells with treatment of A $\beta$ -ACM as compared to only A $\beta$  treatment. Values are expressed as Mean  $\pm$  SEM of six independent experiments. \*\* $p$  < 0.001. (B) Primary cortical neurons were treated with A $\beta$ , with and without rrICAM-1 (50 ng/ml). The graph shows

the recovery in cell viability in A $\beta$  treated cells when subjected to treatment with rrICAM-1. Values are expressed as Mean  $\pm$  SEM of five independent experiments: \*\*\* $p$  < 0.0001.

The morphological integrity of the neurons was checked by immunocytochemistry with MAP2 antibody in all treatment groups including the controls. Dendritic arborization was measured by Sholl analysis (*Sholl D.A., 1953*). Imaging showed that rrICAM-1 treatment ensured sufficient recovery of the disintegrated neuronal process among the A $\beta$  treated neurons (Fig. 13A,B). Further apoptosis was checked by western blot with cleaved PARP antibody and significant decrease in cleaved PARP level was observed upon treatment with rrICAM-1 treated primary neurons even in presence of A $\beta$  compared to only neurons which were solely treated with A $\beta$  (Fig. 13C,D).

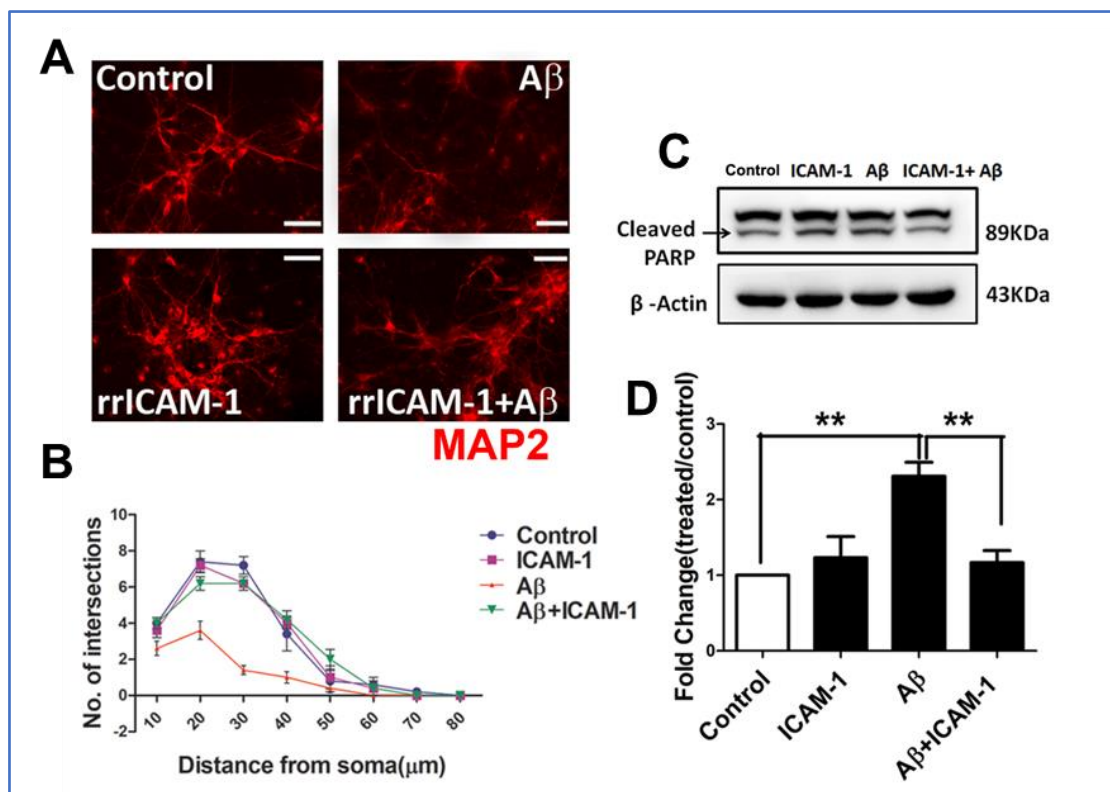


**Figure 13:**(A) Primary cultures of neurons were treated as mentioned above and subjected to immunocytochemistry with antibody against MAP2. 40x Fluorescence images of neurons with and

without treatment of rrlCAM-1 in presence of A $\beta$  showed a morphological recovery with treatment of rrlCAM-1.(B) Represents the corresponding Sholl analysis for the arborisation of neurons present under different treatment. (C) Primary cortical neurons were treated with A $\beta$ , ICAM-1 or ICAM-1+A $\beta$  for 24 h and were subjected to western blot analysis using PARP antibody.(D) Bar diagram shows the fold change in cleaved PARP (normalized with Actin) derived from densitometric analysis. Values are expressed as Mean $\pm$ SEM from three independent experiments; \*\*p<0.001.

Considering all the above findings it can be well concluded that A $\beta$  helps in activating astrocytes which may lead to secretion of sICAM-1.This cytokine helps in improving the health and morphology of neighbouring neurons and reduces cell death in the AD subjects.

## Discussion

Alzheimer's disease (AD) is one of the major forms of neurodegenerative diseases which progress in a complex fashion involving a serious contribution of glia-mediated neuroinflammation, which may be also proclaimed to be a "double-edged sword", having both detrimental and beneficial role. Astrocytes being the most abundant glial cell type, has always taken part in playing an important role in influencing the cellular and pathological processes. Role of astrocytes in neurodegenerative diseases like AD has always evoked controversy for numerous studies having implied the direct role played by glia in partial attenuation of the disease.

In our study, we have shown that astrocyte activation is inevitable in exposure to A $\beta$  and it involves several pathways especially MAPK signalling in causing the differentiation of astrocytes which is known to be a commemoration to astrocyte activation. Astrogliosis is a well-established phenomenon both in animal AD model brain and human AD patient brain. In our investigation regarding the activation of astrocytes we focussed mainly on MAPK pathway, which is known to play a vital role in basic cellular events like proliferation, growth, differentiation and other vital transformations (Kaminska B. 2005, Shaul & Seger, 2007). Several reports also suggest the involvement of MAPK in astrocyte activation and varied inflammatory responses in brain. However the accurate role of MAPK p38 or JNK has not yet been well established in altered morphology of astrocytes in exposure to A $\beta$ . Firstly, in corroboration with previous findings, we have shown that A $\beta$  activates astrocytes causing activation of specific markers like GFAP, S100 $\beta$  and vimentin. Also we have shown that p38 signalling shows a significant upregulation in exposure to A $\beta$  in astrocytes at various timepoints. We checked the downstream molecules of MAPK

signalling such as the c-Jun and p-ATF-2 as well and found a positive co-relation to the above mentioned data.

With exposure to A $\beta$  or following any traumatic signals, astrocytes are known to secrete several molecules, especially cytokines like IL-1, IL-6, and TNF- $\alpha$  (Sajja et al., 2016). Also A $\beta$  can instigate the production of chemokines like MCP1 which actively take part in recruiting the astrocytes at the site of lesion during the neurodegeneration process (Smits et al., 2002; Wyss-Coray et al., 2003). The question which is still being addressed all over is regarding the prevalence of the advantageous or the injurious role of astrocytes in neurodegeneration process in AD.

Although, astrocytes are proclaimed to mediate amyloid plaques degradation, reports also suggest their capability to produce A $\beta$  under specific inflammatory conditions. For example, TGF- $\beta$ 1 (Lesné et al., 2003) or IFN- $\gamma$  along with TNF- $\alpha$  (Zhao et al., 2012) or IL-1 $\beta$  (Blasko et al., 2000) accelerates A $\beta$  production by astrocytes. Large amounts of partially digested A $\beta$  is also known to be engulfed by astroglia eventually causing an autocrine defect and neuronal apoptosis (Söllvander et al., 2014). Moreover, despite the secretion of beneficial trophic factors like GDNF, improving neuronal functioning and cognition in rodents (Pertusa et al., 2008), astroglia may overexpress NGF causing neurotoxicity and degeneration of hippocampal neurons in-vitro (Sáez et al., 2006). However we found in our study, that secretome of A $\beta$  treated astrocytes were causing a holistic improvement in the degenerating neurons, and this led our inquisitive mind to locate the factors, especially the cytokines, which might cause improvement in AD conditions. We performed a cytokine array and observed differential expression in several of the cytokines.

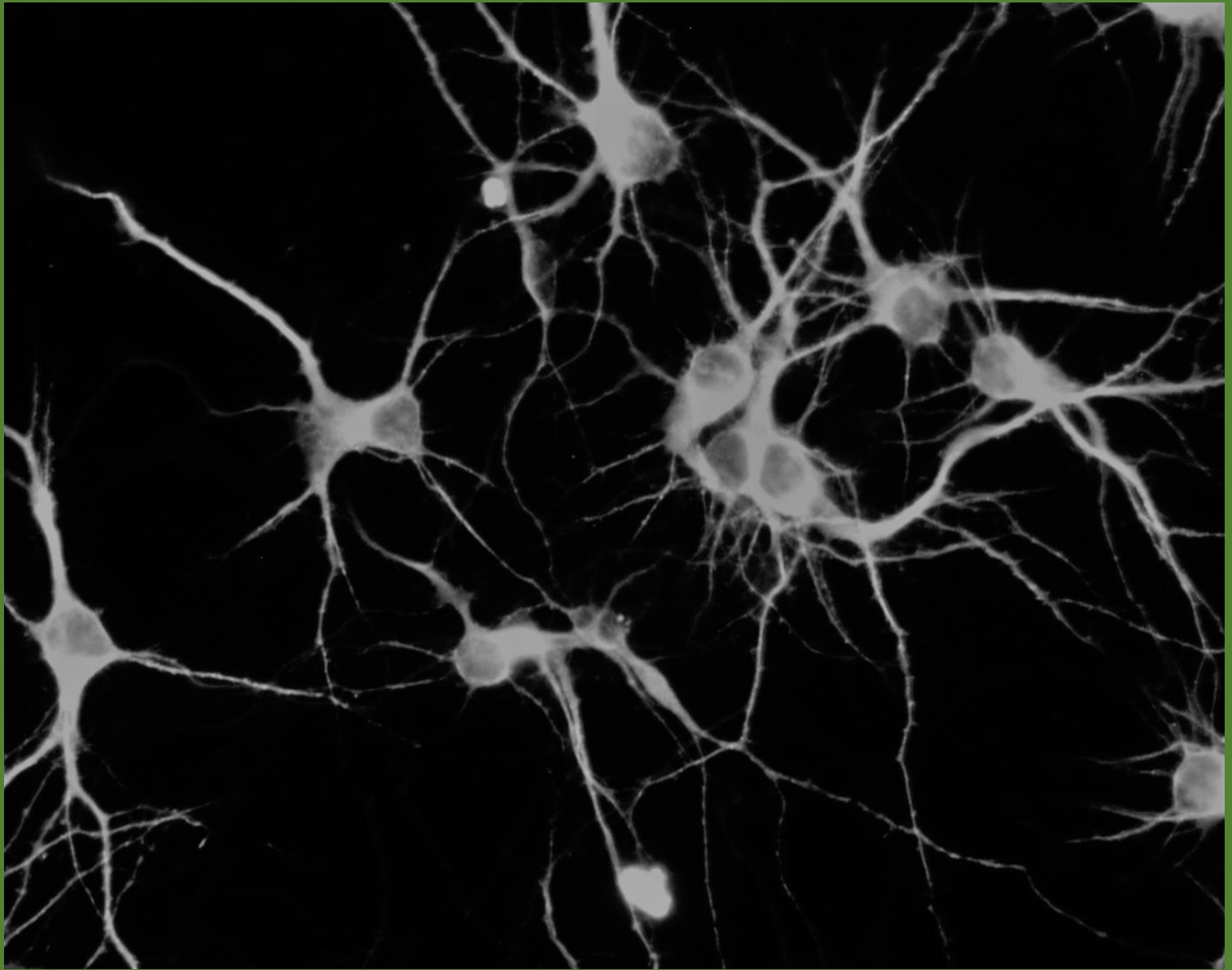
A previous study in our laboratory had shown that one of the cytokines, TIMP-1 was upregulated (Saha et al., 2020) in astrocytes in exposure to A $\beta$ , which provided protection to degenerating neurons at initial time points. So in our work, we selected sICAM-1, in accordance with Kim et al., 2012 , who showed ICAM-1 secreted from MSC-BV2 cells could influence microglia to produce neprilysin causing A $\beta$  degradation, further providing neuronal protection.

Adhesion molecules have been known to be an important player in the regulating several peripheral immune processes, one major example being ICAM-5 another intercellular adhesion molecule, preferentially expressed in dendrites and soma is known well to bring about neuronal development (Yoshihara et al., 1994). It also contributes in stabilising the post synaptic connections  $\beta$ 1 integrins binding (Ning et al., 2013). Previously, ICAM-1 has been found to be compartmentalized in some of the reactive astrocytes surrounding the amyloid plaques in post-mortem brain of AD patients (Akiyama et al., 1993, Miguel-Hidalgo et al., 2007). Also, sICAM-1 shows a marked elevation in CSF in AD brain and often has been proclaimed as a biomarker for neuroinflammation (Nielsen et al., 2007, Wennstrom et al., 2014).

ICAM-1 which on induction with IL-1 and TNF , bind to endothelial cells and with the assistance of receptors like LFA-1/MAC-1, they contribute in transmigration of the tissue of the CNS. Also, ICAM-1-deficient mice experienced increased levels of pathology in gray matter regions of the brain. Numerous studies in a variety of CNS disease models have associated ICAM-1 expression with pathology (Kraus et al., 1998; Mycko et al., 1998; Samoilova et al., 1998; McDonnell et al., 1999). However not much has been elucidated about whether sICAM-1 has any role or whether any underlying mechanism enables it to help provide neuroprotection, if any in A $\beta$

exposed brain cells. Here we showed that sICAM-1 shows an upregulation in astrocytes both in vitro and in vivo in treatment to A $\beta$ . The secretion of the molecule also increased in astrocyte conditioned medium with A $\beta$  treatment. To our excitement when we treated this A $\beta$ -ACM in degenerating neurons we observed an improvement in the neuronal health and viability, however with application of neutralizing antibody against ICAM-1, we found a decreased protection in cell viability of neurons. The same result was observed in treatment with rrICAM-1 which offered protection in degenerating primary neurons in AD conditions. Besides, PARP cleavage assay also confirmed that ICAM-1 was reducing neuronal death in vitro. These results corroborated with some of the previous findings and enabled us to initiate a further journey with a hope that sICAM-1 may be neuroprotective and could bring an aid in AD therapeutics.





# Chapter:2

ICAM-1 : Essential player to reduce amyloid plaque burden and improve cognitive functioning in A $\beta$  infused rats

## Introduction

The primary clinical manifestation of AD, considered quite essential for identifying the disease, is mainly the accumulation of A $\beta$  in the cortical and hippocampal regions of brain. This often leads to an acute progressive decline in cognitive functioning of the patient. It has been long known that major pathological hallmarks of AD include amyloid plaque formation and neurofibrillary tangles (NFTs). Many reports have shown that the synaptic loss found in AD patients form the best correlation with the cognitive decline (Davies et al., 1987; DeKosky and Scheff, 1990; Terry et al., 1991). The prefibrillar forms of A $\beta$ , along with its wide soluble and insoluble embodiments have been suggested to be highly neurotoxic causing disruption of learning and memory (Walsh and Selko, 2004). Most of the clinical therapy suggested by numerous scientists have strictly aimed to bring down the formed A $\beta$  levels in brain. The major enzymes controlling the A $\beta$  reduction, mainly involves the various metalloproteinase (MMP) enzymes, Insulin Degrading enzyme (IDE), Neprilysin. Across the world several research organisations have been searching successful strategies to attenuate the formation and effects of A $\beta$  and human clinical trials have been also initiated for the cause. However it was close to apparent success with Aducanumab trial in 2016, where Aducanumab was an antibody binding to A $\beta$  plaques along with its soluble forms. This showed a decrease in plaque levels in the brain and also slowed down the cognitive decline and memory loss within the subjects having mild clinical predisposition to AD. In our study we have tried to investigate if ICAM-1 could have any specific role in reducing A $\beta$  plaque or reducing the cellular death in animal models of AD.

Because cognitive decline in the disease begins several years before individuals develop dementia the transition from cognitive health through dementia can take a decade or more. The lengthy duration of cognitive symptoms in the disease makes it

difficult to track individuals across the full spectrum from cognitive health through dementia, limiting knowledge about the temporal course of cognitive decline in AD. Since AD known to be disconnecting syndrome, many MRI based techniques have been established to form a connectome study to venture into detailed therapeutic measures for the disease. Animal models have been long used in scientific experiments to perform the detailed study regarding the disease progression of AD. Along with neuroimaging, various cognitive functioning tests have been always regarded as reliable parameters to verify the improvement of neurodegenerative diseases with various drug administration. Here in our study we have focussed on analysing the cognitive functioning in rat with A $\beta$  infused models with several behavioural tests. The anxiety tests along with short term memory association and recognition has been selected as the basic parameter to establish our hypothesis of ICAM-1 being a beneficial cytokine which may improve depressive behaviour in rats.

## Results

### ICAM-1 reduces apoptosis and A $\beta$ plaque load in A $\beta$ -infused cortex in rodents

To ascertain whether ICAM-1 had any protective effect on in-vivo model of AD, the cortical infusion model of AD was used where A $\beta_{1-42}$  was infused in the cortical region of adult rat brain. On 14 DPI, the rats were subjected to IP injection of rrICAM-1 (0.5 $\mu$ g/kg b.w.) and the brain sections were subjected to TUNEL assay in the cortical region near the site of infusion to check the level of apoptosis. In tissue sections from A $\beta$ -infused rats, the % of TUNEL-positive cells were found to be significantly higher in cortical regions as compared to the control. In contrast, TUNEL positive cells decreased significantly when rrICAM-1 was administered intraperitoneally into the A $\beta$ -infused rats (Fig.1). Commemorating with the previous result it showed that ICAM-1 reduced cell death in A $\beta$  infused rat brain cortex in vivo.

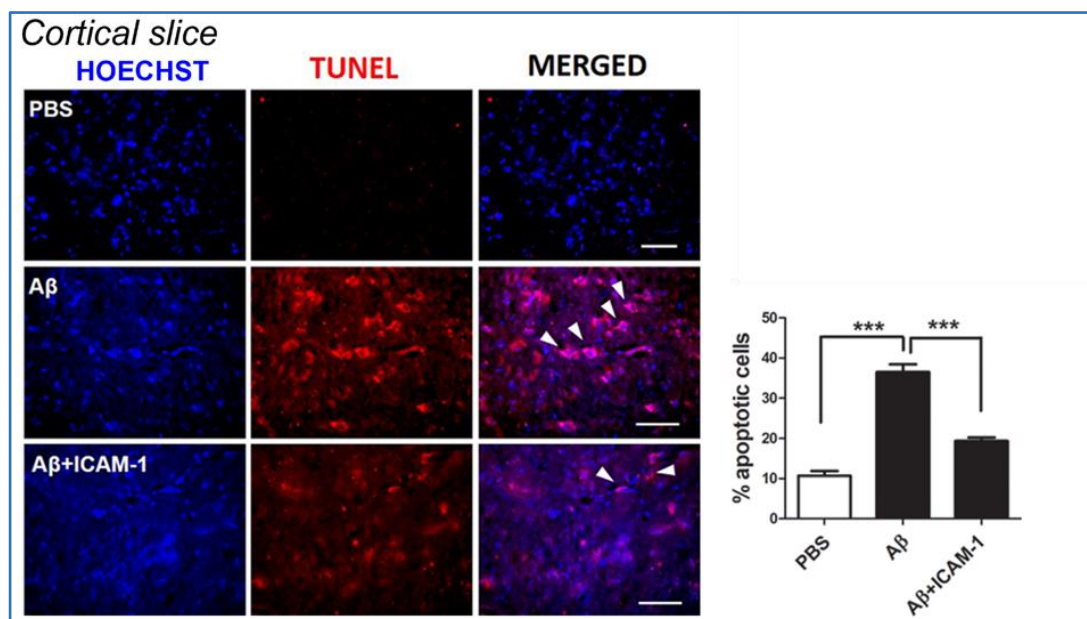


**Figure 1:** TUNEL assay performed to assess the status of apoptosis in brain cortical sections of various treated and untreated groups, 23 DPI of A $\beta$  infusion in cortex. All vertical image panels depicts 20x images (left to right) of cortex – Hoechst, TUNEL and merged. Each horizontal row represents each experimental group, Control, A $\beta$ , and A $\beta$  + ICAM-1 (0.5 $\mu$ g/kg b.w.). A $\beta$  + ICAM-1 treated group showed a significant reduction in the % of apoptotic cells compared to A $\beta$  alone group. Images taken at 20x magnification (n=3 for each group; \*\*\*p < 0.0001).

### **Administration of ICAM-1 fails to improve cognitive functioning in cortically infused A $\beta$ rat model of AD**

Since a significant reduction was found in the TUNEL+ve cells in cortical part of rat brain with ICAM-1 administration, an attempt was made to further observe the effect of the same on behavioral anomalies in cortically A $\beta$ -infused rats. Following the previous infusion and treatment method in the cortex of rat brain only, Open Field Test (OFT) was performed among the various experimental group of rats to determine the anxiety of the rodents. A $\beta$ -infused animals showed a significant increase in the distance travelled compared to control animals indicating a higher level of anxiety and hyperlocomotion. This enhanced distance covered was lessened upon ICAM-1 administration (0.5 $\mu$ g/kg b.w.) in cortical A $\beta$ -infused rats which showed that the anxiety level seemingly reduced with the treatment (Fig. 2A). Furthermore we wanted to check the effect of ICAM-1 on passive avoidance test which highlights the formation of short term memory in rat brain. Results showed that the A $\beta$ -infused animals on the probe day displayed a significantly reduced wait latency suggesting memory loss as compared to the PBS infused. However, unlike the OFT, in passive avoidance test, ICAM-1 treatment failed to show the recovery in wait latency of A $\beta$ -infused rats explaining that the administration of ICAM-1 did not improve short term memory in cortically infused A $\beta$  rats (Fig. 2B,C).

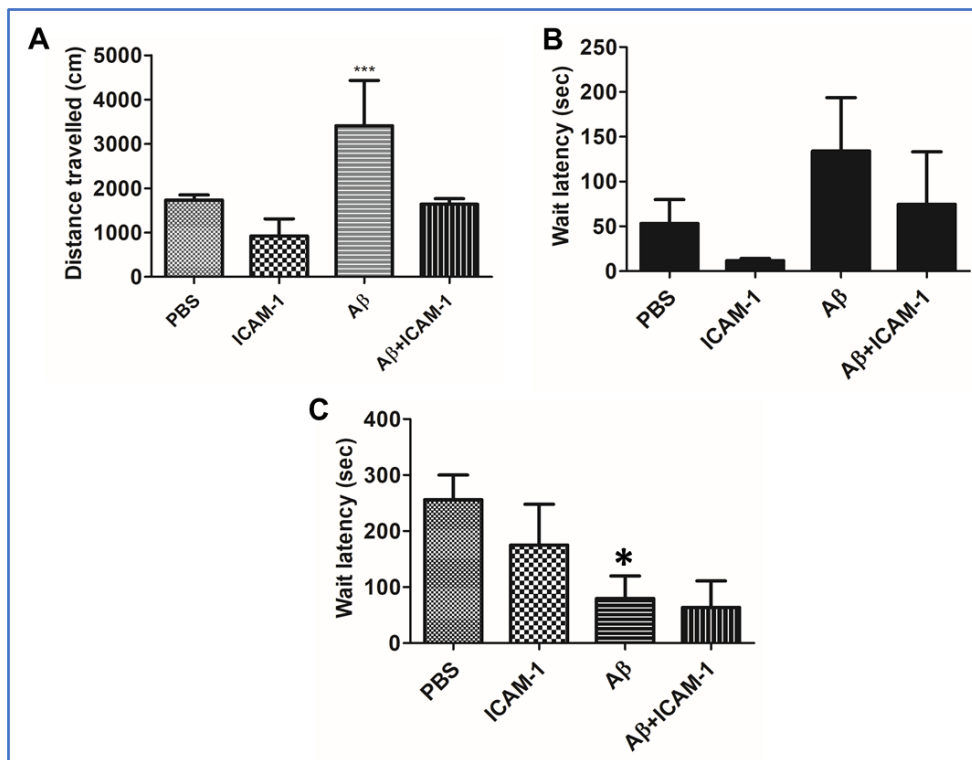


**Figure 2:** Adult rats were infused with 5 $\mu$ l of 100  $\mu$ M oligomeric A $\beta$ <sub>1-42</sub> within brain cortex bilaterally followed by an I.P. systemic administration of rrICAM-1(0.5 $\mu$ g/kg b.w.).(A)Open field test (OFT) showing distance covered by rats, induced by A $\beta$  (\* $p$  < 0.01) was significantly reduced by rrICAM-1 (# $p$ <0.01). (B,C) Passive Avoidance test: The graph represents the significantly lower wait latency time of A $\beta$  groups as compared to the PBS infused control (\* $p$  < 0.05) but no improvement was observed in wait latency among the A $\beta$ +ICAM-1 groups on the probing day. Data set represent the mean  $\pm$  SEM of three independent experiments.

Furthermore the associated memory tests namely the contextual and the cue dependent memory learning test were performed among all the experimental groups of animals. This test is specifically performed to elucidate the associated memory improvement by the implanting fear memory in animals with the help of a series of foot shocks. After several single and multiple trials too, the A $\beta$  infused animals did not show any reduction in the freezing % both in presence and absence of ICAM-1 (Fig.3A-C).

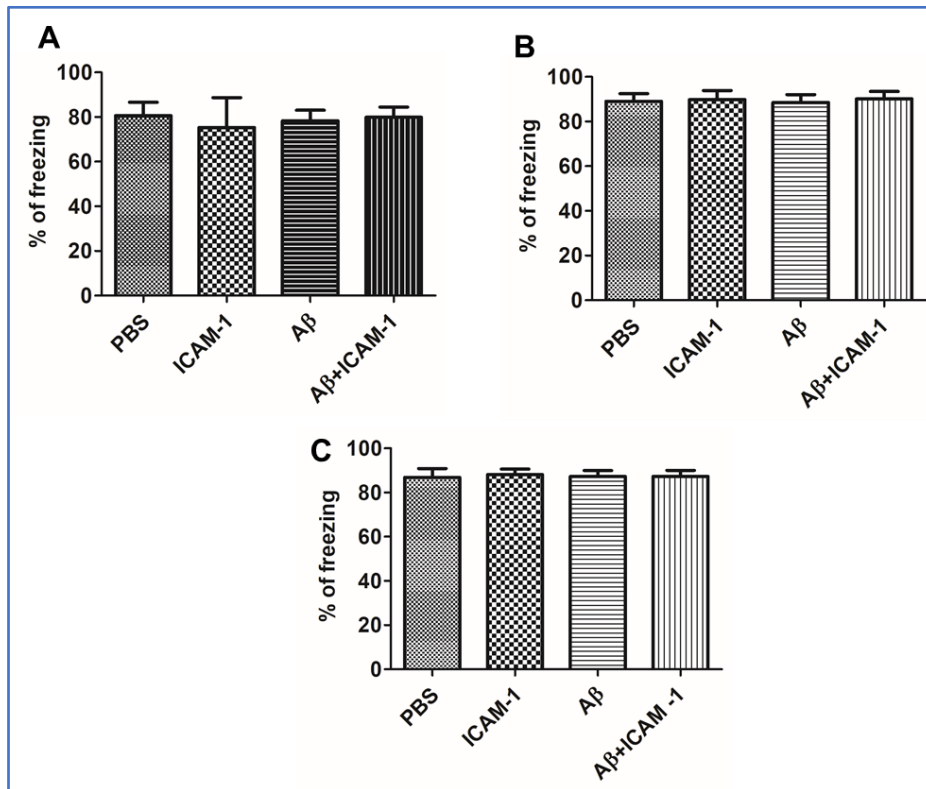


**Figure 3:** To analyze the short term memory retention and cognitive behavior fear conditioning was performed in the A $\beta$  infused rats with or without the intraperitoneal injection of rrICAM-1. **(A)** The graphical data represent non-significant freezing % among all the treated groups of animals. Values are expressed as mean  $\pm$  SEM of three independent experiments. **(B,C)** Cue dependent fear conditioning performed in the rodent groups in single and multi-shock trial. Graphical expression shows unaltered freezing% in all individual treated group. All data have been shown as mean  $\pm$  SEM of three independent experiments.

These results clearly showed that even though infusion of A $\beta$  in the cortical region of brain could result in formation of A $\beta$  plaque and initiate the cell death, yet the model was not suffice to establish a behavioral assessment study of AD. Animal behavior is mainly governed by the hippocampus along with amygdala and entorhinal cortex (Anand and Dhikav, 2012). So in order to establish an animal model to check whether ICAM-1 had any role in improving the behavior in AD rats, bilateral hippocampal infusion of A $\beta$  in rat brain was performed.

## rrICAM-1 causes A $\beta$ load reduction and reduces cellular death in hippocampally A $\beta$ -infused rat model of AD

ICAM-1 finds a primary expression in glial cells, especially in astrocytes and microglia of the CNS (Müller N., 2019). Also report shows that hUCB-MSC is a good source of ICAM-1 which, on transplantation in hippocampus helps in reducing the A $\beta$  plaques in an AD transgenic mouse (Kim *et al.*, 2012). Thus the effect of systemic administration of ICAM-1, may have a chance in facilitating A $\beta$  clearance in A $\beta$ -infused rat brain. To obtain a definitive insight into the fact that ICAM-1 contributes in significantly reducing the A $\beta$  plaque accumulation in rat hippocampus, immunohistochemical studies of rat brain slices were done by probing them with A $\beta$  protein. This revealed a significant reduction in A $\beta$  plaque numbers along with decrease in A $\beta$  plaque burden (~2-4 folds) in hippocampal regions of A $\beta$ -infused rats upon ICAM-1 (0.5 $\mu$ g/kg body weight) treatment (Fig 4A-C).

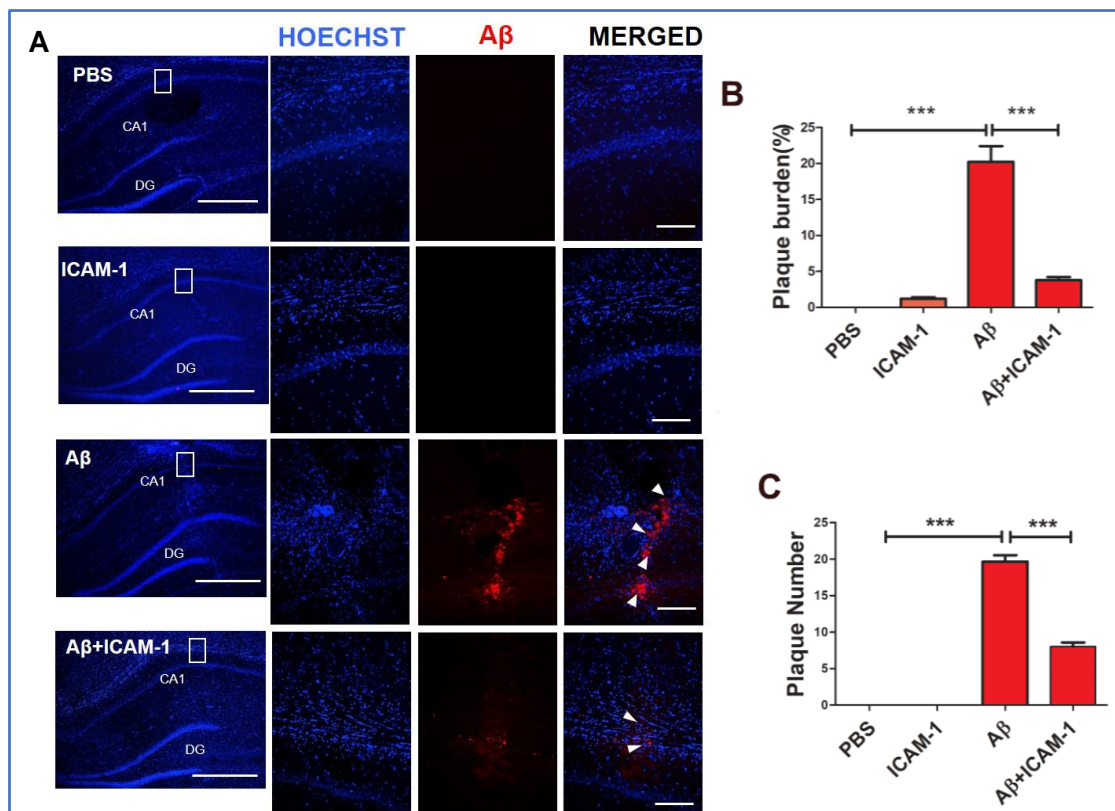




**Figure 4:** (A) Fluorescence imaging of hippocampal slices was done after immunostaining with anti-A $\beta$  antibody. The left vertical panels show the 5x image of the hippocampus and cortex regions of rat brain of all experimental groups (scale bar: 200  $\mu$ m). Remaining panels show the respective 20x images of the same. (left to right: Hoechst, A $\beta$ , merged. Scale bar: 50 $\mu$ m). (B-C) Bar diagrams show significant reduction in A $\beta$  plaque number and % plaque burden respectively with rrICAM-1 treatment. n = 3 for each group, 3 slices of each rat brain:

In order to check the plaque reduction further, we performed Congo-red staining and immunohistochemical analysis by DAB staining in the hippocampal site of infusion (HCSI) of the brain. DAB staining revealed the significant reduction in plaque burden with ICAM-1 administration in vivo (Fig.5A-C).

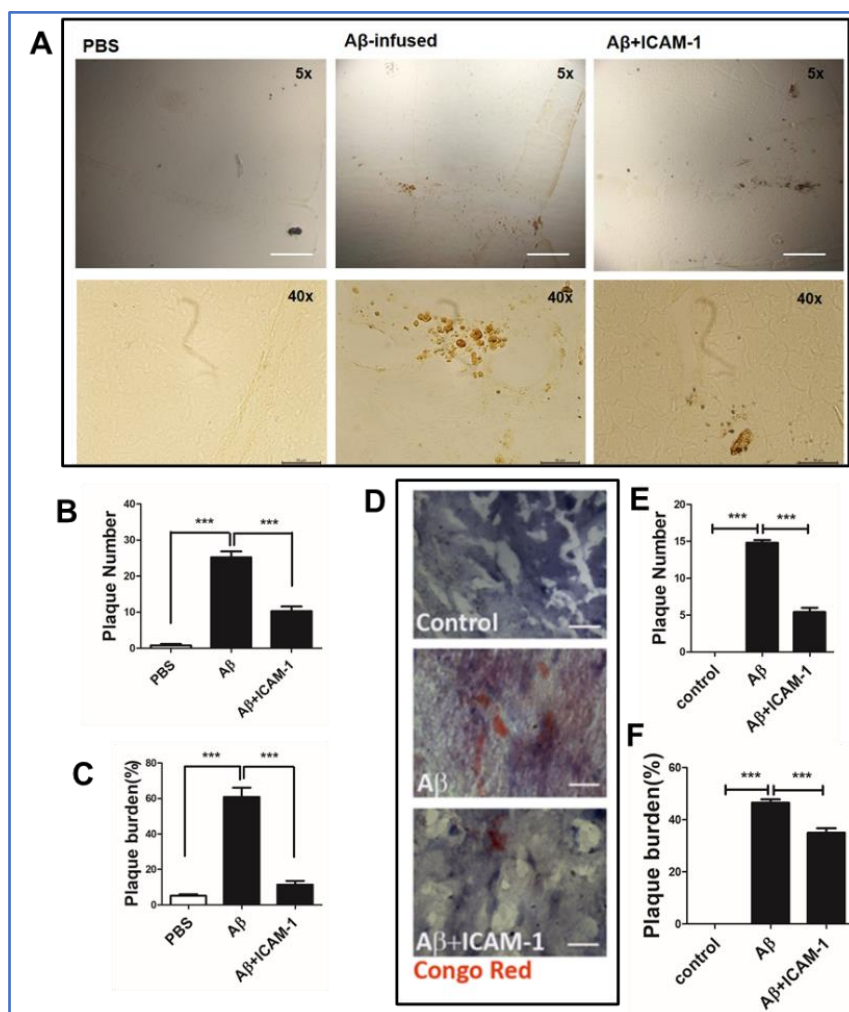


**Figure 5:** (A) DAB imaging of brain slices was done after immunostaining with anti-A $\beta$  antibody. The upper horizontal panel shows the 5x image of adult rat brain slices of all experimental groups along with the plaque formation at the infusion site, scale bar: 200 $\mu$ m. The lower horizontal panels depict the 40x images of all the experimental groups, scale bar:50 $\mu$ m. (B-C) Bar diagrams show significant reduction in A $\beta$  %plaque burden and plaque number respectively with rrlCAM-1 treatment. n=3 for each group, 3 slices of each rat brain:\*\*\*p<0.0001. (D) 40x bright field images of Congo red staining of hippocampal slices from A $\beta$ <sub>1-42</sub> infused rat brains are showing the A $\beta$  plaque formation and reduction in plaque burden and number while treating the same with rrlCAM-1 (0.5 ug/kg body weight). (E-F) Bar diagrams show significant reduction in plaque number and % plaque burden respectively. n = 3 for each group, 3 slices of each rat brain, \*\*\*p < 0.0001, scale bar: 20  $\mu$ m.

The Congo-red staining showed a decrease of about 3 folds in A $\beta$  plaque numbers and almost 20% reduction in plaque load in the hippocampal region in rrlCAM-1 treated A $\beta$ -infused rats. Graphical representation of image was obtained by plotting the plaque burden and plaque number among the untreated and treated groups (Fig. 5D-F).

Next, hippocampally infused AD rats were used to assess the effect of rrlCAM-1 on apoptosis in hippocampus in vivo. On 14th DPI, the rats were given IP injection of rrlCAM-1 with doses 0.25 $\mu$ g/kg and 0.5 $\mu$ g/kg b.w. for 11 days alternately. To check apoptosis, we performed TUNEL staining in the hippocampus. In tissue sections from A $\beta$ -infused rats, the % of TUNEL+ve cells were found to be significantly higher in hippocampal regions than the control sections. In contrast, the numbers of TUNEL positive cells were observed to be reduced on a significant amount when rrlCAM-1 was administered intra-peritoneally (Fig.6)

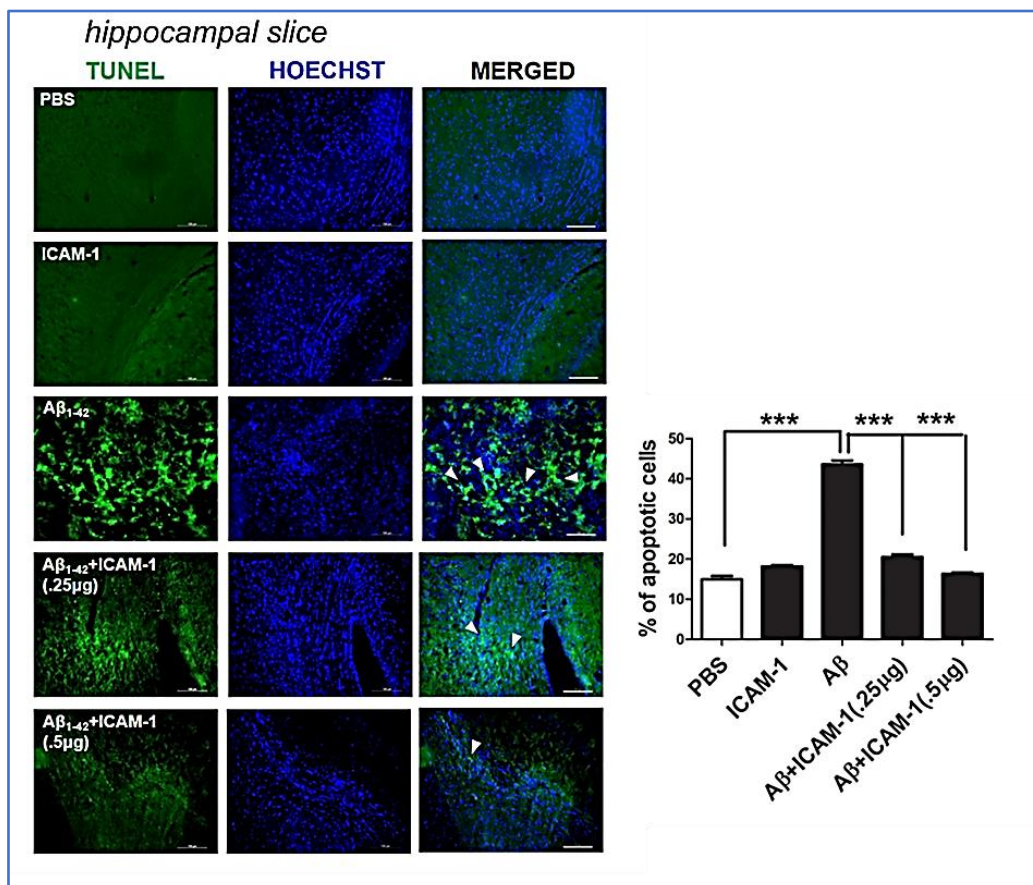


**Figure 6:** Apoptosis showed in the hippocampal region of various control and treated groups of rats 24 DPI of A $\beta$  infusion. The 3 vertical panels show the 20x images (left to right) – TUNEL, Hoechst, and Merged. Each row represents each experimental group, Control, ICAM-1, A $\beta$ , A $\beta$  + ICAM-1 (0.25  $\mu$ g/kg b.w.) and A $\beta$ +ICAM-1(0.5  $\mu$ g/kg b.w.). A $\beta$ +ICAM-1 treated groups displayed a significant reduction in the apoptotic cells % compared to A $\beta$  only group. Right panel shows the bar diagram depicting the % apoptotic cells among all the various experimental groups (n = 3 for each group, \*\*\*p < 0.0001).

So it could be concluded that these in vitro and in vivo data indicate that ICAM-1 contributes to A $\beta$ -ACM mediated neuroprotection and protects neurons against A $\beta$  if administered exogenously.

## **Administration of ICAM-1 leads to enhancement in cognitive functioning in A $\beta$ -infused rat model of AD**

Several reports have shown that the major area of brain which control the memory and cognitive behavior in rodent is primarily the hippocampus, along with associated memory formation by the entorhinal cortex and amygdala (Preston and Eichenbaum, 2013). With a failure to observe an improvement in behavior of cortically infused rats, the task was taken up to establish the hippocampal infusion model of AD to check for the behavioral changes if any. A $\beta$  was infused in the near CA1 region of the hippocampus in brain bilaterally at stereotaxic co-ordinates from bregma: AP: 3.6, L: 2.1, DV: 2.8 mm.

To check the anxiety levels of the rodents, all experimental sets of animals were made to perform an open field test (OFT). A $\beta$ -infused animals displayed higher locomotory activity compared to PBS treated control animals. However, rrICAM-1 administration (0.5 $\mu$ g/kg b.w.) in A $\beta$ -infused rats showed a reduced distance travelled in open platform indicating an improvement in the anxiety level (Fig.7A). Additionally the rats displayed a reduced anxiety level upon ICAM-1 administration as the %centre distance covered increased significantly on treatment as compared to the A $\beta$ -infused rats (Fig. 7B). To further validate the role of ICAM-1 on anxiety and memory in rodents, the elevated plus maze (EPM) study was performed. A $\beta$  infusion in rats showed increased retention transfer latency (RTL) as compared to the initial transfer latency (ITL) and rrICAM-1 treatment helped in decreasing RTL than ITL. ITL–RTL being considered as an important parameter to determine the cognitive memory ability in the EPM test, showed a negative difference in A $\beta$  infused animals. Contrastingly, on rrICAM-1 treatment A $\beta$ -infused rats showed a positive recovery in the ITL-RTL values indicating cognitive memory got improved by it (Fig. 7C).

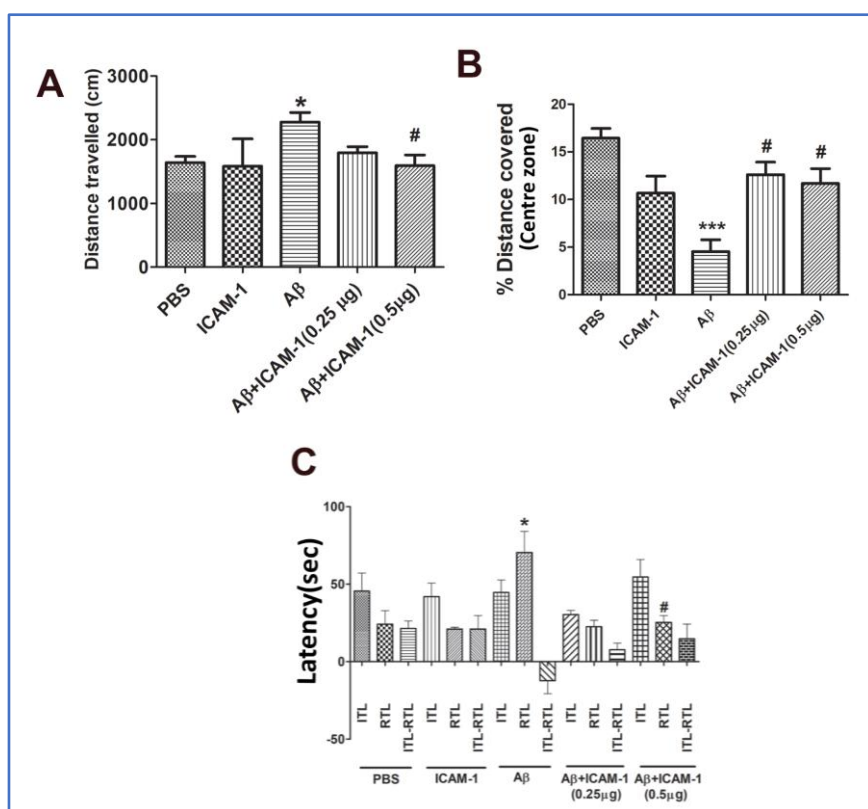


**Figure 7:** Aβ-infused adult rat following the intra-peritoneal administration of rrICAM-1 (0.25 μg/kg b.w. or 0.5 μg/kg b.w.) every alternate day after 11 days, were subjected to various behavioural tests prior to being sacrificed at day 24. **(A,B)** Open field test (OFT) showed that the total distance travelled (cm), induced by Aβ (\*p<0.05) was significantly reduced by 0.5μg/kg b.w. of rrICAM-1 (#p<0.05) along with a significant recovery in the % central distance covered in the same (\*p<0.01). **(C)** In Elevated plus maze test (EPM), retention transfer latency (RTL) on day-2 was significantly less than the initial transfer latency (ITL) on day-1 in all the experimental groups except Aβ animals (\*p<0.05). The difference between ITL and RTL (ITL-RTL) was significantly negative for Aβ group (\*p<0.05) which was reversed to positive values by treatment with 0.5 μg/kg b.w. of ICAM-1 (#p<0.05). Values are expressed as mean ± SEM. (\*) indicates p-values in comparison to PBS group and (#) indicates p-values in comparison to Aβ group.

To further detect the effect of ICAM-1 administration in determining the eagerness of the subject to explore novel objects and memory retention of the same, an additional cognitive task, Novel Object Recognition test was performed. Animals were allowed to explore two similar objects on an open arena on the first day and one of the object

was replaced with a one with different shape and color to determine the exploratory interest of the subject on the novel one the next day. Results showed that loss in ability to recognize the novel object was evident in the A $\beta$  infused animals along with a significant reduction in preference (PI) and discrimination index (DI) in contrast to the control animals. However rrlCAM-1(0.5 $\mu$ g/kg b.w.) treatment, enabled the A $\beta$  infused rodent group to significantly increase the novel object exploration time along with an enhanced PI and DI score. This strengthened the proposal that ICAM-1 positively escalates the recognition and learning memory in A $\beta$ -infused rats (Fig. 8A-C).

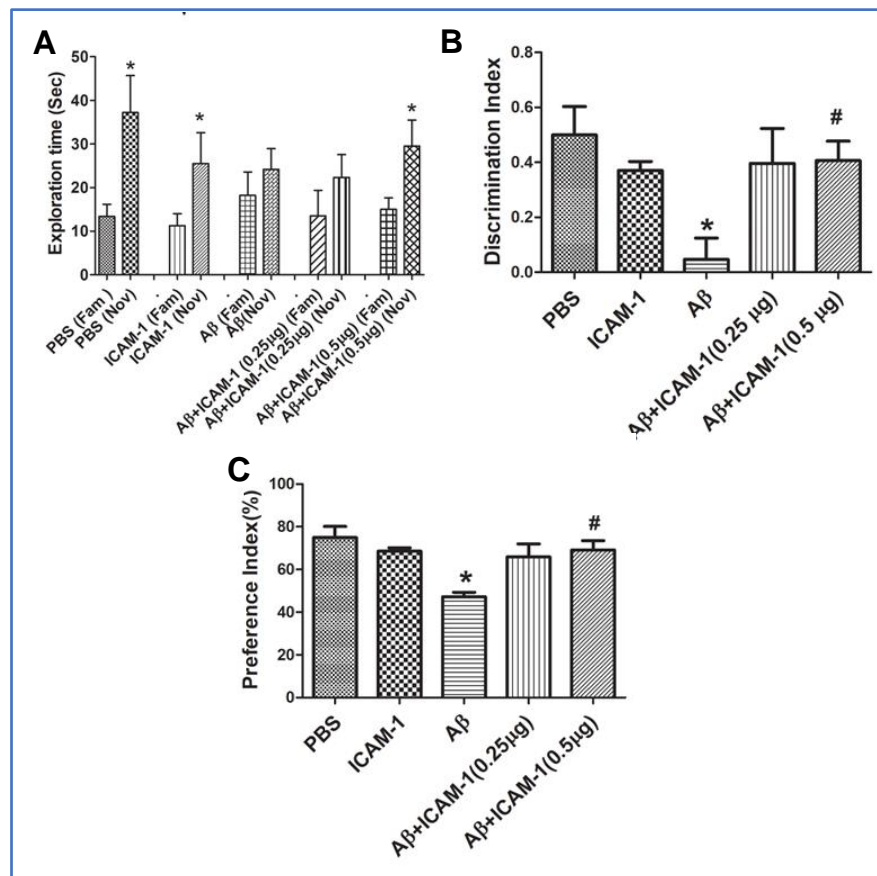


**Figure 8:** Novel object recognition test performed and compared to PBS and ICAM-1 only treated groups both in presence and absence of A $\beta$ . (A) Exploration time taken by A $\beta$ -infused animals at the novel (Nov) object were less than the familiar (Fam) object while A $\beta$ +ICAM-1(0.5  $\mu$ g/kg b.w.) group

found to spend longer time with the novel object than familiar one(\*p < 0.05). **(B)** Preference index for the novel object was significantly lowered in the A $\beta$  group(\*p<0.05) while it was recovered in the A $\beta$ + ICAM-1 (0.5 $\mu$ g/kg b.w.) group (#p<0.05). **(C)** A $\beta$ -infused animals gave a negative discrimination index value (\*p<0.05) while for A $\beta$  + ICAM-1 (0.5 $\mu$ g/kg b.w.) group, it was improved (#p<0.05).

Next, Passive Avoidance test which employs the principle of the innate nature of the animal of preferring a dark niche was performed. The A $\beta$ -infused animals on the probe day displayed a lower wait latency suggesting a suffered memory loss in comparison to the control rats. It was interesting to note that after treating with ICAM-1, animals showed increased wait latency in returning to the dark chamber as compared to A $\beta$  infused ones, explaining the therapeutic role of ICAM-1 leading to recovery of lost memory among the subjects (Fig.9A,B).

Finally, to assess the most essential task which directs towards learning memory formation, fear conditioning test was done among the experimental subjects providing an insight into the tendency of an animal to potentially recall and act to the false fear context while being enclosed within the dark chamber. In contextual fear conditioning test, the mean value of the %freezing of four trials is measured in the probe stage. The A $\beta$ -infused animals displayed much lesser freezing% in comparison to the control animals. This indicated the loss in acquisition of contextual fear conditioning on following day. However administering ICAM-1(0.5  $\mu$ g/kg b.w.) into the A $\beta$ -infused rats improved their percent freezing. This clearly showed that the substantial memory was recovered along with an improvement in cognitive functioning (Fig.9C,D). Also the cue dependent fear conditioning was also performed, but no significant change was observed within the group of rodents, control and A $\beta$  treated.

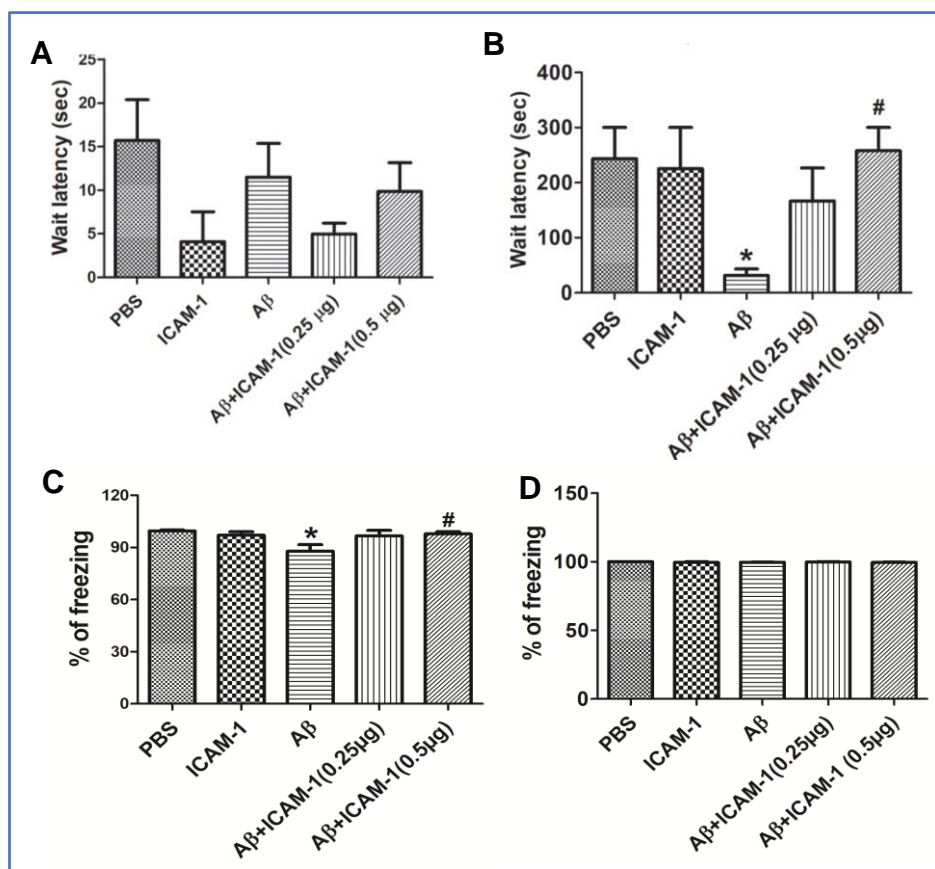


**Figure 9: (A,B)** Passive Avoidance test - the graphs represent the significantly lower wait latency time of A $\beta$  groups (\* $p$ <0.05) and a significant regain in wait latency in the A $\beta$ + ICAM-1 (0.5 $\mu$ g/kg b.w.) group on the probe day (# $p$ <0.01). Data set represent the mean  $\pm$  SEM of three independent experiments: \* $p$ <0.05. (\*) indicates p-values in comparison to PBS group and (#) indicates p-values in comparison to A $\beta$  group. **(C)** Graph indicating the Contextual fear conditioning among A $\beta$ -infused rats in presence and absence of rICAM-1 and freezing % was significantly attenuated in A $\beta$ -infused rats (\* $p$ <0.05) whereas this effect was significantly recovered by ICAM-1 treatment given at a dose of 0.5 $\mu$ g/kg b.w. (# $p$ <0.05). **(D)** Graph showing no significant change among the animal groups on conducting the cue dependent fear conditioning with multiple trials.

Taken together, these findings show that A $\beta$ -infused rats on administration of ICAM-1 intraperitoneally leads to decreased A $\beta$  load in various parts of brain like the cortex



and hippocampus and helps in improving the impaired memory and cognitive functioning of the subjects.

## **Discussion**

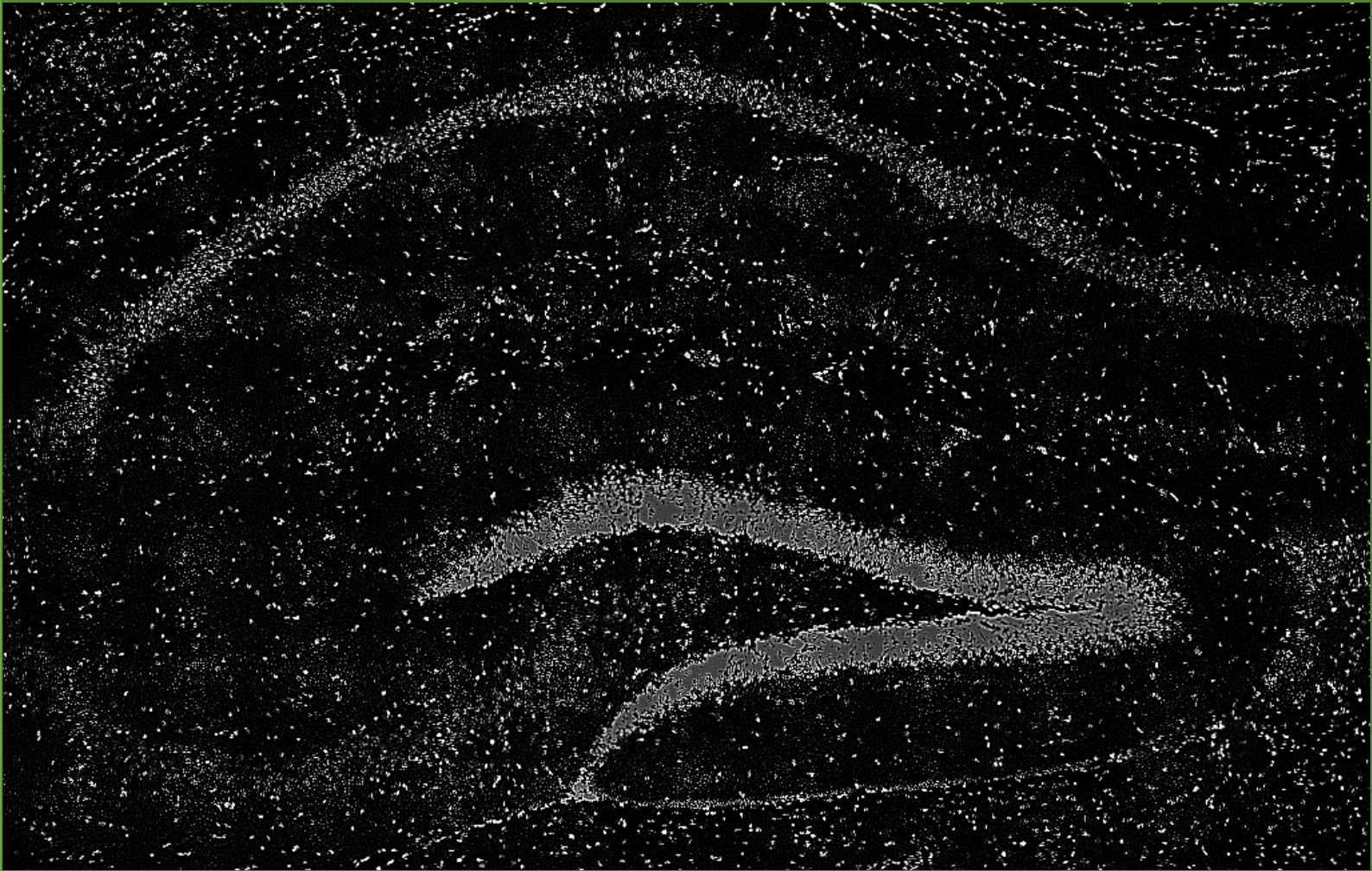
AD has always been one of the most complicated diseases whose underlying mechanism still remain to be elucidated. The post mortem brains of the affected patients have shown degenerating neurons and synapses with diverse accumulation of A $\beta$  plaque and Neurofibrillary Tangles. Scientists have tried various therapy in human and animal model systems to stall the disease and check if the reversal of the memory loss is ever possible.

To therapeutically target AD on previous occasions, several organic and inorganic factors have been tried and tested to check whether they can cause any reduction in accumulated A $\beta$ . For instance, protein kinase A (PKA) and acetyl choline inhibitors when administered have had a decline in the accumulating A $\beta$  plaque along with its production (Su et al., 2003; Huttunen et al., 2009). Also inhibitory agents of zinc and O-glycosylation stalled the APP maturation finally causing a significant decrease in formation of A $\beta$  (Lee et al., 2009; Tomita et al.,1998). Involvement of cytokines, being an intriguing factor, was cultivated to check the attenuating process of AD progression. In our study, we have tried to dig deep into the probability of using cytokine like ICAM-1 as a major factor which might help in reducing the A $\beta$  plaque load. Intraperitoneal ICAM-1 administration showed a significant decrease in plaque load and burden in A $\beta$  infused models of AD (both cortical and hippocampal) along with reduction in the apoptotic cells in brain as indicated by TUNEL assay. The detailed mechanism underlying the process of reducing A $\beta$  may still be scrutinized in details. Some of the earlier reports suggested involvement of several enzymes like

IDE, MMP and neprilysin which often help in cleaving the specific A $\beta$  plaque and reducing the extracellular accumulation of the same. Besides targeting the  $\alpha$  and  $\gamma$ -secretase enzymes is also another mode which has been targeted by various scientists to check the inhibition of A $\beta$  production and maturation in cases of AD.

The extreme interest towards the impaired cognitive functioning as a major symptom of AD onset has been nurtured by clinicians and scientists globally since a long time. Previously in our lab, detailed experiments have shown that cytokine like TIMP-1 when administered within the brain has improved the cognitive functioning of rats affected with AD (Saha *et al.*, 2020). Also use of various acetyl cholinesterase inhibitors and NMDA inhibitors has shown an improvement in behavioral pattern of various subjects of AD. In our study we have tried to find out the effect of ICAM-1 on degenerative behavioral anomaly of A $\beta$  infused rats. Initially rats having A $\beta$  infused in the cortical area were subjected to behavioral analysis in presence of ICAM-1. However not much changes were observed in the cortically A $\beta$  infused rodent groups only to suggest that infusing A $\beta$  in cortical region was not sufficient to establish the AD model. Reports are there which have shown that memory functioning is influenced primarily by the specific regions of brain namely the hippocampus, entorhinal cortex and amygdala which led us to establish the AD model by infusing the A $\beta$  in the hippocampus CA1 region of the rat brain. On systemic infiltration of rat recombinant ICAM-1 by injecting it intraperitoneally several cognitive functioning tests like open field test, elevated plus maze along with novel object recognition tests showed significant improvement in lost memory and cognition suggesting that ICAM-1 could play a potent role in recovering the brain functioning in AD rats. Furthermore, improvement in associated memory learning by

various fear conditioning test with ICAM-1 treatment really suggested an avenue for further therapeutic possibility.



# Chapter:3

Role of ICAM-1 in improving cognition in 5xFAD model and identifying its underlying mechanism

## Introduction

Genetic mice models of AD have contributed tremendously to obtain a detailed insight into the functionality of various active and inactive genes related to the disease. For e.g. transgenic mouse model has been made by mutating the basic genes like APP, secretases including BACE, presenilin-1 and 2, and ADAM 10 and 17 (Shen et al., 1997; Herreman et al., 1999 ; Luo et al., 2001; Hartmann et al.,2002; Lee et al., 2003). Also tau knockout mice models have contributed invaluablely in unearthing the underlying mechanism behind the complex disease mechanism. The major objective behind our work was to initiate the identification of a factor which would eventually help to procure a remedy or at least stall the process of neurodegeneration. To do so, previously in our experiments, A $\beta$  was infused within the hippocampus of rats resulting in a model to identify the effect of ICAM-1 on the same. Furthermore keeping in mind, the progressive nature of the disease and the genetic mutations responsible for the cause, 5xFAD mouse model was used to assess the utility of ICAM-1 in improving the pathology of AD in vivo. 5xFAD mouse model widely used globally is known to have five major mutations. They are Swedish (K670N/M671L), Florida (I716V), and London (V717I) mutations occurring in APP gene, and M146L, L286V mutations in PSEN1 gene enabling scientists to consider it to be a sufficiently suitable model for studying AD pathology. We have tried to check here whether ICAM-1 helps to improve the cognitive behaviors and anxiety in 5xFAD mice. Anxiety tests like open field test and elevated plus maze have been performed to detect the improvement if any in the transgenic mice subjects. Besides other recognition tests, learning memory tests have been performed too with the help of fear conditioning programs.

In 2012 Kim et al. showed that mesenchymal stem cell derived from human umbilical cord blood cells was able to secrete sICAM-1. They reported for the first time that within such a system, not only the protein helped in reducing A $\beta$  plaque load, with enzyme neprilysin but also nurtured the dying neurons helping in preventing their death. So in our study, we searched for appropriate role played by ICAM-1 in improving the degenerative cognitive behaviour and whether neprilysin helped in reducing the A $\beta$  loads in 5xFAD mouse model mimicking familial AD.

Another essential aspect towards installing therapy mediated remission of certain disease is to identify the player molecule which undergoes differential regulation resulting in corresponding signaling cascades. Various pathways like the MAPK pathway, mTOR signaling etc. have been known to get altered during the onset and later stages of AD. However, whether and how ICAM-1 helps the system to overcome these dysregulation and contribute in stalling the disease is still unknown. In our scientific venture we have delved into the details of the signaling which may play a role in ICAM-1 mediated neuroprotection. Several pathway screening had been performed to find the real player and its definitive role in improving cognitive functioning in 5xFAD model of AD.

## Results

### Characterization of 5xFAD mice model

There are several reports regarding the age of AD related pathology onset in 5xFAD mice but not much has been reported regarding the age to be considered which would help in analyzing the behavioral improvement. To determine the anxiety level onset in the transgenic mice, control C56/BL7 and the 5xFAD mice of age 2 months to 7 months were subjected to open field test where results clearly indicated that from 5 months, the mice started displaying an agitative nature. All the mice from 5 months of age and higher, travelled a greater distance and thus showed their hyperactive nature as compared to the control mice (Fig. 1A-E).

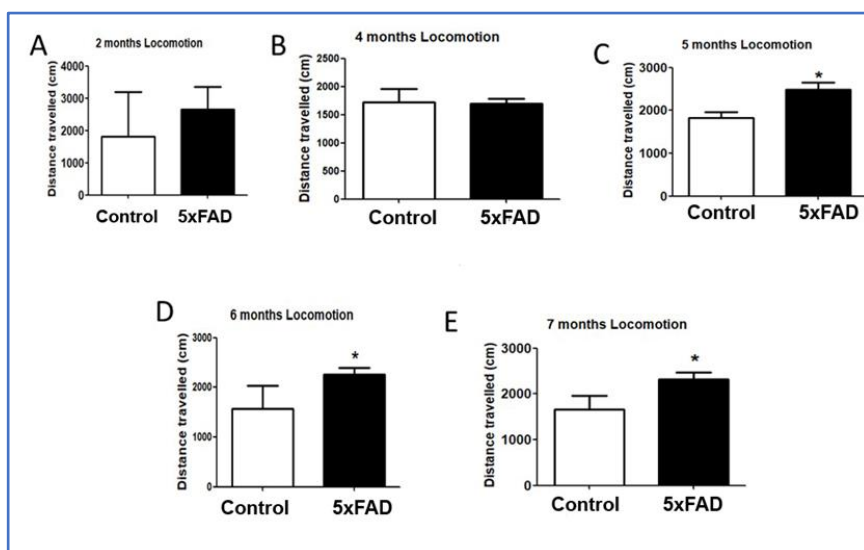


**Figure1:** Graphical representation of behavioural study in 2-7 months old 5xFAD mice. (A-E) Locomotory activity of all control and treated group of mice was tested by open field test (OFT). Bar diagrams show the significant hyperactivity in mice emphasizing their anxiety in age dependent manner starting from 5 months (\* $p < 0.05$ ).

Furthermore to check the onset of plaque formation, 20 $\mu$ m cryo-sections of the transgenic mice brain were taken and subjected to immunohistochemistry with DAB

staining against A $\beta$ . The microscopic images of the age dependent transgenic mice clearly showed that plaque formation was evident from 2months of age, the progression being in correlation to the increasing age (Fig. 2).

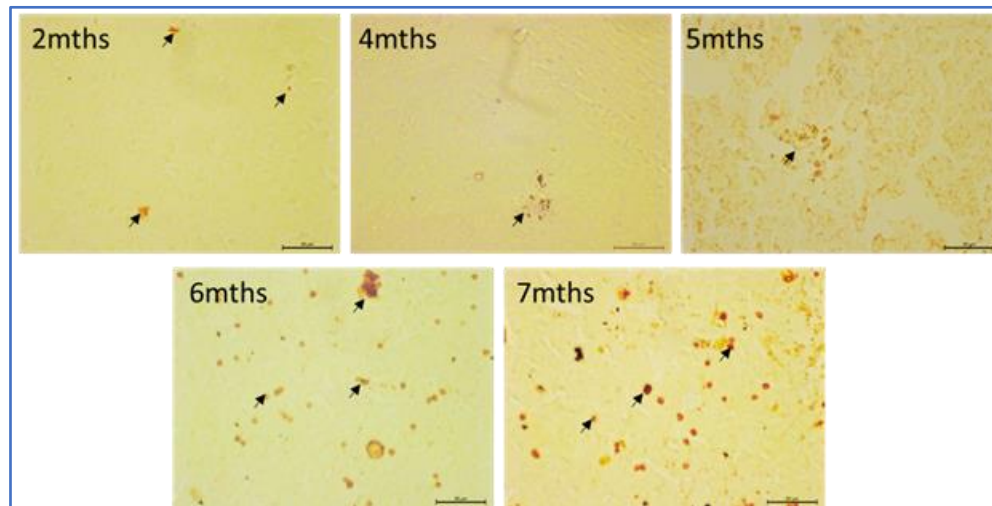


**Figure 2:** Age dependent formation of A $\beta$  plaque in 5xFAD transgenic mice. Immunostaining with DAB against A $\beta$  was performed in 20 $\mu$ m cryo-sections of fixed 5xFAD mice brain of different ages as indicated in the figure. 40x bright field images showing increase in A $\beta$  plaque formation from 2-7 months. Arrow indicates plaques formed in brain, scale bar: 50 $\mu$ m.

### **ICAM-1 reduces TUNEL+ve cells in 5xFAD mice brain**

Next, we used WT and 5xFAD transgenic mice to assess the effect of rrICAM-1 on apoptosis *in vivo*. The mice were subjected to I.P. injection of rrICAM-1 (1 $\mu$ g/kg b.w.) on alternate day for 21 days until sacrifice. We performed TUNEL staining in the brain sections to check the apoptosis both in hippocampal and cortical brain regions. In tissue sections from 5xFAD mice, the % of TUNEL-positive cells were found to be significantly higher in both cortical and hippocampal regions than the control (WT) sections (Fig. 3, Fig. 4). In contrast, the numbers of TUNEL positive cells were found to be decreased significantly in both the brain regions when rrICAM-1 was administered intra-peritoneally (Fig. 3, Fig. 4). Taken together, these *in vitro* and *in*



*in vivo* data indicate that ICAM-1 contributes to A $\beta$ -ACM mediated neuroprotection and protects neurons against A $\beta$  if administered exogenously.

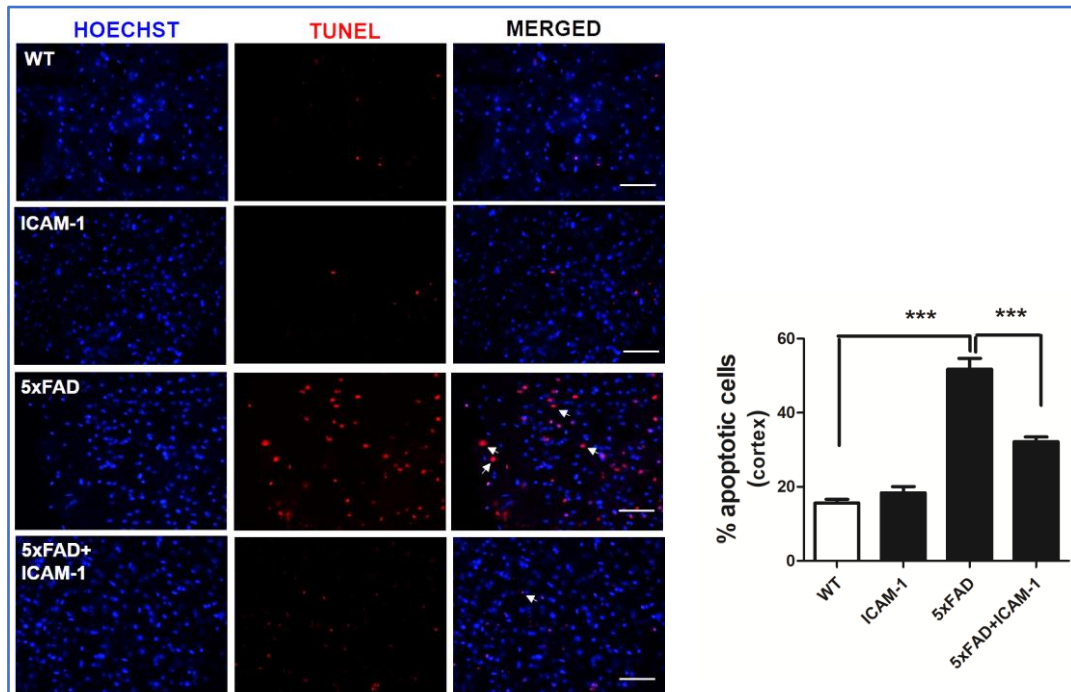


**Figure 3:** Apoptosis in the cortical regions of the different treatment groups of wild type and 5xFAD mice. The 3 vertical panels show the 20x images (left to right) – Hoechst, TUNEL and merged. Each row represents each experimental group: WT, ICAM-1, 5xFAD, and 5xFAD+ICAM-1 (1 $\mu$ g/kg b.w.). 5xFAD+ ICAM-1 treated group showed a significant reduction in the % of apoptotic cells compared to A $\beta$  alone group (n = 3 for each group, 3 slices of each rat brain, 500 cells/ slice at 20 $\times$  magnification: \*\*\*p<0.0001(scale bar: 30 $\mu$ m).

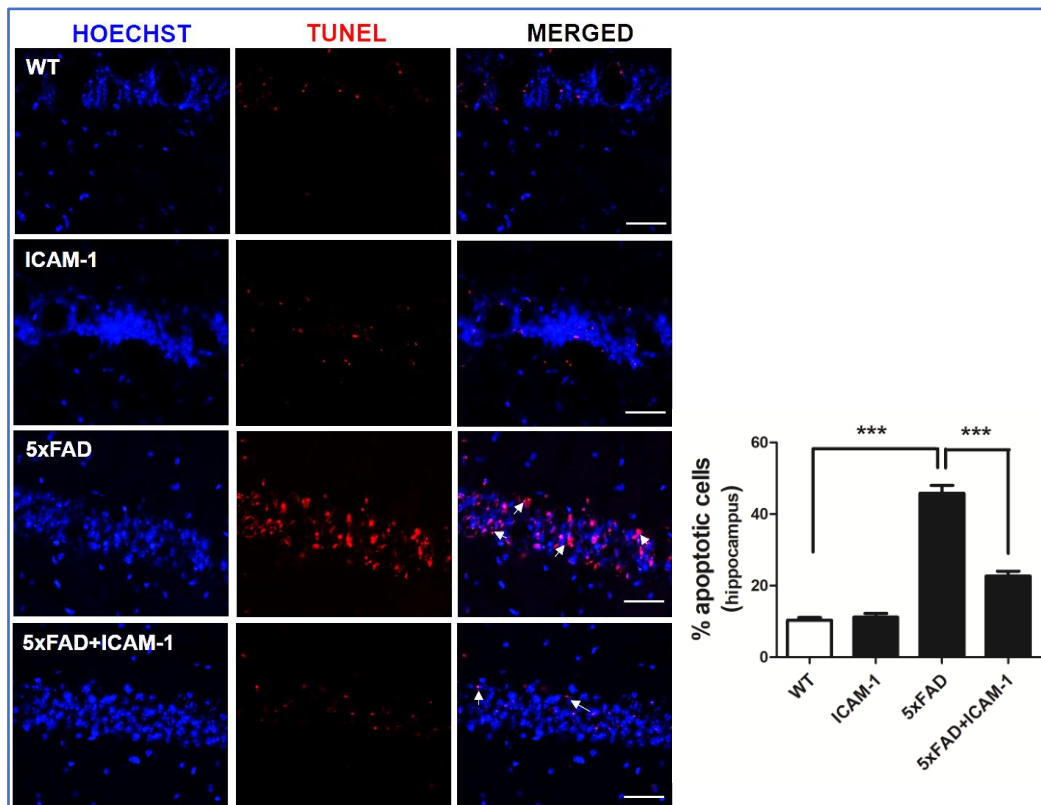


**Figure 4:** Apoptosis in the hippocampus of the different WT and 5xFAD treatment groups. The 3 vertical panels show the 20x images (left to right)—Hoechst, TUNEL and merged. Each row represents each experimental group, WT, ICAM-1, 5xFAD, 5xFAD+ICAM-1 (1µg/kg b.w.). 5xFAD+ICAM-1 treated groups showed a significant reduction in the % of apoptotic cells compared to 5xFAD alone group (n=3 for each group, 3 slices of each rat brain, 500 cells/ slice at 20x magnification) \*\*\*p<0.0001 (scale bar: 30 µm).

### ICAM-1 treatment reduces Aβ plaque and increases neprilysin in 5xFAD mice model

From our previous experiments performed in Aβ infused rat brain, it was seen clearly that ICAM-1 was quite efficient in reducing the accumulated plaque number and burden both in cortex and hippocampus. Many earlier reports also suggest reduction in Aβ plaque as a therapeutic strategy to deal with ushering neurodegeneration of AD. Several enzyme like the neprilysin, metalloproteinase (MMP) and IDE have been identified with ability to degrade Aβ aggregates (Iwata et al., 2001; Iwata et al., 2000). Next, we sought to look whether administration of rrlCAM-1 produced

any similar recovering effect in transgenic mouse brain or not. To check that, 5 months old 5xFAD mice were subjected to intraperitoneal injection of rrICAM-1 on every alternate day for 21 days until sacrifice. Perfused brains were subjected to cryosectioning. Immunohistochemistry of brain slices of ICAM-1 treated 5xFAD mice, both in fluorescence and DAB staining, showed a significant decrease in plaque number and plaque load of A $\beta$  as compared to the 5xFAD mouse (Fig. 5A-C, Fig. 6A-C).

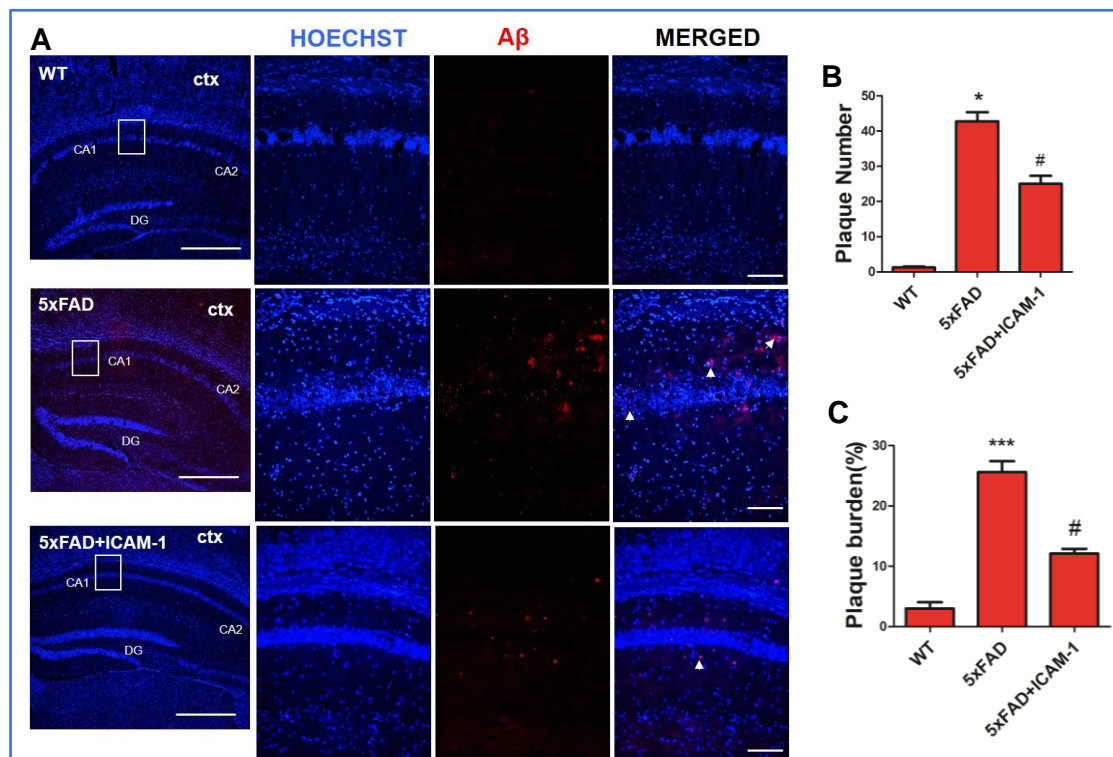


**Figure 5:** 5xFAD mice along with their wild type control C57BL/6 were treated with rrICAM-1 (1 $\mu$ g/kg b.w.). Immunostaining of hippocampus of all slices performed with anti-A $\beta$  antibody, were subjected to fluorescence imaging. (A) The first vertical panel shows the 5x image of HCSI region of mice brain of all experimental groups (scale bar: 200 $\mu$ m). The last three vertical panels depict the 20x images (left to right–Hoechst, A $\beta$  and merged), scale bar: 50 $\mu$ m. (B,C) Bar diagrams show significant reduction in A $\beta$  plaque number and % plaque burden respectively with rrICAM-1 treatment. n = 3 for each group, 3 slices of each rat brain: \*\*\*p<0.0001, \*p<0.01. # depicts \*p<0.01, showing significant decrease in plaque number and burden in 5xFAD+ICAM-1 as compared to 5xFAD mice.

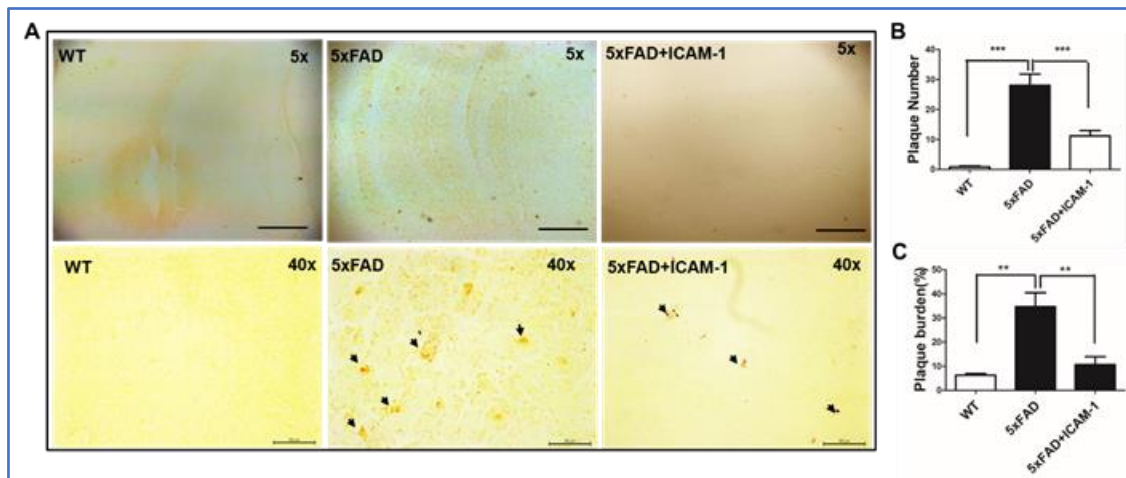


**Figure 6:** (A) 5xFAD mice along with their wild type control C56BL/7 were treated with rrICAM-1 (1  $\mu\text{g}/\text{kg}$  b.w.). Immunostaining of hippocampus of all slices performed with anti-A $\beta$  antibody, were subjected to DAB staining. The upper horizontal panel show the 5x image of HCSI region of mice brain of all experimental groups, scale bar: 200  $\mu\text{m}$ . The lower horizontal panels depict the 40x images (left to right – WT, 5xFAD and 5xFAD+ICAM-1), scale bar: 50  $\mu\text{m}$ . (B-C) Bar diagrams show significant reduction in A $\beta$  plaque number and % plaque burden respectively with rrICAM-1 treatment in 5xFAD mice.  $n = 3$  for each group, 3 slices of each mouse brain: \*\*\* $p < 0.0001$ , \*\* $p < 0.001$

Nephrilysin is one of the important enzymes that is able to degrade A $\beta$  aggregate and resist the accumulation of the A $\beta$  plaque burden. We checked the plaque load of 5xFAD mice at different ages starting from 2 months. We found that although A $\beta$  plaques appear even in 2 months but a substantial level reached by 5 months (Fig. 2) and thus we performed immunohistochemical analysis of neprilysin protein in brain sections of 5 months old 5xFAD mouse. Our results showed that upon ICAM-1 treatment, a significant increase in neprilysin expression (about 20%) takes place in the cortical region of this model (Fig. 7).

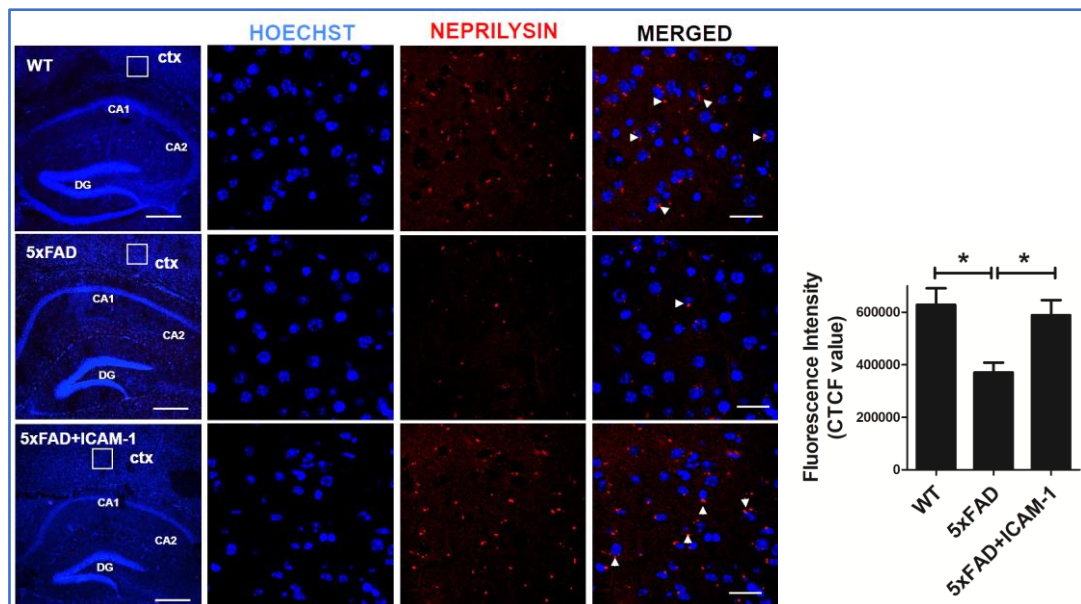


**Figure 7:** Fluorescence images of 5x (scale bar: 100 $\mu$ m) and confocal images of 40x (scale bar: 15 $\mu$ m) of brain slices of WT, 5xFAD and 5xFAD+ICAM-1 mice show neprilysin indicated in red, Hoechst in blue. Each row represents each experimental group: WT, 5xFAD and 5xFAD + ICAM-1 (1 $\mu$ g/kg b.w.): n=3 for each group, 3 slices of each rat brain \*p<0.01. Insets in 5x images shown as the 40x magnified images.

Collectively, these findings indicate that ICAM-1 decreases A $\beta$  plaque formation and burden of the same, through modulation of the expression of A $\beta$  degrading enzyme, neprilysin *in vivo* in a transgenic model of AD.

### **5xFAD transgenic mice show an improvement in learning and cognitive behavior with intraperitoneal administration of rrICAM-1.**

A $\beta$ -infused within rat hippocampus was more of an acute model which was obtained by injecting synthetic A $\beta$  locally, So to assess the systemic efficacy of ICAM-1 in AD transgenic model where multiple mutations were present, recovery in memory and cognitive functioning was checked in 5xFAD mouse. The 5xFAD mice were subjected to I.P. injection of rrICAM-1 in two doses (0.5 $\mu$ g/kg b.w. & 1 $\mu$ g/kg b.w.)

every alternative day until performance. Open Field Test showed significant decrease in total distance travelled by the rrICAM-1-5xFAD mice compared to the 5xFAD mice, whereas the % central distance travelled was increased in both the doses (Fig. 8A,B). To further ascertain whether ICAM-1 caused any further improvement in spatial memory and the reduction in anxiety of the cohort of mice, the experimental animals were subjected to Elevated Plus Maze test. The decrease in (ITL-RTL) in 5xFAD as compared to WT, was regained back on rrICAM-1 treatment (Fig. 8C). However, when anxiety test was performed in EPM, rarely any change was observed in 5xFAD as compared to the wild type C57BL/6 (Fig. 8D).

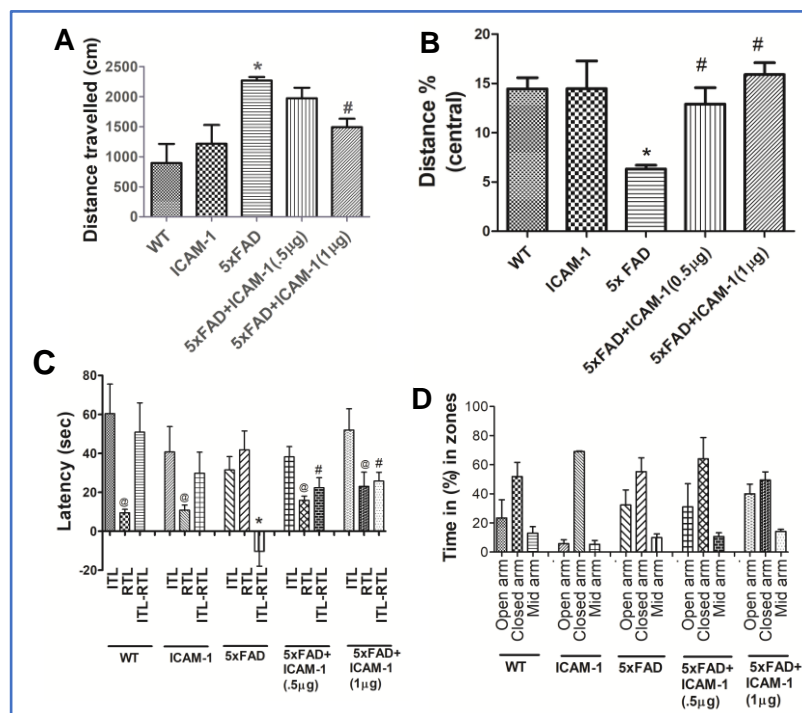


**Figure 8:** I.P. rrICAM-1 administered to 5 months-aged 5xFAD mice on alternative day for 21 days till sacrifice control being the C57BL/6(WT) injected with sterile PBS. (A-B) OFT of all experimental groups of mice showed a significant reduction in distance travelled along with an increase in the %central distance covered by 5xFAD+ICAM-1 (1µg/kg b.w.) group (#p<0.01) as compared to 5xFAD mice (\*p <0.005). Values are expressed as mean ± SEM of three independent experiments. (C) EPM test performed where, (RTL) on day-2 was significantly lower than (ITL) on day-1 among all

experimental groups except 5xFAD mice (@  $p < 0.05$ ). The difference between ITL and RTL (ITL-RTL) was significantly negative for 5xFAD group ( $*p < 0.05$ ) which was reversed to positive values by treatment with both doses of ICAM-1 ( $\#p < 0.05$ ). Values are expressed as mean  $\pm$  SEM. (\*) indicates p-values when compared to WT group and (#) indicates p-values with respect to 5xFAD group. (D) In EPM test, Test performed in association with the % of anxiety in specific zones showed no significant alteration. (Control  $n=6$ , ICAM-1  $n=6$ , 5x FAD  $n=6$ , 5xFAD+ICAM-1 (0.5 $\mu$ g/kg body weight)  $n=6$ , 5xFAD+ICAM-1(1 $\mu$ g/kg body weight)  $n=6$ ). Values are expressed as mean  $\pm$  SEM of three independent experiments.

Next, to further check whether ICAM-1 could actually improve learning memory and preference, Novel Object Recognition test was performed in 5xFAD mice both in presence and absence of the recombinant protein. rrICAM-1 treated animals displayed greater interest towards the novel object displaying a higher exploration time as compared to the wild type (Fig. 9A). Also as for the discrimination and preference index between the familiar and novel object was concerned, rrICAM-1+5xFAD mice showed a better ability to recognize the novel objects than 5xFAD mice in a dose dependent manner (Fig. 9B,C)

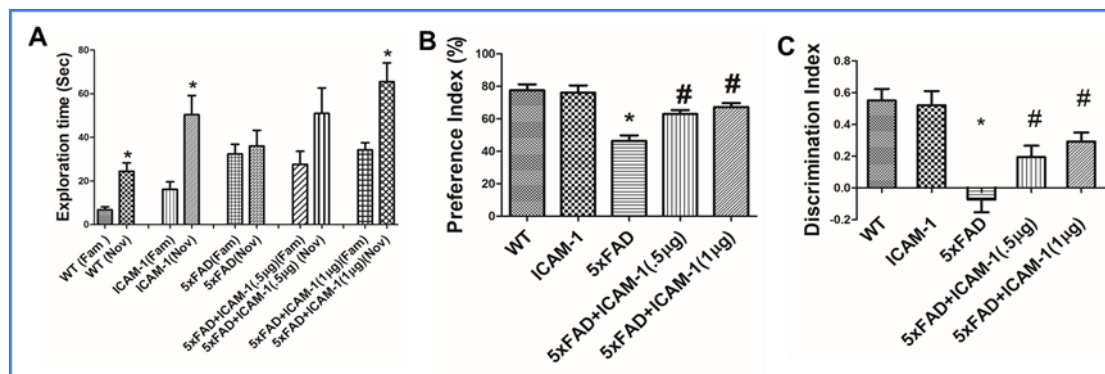


**Figure 9:** (A) In NOR-probe day, in comparison to WT and ICAM-1 treated groups, exploration time spent by 5xFAD mice at the novel (Nov) object was less than the familiar (Fam) object whereas 5xFAD+ICAM-1(1 $\mu$ g/kg b.w.) group spent significantly longer time with the novel object than familiar object ( $*p < 0.05$ ). (B) 5xFAD mice showed negative discrimination index ( $*p < 0.05$ ) while 5xFAD+ICAM-1 displayed a significantly positive response in discrimination ( $\#p < 0.05$ ). (C) Preference index for the novel object was significantly lowered in the 5xFAD group ( $*p < 0.05$ ) while it was significantly

higher in the 5x FAD+ICAM-1 (1µg/kg b.w.) group than the Aβ group (#p<0.05). All values expressed as mean ± SEM of three independent experiments.

Fear related memory is by far the most important associated memory and helps to create a bigger picture regarding assessment of the cognitive degeneration or improvement. So, to further check the effect of ICAM-1 on learning memory and functioning in 5xFAD, fear conditioning tests both contextual and cue dependent were performed. A significant decrease in freezing behavior of 5xFAD indicated reduced contextually formed memory, which showed a positive recovery with ICAM-1 treatment in a dose dependent manner (Fig. 10A). To determine the involvement of rrlCAM-1 in cue dependent associated memory formation, we subjected the mice cohort to one trial and multi trial cue dependent fear conditioning tests. ICAM-1 treated 5xFAD mice showed a significant increase in freezing% suggesting improvement in fear associated memory formation compared to the 5xFAD mice (Fig. 10B,C).

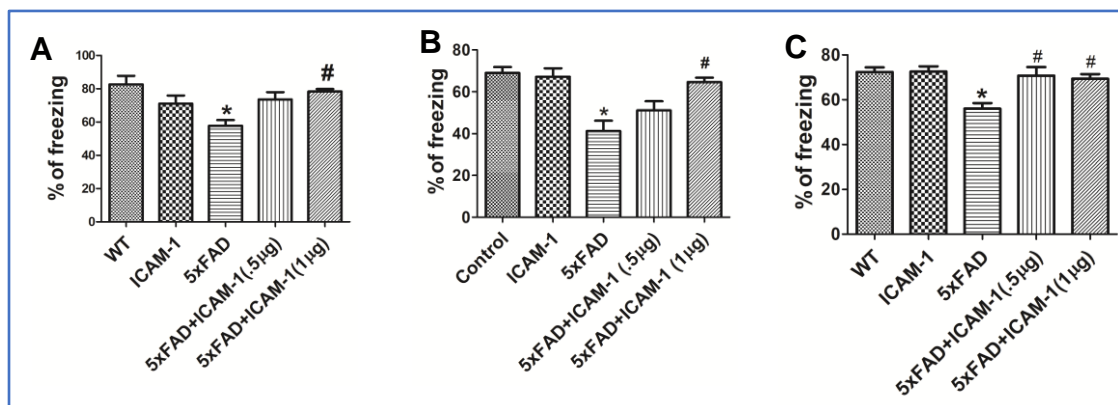


**Figure 10:**(A-C) Contextual and cue dependent fear (one trial and multi-trial) conditioning performed in 5xFAD mice both in presence and absence of intraperitoneal injection of rrlCAM-1. Graphical data represent the significant regain in %freezing of 5xFAD+ICAM-1 (1µg/kg b.w.) group as compared to the 5xFAD group which showed a significant decrease compared to WT group. Values are expressed as mean±SEM of three independent experiments: \*p<0.05.



## ICAM-1 provides neuroprotection by mitigating the action of NF- $\kappa$ B both in in vitro and in vivo models of AD

Unraveling the mystery behind the mechanism of any phenomenon has always been a challenge for the scientists. In search for the detailed molecular pattern through which ICAM-1 might render neuroprotection and cognitive recovery, signaling molecules were screened to identify the one responsible for improving the neuronal health in AD. Western blotting against important cellular proteins like mTOR, phospho and total forms of PKC was performed from hippocampus of PBS and ICAM-1 infused rats, both in absence and presence of ICAM-1, to check the probable metabolic changes in brain. The results obtained were insignificant (Fig.11A,B).

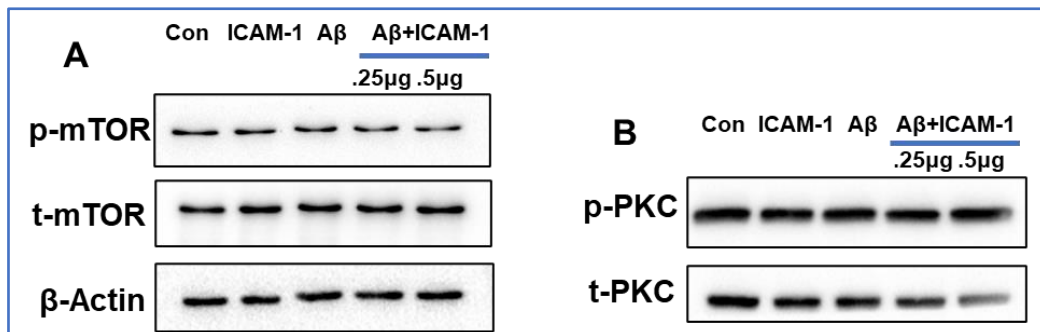


**Figure 11:(A,B)** Western blot of A $\beta$  infused animals along with their respective control both in presence and absence of A $\beta$  administration. Protein p-mTOR and p-PKC showed no significant change among the experimental groups.

Also similar experiment was performed to check the protein activation level of p-p38 MAPK, p-JNK, p-ERK in same group of animals. Western blotting showed clearly

that no change was visible in either of the proteins with or without treatment on ICAM-1 on the A $\beta$  infused rat brain (Fig12 A-C).

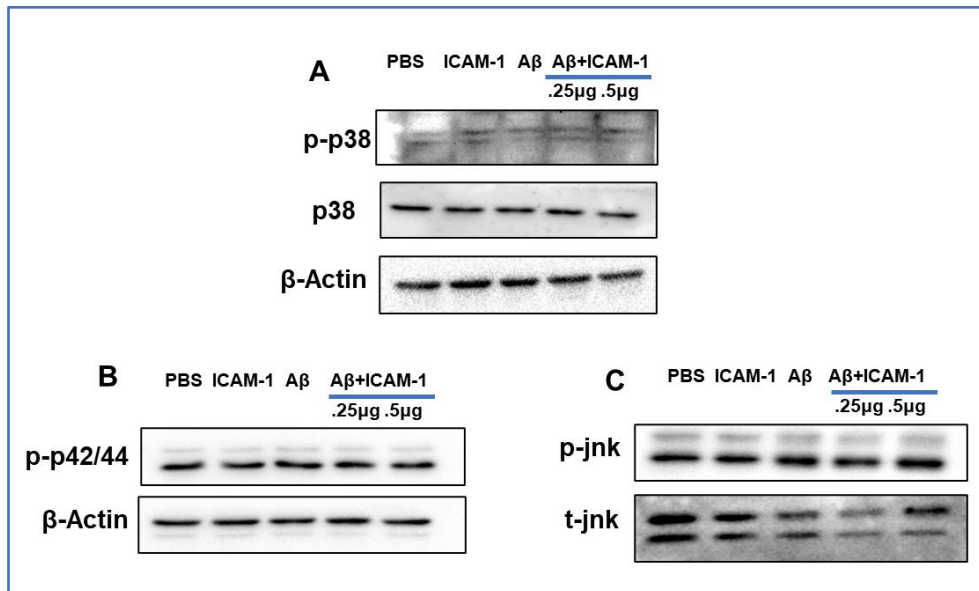


**Figure 12:** (A-C) Western blot of A $\beta$  infused animals along with their respective control both in presence and absence of A $\beta$  administration. MAPK specific proteins p-p38, p-ERK and p-JNK showed no significant change among the experimental groups.

Among all the transcription factors, NF- $\kappa$ B is well known to be the major inflammation marker. NF- $\kappa$ B, which on many occasions has been seen to be unregulated in neurons, are also known to be involved in maintaining synaptic conglomeration along with, learning and memory in AD (Kaltschmidt et al., 1997; Mattson & Meffert, 2006). Although various studies indicate that NF- $\kappa$ B can draw out ICAM-1 expression during neuroinflammation, yet by far no evidence confirms that ICAM-1 contributes in regulating the functionality of NF- $\kappa$ B activity. To check the possibility of this phenomenon, the NF- $\kappa$ B expression in both AD models of rats and 5xFAD mice with systemic administration of ICAM-1 was tested with the help of western blot. In both

of these AD models, we found a significant upregulation of NF- $\kappa$ B in cortical and hippocampal tissues (Fig.13A,B). Interestingly upon treatment with ICAM-1, a significant decrease of about 2 folds in NF- $\kappa$ B levels was found in tissues of AD models. This was similar for primary cultured neurons also suggesting that ICAM-1 treatment led to decrease in overtly expressed NF- $\kappa$ B both in vitro and in vivo (Fig.13C).

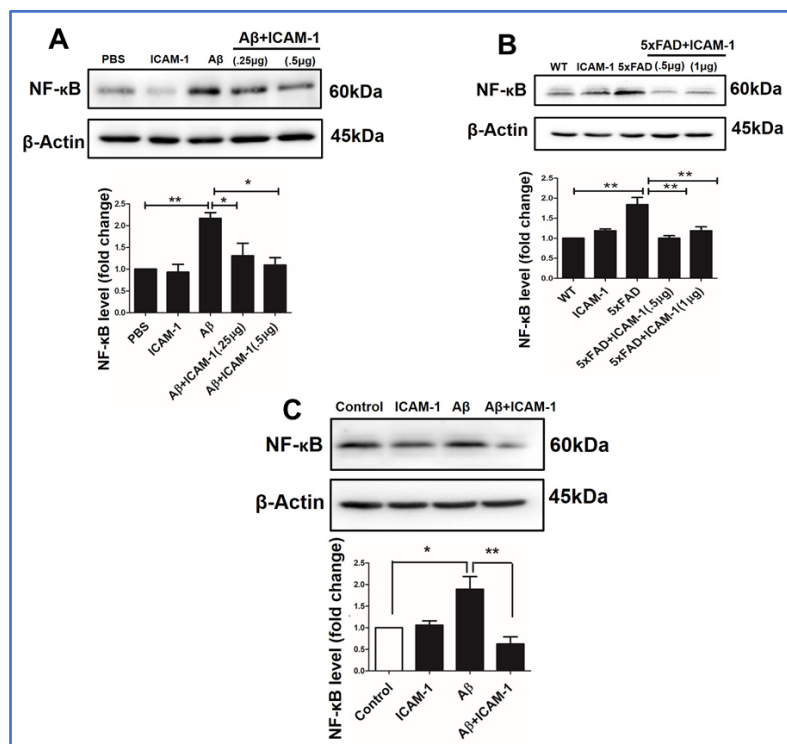


**Figure 13:**(A) A $\beta$ <sub>1-42</sub> was infused in adult rat brain and rICAM-1 was treated. Brain tissues of all experimental groups were collected and subjected to western blotting against NF- $\kappa$ B, with  $\beta$ -actin as the loading control, \*\*p<0.001, \*p<0.01. (B) WT and 5xFAD mice both were treated with ICAM-1 and western blotting was performed against NF- $\kappa$ B.\*\*p<0.001.(C) Western blotting and its analysis depicting differential expression of NF- $\kappa$ B in primary neurons when subjected to ICAM-1 treatment in treated and control neurons. Values expressed as mean  $\pm$  SEM from three independent experiments.\*\*p<0.001, \*p<0.01.

To further confirm this observation, 20 $\mu$ m coronal sections from 5xFAD mice were taken and immunohistochemical staining was done. Confocal imaging of the same

was done in the tissues being treated and untreated with ICAM-1. The increased NF- $\kappa$ B in 5xFAD brain was found to be decreased significantly upon ICAM-1 treatment (Fig.14).

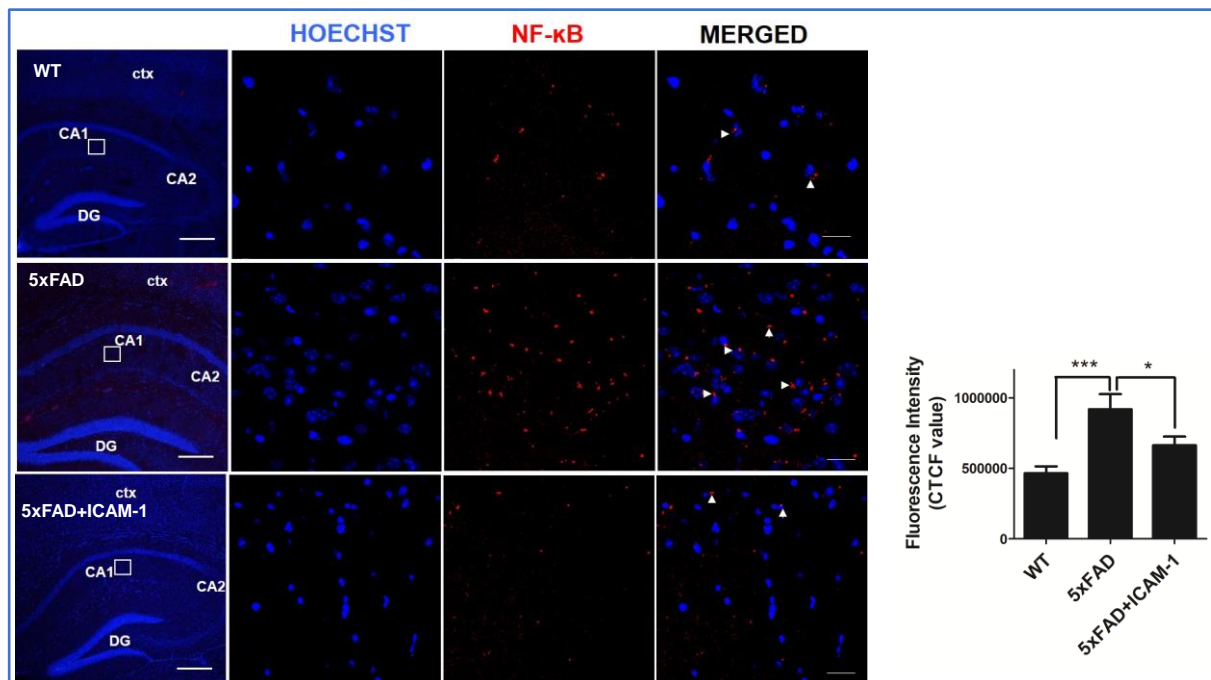


**Figure 14:** Confocal microscopic images taken at 20x magnification of WT, 5xFAD and 5xFAD+ICAM-1 (shown in vertical 3 panels) mice in hippocampus, showing upregulation in NF- $\kappa$ B detected by immunostaining with NF- $\kappa$ B antibody (Red). Nucleus stained by Hoechst (Blue). Right panel shows the graphical representation of the fluorescence intensity of three different experimental groups expressed as the CTCF score. Values expressed as mean  $\pm$  SEM from three independent experiments. \*\*\* $p$ <0.0001, \* $p$ <0.01.

### ICAM-1 changes level of apoptotic proteins in primary neuron

Huge amount of evidences reveal that various pro- and anti-apoptotic genes get their expression controlled by transcription factor NF- $\kappa$ B (Inta et al., 2006). So the level of pro-apoptotic protein Bim and anti-apoptotic proteins Bcl-2 and Bcl-xL was checked by western blotting. This strengthened the possibility NF- $\kappa$ B and its downstream targets being involved in ICAM-1 mediated neuroprotection in AD. The

results obtained elucidated that A $\beta$  mediated upregulation of Bim was reduced with ICAM-1 treatment in cultured primary neurons (Fig.15A) and also Bcl-2 and Bcl-xL levels were significantly restored even in the presence of A $\beta$  when co-treated with ICAM-1(Fig.15B,C).

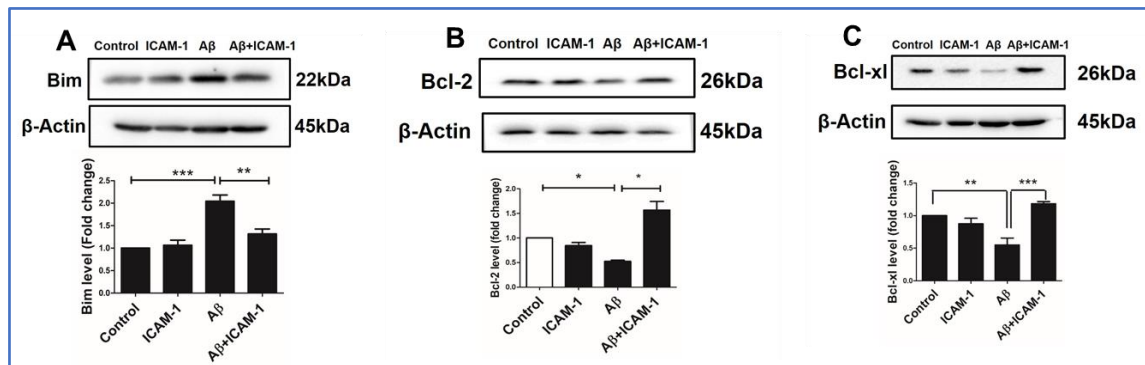


**Figure 15:** (A-C) Primary neurons harvested and western blotting against Bim, Bcl-2, Bcl-xL was done with  $\beta$ -actin as the loading control. Lower panel suggests the analyzed densitometry corresponding to each of the blots. Values expressed as mean  $\pm$  SEM from three independent experiments: \*\*\* $p$ <0.0001, \*\* $p$ <0.001, \* $p$ <0.01.

### Inhibiting NF- $\kappa$ B reduces anxiety and improves cognitive memory in 5xFAD mice

From our earlier experiments and studies it was found that NF- $\kappa$ B showed a significant upregulation when treated with A $\beta$  and also in 5xFAD transgenic mice. However, the same showed a reduction in presence of ICAM-1. So it was essential to check whether deficiency in NF- $\kappa$ B held any significant outcomes on behavioral deficits caused due to Alzheimer's Disease. In order to learn the roles played by NF- $\kappa$ B, in rescuing memory failure, cognitive malfunctioning or anxiety like behavior, inhibitor of NF- $\kappa$ B namely pyrrolidine dithiocarbamate (PDTC) was introduced systemically into the wild-type C56BL/7 and 5xFAD transgenic mice. The dose used here was 50mg/kg b.w. for 7 days, following which several behavioral tests were performed on the animals. Firstly the OFT was done. The results obtained on

administration of PDTC, showed a significant reduction in the anxiety which was common in 5xFAD mice. This was compared to wild type C56BL/7 and also to the untreated transgenic mice (Fig.16A, B). Also, the EPM test results, showed a significant lessening in RTL and positive difference was observed between ITL and RTL when 5xFAD mice were treated with PDTC. This was compared to higher RTL and (ITL-RTL) in untreated 5xFAD mice implying an improvement in cognitive functioning of the subjects (Fig 16C).

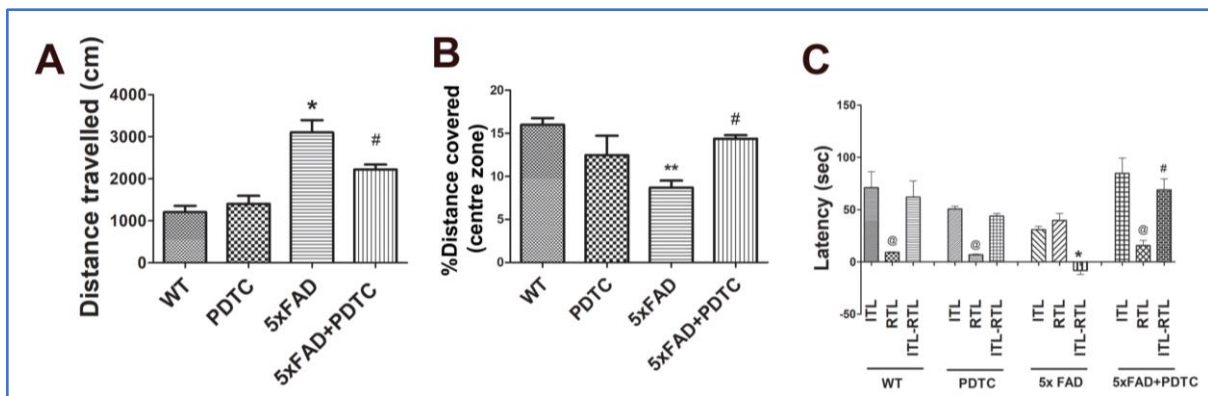


**Figure 16:** Effect of PDTC on cognitive functioning in 5xFAD mice. 5-month-old 5xFAD mice and corresponding age-matched WT mice were subjected to intraperitoneal administration of 50 mg/kg b.w. of PDTC, inhibitor of NF- $\kappa$ B, for 7 days whereby the mice cohorts were subjected to behavioral experiments and analyzed for results as indicated below. (A,B) OFT-graphical data represent a significant reduction in distance travelled and recovered % central distance covered by 5xFAD+PDTC (50 mg/kg) (# $p$ <0.01) group as compared to the increase in 5xFAD mice (\* $p$ <0.005). Data represent mean  $\pm$  SEM of three independent experiments, (A)\* $p$ <0.05, # $p$ <0.01 (B)\*\* $p$ <0.001, # $p$ <0.05 (C) In EPM test, retention transfer latency (RTL) on day-2 was significantly less than the initial transfer latency (ITL) on day-1 in all the experimental groups except 5xFAD mice (@ $p$ <0.05). The difference between ITL and RTL (ITL-RTL) was significantly negative for 5xFAD group (\* $p$ <0.05) which was reversed to positive values by treatment with 50 mg/kg b.w. PDTC administration (# $p$ <0.05). Values are expressed as mean  $\pm$  SEM. (\*) indicates  $p$ -values in comparison to WT group and (#) indicates  $p$ -values in comparison to 5xFAD group.

Novel Object Recognition helps to measure the occurrent state of spatial learning and short-term memory. Administration of PDTC displayed an improvement in the

exploration time towards the novel object as compared to the familiar object was observed in 5xFAD mice. Besides positive preference towards new object and discrimination ability of the subject determined by the preference index and discrimination index respectively was also found to improve with ICAM-1 treatment on 5xFAD mice (Fig 17A-C).

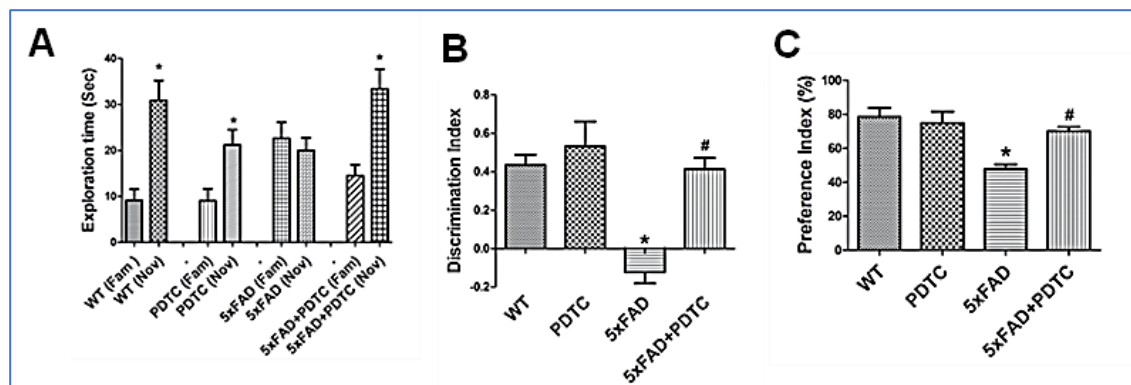


**Figure 17:** NOR on probe day (A) In comparison to WT and PDTC treated groups, time taken for exploration by 5xFAD mice near novel (Nov) object was less than the familiar (Fam) object whereas 5xFAD+PDTC (50 mg/kg) group spent significantly longer time with novel object than familiar object (\* $p < 0.05$ ). (B) 5xFAD mice gave a negative discrimination index value (\* $p < 0.05$ ) while for 5xFAD+PDTC (50 mg/kg), data showed to be significantly positive (# $p < 0.05$ ). (C) Preference index for the novel object was much lower in the 5xFAD group (\* $p < 0.05$ ) while it became significantly higher in the 5xFAD+PDTC (50 mg/kg) group as compared to the 5xFAD group (# $p < 0.05$ ). Values are expressed as mean  $\pm$  SEM of three independent experiments.

Finally hippocampus associated short-term and long-term memory was tested with the cue-dependent memory tests single and multi-trial was assessed. The percent freezing showed a significant increase upon PDTC administration which decreased in 5xFAD mice. This was compared to wild type both in single and multi-trial cue-dependent fear conditioning tests designating that NF- $\kappa$ B inhibition helped in recovery of short and long term associated memory malfunctioning (Fig 18 A,B).

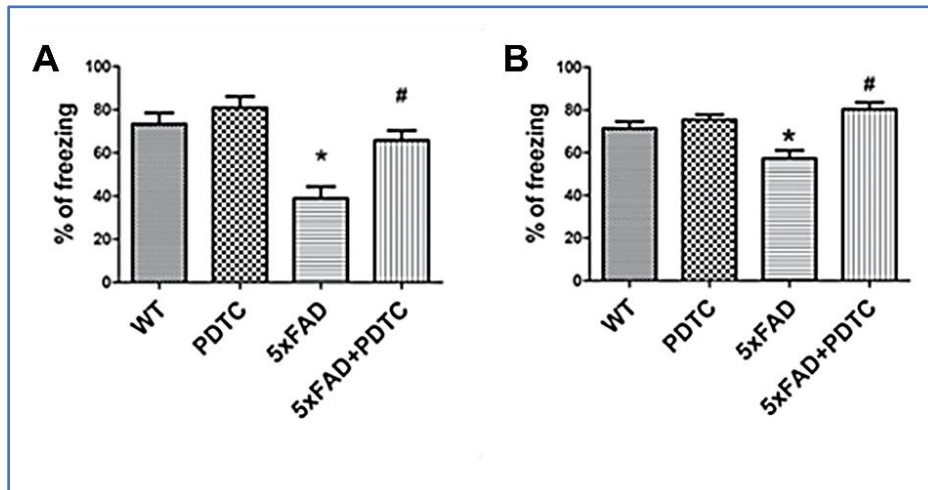


**Figure 18:** Cue dependent fear conditioning was performed in the mice groups in two different methods of single shock trial and multi shock trial. (A) and (B) show the graphical expression of altered percent freezing in individual group. Values are expressed as mean  $\pm$  SEM of three independent experiments (A)\* $p < 0.05$  # $p < 0.05$  (B) \* $p < 0.05$  # $p < 0.05$ .

Taken together, it can be concluded that transcription factor NF- $\kappa$ B on being upregulated plays an essential role in A $\beta$  influenced neuronal death and toxicity after which ushers the cognitive memory decline leading to neurodegeneration. Systemic administration of ICAM-1 could help in blocking the NF- $\kappa$ B upregulation leading to recovery of the detailed cellular damage and cognitive shortfall in models of AD.



## Discussion

Since long time scientists have been trying to decode some serious therapeutic strategy which could contribute in designing a remedial method for AD. One major method involved in the journey has been an attempt to identify specific biomarkers which can be targeted as identifying agent to the disease. Among several cytokines which are known to display a differential expression in exposure to A $\beta$ , we had identified a cytokine molecule namely soluble ICAM-1 during our initial study. Previous reports have suggested that in AD, there is a marked elevation of sICAM-1 in CSF and may hence be a probable candidate for being a biomarker during neuroinflammation (*Wennstrom et al., 2014*). Also the fact that sICAM-1 was also located in CSF of those patients who were initially not suffering from dementia but subsequently developed a significant deterioration in memory retention and cognitive functioning, makes sICAM-1 a potential preclinical biomarker (*Janelidze et al., 2018*). Even though typically ICAM-1 mainly functions as a cell adhesion molecule, yet recent studies enlighten its role in variety of neurological disorders (*Kim et al., 2012, Muller N., 2019*). Also mICAM-1 plays an significant role in allowing the infiltration of various immune cells across BBB with the help of its cognate receptor (LFA-1) and help in causing neuroinflammation (*Witkowska & Borawska, 2004, Lawson & Wolf, 2009*). Keeping all these benefits in mind, we hypothesized the probability of ICAM-1 having a potential role in staling the method of neurodegeneration and helping in recovering cognitive functioning in animal models of AD. Our studies reveal that injecting ICAM-1 in 5xFAD mice reduced A $\beta$  load by inducing NEP and improved learning memory in experimental subjects. While the transgenic subjects showed an anxious behavior induced by deposition of A $\beta$ , systemic administration of rrICAM-1

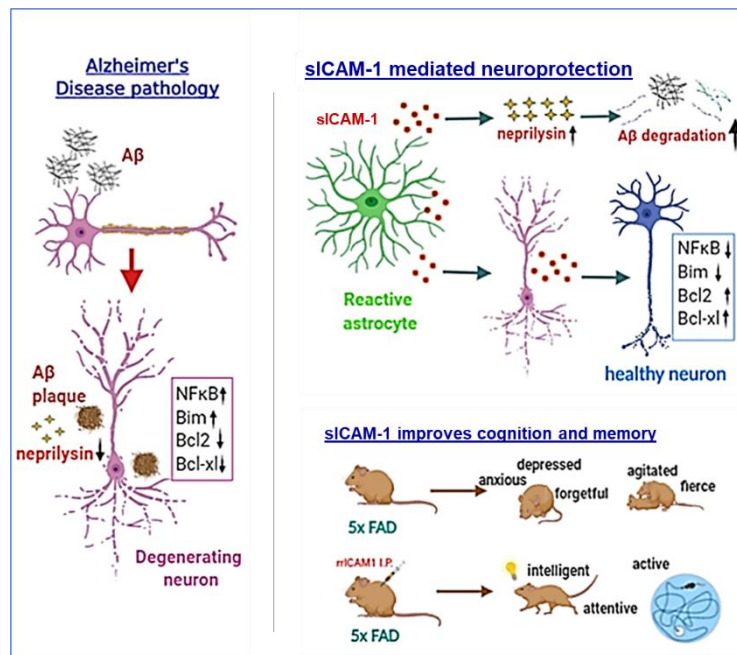
helped in improving the symptoms of hyperactivity in the subjects. Also short term and long term associated memory recovery was checked by various novel object recognition and fear conditioning tests. All of these suggested that ICAM-1 treatment improved cognitive abilities in this transgenic model of AD.

Furthermore we tried to explore the underlying mechanism which guided the neuroprotective functioning of ICAM-1. A lot of research has been done regarding the identification of various pathways activated in AD. Among our screening process we found NF- $\kappa$ B to be a key player which gets upregulated in exposure to A $\beta$  both in vitro and in vivo models of AD. However by treating the subjects with ICAM-1, NF- $\kappa$ B expression was found to be significantly downregulated. Transcription factor NF- $\kappa$ B has often been known to influence the downstream apoptotic protein like Bim and Bcl-2 genes (Lanzillotta et al., 2010; Sarnico et al., 2009). So it was seen that ICAM-1 injection significantly decreased the A $\beta$ -induced Bim upregulation and Bcl-2 and Bcl-xL levels were restored back in the primary cultured cellular AD model. Finally it was checked whether ICAM-1 influenced recovery of rodent cognitive functioning was NF- $\kappa$ B mediated or not. To do that, PDTC, an inhibitor of NF- $\kappa$ B was administered within system in WT and 5xFAD mice and all the behavioral tests were performed. All of them indicated that downregulating the excess NF- $\kappa$ B helped in recovering lost memory and cognitive malfunctioning in 5xFAD mice.

Since long time , clinicians and basic scientists have collaborated in search of a biomarker such that a holistic therapy could be carved in various neurodegenerative diseases like AD. Our current work strongly suggests that ICAM-1 has strong potential as a therapeutic agent as it is seen improving the cognitive functioning even in transgenic mouse model. This perspective calls for reassessing the importance of cytokines in neuroprotective venture, also elaborating the limited role of ICAM-1 as

adhesion molecules merely enabling helping in assisting transmembrane attachments.

# SUMMARY



- ✧ Aβ increases ICAM-1 in astrocyte, contributing significantly in improving the neuronal health and viability both in vitro and in vivo.
- ✧ ICAM-1 reduces Aβ plaque load in 5xFAD mice by increasing Neprilysin.
- ✧ ICAM-1 improves cognitive behavior and memory in Aβ infused and 5xFAD mice AD model.
- ✧ ICAM-1 modulates NF-κB to improve neuronal health & regulates apoptotic protein like Bim, Bcl-2 and Bcl-xL in neurons.
- ✧ Targeting NF-κB could contribute in reducing cognitive decline in 5xFAD transgenic mice



CONCLUSIVE  
DISCUSSION

Decades of research has reflected the fact that astroglia at later stage of Alzheimer's disease (AD) contribute primarily in creating a toxic milieu adding to the fact that synaptic signaling disturbance contribute in causing cognitive impairment (Chung et al., 2015; Perez-Nievas & Serrano-Pozo, 2018). Neuronal cross talk along with synaptic functioning is mainly possible through a variety of intercellularly secreted cytokines and other soluble growth factors. In our study we have found that sICAM-1 secreted from astrocytes in excess, with A $\beta$  treatment attempts to rescue neuronal degeneration and death caused in the process. ICAM-1 level found to be upregulated in in vivo AD model is found to reduce A $\beta$  plaque burden. Moreover, systemic injection of rrICAM-1 in AD rodent model attenuates the cognitive and learning malfunctioning in the subjects too. Furthermore, our experimental strategies have revealed that ICAM-1 assures neuronal protection causing neutralization of pro-apoptotic signaling of NF- $\kappa$ B. Finally, our data showing that inhibition of NF- $\kappa$ B mitigates learning deficits, suggest NF- $\kappa$ B to be a potential target molecule in AD therapy.

Though not a prominent molecule in neuronal signaling arcade, ICAM-1 was found to be present within certain reactive astrocytes near amyloid plaques in several post-mortem brain of AD patient. (Akiyama et al., 1993; Miguel-Hidalgo et al., 2007). Also, increased trace of sICAM-1 found in CSF in AD brain, has caused it to be regarded as biomarker for neuroinflammation (Nielsen et al., 2007). However, the mechanism involved within cellular milieu in response to sICAM-1 in AD are yet to be found out. Our study shows that A $\beta$  treatment results in higher secretion of sICAM-1 within the astrocyte conditioned media and co-localization of ICAM-1 with GFAP activated astrocytes are also evident from immunohistochemical imaging. Traditionally, ICAM-1 being an essential adherence protein has mostly involved its purpose in cell-cell

interactions and adhesion until recently where detailed studies have revealed its role played in several neurological disorders. For example, ICAM-1 helps immune cells to cross BBB causing neuroinflammation (Greenwood et al. 2002) and helps in reducing A $\beta$  plaque accumulation with the help of Neprilysin (Kim et al., 2012). In our study too we found that systemic administration of rrICAM-1 into the A $\beta$ -infused rat and 5xFAD mice helped in lowering the A $\beta$  plaque burden by inducing Neprilysin, also improving the cognitive functioning among the subjects.

Activated astrocytes are known to dissolve the A $\beta$  by activating several enzymes like NEP, insulin degrading enzyme (IDE) and MMPs (Leal et al., 2006; Yin et al., 2006). However, during the early to late stage transition of AD progress, complex and consecutive flow of cytokine signaling is essential to bring in the degradation (Ries & Sastre, 2016) In this respect, IL-1 $\beta$ , IL-6 and other pro-inflammatory cytokines like TNF- $\alpha$  causes transient accumulation of A $\beta$  whereas anti-inflammatory cytokines like IL-10 help in attenuating A $\beta$  deposition. On the other hand, reports indicating IL-10 might help in promoting A $\beta$  pathology, also suggest otherwise (Yamamoto et al., 2008). So it was essential to investigate the convoluted activities of the cytokines secreted from reactive astrocytes in various stages of AD. Interestingly, our studies revealed that ICAM-1 administration within in vivo system showed reduction in A $\beta$  plaque number and burden across cortex and hippocampus areas in 5xFAD mouse. This finding helped showed commemoration with our earlier report of astrocyte activation being neuroprotective in early stages of AD.

Researchers have often found an intrinsic relation between A $\beta$  plaque load and memory impairment bringing in cognitive anomaly (Nelson et al., 2012). This motivated us to further check if any restoration in cognitive functioning was happening in AD models. The AD model used in our study comprised of A $\beta$ -infused



rats and 5xFAD mice which clearly displayed symptoms of anxiety and reduced exploratory capability. However on administration of ICAM-1, all the symptoms were found reduced and improvement in their novelty seeking behavior was noticed. Moreover, various short-term and associated memory improving performance tests like the passive avoidance tests and the fear conditioning tests were also performed only to find a significant improvement in retaining the improved memory in both AD models following ICAM-1 injection.

Regarding the signaling pathways underlying ICAM-1 treatment, majority of findings involve vascular endothelial cells and immune cell system. ICAM-1 shows close interaction with LFA-1 receptor on microglia (*Kim et al., 2012*) and T-cells activating ERK and JNK pathways (Hubbard & Rothlein, 2000). Here in our study, we have checked the possible pathways like PKC, p-38, p-JNK, p-mTOR along with NF- $\kappa$ B which might be involved in ICAM-1 mediated signaling. Although NF- $\kappa$ B expression remains essential for neuronal survival (Bhakar et al., 2002), yet reports also suggest A $\beta$  triggered neuronal degeneration may also occur through NF- $\kappa$ B activation (Chami et al., 2012). The results obtained by us clearly showed that A $\beta$  was able to upregulate NF- $\kappa$ B in cellular and in vivo models of AD. However, with ICAM-1 treatment, significant reduction of the same was found. Being a pleiotropic regulator of cell death and neuroinflammation, NF- $\kappa$ B may positively or negatively activate several pro-apoptotic and anti-apoptotic proteins players (*Inta et al., 2006, Lanzillotta et al., 2010; Sohur et al., 1999*). So, to study the anti-survival effect of NF- $\kappa$ B, the level of pro-apoptotic protein Bim and anti-apoptotic proteins, Bcl-2 and Bcl-xL were further checked in AD models along with the treating effect of ICAM-1. Our finding suggested that ICAM-1 administration could bring about a significant reduction in the Bim upregulation and restoration of the Bcl-2 and Bcl-xL expression were possible

too in the system. Finally, importance of deactivating NF- $\kappa$ B to instigate ICAM-1 mediated memory improvement was also checked in our study where we treated 5xFAD mice with PDTTC, an inhibitor of NF- $\kappa$ B, only to find that this caused a significant recovery of cognition and memory deficiency. Numerous reports provided strong correlation between neuronal survival and NF- $\kappa$ B activity (*Mattson & Meffert, 2006*). However, dual roles of NF- $\kappa$ B is also evident where neuroprotection is common early phases of AD but eventually at later stages a deleterious effect on the neuroprotective genes is possible (Srinivasan & Lahiri, 2015). So, this hypothesis required a strong validation in disease onset and progressive severity of the same which may also be explained by a finding which says that attenuation of cognitive impairment is possible by deactivating NF- $\kappa$ B signalling by minocycline in rodents with diabetes (Cai et al., 2011). Our results validate the possibility of inhibition of NF- $\kappa$ B pathway being a therapeutic target for improving cognitive functioning in 5xFAD mice. However, further work and detailed research is necessary because NF- $\kappa$ B activation may also occur independent to ICAM-1 mediated signaling (Lawson et al., 1999).

Since long time, physicians and clinical researchers have often made an attempt to decide upon the intrinsic role played by astroglia in neurodegenerative disease like AD in a bigger holistic fashion. Our current hypothesis and the detailed study strongly imply that soluble ICAM-1 secreted by astrocyte can be a therapeutic biomarker in AD. Hence, a halt to the disease may be brought about either by altering the astrocytic secretion of sICAM-1 or including it within the system through a minimal invasive method.

# REFERENCES

- Abate G, Marziano M, Rungratanawanich W, Memo M, Uberti D. Nutrition and AGE-ing: Focusing on Alzheimer's Disease. *Oxid Med Cell Longev*. 2017;2017:7039816.
- Adlard PA, Bush AI. Metals and Alzheimer's disease. *J Alzheimers Dis*. 2006;10(2-3):145-163.
- Akiyama H, Kawamata T, Yamada T, Tooyama I, Ishii T, McGeer PL. Expression of intercellular adhesion molecule (ICAM)-1 by a subset of astrocytes in Alzheimer disease and some other degenerative neurological disorders. *Acta Neuropathol*. 1993;85(6):628-634.
- Albert MS, DeKosky ST, Dickson D, et al. The diagnosis of mild cognitive impairment due to Alzheimer's disease: recommendations from the National Institute on Aging-Alzheimer's Association workgroups on diagnostic guidelines for Alzheimer's disease. *Alzheimers Dement*. 2011;7(3):270-279.
- Albright CF, Dockens RC, Meredith JE Jr, et al. Pharmacodynamics of selective inhibition of  $\gamma$ -secretase by avagacestat. *J Pharmacol Exp Ther*. 2013;344(3):686-695.
- Alcolea D, Martínez-Lage P, Sánchez-Juan P, et al. Amyloid precursor protein metabolism and inflammation markers in preclinical Alzheimer disease. *Neurology*. 2015;85(7):626-633.
- Alford S, Patel D, Perakakis N, Mantzoros CS. Obesity as a risk factor for Alzheimer's disease: weighing the evidence. *Obes Rev*. 2018;19(2):269-280.
- Allen NJ, Bennett ML, Foo LC, et al. Astrocyte glypicans 4 and 6 promote formation of excitatory synapses via GluA1 AMPA receptors. *Nature*. 2012;486(7403):410-414.
- Alonso AC, Grundke-Iqbal I, Iqbal K. Alzheimer's disease hyperphosphorylated tau sequesters normal tau into tangles of filaments and disassembles microtubules. *Nat Med*. 1996;2(7):783-787.
- Alonso AC, Zaidi T, Grundke-Iqbal I, Iqbal K. Role of abnormally phosphorylated tau in the breakdown of microtubules in Alzheimer disease. *Proc Natl Acad Sci U S A*. 1994;91(12):5562-5566.
- Alzheimer A, Stelzmann RA, Schnitzlein HN, Murtagh FR. An English translation of Alzheimer's 1907 paper, "Über eine eigenartige Erkrankung der Hirnrinde". *Clin Anat*. 1995;8(6):429-431.
- Anand KS, Dhikav V. Hippocampus in health and disease: An overview. *Ann Indian Acad Neurol*. 2012;15(4):239-246.
- Anderson MA, Burda JE, Ren Y, et al. Astrocyte scar formation aids central nervous system axon regeneration. *Nature*. 2016;532(7598):195-200.
- Andrew RJ, De Rossi P, Nguyen P, et al. Reduction of the expression of the late-onset Alzheimer's disease (AD) risk-factor *BIN1* does not affect amyloid pathology in an AD mouse model. *J Biol Chem*. 2019;294(12):4477-4487.
- Anjum I, Fayyaz M, Wajid A, Sohail W, Ali A. Does Obesity Increase the Risk of Dementia: A Literature Review. *Cureus*. 2018;10(5):e2660.
- Antunes M, Biala G. The novel object recognition memory: neurobiology, test procedure, and its modifications. *Cogn Process*. 2012;13(2):93-110.:979-982.
- Apostolova LG, Green AE, Babakchian S, et al. Hippocampal atrophy and ventricular enlargement in normal aging, mild cognitive impairment (MCI), and Alzheimer Disease. *Alzheimer Dis Assoc Disord*. 2012;26(1):17-27.
- Arnsten AFT, Datta D, Tredici KD, Braak H. Hypothesis: Tau pathology is an initiating factor in sporadic Alzheimer's disease. *Alzheimers Dement*. 2021;17(1):115-124.
- Askarizadeh A, Barreto GE, Henney NC, Majeed M, Sahebkar A. Neuroprotection by curcumin: A review on brain delivery strategies. *Int J Pharm*. 2020;585:119476.
- Attems J, Yamaguchi H, Saido TC, Thal DR. Capillary CAA and perivascular A $\beta$ -deposition: two distinct features of Alzheimer's disease pathology. *J Neurol Sci*. 2010;299(1-2):155-162.
- Avila J. Alzheimer disease: caspases first. *Nat Rev Neurol*. 2010;6(11):587-588.
- Babic T. The cholinergic hypothesis of Alzheimer's disease: a review of progress. *J Neurol Neurosurg Psychiatry*. 1999;67(4):558.

- Bakota L, Brandt R. Tau Biology and Tau-Directed Therapies for Alzheimer's Disease. *Drugs*. 2016;76(3):301-313.
- Barker WW, Luis CA, Kashuba A, et al. Relative frequencies of Alzheimer disease, Lewy body, vascular and frontotemporal dementia, and hippocampal sclerosis in the State of Florida Brain Bank. *Alzheimer Dis Assoc Disord*. 2002;16(4):203-212.
- Barres BA. The mystery and magic of glia: a perspective on their roles in health and disease. *Neuron*. 2008;60(3):430-440.
- Bateman RJ, Xiong C, Benzinger TL, et al. Clinical and biomarker changes in dominantly inherited Alzheimer's disease [published correction appears in *N Engl J Med*. 2012 Aug 23;367(8):780]. *N Engl J Med*. 2012;367(9):795-804.
- Battefeld A, Klooster J, Kole MH. Myelinating satellite oligodendrocytes are integrated in a glial syncytium constraining neuronal high-frequency activity. *Nat Commun*. 2016;7:11298.
- Beccari S, Diaz-Aparicio I, Sierra A. Quantifying Microglial Phagocytosis of Apoptotic Cells in the Brain in Health and Disease. *Curr Protoc Immunol*. 2018;122(1):e49.
- Benilova I, Gallardo R, Ungureanu AA, et al. The Alzheimer disease protective mutation A2T modulates kinetic and thermodynamic properties of amyloid- $\beta$  (A $\beta$ ) aggregation. *J Biol Chem*. 2014;289(45):30977-30989.
- Bergles DE, Jahr CE. Synaptic activation of glutamate transporters in hippocampal astrocytes. *Neuron*. 1997;19(6):1297-1308.
- Beyreuther K, Masters CL. Amyloid precursor protein (APP) and beta A4 amyloid in the etiology of Alzheimer's disease: precursor-product relationships in the derangement of neuronal function. *Brain Pathol*. 1991;1(4):241-251.
- Bhakar AL, Tannis LL, Zeindler C, et al. Constitutive nuclear factor-kappa B activity is required for central neuron survival. *J Neurosci*. 2002;22(19):8466-8475.
- Bi C, Bi S, Li B. Processing of Mutant  $\beta$ -Amyloid Precursor Protein and the Clinicopathological Features of Familial Alzheimer's Disease. *Aging Dis*. 2019;10(2):383-403.
- Biswas SC, Ryu E, Park C, Malagelada C, Greene LA. Puma and p53 play required roles in death evoked in a cellular model of Parkinson disease. *Neurochem Res*. 2005;30(6-7):839-845.
- Blasko I, Veerhuis R, Stampfer-Kountchev M, Saurwein-Teissl M, Eikelenboom P, Grubeck-Loebenstein B. Costimulatory effects of interferon-gamma and interleukin-1beta or tumor necrosis factor alpha on the synthesis of Abeta1-40 and Abeta1-42 by human astrocytes. *Neurobiol Dis*. 2000;7(6 Pt B):682-689.
- Boller F, Verny M, Hugonot-Diener L, Saxton J. Clinical features and assessment of severe dementia. A review. *Eur J Neurol*. 2002;9(2):125-136.
- Boonruamkaew P, Chonpathompikunlert P, Vong LB, et al. Chronic treatment with a smart antioxidative nanoparticle for inhibition of amyloid plaque propagation in Tg2576 mouse model of Alzheimer's disease. *Sci Rep*. 2017;7(1):3785.
- Böttcher C, Schlickeiser S, Sneuboer MAM, et al. Human microglia regional heterogeneity and phenotypes determined by multiplexed single-cell mass cytometry. *Nat Neurosci*. 2019;22(1):78-90.
- Bouchon A, Hernández-Munain C, Cella M, Colonna M. A DAP12-mediated pathway regulates expression of CC chemokine receptor 7 and maturation of human dendritic cells. *J Exp Med*. 2001;194(8):1111-1122.
- Boulanger JJ, Messier C. From precursors to myelinating oligodendrocytes: contribution of intrinsic and extrinsic factors to white matter plasticity in the adult brain. *Neuroscience*. 2014;269:343-366.
- Bozyczko-Coyne D, O'Kane TM, Wu ZL, et al. CEP-1347/KT-7515, an inhibitor of SAPK/JNK pathway activation, promotes survival and blocks multiple events associated with Abeta-induced cortical neuron apoptosis. *J Neurochem*. 2001;77(3):849-863.

- Braak H, Braak E. Neuropathological staging of Alzheimer-related changes. *Acta Neuropathol.* 1991;82(4):239-259.
- Braak H, Del Tredici K. The preclinical phase of the pathological process underlying sporadic Alzheimer's disease. *Brain.* 2015;138(Pt 10):2814-2833. doi:10.1093/brain/awv236
- Bradburn S, Murgatroyd C, Ray N. Neuroinflammation in mild cognitive impairment and Alzheimer's disease: A meta-analysis. *Ageing Res Rev.* 2019;50:1-8.
- Breijyeh Z, Karaman R. Comprehensive Review on Alzheimer's Disease: Causes and Treatment. *Molecules.* 2020;25(24):5789.
- Buckley JS, Salpeter SR. A Risk-Benefit Assessment of Dementia Medications: Systematic Review of the Evidence. *Drugs Aging.* 2015;32(6):453-467.
- Buckley RF, Hanseeuw B, Schultz AP, et al. Region-Specific Association of Subjective Cognitive Decline With Tauopathy Independent of Global  $\beta$ -Amyloid Burden. *JAMA Neurol.* 2017;74(12):1455-1463.
- Buée L, Bussièrè T, Buée-Scherrer V, Delacourte A, Hof PR. Tau protein isoforms, phosphorylation and role in neurodegenerative disorders. *Brain Res Brain Res Rev.* 2000;33(1):95-130.
- Buffo A, Rolando C, Ceruti S. Astrocytes in the damaged brain: molecular and cellular insights into their reactive response and healing potential. *Biochem Pharmacol.* 2010;79(2):77-89.
- Butovsky O, Jedrychowski MP, Moore CS, et al. Identification of a unique TGF- $\beta$ -dependent molecular and functional signature in microglia [published correction appears in *Nat Neurosci.* 2014 Sep;17(9):1286]. *Nat Neurosci.* 2014;17(1):131-143.
- Cai Y, An SS, Kim S. Mutations in presenilin 2 and its implications in Alzheimer's disease and other dementia-associated disorders. *Clin Interv Aging.* 2015;10:1163-1172.
- Cai Z, Zhao Y, Yao S, Bin Zhao B. Increases in  $\beta$ -amyloid protein in the hippocampus caused by diabetic metabolic disorder are blocked by minocycline through inhibition of NF- $\kappa$ B pathway activation. *Pharmacol Rep.* 2011;63(2):381-391.
- Calsolaro V, Edison P. Neuroinflammation in Alzheimer's disease: Current evidence and future directions. *Alzheimers Dement.* 2016;12(6):719-732.
- Caselli RJ, Reiman EM. Characterizing the preclinical stages of Alzheimer's disease and the prospect of presymptomatic intervention. *J Alzheimers Dis.* 2013;33 Suppl 1(0 1):S405-S416.
- Chaitanya GV, Steven AJ, Babu PP. PARP-1 cleavage fragments: signatures of cell-death proteases in neurodegeneration. *Cell Commun Signal.* 2010;8:31.
- Chami L, Buggia-Prévot V, Duplan E, et al. Nuclear factor- $\kappa$ B regulates  $\beta$ APP and  $\beta$ - and  $\gamma$ -secretases differently at physiological and supraphysiological A $\beta$  concentrations [published correction appears in *J Biol Chem.* 2013 Jul 5;288(27):19645
- Chang J, Liu F, Lee M, et al. NF- $\kappa$ B inhibits osteogenic differentiation of mesenchymal stem cells by promoting  $\beta$ -catenin degradation [published correction appears in *Proc Natl Acad Sci U S A.* 2013 Aug 13;110(33):13690]. *Proc Natl Acad Sci U S A.* 2013;110(23):9469-9474.
- Chávez-Gutiérrez L, Bammens L, Benilova I, et al. The mechanism of  $\gamma$ -Secretase dysfunction in familial Alzheimer disease. *EMBO J.* 2012;31(10):2261-2274.
- Chen G, Chen KS, Knox J, et al. A learning deficit related to age and beta-amyloid plaques in a mouse model of Alzheimer's disease. *Nature.* 2000;408(6815):975-979.
- Chen H, Liu S, Ji L, et al. Folic Acid Supplementation Mitigates Alzheimer's Disease by Reducing Inflammation: A Randomized Controlled Trial. *Mediators Inflamm.* 2016;2016:5912146.
- Chen W, He B, Tong W, Zeng J, Zheng P. Astrocytic Insulin-Like Growth Factor-1 Protects Neurons Against Excitotoxicity. *Front Cell Neurosci.* 2019;13:298. Published 2019 Jul 9.
- Chételat G, La Joie R, Villain N, et al. Amyloid imaging in cognitively normal individuals, at-risk populations and preclinical Alzheimer's disease. *Neuroimage Clin.* 2013;2:356-365.

- Choi SH, Kim YH, Hebisch M, et al. A three-dimensional human neural cell culture model of Alzheimer's disease. *Nature*. 2014;515(7526):274-278.
- Choi SS, Lee HJ, Lim I, Satoh J, Kim SU. Human astrocytes: secretome profiles of cytokines and chemokines. *PLoS One*. 2014;9(4):e92325.
- Chukwu JE, Pedersen JT, Pedersen LØ, Volbracht C, Sigurdsson EM, Kong XP. Tau Antibody Structure Reveals a Molecular Switch Defining a Pathological Conformation of the Tau Protein. *Sci Rep*. 2018;8(1):6209.
- Chung D, Christopoulos GI, King-Casas B, Ball SB, Chiu PH. Social signals of safety and risk confer utility and have asymmetric effects on observers' choices. *Nat Neurosci*. 2015;18(6):912-916.
- Colomina MT, Peris-Sampedro F. Aluminum and Alzheimer's Disease. *Adv Neurobiol*. 2017;18:183-197.
- Colović MB, Krstić DZ, Lazarević-Pašti TD, Bondžić AM, Vasić VM. Acetylcholinesterase inhibitors: pharmacology and toxicology. *Curr Neuropharmacol*. 2013;11(3):315-335.
- Combs CK, Karlo JC, Kao SC, Landreth GE. beta-Amyloid stimulation of microglia and monocytes results in TNFalpha-dependent expression of inducible nitric oxide synthase and neuronal apoptosis. *J Neurosci*. 2001;21(4):1179-1188.
- Condello C, Yuan P, Schain A, Grutzendler J. Microglia constitute a barrier that prevents neurotoxic protofibrillar Aβ42 hotspots around plaques. *Nat Commun*. 2015;6:6176. Published 2015 Jan 29.
- Cribbs DH, Poon WW, Rissman RA, Blurton-Jones M. Caspase-mediated degeneration in Alzheimer's disease. *Am J Pathol*. 2004;165(2):353-355.
- Croze ML, Zimmer L. Ozone Atmospheric Pollution and Alzheimer's Disease: From Epidemiological Facts to Molecular Mechanisms. *J Alzheimers Dis*. 2018;62(2):503-522.
- Crusio WE. Genetic dissection of mouse exploratory behaviour. *Behav Brain Res*. 2001;125(1-2):127-132.
- Cuesto G, Enriquez-Barreto L, Caramés C, et al. Phosphoinositide-3-kinase activation controls synaptogenesis and spinogenesis in hippocampal neurons. *J Neurosci*. 2011;31(8):2721-2733.
- Culmsee C, Gerling N, Lehmann M, et al. Nerve growth factor survival signaling in cultured hippocampal neurons is mediated through TrkA and requires the common neurotrophin receptor P75. *Neuroscience*. 2002;115(4):1089-1108.
- Dai MH, Zheng H, Zeng LD, Zhang Y. The genes associated with early-onset Alzheimer's disease. *Oncotarget*. 2017;9(19):15132-15143.
- D'Amelio M, Cavallucci V, Cecconi F. Neuronal caspase-3 signaling: not only cell death. *Cell Death Differ*. 2010;17(7):1104-1114.
- Danysz W, Parsons CG. Alzheimer's disease, β-amyloid, glutamate, NMDA receptors and memantine--searching for the connections. *Br J Pharmacol*. 2012;167(2):324-352.
- Davies CA, Mann DM, Sumpter PQ, Yates PO. A quantitative morphometric analysis of the neuronal and synaptic content of the frontal and temporal cortex in patients with Alzheimer's disease. *J Neurol Sci*. 1987;78(2):151-164.
- Davis DG, Schmitt FA, Wekstein DR, Markesbery WR. Alzheimer neuropathologic alterations in aged cognitively normal subjects. *J Neuropathol Exp Neurol*. 1999;58(4):376-388.
- De Nadai T, Marchetti L, Di Rienzo C, et al. Precursor and mature NGF live tracking: one versus many at a time in the axons [published correction appears in *Sci Rep*. 2016;6:23308]. *Sci Rep*. 2016;6:20272.
- de Oliveira LG, Angelo YS, Iglesias AH, Peron JPS. Unraveling the Link Between Mitochondrial Dynamics and Neuroinflammation. *Front Immunol*. 2021;12:624919.
- De Strooper B, Saftig P, Craessaerts K, et al. Deficiency of presenilin-1 inhibits the normal cleavage of amyloid precursor protein. *Nature*. 1998;391(6665):387-390.

- De Strooper B. Loss-of-function presenilin mutations in Alzheimer disease. Talking Point on the role of presenilin mutations in Alzheimer disease. *EMBO Rep.* 2007;8(2):141-146.
- Dean RL 3rd, Scozzafava J, Goas JA, Regan B, Beer B, Bartus RT. Age-related differences in behavior across the life span of the C57BL/6J mouse. *Exp Aging Res.* 1981;7(4):427-451.
- DeCarli C, Miller BL, Swan GE, Reed T, Wolf PA, Carmelli D. Cerebrovascular and brain morphologic correlates of mild cognitive impairment in the National Heart, Lung, and Blood Institute Twin Study. *Arch Neurol.* 2001;58(4):643-647.
- DeKosky ST, Scheff SW. Synapse loss in frontal cortex biopsies in Alzheimer's disease: correlation with cognitive severity. *Ann Neurol.* 1990;27(5):457-464.
- Del Bo R, Angeretti N, Lucca E, De Simoni MG, Forloni G. Reciprocal control of inflammatory cytokines, IL-1 and IL-6, and beta-amyloid production in cultures. *Neurosci Lett.* 1995;188(1):70-74.
- DeTure MA, Dickson DW. The neuropathological diagnosis of Alzheimer's disease. *Mol Neurodegener.* 2019;14(1):32.
- Dickson DW, Crystal HA, Mattiace LA, et al. Identification of normal and pathological aging in prospectively studied nondemented elderly humans. *Neurobiol Aging.* 1992;13(1):179-189.
- Dickson DW. The pathogenesis of senile plaques. *J Neuropathol Exp Neurol.* 1997;56(4):321-339.
- Diniz LP, Tortelli V, Matias I, et al. Astrocyte Transforming Growth Factor Beta 1 Protects Synapses against A $\beta$  Oligomers in Alzheimer's Disease Model. *J Neurosci.* 2017;37(28):6797-6809.
- Diorio D, Welner SA, Butterworth RF, Meaney MJ, Suranyi-Cadotte BE. Peripheral benzodiazepine binding sites in Alzheimer's disease frontal and temporal cortex. *Neurobiol Aging.* 1991;12(3):255-258.
- DiSabato DJ, Quan N, Godbout JP. Neuroinflammation: the devil is in the details. *J Neurochem.* 2016;139 Suppl 2(Suppl 2):136-153. doi:10.1111/jnc.13607
- Dordoe C, Chen K, Huang W, et al. Roles of Fibroblast Growth Factors and Their Therapeutic Potential in Treatment of Ischemic Stroke. *Front Pharmacol.* 2021;12:671131.
- Drechsel DN, Hyman AA, Cobb MH, Kirschner MW. Modulation of the dynamic instability of tubulin assembly by the microtubule-associated protein tau. *Mol Biol Cell.* 1992;3(10):1141-1154.
- Du Y, Zhao Y, Li C, et al. Inhibition of PKC $\delta$  reduces amyloid- $\beta$  levels and reverses Alzheimer disease phenotypes. *J Exp Med.* 2018;215(6):1665-1677. doi:10.1084/jem.20171193
- Dunn N, Mullee M, Perry VH, Holmes C. Association between dementia and infectious disease: evidence from a case-control study. *Alzheimer Dis Assoc Disord.* 2005;19(2):91-94.
- Edison P, Archer HA, Hinz R, et al. Amyloid, hypometabolism, and cognition in Alzheimer disease: an [11C]PIB and [18F]FDG PET study. *Neurology.* 2007;68(7):501-508.
- Edison P, Brooks DJ. Role of Neuroinflammation in the Trajectory of Alzheimer's Disease and in vivo Quantification Using PET. *J Alzheimers Dis.* 2018;64(s1):S339-S351.
- Egensperger R, Kösel S, von Eitzen U, Graeber MB. Microglial activation in Alzheimer disease: Association with APOE genotype. *Brain Pathol.* 1998;8(3):439-447.
- El Kadmiri N, Said N, Slassi I, El Moutawakil B, Nadifi S. Biomarkers for Alzheimer Disease: Classical and Novel Candidates' Review. *Neuroscience.* 2018;370:181-190.
- Elewa HF, Hilali H, Hess DC, Machado LS, Fagan SC. Minocycline for short-term neuroprotection. *Pharmacotherapy.* 2006;26(4):515-521.
- Ennaceur A. One-trial object recognition in rats and mice: methodological and theoretical issues. *Behav Brain Res.* 2010;215(2):244-254.
- Eroglu C, Barres BA. Regulation of synaptic connectivity by glia. *Nature.* 2010;468(7321):223-231.



- Erta M, Giralt M, Esposito FL, Fernandez-Gayol O, Hidalgo J. Astrocytic IL-6 mediates locomotor activity, exploration, anxiety, learning and social behavior. *Horm Behav.* 2015;73:64-74.
- Etminan M, Gill S, Samii A. Effect of non-steroidal anti-inflammatory drugs on risk of Alzheimer's disease: systematic review and meta-analysis of observational studies. *BMJ.* 2003;327(7407):128.
- Eulenburg V, Gomez J. Neurotransmitter transporters expressed in glial cells as regulators of synapse function. *Brain Res Rev.* 2010;63(1-2):103-112.
- Fagan AM, Mintun MA, Shah AR, et al. Cerebrospinal fluid tau and ptau(181) increase with cortical amyloid deposition in cognitively normal individuals: implications for future clinical trials of Alzheimer's disease. *EMBO Mol Med.* 2009;1(8-9):371-380.
- Fan Z, Aman Y, Ahmed I, et al. Influence of microglial activation on neuronal function in Alzheimer's and Parkinson's disease dementia. *Alzheimers Dement.* 2015;11(6):608-21.e7.
- Fanselow MS, Tighe TJ. Contextual conditioning with massed versus distributed unconditional stimuli in the absence of explicit conditional stimuli. *J Exp Psychol Anim Behav Process.* 1988;14(2):187-199.
- Femminella GD, Ninan S, Atkinson R, Fan Z, Brooks DJ, Edison P. Does Microglial Activation Influence Hippocampal Volume and Neuronal Function in Alzheimer's Disease and Parkinson's Disease Dementia?. *J Alzheimers Dis.* 2016;51(4):1275-1289.
- Fernandez MA, Klutkowski JA, Freret T, Wolfe MS. Alzheimer presenilin-1 mutations dramatically reduce trimming of long amyloid  $\beta$ -peptides (A $\beta$ ) by  $\gamma$ -secretase to increase 42-to-40-residue A $\beta$ . *J Biol Chem.* 2014;289(45):31043-31052.
- Ferreira-Vieira TH, Guimaraes IM, Silva FR, Ribeiro FM. Alzheimer's disease: Targeting the Cholinergic System. *Curr Neuropharmacol.* 2016;14(1):101-115.
- Floden AM, Li S, Combs CK. Beta-amyloid-stimulated microglia induce neuron death via synergistic stimulation of tumor necrosis factor alpha and NMDA receptors. *J Neurosci.* 2005;25(10):2566-2575.
- Fogarty MP, Downer EJ, Campbell V. A role for c-Jun N-terminal kinase 1 (JNK1), but not JNK2, in the beta-amyloid-mediated stabilization of protein p53 and induction of the apoptotic cascade in cultured cortical neurons. *Biochem J.* 2003;371(Pt 3):789-798.
- Foster EM, Dangla-Valls A, Lovestone S, Ribe EM, Buckley NJ. Clusterin in Alzheimer's Disease: Mechanisms, Genetics, and Lessons From Other Pathologies. *Front Neurosci.* 2019;13:164.
- Francis PT, Sims NR, Procter AW, Bowen DM. Cortical pyramidal neurone loss may cause glutamatergic hypoactivity and cognitive impairment in Alzheimer's disease: investigative and therapeutic perspectives. *J Neurochem.* 1993;60(5):1589-1604.
- Frank S, Burbach GJ, Bonin M, et al. TREM2 is upregulated in amyloid plaque-associated microglia in aged APP23 transgenic mice. *Glia.* 2008;56(13):1438-1447.
- Fratiglioni L, Launer LJ, Andersen K, et al. Incidence of dementia and major subtypes in Europe: A collaborative study of population-based cohorts. Neurologic Diseases in the Elderly Research Group. *Neurology.* 2000;54(11 Suppl 5):S10-S15.
- Fricker M, Vilalta A, Tolkovsky AM, Brown GC. Caspase inhibitors protect neurons by enabling selective necroptosis of inflamed microglia. *J Biol Chem.* 2013;288(13):9145-9152.
- Frost GR, Li YM. The role of astrocytes in amyloid production and Alzheimer's disease. *Open Biol.* 2017;7(12):170228.
- Fülöp T, Itzhaki RF, Balin BJ, Miklossy J, Barron AE. Role of Microbes in the Development of Alzheimer's Disease: State of the Art - An International Symposium Presented at the 2017 IAGG Congress in San Francisco. *Front Genet.* 2018;9:362.
- Funato H, Yoshimura M, Yamazaki T, et al. Astrocytes containing amyloid beta-protein (A $\beta$ )-positive granules are associated with A $\beta$ 40-positive diffuse plaques in the aged human brain. *Am J Pathol.* 1998;152(4):983-992.

- Funk KE, Mrak RE, Kuret J. Granulovacuolar degeneration (GVD) bodies of Alzheimer's disease (AD) resemble late-stage autophagic organelles. *Neuropathol Appl Neurobiol.* 2011;37(3):295-306.
- Furgerson M, Clark JK, Crystal JD, Wagner JJ, Fechheimer M, Furukawa R. Hirano body expression impairs spatial working memory in a novel mouse model. *Acta Neuropathol Commun.* 2014;2:131.
- Gadea A, Schinelli S, Gallo V. Endothelin-1 regulates astrocyte proliferation and reactive gliosis via a JNK/c-Jun signaling pathway. *J Neurosci.* 2008;28(10):2394-2408.
- Garcia-Lopez P, Garcia-Marin V, Freire M. The histological slides and drawings of cajal. *Front Neuroanat.* 2010;4:9. Published 2010 Mar 10. doi:10.3389/neuro.05.009.2010
- Garwood CJ, Cooper JD, Hanger DP, Noble W. Anti-inflammatory impact of minocycline in a mouse model of tauopathy. *Front Psychiatry.* 2010;1:136.
- Garwood CJ, Pooler AM, Atherton J, Hanger DP, Noble W. Astrocytes are important mediators of A $\beta$ -induced neurotoxicity and tau phosphorylation in primary culture. *Cell Death Dis.* 2011;2(6):e167.
- Giau VV, Bagyinszky E, An SS, Kim SY. Role of apolipoprotein E in neurodegenerative diseases. *Neuropsychiatr Dis Treat.* 2015;11:1723-1737.
- Gibson PH, Tomlinson BE. Numbers of Hirano bodies in the hippocampus of normal and demented people with Alzheimer's disease. *J Neurol Sci.* 1977;33(1-2):199-206.
- Ginhoux F, Greter M, Leboeuf M, et al. Fate mapping analysis reveals that adult microglia derive from primitive macrophages. *Science.* 2010;330(6005):841-845.
- Glass CK, Saijo K, Winner B, Marchetto MC, Gage FH. Mechanisms underlying inflammation in neurodegeneration. *Cell.* 2010;140(6):918-934.
- Glenner GG, Wong CW. Alzheimer's disease: initial report of the purification and characterization of a novel cerebrovascular amyloid protein. *Biochem Biophys Res Commun.* 1984;120(3):885-890.
- Goedert M. Oskar Fischer and the study of dementia. *Brain.* 2009;132(Pt 4):1102-1111.
- Golde TE. Alzheimer disease therapy: can the amyloid cascade be halted?. *J Clin Invest.* 2003;111(1):11-18.
- Goldmann T, Tay TL, Prinz M. Love and death: microglia, NLRP3 and the Alzheimer's brain. *Cell Res.* 2013;23(5):595-596.
- Gomez-Arboledas A, Davila JC, Sanchez-Mejias E, et al. Phagocytic clearance of presynaptic dystrophies by reactive astrocytes in Alzheimer's disease. *Glia.* 2018;66(3):637-653.
- Gómez-Isla T, Hollister R, West H, et al. Neuronal loss correlates with but exceeds neurofibrillary tangles in Alzheimer's disease. *Ann Neurol.* 1997;41(1):17-24.
- Gozes I. Tau as a drug target in Alzheimer's disease. *J Mol Neurosci.* 2002;19(3):337-338.
- Green RC, Schneider LS, Amato DA, et al. Effect of tarenflurbil on cognitive decline and activities of daily living in patients with mild Alzheimer disease: a randomized controlled trial. *JAMA.* 2009;302(23):2557-2564.
- Greenwood J, Etienne-Manneville S, Adamson P, Couraud PO. Lymphocyte migration into the central nervous system: implication of ICAM-1 signalling at the blood-brain barrier. *Vascul Pharmacol.* 2002;38(6):315-322.
- Greter M, Lelios I, Croxford AL. Microglia Versus Myeloid Cell Nomenclature during Brain Inflammation. *Front Immunol.* 2015;6:249.
- Grimaldi LM, Zappalà G, Iemolo F, et al. A pilot study on the use of interferon beta-1a in early Alzheimer's disease subjects. *J Neuroinflammation.* 2014;11:30.
- Grossi C, Francese S, Casini A, et al. Clioquinol decreases amyloid-beta burden and reduces working memory impairment in a transgenic mouse model of Alzheimer's disease. *J Alzheimers Dis.* 2009;17(2):423-440.
- Gu Y, Ma LJ, Bai XX, et al. Mitogen-activated protein kinase phosphatase 1 protects PC12 cells from amyloid beta-induced neurotoxicity. *Neural Regen Res.* 2018;13(10):1842-1850.

- Guerreiro R, Bras J. The age factor in Alzheimer's disease. *Genome Med.* 2015;7:106.
- Guerreiro R, Wojtas A, Bras J, et al. TREM2 variants in Alzheimer's disease. *N Engl J Med.* 2013;368(2):117-127.
- Guillemot F. Cell fate specification in the mammalian telencephalon. *Prog Neurobiol.* 2007;83(1):37-52.
- Guyon A, Rousseau J, Lamothe G, Tremblay JP. The protective mutation A673T in amyloid precursor protein gene decreases A $\beta$  peptides production for 14 forms of Familial Alzheimer's Disease in SH-SY5Y cells. *PLoS One.* 2020;15(12):e0237122.
- Halle A, Hornung V, Petzold GC, et al. The NALP3 inflammasome is involved in the innate immune response to amyloid-beta. *Nat Immunol.* 2008;9(8):857-865.
- Hammond RS, Tull LE, Stackman RW. On the delay-dependent involvement of the hippocampus in object recognition memory. *Neurobiol Learn Mem.* 2004;82(1):26-34.
- Hampel H, Mesulam MM, Cuello AC, et al. The cholinergic system in the pathophysiology and treatment of Alzheimer's disease. *Brain.* 2018;141(7):1917-1933.
- Hanisch UK, Kettenmann H. Microglia: active sensor and versatile effector cells in the normal and pathologic brain. *Nat Neurosci.* 2007;10(11):1387-1394.
- Hanisch UK. Microglia as a source and target of cytokines. *Glia.* 2002;40(2):140-155.
- Hanseuw BJ, Betensky RA, Jacobs HIL, et al. Association of Amyloid and Tau With Cognition in Preclinical Alzheimer Disease: A Longitudinal Study [published correction appears in JAMA Neurol. 2019 Aug 1;76(8):986]. *JAMA Neurol.* 2019;76(8):915-924.
- Hanzel CE, Pichet-Binette A, Pimentel LS, et al. Neuronal driven pre-plaque inflammation in a transgenic rat model of Alzheimer's disease. *Neurobiol Aging.* 2014;35(10):2249-2262.
- Hardy J, Allsop D. Amyloid deposition as the central event in the aetiology of Alzheimer's disease. *Trends Pharmacol Sci.* 1991;12(10):383-388.
- Hardy J, Selkoe DJ. The amyloid hypothesis of Alzheimer's disease: progress and problems on the road to therapeutics [published correction appears in Science 2002 Sep 27;297(5590):2209]. *Science.* 2002;297(5580):353-356.
- Hardy JA, Higgins GA. Alzheimer's disease: the amyloid cascade hypothesis. *Science.* 1992;256(5054):184-185.
- Harris CA, Deshmukh M, Tsui-Pierchala B, Maroney AC, Johnson EM Jr. Inhibition of the c-Jun N-terminal kinase signaling pathway by the mixed lineage kinase inhibitor CEP-1347 (KT7515) preserves metabolism and growth of trophic factor-deprived neurons. *J Neurosci.* 2002;22(1):103-113.
- Harris JA, Devidze N, Verret L, et al. Transsynaptic progression of amyloid- $\beta$ -induced neuronal dysfunction within the entorhinal-hippocampal network. *Neuron.* 2010;68(3):428-441.
- Harris ME, Carney JM, Cole PS, et al. beta-Amyloid peptide-derived, oxygen-dependent free radicals inhibit glutamate uptake in cultured astrocytes: implications for Alzheimer's disease. *Neuroreport.* 1995;6(14):1875-1879.
- Hartmann D, de Strooper B, Serneels L, et al. The disintegrin/metalloprotease ADAM 10 is essential for Notch signalling but not for alpha-secretase activity in fibroblasts. *Hum Mol Genet.* 2002;11(21):2615-2624.
- Hayes A, Thaker U, Iwatsubo T, Pickering-Brown SM, Mann DM. Pathological relationships between microglial cell activity and tau and amyloid beta protein in patients with Alzheimer's disease. *Neurosci Lett.* 2002;331(3):171-174.
- Haynes SE, Hollopeter G, Yang G, et al. The P2Y<sub>12</sub> receptor regulates microglial activation by extracellular nucleotides. *Nat Neurosci.* 2006;9(12):1512-1519.
- He F, Ge W, Martinowich K, et al. A positive autoregulatory loop of Jak-STAT signaling controls the onset of astroglialogenesis. *Nat Neurosci.* 2005;8(5):616-625.
- Heneka MT, Carson MJ, El Khoury J, et al. Neuroinflammation in Alzheimer's disease. *Lancet Neurol.* 2015;14(4):388-405.

- Heneka MT, Kummer MP, Latz E. Innate immune activation in neurodegenerative disease. *Nat Rev Immunol.* 2014;14(7):463-477.
- Heneka MT, McManus RM, Latz E. Inflammasome signalling in brain function and neurodegenerative disease [published correction appears in *Nat Rev Neurosci.* 2019 Mar;20(3):187]. *Nat Rev Neurosci.* 2018;19(10):610-621.
- Herreman A, Hartmann D, Annaert W, et al. Presenilin 2 deficiency causes a mild pulmonary phenotype and no changes in amyloid precursor protein processing but enhances the embryonic lethal phenotype of presenilin 1 deficiency. *Proc Natl Acad Sci U S A.* 1999;96(21):11872-11877.
- Herz J, Filiano AJ, Smith A, Yogev N, Kipnis J. Myeloid Cells in the Central Nervous System. *Immunity.* 2017;46(6):943-956.
- Hirano A, Dembitzer HM, Kurland LT, Zimmerman HM. The fine structure of some intraganglionic alterations. Neurofibrillary tangles, granulovacuolar bodies and "rod-like" structures as seen in Guam amyotrophic lateral sclerosis and parkinsonism-dementia complex. *J Neuropathol Exp Neurol.* 1968;27(2):167-182.
- Hirano A. Hirano bodies and related neuronal inclusions. *Neuropathol Appl Neurobiol.* 1994;20(1):3-11.
- Holler CJ, Davis PR, Beckett TL, et al. Bridging integrator 1 (BIN1) protein expression increases in the Alzheimer's disease brain and correlates with neurofibrillary tangle pathology. *J Alzheimers Dis.* 2014;42(4):1221-1227.
- Hollingworth P, Harold D, Sims R, et al. Common variants at ABCA7, MS4A6A/MS4A4E, EPHA1, CD33 and CD2AP are associated with Alzheimer's disease. *Nat Genet.* 2011;43(5):429-435.
- Holtman IR, Raj DD, Miller JA, et al. Induction of a common microglia gene expression signature by aging and neurodegenerative conditions: a co-expression meta-analysis. *Acta Neuropathol Commun.* 2015;3:31.
- Holtzman DM, Bales KR, Paul SM, DeMattos RB. Abeta immunization and anti-Abeta antibodies: potential therapies for the prevention and treatment of Alzheimer's disease. *Adv Drug Deliv Rev.* 2002;54(12):1603-1613.
- Hong S, Beja-Glasser VF, Nfonoyim BM, et al. Complement and microglia mediate early synapse loss in Alzheimer mouse models. *Science.* 2016;352(6286):712-716.
- Hongpaisan J, Sun MK, Alkon DL. PKC  $\epsilon$  activation prevents synaptic loss, A $\beta$  elevation, and cognitive deficits in Alzheimer's disease transgenic mice. *J Neurosci.* 2011;31(2):630-643.
- Hong-Qi Y, Zhi-Kun S, Sheng-Di C. Current advances in the treatment of Alzheimer's disease: focused on considerations targeting A $\beta$  and tau. *Transl Neurodegener.* 2012;1(1):21.
- Hopperton KE, Mohammad D, Trépanier MO, Giuliano V, Bazinet RP. Markers of microglia in post-mortem brain samples from patients with Alzheimer's disease: a systematic review. *Mol Psychiatry.* 2018;23(2):177-198.
- Hoshiko M, Arnoux I, Avignone E, Yamamoto N, Audinat E. Deficiency of the microglial receptor CX3CR1 impairs postnatal functional development of thalamocortical synapses in the barrel cortex. *J Neurosci.* 2012;32(43):15106-15111.
- Hsu D, Marshall GA. Primary and Secondary Prevention Trials in Alzheimer Disease: Looking Back, Moving Forward. *Curr Alzheimer Res.* 2017;14(4):426-440.
- Huat TJ, Camats-Perna J, Newcombe EA, Valmas N, Kitazawa M, Medeiros R. Metal Toxicity Links to Alzheimer's Disease and Neuroinflammation. *J Mol Biol.* 2019;431(9):1843-1868.
- Hubbard AK, Rothlein R. Intercellular adhesion molecule-1 (ICAM-1) expression and cell signaling cascades. *Free Radic Biol Med.* 2000;28(9):1379-1386.
- Husemann J, Loike JD, Kodama T, Silverstein SC. Scavenger receptor class B type I (SR-BI) mediates adhesion of neonatal murine microglia to fibrillar beta-amyloid. *J Neuroimmunol.* 2001;114(1-2):142-150.

- Huttunen HJ, Peach C, Bhattacharyya R, et al. Inhibition of acyl-coenzyme A: cholesterol acyl transferase modulates amyloid precursor protein trafficking in the early secretory pathway. *FASEB J*. 2009;23(11):3819-3828.
- Hyman BT, Van Hoesen GW, Damasio AR, Barnes CL. Alzheimer's disease: cell-specific pathology isolates the hippocampal formation. *Science*. 1984;225(4667):1168-1170.
- Imbimbo BP, Lombard J, Pomara N. Pathophysiology of Alzheimer's disease. *Neuroimaging Clin N Am*. 2005;15(4):727-ix.
- in t' Veld BA, Ruitenbergh A, Hofman A, et al. Nonsteroidal antiinflammatory drugs and the risk of Alzheimer's disease. *N Engl J Med*. 2001;345(21):1515-1521.
- Inta I, Paxian S, Maegele I, et al. Bim and Noxa are candidates to mediate the deleterious effect of the NF-kappa B subunit RelA in cerebral ischemia. *J Neurosci*. 2006;26(50):12896-12903
- Iwata N, Tsubuki S, Takaki Y, et al. Identification of the major Abeta1-42-degrading catabolic pathway in brain parenchyma: suppression leads to biochemical and pathological deposition. *Nat Med*. 2000;6(2):143-150.
- Iwata N, Tsubuki S, Takaki Y, et al. Metabolic regulation of brain Abeta by neprilysin. *Science*. 2001;292(5521):1550-1552.
- Jahn H. Memory loss in Alzheimer's disease. *Dialogues Clin Neurosci*. 2013;15(4):445-454.
- Janelidze S, Mattsson N, Stomrud E, et al. CSF biomarkers of neuroinflammation and cerebrovascular dysfunction in early Alzheimer disease. *Neurology*. 2018;91(9):e867-e877.
- Jansen IE, Savage JE, Watanabe K, et al. Genome-wide meta-analysis identifies new loci and functional pathways influencing Alzheimer's disease risk [published correction appears in *Nat Genet*. 2020 Mar;52(3):354]. *Nat Genet*. 2019;51(3):404-413.
- Janus C, Pearson J, McLaurin J, et al. A beta peptide immunization reduces behavioural impairment and plaques in a model of Alzheimer's disease. *Nature*. 2000;408(6815):979-982.
- Jessen F, Feyen L, Freymann K, et al. Volume reduction of the entorhinal cortex in subjective memory impairment. *Neurobiol Aging*. 2006;27(12):1751-1756.
- Jessen F, Wiese B, Bachmann C, et al. Prediction of dementia by subjective memory impairment: effects of severity and temporal association with cognitive impairment. *Arch Gen Psychiatry*. 2010;67(4):414-422.
- Jessen NA, Munk AS, Lundgaard I, Nedergaard M. The Glymphatic System: A Beginner's Guide. *Neurochem Res*. 2015;40(12):2583-2599.
- Jiang T, Tan L, Zhu XC, et al. Upregulation of TREM2 ameliorates neuropathology and rescues spatial cognitive impairment in a transgenic mouse model of Alzheimer's disease. *Neuropsychopharmacology*. 2014;39(13):2949-2962.
- Jo S, Yarishkin O, Hwang YJ, et al. GABA from reactive astrocytes impairs memory in mouse models of Alzheimer's disease. *Nat Med*. 2014;20(8):886-896.
- Johnson JW, Kotermanski SE. Mechanism of action of memantine. *Curr Opin Pharmacol*. 2006;6(1):61-67.
- Jonsson T, Atwal JK, Steinberg S, et al. A mutation in APP protects against Alzheimer's disease and age-related cognitive decline. *Nature*. 2012;488(7409):96-99.
- Jonsson T, Stefansson H, Steinberg S, et al. Variant of TREM2 associated with the risk of Alzheimer's disease. *N Engl J Med*. 2013;368(2):107-116.
- Kaltschmidt B, Uherek M, Volk B, Baeuerle PA, Kaltschmidt C. Transcription factor NF-kappaB is activated in primary neurons by amyloid beta peptides and in neurons surrounding early plaques from patients with Alzheimer disease. *Proc Natl Acad Sci U S A*. 1997;94(6):2642-2647.
- Kametani F, Hasegawa M. Reconsideration of Amyloid Hypothesis and Tau Hypothesis in Alzheimer's Disease. *Front Neurosci*. 2018;12:25.

- Kaminska B. MAPK signalling pathways as molecular targets for anti-inflammatory therapy--from molecular mechanisms to therapeutic benefits. *Biochim Biophys Acta*. 2005;1754(1-2):253-262.
- Kanski R, van Strien ME, van Tijn P, Hol EM. A star is born: new insights into the mechanism of astrogenesis. *Cell Mol Life Sci*. 2014;71(3):433-447.
- Karantzoulis S, Galvin JE. Distinguishing Alzheimer's disease from other major forms of dementia. *Expert Rev Neurother*. 2011;11(11):1579-1591.
- Kaufman AC, Salazar SV, Haas LT, et al. Fyn inhibition rescues established memory and synapse loss in Alzheimer mice. *Ann Neurol*. 2015;77(6):953-971.
- Keren-Shaul H, Spinrad A, Weiner A, et al. A Unique Microglia Type Associated with Restricting Development of Alzheimer's Disease. *Cell*. 2017;169(7):1276-1290.e17.
- Kero M, Paetau A, Polvikoski T, et al. Amyloid precursor protein (APP) A673T mutation in the elderly Finnish population. *Neurobiol Aging*. 2013;34(5):1518.e1-1518.e15183.
- Kettenmann H, Verkhratsky A. Neuroglia: the 150 years after. *Trends Neurosci*. 2008;31(12):653-659.
- KIDD M. Paired helical filaments in electron microscopy of Alzheimer's disease. *Nature*. 1963;197:192-193.
- Kierdorf K, Prinz M. Microglia in steady state. *J Clin Invest*. 2017;127(9):3201-3209.
- Kim CC, Nakamura MC, Hsieh CL. Brain trauma elicits non-canonical macrophage activation states. *J Neuroinflammation*. 2016;13(1):117.
- Kim J, Basak JM, Holtzman DM. The role of apolipoprotein E in Alzheimer's disease. *Neuron*. 2009;63(3):287-303.
- Kim J, Eltorai AE, Jiang H, et al. Anti-apoE immunotherapy inhibits amyloid accumulation in a transgenic mouse model of A $\beta$  amyloidosis. *J Exp Med*. 2012;209(12):2149-2156.
- Kim JY, Kim DH, Kim JH, et al. Soluble intracellular adhesion molecule-1 secreted by human umbilical cord blood-derived mesenchymal stem cell reduces amyloid- $\beta$  plaques. *Cell Death Differ*. 2012;19(4):680-691.
- Kim T, Hinton DJ, Choi DS. Protein kinase C-regulated a $\beta$  production and clearance. *Int J Alzheimers Dis*. 2011;2011:857368.
- Kimelberg HK, Goderie SK, Higman S, Pang S, Waniewski RA. Swelling-induced release of glutamate, aspartate, and taurine from astrocyte cultures. *J Neurosci*. 1990;10(5):1583-1591.
- Kisler K, Nelson AR, Montagne A, Zlokovic BV. Cerebral blood flow regulation and neurovascular dysfunction in Alzheimer disease. *Nat Rev Neurosci*. 2017;18(7):419-434. doi:10.1038/nrn.2017.48
- Kitazawa M, Yamasaki TR, LaFerla FM. Microglia as a potential bridge between the amyloid beta-peptide and tau. *Ann N Y Acad Sci*. 2004;1035:85-103.
- Köhler C. Granulovacuolar degeneration: a neurodegenerative change that accompanies tau pathology. *Acta Neuropathol*. 2016;132(3):339-359.
- Koyama A, Hashimoto M, Tanaka H, et al. Malnutrition in Alzheimer's Disease, Dementia with Lewy Bodies, and Frontotemporal Lobar Degeneration: Comparison Using Serum Albumin, Total Protein, and Hemoglobin Level. *PLoS One*. 2016;11(6):e0157053.
- Kraus J, Oschmann P, Engelhardt B, et al. Soluble and cell surface ICAM-1 as markers for disease activity in multiple sclerosis. *Acta Neurol Scand*. 1998;98(2):102-109.
- Kreutzberg GW. Microglia: a sensor for pathological events in the CNS. *Trends Neurosci*. 1996;19(8):312-318.
- Kumar A, Singh A, Ekavali. A review on Alzheimer's disease pathophysiology and its management: an update. *Pharmacol Rep*. 2015;67(2):195-203.
- Lafon-Cazal M, Adjali O, Galéotti N, et al. Proteomic analysis of astrocytic secretion in the mouse. Comparison with the cerebrospinal fluid proteome. *J Biol Chem*. 2003;278(27):24438-24448.

- Lambert JC, Ibrahim-Verbaas CA, Harold D, et al. Meta-analysis of 74,046 individuals identifies 11 new susceptibility loci for Alzheimer's disease. *Nat Genet.* 2013;45(12):1452-1458.
- Lanouis e HM, Nicolas G, Wallon D, et al. APP, PSEN1, and PSEN2 mutations in early-onset Alzheimer disease: A genetic screening study of familial and sporadic cases. *PLoS Med.* 2017;14(3):e1002270.
- Lanz TA, Wood KM, Richter KE, et al. Pharmacodynamics and pharmacokinetics of the gamma-secretase inhibitor PF-3084014. *J Pharmacol Exp Ther.* 2010;334(1):269-277.
- Lanzillotta A, Sarnico I, Ingrassia R, et al. The acetylation of RelA in Lys310 dictates the NF- B-dependent response in post-ischemic injury. *Cell Death Dis.* 2010;1(11):e96.
- Latina V, Caioli S, Zona C, Ciotti MT, Amadoro G, Calissano P. Impaired NGF/TrkA Signaling Causes Early AD-Linked Presynaptic Dysfunction in Cholinergic Primary Neurons. *Front Cell Neurosci.* 2017;11:68.
- Lawson C, Ainsworth M, Yacoub M, Rose M. Ligation of ICAM-1 on endothelial cells leads to expression of VCAM-1 via a nuclear factor-kappaB-independent mechanism. *J Immunol.* 1999;162(5):2990-2996.
- Lawson C, Wolf S. ICAM-1 signaling in endothelial cells. *Pharmacol Rep.* 2009;61(1):22-32.
- Leal MC, Dorfman VB, Gamba AF, et al. Plaque-associated overexpression of insulin-degrading enzyme in the cerebral cortex of aged transgenic tg2576 mice with Alzheimer pathology. *J Neuropathol Exp Neurol.* 2006;65(10):976-987.
- Lee DC, Sunnarborg SW, Hinkle CL, et al. TACE/ADAM17 processing of EGFR ligands indicates a role as a physiological convertase. *Ann N Y Acad Sci.* 2003;995:22-38.
- Lee HJ, Seo HI, Cha HY, Yang YJ, Kwon SH, Yang SJ. Diabetes and Alzheimer's Disease: Mechanisms and Nutritional Aspects. *Clin Nutr Res.* 2018;7(4):229-240.
- Lee J, Kim CH, Kim DG, Ahn YS. Zinc Inhibits Amyloid beta Production from Alzheimer's Amyloid Precursor Protein in SH-SY5Y Cells. *Korean J Physiol Pharmacol.* 2009;13(3):195-200.
- Lee S, Varvel NH, Konerth ME, et al. CX3CR1 deficiency alters microglial activation and reduces beta-amyloid deposition in two Alzheimer's disease mouse models. *Am J Pathol.* 2010;177(5):2549-2562.
- Lesn e S, Docagne F, Gabriel C, et al. Transforming growth factor-beta 1 potentiates amyloid-beta generation in astrocytes and in transgenic mice. *J Biol Chem.* 2003;278(20):18408-18418.
- Li D, Liu N, Zhao HH, et al. Interactions between Sirt1 and MAPKs regulate astrocyte activation induced by brain injury in vitro and in vivo. *J Neuroinflammation.* 2017;14(1):67.
- Li NM, Liu KF, Qiu YJ, Zhang HH, Nakanishi H, Qing H. Mutations of beta-amyloid precursor protein alter the consequence of Alzheimer's disease pathogenesis. *Neural Regen Res.* 2019;14(4):658-665.
- Li Y, Rinne JO, Mosconi L, et al. Regional analysis of FDG and PIB-PET images in normal aging, mild cognitive impairment, and Alzheimer's disease. *Eur J Nucl Med Mol Imaging.* 2008;35(12):2169-2181.
- Lian H, Litvinchuk A, Chiang AC, Aithmitti N, Jankowsky JL, Zheng H. Astrocyte-Microglia Cross Talk through Complement Activation Modulates Amyloid Pathology in Mouse Models of Alzheimer's Disease. *J Neurosci.* 2016;36(2):577-589.
- Lian H, Yang L, Cole A, et al. NF B-activated astroglial release of complement C3 compromises neuronal morphology and function associated with Alzheimer's disease. *Neuron.* 2015;85(1):101-115.
- Lian H, Zheng H. Signaling pathways regulating neuron-glia interaction and their implications in Alzheimer's disease. *J Neurochem.* 2016;136(3):475-491.
- Licznarski P, Jonas EA. BDNF signaling: Harnessing stress to battle mood disorder. *Proc Natl Acad Sci U S A.* 2018;115(15):3742-3744.

- Liddelow SA, Barres BA. Reactive Astrocytes: Production, Function, and Therapeutic Potential. *Immunity*. 2017;46(6):957-967.
- Liddelow SA, Guttenplan KA, Clarke LE, et al. Neurotoxic reactive astrocytes are induced by activated microglia. *Nature*. 2017;541(7638):481-487. doi:10.1038/nature21029
- Liguori I, Russo G, Curcio F, et al. Oxidative stress, aging, and diseases. *Clin Interv Aging*. 2018;13:757-772.
- Lisman J, Buzsáki G, Eichenbaum H, Nadel L, Ranganath C, Redish AD. Viewpoints: how the hippocampus contributes to memory, navigation and cognition. *Nat Neurosci*. 2017;20(11):1434-1447.
- Liu CC, Liu CC, Kanekiyo T, Xu H, Bu G. Apolipoprotein E and Alzheimer disease: risk, mechanisms and therapy *Nat Rev Neurol*. 2013;9(2):106-118.
- Liu J, Chang L, Song Y, Li H, Wu Y. The Role of NMDA Receptors in Alzheimer's Disease. *Front Neurosci*. 2019;13:43. Published 2019 Feb 8. doi:10.3389/fnins.2019.00043
- Liu S, Liu Y, Hao W, et al. TLR2 is a primary receptor for Alzheimer's amyloid  $\beta$  peptide to trigger neuroinflammatory activation. *J Immunol*. 2012;188(3):1098-1107.
- Liu X, Jiao B, Shen L. The Epigenetics of Alzheimer's Disease: Factors and Therapeutic Implications. *Front Genet*. 2018;9:579. Published 2018 Nov 30.
- Liu Z, Condello C, Schain A, Harb R, Grutzendler J. CX3CR1 in microglia regulates brain amyloid deposition through selective protofibrillar amyloid- $\beta$  phagocytosis. *J Neurosci*. 2010;30(50):17091-17101.
- Longo FM, Massa SM. Small-molecule modulation of neurotrophin receptors: a strategy for the treatment of neurological disease. *Nat Rev Drug Discov*. 2013;12(7):507-525.
- Loy R, Tariot PN. Neuroprotective properties of valproate: potential benefit for AD and tauopathies. *J Mol Neurosci*. 2002;19(3):303-307.
- Luo Y, Bolon B, Kahn S, et al. Mice deficient in BACE1, the Alzheimer's beta-secretase, have normal phenotype and abolished beta-amyloid generation. *Nat Neurosci*. 2001;4(3):231-232.
- Lyman M, Lloyd DG, Ji X, Vizcaychipi MP, Ma D. Neuroinflammation: the role and consequences. *Neurosci Res*. 2014;79:1-12.
- Malarkey EB, Parpura V. Mechanisms of glutamate release from astrocytes. *Neurochem Int*. 2008;52(1-2):142-154.
- Malcangio M, Lessmann V. A common thread for pain and memory synapses? Brain-derived neurotrophic factor and trkB receptors. *Trends Pharmacol Sci*. 2003;24(3):116-121.
- Malko P, Syed Mortadza SA, McWilliam J, Jiang LH. TRPM2 Channel in Microglia as a New Player in Neuroinflammation Associated With a Spectrum of Central Nervous System Pathologies. *Front Pharmacol*. 2019;10:239.
- Maloney JA, Bainbridge T, Gustafson A, et al. Molecular mechanisms of Alzheimer disease protection by the A673T allele of amyloid precursor protein. *J Biol Chem*. 2014;289(45):30990-31000.
- Mandrekar-Colucci S, Karlo JC, Landreth GE. Mechanisms underlying the rapid peroxisome proliferator-activated receptor- $\gamma$ -mediated amyloid clearance and reversal of cognitive deficits in a murine model of Alzheimer's disease. *J Neurosci*. 2012;32(30):10117-10128.
- Martin E, Boucher C, Fontaine B, Delarasse C. Distinct inflammatory phenotypes of microglia and monocyte-derived macrophages in Alzheimer's disease models: effects of aging and amyloid pathology. *Aging Cell*. 2017;16(1):27-38.
- Martineau M, Parpura V, Mothet JP. Cell-type specific mechanisms of D-serine uptake and release in the brain. *Front Synaptic Neurosci*. 2014;6:12.
- Martinez-Coria H, Green KN, Billings LM, et al. Memantine improves cognition and reduces Alzheimer's-like neuropathology in transgenic mice. *Am J Pathol*. 2010;176(2):870-880.
- Martinon F, Burns K, Tschopp J. The inflammasome: a molecular platform triggering activation of inflammatory caspases and processing of proIL-beta. *Mol Cell*. 2002;10(2):417-426.



- Masliah E, Hansen L, Albright T, Mallory M, Terry RD. Immunoelectron microscopic study of synaptic pathology in Alzheimer's disease. *Acta Neuropathol.* 1991;81(4):428-433.
- Massa SM, Xie Y, Yang T, et al. Small, nonpeptide p75NTR ligands induce survival signaling and inhibit proNGF-induced death. *J Neurosci.* 2006;26(20):5288-5300.
- Masuda T, Sankowski R, Staszewski O, et al. Spatial and temporal heterogeneity of mouse and human microglia at single-cell resolution [published correction appears in Nature. 2019 Apr;568(7751):E4]. *Nature.* 2019;566(7744):388-392.
- Matsumoto K, Shimizu N. Activation of the phospholipase C signaling pathway in nerve growth factor-treated neurons by carbon nanotubes. *Biomaterials.* 2013;34(24):5988-5994.
- Mattson MP, Meffert MK. Roles for NF-kappaB in nerve cell survival, plasticity, and disease. *Cell Death Differ.* 2006;13(5):852-860.
- Maurer SV, Williams CL. The Cholinergic System Modulates Memory and Hippocampal Plasticity via Its Interactions with Non-Neuronal Cells. *Front Immunol.* 2017;8:1489.
- May PC, Dean RA, Lowe SL, et al. Robust central reduction of amyloid- $\beta$  in humans with an orally available, non-peptidic  $\beta$ -secretase inhibitor. *J Neurosci.* 2011;31(46):16507-16516.
- May PC, Willis BA, Lowe SL, et al. The potent BACE1 inhibitor LY2886721 elicits robust central A $\beta$  pharmacodynamic responses in mice, dogs, and humans. *J Neurosci.* 2015;35(3):1199-1210.
- Mazanetz MP, Fischer PM. Untangling tau hyperphosphorylation in drug design for neurodegenerative diseases. *Nat Rev Drug Discov.* 2007;6(6):464-479.
- McCubrey JA, Lahair MM, Franklin RA. Reactive oxygen species-induced activation of the MAP kinase signaling pathways. *Antioxid Redox Signal.* 2006;8(9-10):1775-1789.
- McDonald MP, Overmier JB. Present imperfect: a critical review of animal models of the mnemonic impairments in Alzheimer's disease. *Neurosci Biobehav Rev.* 1998;22(1):99-120.
- McDonnell GV, McMillan SA, Douglas JP, Droogan AG, Hawkins SA. Serum soluble adhesion molecules in multiple sclerosis: raised sVCAM-1, sICAM-1 and sE-selectin in primary progressive disease. *J Neurol.* 1999;246(2):87-92.
- McGaugh JL, Cahill L, Roozendaal B. Involvement of the amygdala in memory storage: interaction with other brain systems. *Proc Natl Acad Sci U S A.* 1996;93(24):13508-13514.
- McGeer PL, McGeer EG. Local neuroinflammation and the progression of Alzheimer's disease. *J Neurovirol.* 2002;8(6):529-538.
- McGeer PL, McGeer EG. The amyloid cascade-inflammatory hypothesis of Alzheimer disease: implications for therapy. *Acta Neuropathol.* 2013;126(4):479-497.
- McKhann GM, Knopman DS, Chertkow H, et al. The diagnosis of dementia due to Alzheimer's disease: recommendations from the National Institute on Aging-Alzheimer's Association workgroups on diagnostic guidelines for Alzheimer's disease. *Alzheimers Dement.* 2011;7(3):263-269.
- McNamara RK, Skelton RW. Assessment of a cholinergic contribution to chlordiazepoxide-induced deficits of place learning in the Morris water maze. *Pharmacol Biochem Behav.* 1992;41(3):529-538.
- McQuade A, Blurton-Jones M. Microglia in Alzheimer's Disease: Exploring How Genetics and Phenotype Influence Risk. *J Mol Biol.* 2019;431(9):1805-1817.
- Metz LM, Li DKB, Traboulsee AL, et al. Trial of Minocycline in a Clinically Isolated Syndrome of Multiple Sclerosis. *N Engl J Med.* 2017;376(22):2122-2133.
- Michaelis ML, Chen Y, Hill S, et al. Amyloid peptide toxicity and microtubule-stabilizing drugs. *J Mol Neurosci.* 2002;19(1-2):101-105.
- Micheau O, Tschopp J. Induction of TNF receptor I-mediated apoptosis via two sequential signaling complexes. *Cell.* 2003;114(2):181-190.
- Miguel-Álvarez M, Santos-Lozano A, Sanchis-Gomar F, et al. Non-steroidal anti-inflammatory drugs as a treatment for Alzheimer's disease: a systematic review and meta-analysis of treatment effect. *Drugs Aging.* 2015;32(2):139-147.

- Miguel-Hidalgo JJ, Nithuairisg S, Stockmeier C, Rajkowska G. Distribution of ICAM-1 immunoreactivity during aging in the human orbitofrontal cortex. *Brain Behav Immun.* 2007;21(1):100-111.
- MILLER GA. The magical number seven plus or minus two: some limits on our capacity for processing information. *Psychol Rev.* 1956;63(2):81-97.
- Min SW, Sohn PD, Li Y, et al. SIRT1 Deacetylates Tau and Reduces Pathogenic Tau Spread in a Mouse Model of Tauopathy. *J Neurosci.* 2018;38(15):3680-3688.
- Minett T, Classey J, Matthews FE, et al. Microglial immunophenotype in dementia with Alzheimer's pathology. *J Neuroinflammation.* 2016;13(1):135.
- Miranda M, Morici JF, Zanoni MB, Bekinschtein P. Brain-Derived Neurotrophic Factor: A Key Molecule for Memory in the Healthy and the Pathological Brain. *Front Cell Neurosci.* 2019;13:363.
- Mishra A, Kim HJ, Shin AH, Thayer SA. Synapse loss induced by interleukin-1 $\beta$  requires pre- and post-synaptic mechanisms. *J Neuroimmune Pharmacol.* 2012;7(3):571-578. doi:10.1007/s11481-012-9342-7
- Mittal M, Siddiqui MR, Tran K, Reddy SP, Malik AB. Reactive oxygen species in inflammation and tissue injury. *Antioxid Redox Signal.* 2014;20(7):1126-1167.
- Montine TJ, Phelps CH, Beach TG, et al. National Institute on Aging-Alzheimer's Association guidelines for the neuropathologic assessment of Alzheimer's disease: a practical approach. *Acta Neuropathol.* 2012;123(1):1-11.
- Morest DK, Silver J. Precursors of neurons, neuroglia, and ependymal cells in the CNS: what are they? Where are they from? How do they get where they are going?. *Glia.* 2003;43(1):6-18.
- Morgan D, Diamond DM, Gottschall PE, et al. A beta peptide vaccination prevents memory loss in an animal model of Alzheimer's disease [published correction appears in Nature 2001 Aug 9;412(6847):660]. *Nature.* 2000;408(6815):982-985.
- Morishima Y, Gotoh Y, Zieg J, et al. Beta-amyloid induces neuronal apoptosis via a mechanism that involves the c-Jun N-terminal kinase pathway and the induction of Fas ligand. *J Neurosci.* 2001;21(19):7551-7560.
- Morris JC, Heyman A, Mohs RC, et al. The Consortium to Establish a Registry for Alzheimer's Disease (CERAD). Part I. Clinical and neuropsychological assessment of Alzheimer's disease. *Neurology.* 1989;39(9):1159-1165.
- Morris JC, Storandt M, Miller JP, et al. Mild cognitive impairment represents early-stage Alzheimer disease. *Arch Neurol.* 2001;58(3):397-405.
- Morris JC. Clinical dementia rating: a reliable and valid diagnostic and staging measure for dementia of the Alzheimer type. *Int Psychogeriatr.* 1997;9 Suppl 1:173-178.
- Morris JC. Early-stage and preclinical Alzheimer disease. *Alzheimer Dis Assoc Disord.* 2005;19(3):163-165.
- Mortadza SS, Sim JA, Stacey M, Jiang LH. Signalling mechanisms mediating Zn<sup>2+</sup>-induced TRPM2 channel activation and cell death in microglial cells. *Sci Rep.* 2017;7:45032.
- Moulton PV, Yang W. Air pollution, oxidative stress, and Alzheimer's disease. *J Environ Public Health.* 2012;2012:472751.
- Moussa C, Hebron M, Huang X, et al. Resveratrol regulates neuro-inflammation and induces adaptive immunity in Alzheimer's disease. *J Neuroinflammation.* 2017;14(1):1.
- Müller N. The Role of Intercellular Adhesion Molecule-1 in the Pathogenesis of Psychiatric Disorders. *Front Pharmacol.* 2019;10:1251.
- Munoz L, Ammit AJ. Targeting p38 MAPK pathway for the treatment of Alzheimer's disease. *Neuropharmacology.* 2010;58(3):561-568.
- Murgas P, Godoy B, von Bernhardt R. A $\beta$  potentiates inflammatory activation of glial cells induced by scavenger receptor ligands and inflammatory mediators in culture. *Neurotox Res.* 2012;22(1):69-78.

- Muzambi R, Bhaskaran K, Brayne C, Davidson JA, Smeeth L, Warren-Gash C. Common Bacterial Infections and Risk of Dementia or Cognitive Decline: A Systematic Review. *J Alzheimers Dis.* 2020;76(4):1609-1626.
- Mycko MP, Kwinkowski M, Tronczynska E, Szymanska B, Selmaj KW. Multiple sclerosis: the increased frequency of the ICAM-1 exon 6 gene point mutation genetic type K469. *Ann Neurol.* 1998;44(1):70-75.
- Nagai M, Re DB, Nagata T, et al. Astrocytes expressing ALS-linked mutated SOD1 release factors selectively toxic to motor neurons. *Nat Neurosci.* 2007;10(5):615-622.
- Nakashima K, Yanagisawa M, Arakawa H, Taga T. Astrocyte differentiation mediated by LIF in cooperation with BMP2. *FEBS Lett.* 1999;457(1):43-46.
- Nakazawa T, Komai S, Tezuka T, et al. Characterization of Fyn-mediated tyrosine phosphorylation sites on GluR epsilon 2 (NR2B) subunit of the N-methyl-D-aspartate receptor. *J Biol Chem.* 2001;276(1):693-699.
- National Institute on Aging: Why Population Aging Matters: a Global Perspective. NIH Publ. No. 07- 6134. Bethesda, National Institute on Aging, 2007.
- Nelson PT, Alafuzoff I, Bigio EH, et al. Correlation of Alzheimer disease neuropathologic changes with cognitive status: a review of the literature. *J Neuropathol Exp Neurol.* 2012;71(5):362-381.
- Neniskyte U, Neher JJ, Brown GC. Neuronal death induced by nanomolar amyloid  $\beta$  is mediated by primary phagocytosis of neurons by microglia. *J Biol Chem.* 2011;286(46):39904-39913.
- Nielsen HM, Londos E, Minthon L, Janciauskiene SM. Soluble adhesion molecules and angiotensin-converting enzyme in dementia. *Neurobiol Dis.* 2007;26(1):27-35.
- Niikura T, Tajima H, Kita Y. Neuronal cell death in Alzheimer's disease and a neuroprotective factor, humanin. *Curr Neuropharmacol.* 2006;4(2):139-147.
- Ning L, Tian L, Smirnov S, et al. Interactions between ICAM-5 and  $\beta$ 1 integrins regulate neuronal synapse formation. *J Cell Sci.* 2013;126(Pt 1):77-89.
- Niu J, Tsai HH, Hoi KK, et al. Aberrant oligodendroglial-vascular interactions disrupt the blood-brain barrier, triggering CNS inflammation. *Nat Neurosci.* 2019;22(5):709-718
- Nixon RA, Wegiel J, Kumar A, et al. Extensive involvement of autophagy in Alzheimer disease: an immuno-electron microscopy study. *J Neuropathol Exp Neurol.* 2005;64(2):113-122.
- Okamura N, Yanai K. Brain imaging: Applications of tau PET imaging. *Nat Rev Neurol.* 2017;13(4):197-198.
- Okochi M, Tagami S, Yanagida K, et al.  $\gamma$ -secretase modulators and presenilin 1 mutants act differently on presenilin/ $\gamma$ -secretase function to cleave A $\beta$ 42 and A $\beta$ 43. *Cell Rep.* 2013;3(1):42-51.
- Orre M, Kamphuis W, Osborn LM, et al. Isolation of glia from Alzheimer's mice reveals inflammation and dysfunction. *Neurobiol Aging.* 2014;35(12):2746-2760.
- Ortega-Martínez S. A new perspective on the role of the CREB family of transcription factors in memory consolidation via adult hippocampal neurogenesis. *Front Mol Neurosci.* 2015;8:46.
- Osborn, Lana M et al. "Astrogliosis: An integral player in the pathogenesis of Alzheimer's disease." *Progress in neurobiology* 144 (2016): 121-41.
- Overk CR, Masliah E. Pathogenesis of synaptic degeneration in Alzheimer's disease and Lewy body disease. *Biochem Pharmacol.* 2014;88(4):508-516.
- Paidi RK, Nthenge-Ngumbau DN, Singh R, Kankanala T, Mehta H, Mohanakumar KP. Mitochondrial Deficits Accompany Cognitive Decline Following Single Bilateral Intracerebroventricular Streptozotocin. *Curr Alzheimer Res.* 2015;12(8):785-795.
- Palop JJ, Mucke L. Epilepsy and cognitive impairments in Alzheimer disease. *Arch Neurol.* 2009;66(4):435-440.

- Palop JJ, Mucke L. Synaptic depression and aberrant excitatory network activity in Alzheimer's disease: two faces of the same coin?. *Neuromolecular Med.* 2010;12(1):48-55.
- Panza F, Solfrizzi V, Imbimbo BP, Logroscino G. Amyloid-directed monoclonal antibodies for the treatment of Alzheimer's disease: the point of no return?. *Expert Opin Biol Ther.* 2014;14(10):1465-1476.
- Paoli F, Spignoli G, Pepeu G. Oxiracetam and D-pyroglutamic acid antagonize a disruption of passive avoidance behaviour induced by the N-methyl-D-aspartate receptor antagonist 2-amino-5-phosphonovalerate. *Psychopharmacology (Berl).* 1990;100(1):130-131.
- Paolicelli RC, Bolasco G, Pagani F, et al. Synaptic pruning by microglia is necessary for normal brain development. *Science.* 2011;333(6048):1456-1458.
- Parachikova A, Vasilevko V, Cribbs DH, LaFerla FM, Green KN. Reductions in amyloid-beta-derived neuroinflammation, with minocycline, restore cognition but do not significantly affect tau hyperphosphorylation. *J Alzheimers Dis.* 2010;21(2):527-542.
- Pardridge WM. Neurotrophins, neuroprotection and the blood-brain barrier. *Curr Opin Investig Drugs.* 2002;3(12):1753-1757.
- Park DS, Morris EJ, Padmanabhan J, Shelanski ML, Geller HM, Greene LA. Cyclin-dependent kinases participate in death of neurons evoked by DNA-damaging agents. *J Cell Biol.* 1998;143(2):457-467.
- Paroni G, Bisceglia P, Seripa D. Understanding the Amyloid Hypothesis in Alzheimer's Disease. *J Alzheimers Dis.* 2019;68(2):493-510.
- Parsons CG, Danysz W, Dekundy A, Pulte I. Memantine and cholinesterase inhibitors: complementary mechanisms in the treatment of Alzheimer's disease. *Neurotox Res.* 2013;24(3):358-369.
- Pegueroles J, Jiménez A, Vilaplana E, et al. Obesity and Alzheimer's disease, does the obesity paradox really exist? A magnetic resonance imaging study. *Oncotarget.* 2018;9(78):34691-34698.
- Pei JJ, Björkdahl C, Zhang H, Zhou X, Winblad B. p70 S6 kinase and tau in Alzheimer's disease. *J Alzheimers Dis.* 2008;14(4):385-392.
- Pei JJ, Braak H, An WL, et al. Up-regulation of mitogen-activated protein kinases ERK1/2 and MEK1/2 is associated with the progression of neurofibrillary degeneration in Alzheimer's disease. *Brain Res Mol Brain Res.* 2002;109(1-2):45-55.
- Pekny M, Wilhelmsson U, Pekna M. The dual role of astrocyte activation and reactive gliosis. *Neurosci Lett.* 2014;565:30-38.
- Pepeu G. Overview and perspective on the therapy of Alzheimer's disease from a preclinical viewpoint. *Prog Neuropsychopharmacol Biol Psychiatry.* 2001;25(1):193-209.
- Perez-Nievas BG, Serrano-Pozo A. Deciphering the Astrocyte Reaction in Alzheimer's Disease. *Front Aging Neurosci.* 2018;10:114. Published 2018 Apr 25.
- Perl DP. Neuropathology of Alzheimer's disease. *Mt Sinai J Med.* 2010;77(1):32-42.
- Perry VH, Gordon S. Macrophages and microglia in the nervous system. *Trends Neurosci.* 1988;11(6):273-277.
- Perry VH, Holmes C. Microglial priming in neurodegenerative disease. *Nat Rev Neurol.* 2014;10(4):217-224.
- Pertusa M, García-Matas S, Mameri H, et al. Expression of GDNF transgene in astrocytes improves cognitive deficits in aged rats. *Neurobiol Aging.* 2008;29(9):1366-1379.
- Peter J, Scheef L, Abdulkadir A, et al. Gray matter atrophy pattern in elderly with subjective memory impairment. *Alzheimers Dement.* 2014;10(1):99-108.
- Peters JM, Hummel T, Kratzsch T, Lötsch J, Skarke C, Frölich L. Olfactory function in mild cognitive impairment and Alzheimer's disease: an investigation using psychophysical and electrophysiological techniques. *Am J Psychiatry.* 2003;160(11):1995-2002.
- Petersen RC, Doody R, Kurz A, et al. Current concepts in mild cognitive impairment. *Arch Neurol.* 2001;58(12):1985-1992.

- Philippens IH, Ormel PR, Baarends G, Johansson M, Remarque EJ, Doverskog M. Acceleration of Amyloidosis by Inflammation in the Amyloid-Beta Marmoset Monkey Model of Alzheimer's Disease. *J Alzheimers Dis.* 2017;55(1):101-113.
- Piccio L, Buonsanti C, Mariani M, et al. Blockade of TREM-2 exacerbates experimental autoimmune encephalomyelitis. *Eur J Immunol.* 2007;37(5):1290-1301.
- Pizzino G, Irrera N, Cucinotta M, et al. Oxidative Stress: Harms and Benefits for Human Health. *Oxid Med Cell Longev.* 2017;2017:8416763.
- Plotnikov A, Zehorai E, Procaccia S, Seger R. The MAPK cascades: signaling components, nuclear roles and mechanisms of nuclear translocation. *Biochim Biophys Acta.* 2011;1813(9):1619-1633.
- Pradhan J, Noakes PG, Bellingham MC. The Role of Altered BDNF/TrkB Signaling in Amyotrophic Lateral Sclerosis. *Front Cell Neurosci.* 2019;13:368.
- Prasher VP, Farrer MJ, Kessling AM, et al. Molecular mapping of Alzheimer-type dementia in Down's syndrome. *Ann Neurol.* 1998;43(3):380-383.
- Preston AR, Eichenbaum H. Interplay of hippocampus and prefrontal cortex in memory. *Curr Biol.* 2013;23(17):R764-R773.
- Price JL, McKeel DW Jr, Buckles VD, et al. Neuropathology of nondemented aging: presumptive evidence for preclinical Alzheimer disease. *Neurobiol Aging.* 2009;30(7):1026-1036.
- Prince MJ. The 10/66 dementia research group - 10 years on. *Indian J Psychiatry.* 2009;51 Suppl 1(Suppl1):S8-S15.
- Prokop S, Miller KR, Heppner FL. Microglia actions in Alzheimer's disease. *Acta Neuropathol.* 2013;126(4):461-477.
- Prybylowski K, Chang K, Sans N, Kan L, Vicini S, Wenthold RJ. The synaptic localization of NR2B-containing NMDA receptors is controlled by interactions with PDZ proteins and AP-2. *Neuron.* 2005;47(6):845-857.
- Qin S, Niu W, Iqbal N, Smith DK, Zhang CL. Orphan nuclear receptor TLX regulates astrogenesis by modulating BMP signaling. *Front Neurosci.* 2014;8:74.
- Qi-Takahara Y, Morishima-Kawashima M, Tanimura Y, et al. Longer forms of amyloid beta protein: implications for the mechanism of intramembrane cleavage by gamma-secretase. *J Neurosci.* 2005;25(2):436-445.
- Qiu C, Kivipelto M, von Strauss E. Epidemiology of Alzheimer's disease: occurrence, determinants, and strategies toward intervention. *Dialogues Clin Neurosci.* 2009;11(2):111-128.
- Rahayel S, Frasnelli J, Joubert S. The effect of Alzheimer's disease and Parkinson's disease on olfaction: a meta-analysis. *Behav Brain Res.* 2012;231(1):60-74.
- Rajamohamedsait H, Rasool S, Rajamohamedsait W, Lin Y, Sigurdsson EM. Prophylactic Active Tau Immunization Leads to Sustained Reduction in Both Tau and Amyloid- $\beta$  Pathologies in 3xTg Mice. *Sci Rep.* 2017;7(1):17034.
- Raman M, Chen W, Cobb MH. Differential regulation and properties of MAPKs. *Oncogene.* 2007;26(22):3100-3112.
- Ransohoff RM, Perry VH. Microglial physiology: unique stimuli, specialized responses. *Annu Rev Immunol.* 2009;27:119-145.
- Ransohoff RM. A polarizing question: do M1 and M2 microglia exist?. *Nat Neurosci.* 2016;19(8):987-991.
- Reisberg B, Doody R, Stöffler A, et al. Memantine in moderate-to-severe Alzheimer's disease. *N Engl J Med.* 2003;348(14):1333-1341.
- Ricciarelli R, Fedele E. The Amyloid Cascade Hypothesis in Alzheimer's Disease: It's Time to Change Our Mind. *Curr Neuropharmacol.* 2017;15(6):926-935.
- Riedel BC, Thompson PM, Brinton RD. Age, APOE and sex: Triad of risk of Alzheimer's disease. *J Steroid Biochem Mol Biol.* 2016;160:134-147.

- Ries M, Sastre M. Mechanisms of A $\beta$  Clearance and Degradation by Glial Cells. *Front Aging Neurosci.* 2016;8:160.
- Rodríguez-Arellano JJ, Parpura V, Zorec R, Verkhratsky A. Astrocytes in physiological aging and Alzheimer's disease. *Neuroscience.* 2016;323:170-182.
- Roth KA. Caspases, apoptosis, and Alzheimer disease: causation, correlation, and confusion. *J Neuropathol Exp Neurol.* 2001;60(9):829-838.
- Rouach N, Koulakoff A, Abudara V, Willecke K, Giaume C. Astroglial metabolic networks sustain hippocampal synaptic transmission. *Science.* 2008;322(5907):1551-1555.
- Ryan NS, Rossor MN, Fox NC. Alzheimer's disease in the 100 years since Alzheimer's death. *Brain.* 2015;138(Pt 12):3816-3821.
- Sáez ET, Pehar M, Vargas MR, Barbeito L, Maccioni RB. Production of nerve growth factor by beta-amyloid-stimulated astrocytes induces p75NTR-dependent tau hyperphosphorylation in cultured hippocampal neurons. *J Neurosci Res.* 2006;84(5):1098-1106.
- Sah DW, Ossipo MH, Porreca F. Neurotrophic factors as novel therapeutics for neuropathic pain. *Nat Rev Drug Discov.* 2003;2(6):460-472.
- Saha P, Biswas SC. Amyloid- $\beta$  induced astrocytosis and astrocyte death: Implication of FoxO3a-Bim-caspase3 death signaling. *Mol Cell Neurosci.* 2015;68:203-211.
- Saha P, Guha S, Biswas SC. P38K and JNK pathways are induced by amyloid- $\beta$  in astrocyte: Implication of MAPK pathways in astrogliosis in Alzheimer's disease. *Mol Cell Neurosci.* 2020;108:103551.
- Saha P, Sarkar S, Paidi RK, Biswas SC. TIMP-1: A key cytokine released from activated astrocytes protects neurons and ameliorates cognitive behaviours in a rodent model of Alzheimer's disease. *Brain Behav Immun.* 2020;87:804-819.
- Sajja VS, Hlavac N, VandeVord PJ. Role of Glia in Memory Deficits Following Traumatic Brain Injury: Biomarkers of Glia Dysfunction. *Front Integr Neurosci.* 2016;10:7.
- Samoilova EB, Horton JL, Chen Y. Experimental autoimmune encephalomyelitis in intercellular adhesion molecule-1-deficient mice. *Cell Immunol.* 1998;190(1):83-89.
- Sanphui P, Biswas SC. FoxO3a is activated and executes neuron death via Bim in response to  $\beta$ -amyloid. *Cell Death Dis.* 2013;4(5):e625. Published 2013 May 9.
- Santello M, Toni N, Volterra A. Astrocyte function from information processing to cognition and cognitive impairment. *Nat Neurosci.* 2019;22(2):154-166.
- Santos CY, Snyder PJ, Wu WC, Zhang M, Echeverria A, Alber J. Pathophysiologic relationship between Alzheimer's disease, cerebrovascular disease, and cardiovascular risk: A review and synthesis. *Alzheimers Dement (Amst).* 2017;7:69-87.
- Sarafian TA, Montes C, Imura T, et al. Disruption of astrocyte STAT3 signaling decreases mitochondrial function and increases oxidative stress in vitro. *PLoS One.* 2010;5(3):e9532.
- Sarnico I, Lanzillotta A, Boroni F, et al. NF-kappaB p50/RelA and c-Rel-containing dimers: opposite regulators of neuron vulnerability to ischaemia. *J Neurochem.* 2009;108(2):475-485.
- Sarter M, Hagan J, Dudchenko P. Behavioral screening for cognition enhancers: from indiscriminate to valid testing: Part I. *Psychopharmacology (Berl).* 1992;107(2-3):144-159.
- Sauer H, Francis JM, Jiang H, Hamilton GS, Steiner JP. Systemic treatment with GPI 1046 improves spatial memory and reverses cholinergic neuron atrophy in the medial septal nucleus of aged mice. *Brain Res.* 1999;842(1):109-118.
- Saunders A, Macosko EZ, Wysoker A, et al. Molecular Diversity and Specializations among the Cells of the Adult Mouse Brain. *Cell.* 2018;174(4):1015-1030.e16.
- Saunders AM. Gene identification in Alzheimer's disease. *Pharmacogenomics.* 2001;2(3):239-249.
- Savage MJ, Lin YG, Ciallella JR, Flood DG, Scott RW. Activation of c-Jun N-terminal kinase and p38 in an Alzheimer's disease model is associated with amyloid deposition. *J Neurosci.* 2002;22(9):3376-3385.

- Schafer DP, Lehrman EK, Kautzman AG, et al. Microglia sculpt postnatal neural circuits in an activity and complement-dependent manner. *Neuron*. 2012;74(4):691-705. doi:10.1016/j.neuron.2012.03.026
- Schafer DP, Lehrman EK, Kautzman AG, et al. Microglia sculpt postnatal neural circuits in an activity and complement-dependent manner. *Neuron*. 2012;74(4):691-705.
- Scheff SW, Price DA, Schmitt FA, Mufson EJ. Hippocampal synaptic loss in early Alzheimer's disease and mild cognitive impairment. *Neurobiol Aging*. 2006;27(10):1372-1384.
- Scheff SW, Price DA, Schmitt FA, Scheff MA, Mufson EJ. Synaptic loss in the inferior temporal gyrus in mild cognitive impairment and Alzheimer's disease. *J Alzheimers Dis*. 2011;24(3):547-557.
- Scheuner D, Eckman C, Jensen M, et al. Secreted amyloid beta-protein similar to that in the senile plaques of Alzheimer's disease is increased in vivo by the presenilin 1 and 2 and APP mutations linked to familial Alzheimer's disease. *Nat Med*. 1996;2(8):864-870.
- Schmid CD, Sautkulis LN, Danielson PE, et al. Heterogeneous expression of the triggering receptor expressed on myeloid cells-2 on adult murine microglia. *J Neurochem*. 2002;83(6):1309-1320.
- Schöll M, Lockhart SN, Schonhaut DR, et al. PET Imaging of Tau Deposition in the Aging Human Brain. *Neuron*. 2016;89(5):971-982.
- Schulz C, Gomez Perdiguero E, Chorro L, et al. A lineage of myeloid cells independent of Myb and hematopoietic stem cells. *Science*. 2012;336(6077):86-90.
- Schwarz AJ, Yu P, Miller BB, et al. Regional profiles of the candidate tau PET ligand 18F-AV-1451 recapitulate key features of Braak histopathological stages. *Brain*. 2016;139(Pt 5):1539-1550.
- Sekar A, Bialas AR, de Rivera H, et al. Schizophrenia risk from complex variation of complement component 4. *Nature*. 2016;530(7589):177-183.
- Selkoe DJ, Schenk D. Alzheimer's disease: molecular understanding predicts amyloid-based therapeutics. *Annu Rev Pharmacol Toxicol*. 2003;43:545-584.
- Selkoe DJ. The molecular pathology of Alzheimer's disease. *Neuron*. 1991;6(4):487-498.
- Serrano-Pozo A, Betensky RA, Frosch MP, Hyman BT. Plaque-Associated Local Toxicity Increases over the Clinical Course of Alzheimer Disease. *Am J Pathol*. 2016;186(2):375-384.
- Serrano-Pozo A, Frosch MP, Masliah E, Hyman BT. Neuropathological alterations in Alzheimer disease. *Cold Spring Harb Perspect Med*. 2011 Sep;1(1):a006189.
- Serrano-Pozo A, Mielke ML, Gómez-Isla T, et al. Reactive glia not only associates with plaques but also parallels tangles in Alzheimer's disease. *Am J Pathol*. 2011;179(3):1373-1384.
- Sevigny J, Chiao P, Bussière T, et al. The antibody aducanumab reduces A $\beta$  plaques in Alzheimer's disease. *Nature*. 2016;537(7618):50-56.
- Shaul YD, Seger R. The MEK/ERK cascade: from signaling specificity to diverse functions. *Biochim Biophys Acta*. 2007;1773(8):1213-1226.
- Sheldon AL, Robinson MB. The role of glutamate transporters in neurodegenerative diseases and potential opportunities for intervention. *Neurochem Int*. 2007;51(6-7):333-355.
- Shen J, Bronson RT, Chen DF, Xia W, Selkoe DJ, Tonegawa S. Skeletal and CNS defects in Presenilin-1-deficient mice. *Cell*. 1997;89(4):629-639.
- Shen J, Kelleher RJ 3rd. The presenilin hypothesis of Alzheimer's disease: evidence for a loss-of-function pathogenic mechanism. *Proc Natl Acad Sci U S A*. 2007;104(2):403-409.
- Shi Q, Chowdhury S, Ma R, et al. Complement C3 deficiency protects against neurodegeneration in aged plaque-rich APP/PS1 mice. *Sci Transl Med*. 2017;9(392):eaaf6295.
- Shoji M, Iwakami N, Takeuchi S, et al. JNK activation is associated with intracellular beta-amyloid accumulation. *Brain Res Mol Brain Res*. 2000;85(1-2):221-233.

- SHOLL DA. Dendritic organization in the neurons of the visual and motor cortices of the cat. *J Anat.* 1953;87(4):387-406.
- Sieber MW, Jaenisch N, Brehm M, et al. Attenuated inflammatory response in triggering receptor expressed on myeloid cells 2 (TREM2) knock-out mice following stroke. *PLoS One.* 2013;8(1):e52982.
- Sierra A, de Castro F, Del Río-Hortega J, Rafael Iglesias-Rozas J, Garrosa M, Kettenmann H. The "Big-Bang" for modern glial biology: Translation and comments on Pío del Río-Hortega 1919 series of papers on microglia. *Glia.*
- Simon E, Obst J, Gomez-Nicola D. The Evolving Dialogue of Microglia and Neurons in Alzheimer's Disease: Microglia as Necessary Transducers of Pathology. *Neuroscience.* 2019;405:24-34.
- Sims NR, Bowen DM, Allen SJ, et al. Presynaptic cholinergic dysfunction in patients with dementia. *J Neurochem.* 1983;40(2):503-509.
- Smith MA, Casadesus G, Joseph JA, Perry G. Amyloid-beta and tau serve antioxidant functions in the aging and Alzheimer brain. *Free Radic Biol Med.* 2002;33(9):1194-1199.
- Smith SJ, Fenwick PS, Nicholson AG, et al. Inhibitory effect of p38 mitogen-activated protein kinase inhibitors on cytokine release from human macrophages. *Br J Pharmacol.* 2006;149(4):393-404.
- Smits HA, Rijmsus A, van Loon JH, et al. Amyloid-beta-induced chemokine production in primary human macrophages and astrocytes. *J Neuroimmunol.* 2002;127(1-2):160-168.
- Snow WM, Albeni BC. Neuronal Gene Targets of NF- $\kappa$ B and Their Dysregulation in Alzheimer's Disease. *Front Mol Neurosci.* 2016;9:118.
- Sochocka M, Zwolińska K, Leszek J. The Infectious Etiology of Alzheimer's Disease. *Curr Neuropharmacol.* 2017;15(7):996-1009.
- Sofroniew MV, Vinters HV. Astrocytes: biology and pathology. *Acta Neuropathol.* 2010;119(1):7-35.
- Sohur US, Dixit MN, Chen CL, Byrom MW, Kerr LA. Rel/NF-kappaB represses bcl-2 transcription in pro-B lymphocytes. *Gene Expr.* 1999;8(4):219-229.
- Söllvander S, Nikitidou E, Brolin R, et al. Accumulation of amyloid- $\beta$  by astrocytes result in enlarged endosomes and microvesicle-induced apoptosis of neurons. *Mol Neurodegener.* 2016;11(1):38.
- Spangenberg EE, Green KN. Inflammation in Alzheimer's disease: Lessons learned from microglia-depletion models. *Brain Behav Immun.* 2017;61:1-11.
- Spanos F, Liddel SA. An Overview of Astrocyte Responses in Genetically Induced Alzheimer's Disease Mouse Models. *Cells.* 2020;9(11):2415.
- Sperling RA, Aisen PS, Beckett LA, et al. Toward defining the preclinical stages of Alzheimer's disease: recommendations from the National Institute on Aging-Alzheimer's Association workgroups on diagnostic guidelines for Alzheimer's disease. *Alzheimers Dement.* 2011;7(3):280-292.
- Srinivasan M, Lahiri DK. Significance of NF- $\kappa$ B as a pivotal therapeutic target in the neurodegenerative pathologies of Alzheimer's disease and multiple sclerosis. *Expert Opin Ther Targets.* 2015;19(4):471-487.
- Stampfer MJ. Cardiovascular disease and Alzheimer's disease: common links. *J Intern Med.* 2006;260(3):211-223.
- Steele ML, Robinson SR. Reactive astrocytes give neurons less support: implications for Alzheimer's disease. *Neurobiol Aging.* 2012;33(2).
- Stevens B, Allen NJ, Vazquez LE, et al. The classical complement cascade mediates CNS synapse elimination. *Cell.* 2007;131(6):1164-1178.
- Streit WJ, Braak H, Xue QS, Bechmann I. Dystrophic (senescent) rather than activated microglial cells are associated with tau pathology and likely precede neurodegeneration in Alzheimer's disease. *Acta Neuropathol.* 2009;118(4):475-485.



- Strittmatter WJ, Saunders AM, Schmechel D, et al. Apolipoprotein E: high-avidity binding to beta-amyloid and increased frequency of type 4 allele in late-onset familial Alzheimer disease. *Proc Natl Acad Sci U S A*. 1993;90(5):1977-1981.
- Su Y, Ryder J, Ni B. Inhibition of Abeta production and APP maturation by a specific PKA inhibitor. *FEBS Lett*. 2003;546(2-3):407-410.
- Sutphen CL, Jasielec MS, Shah AR, et al. Longitudinal Cerebrospinal Fluid Biomarker Changes in Preclinical Alzheimer Disease During Middle Age. *JAMA Neurol*. 2015;72(9):1029-1042.
- Swardfager W, Lanctôt K, Rothenburg L, Wong A, Cappell J, Herrmann N. A meta-analysis of cytokines in Alzheimer's disease. *Biol Psychiatry*. 2010;68(10):930-941.
- Takami M, Nagashima Y, Sano Y, et al. gamma-Secretase: successive tripeptide and tetrapeptide release from the transmembrane domain of beta-carboxyl terminal fragment. *J Neurosci*. 2009;29(41):13042-13052.
- Talman V, Pascale A, Jääntti M, Amadio M, Tuominen RK. Protein Kinase C Activation as a Potential Therapeutic Strategy in Alzheimer's Disease: Is there a Role for Embryonic Lethal Abnormal Vision-like Proteins?. *Basic Clin Pharmacol Toxicol*. 2016;119(2):149-160.
- Tarasoff-Conway JM, Carare RO, Osorio RS, et al. Clearance systems in the brain-implications for Alzheimer disease. *Nat Rev Neurol*. 2015;11(8):457-470.
- Tare M, Modi RM, Nainaparampil JJ, et al. Activation of JNK signaling mediates amyloid- $\beta$ -dependent cell death. *PLoS One*. 2011;6(9):e24361.
- Tcw J, Goate AM. Genetics of  $\beta$ -Amyloid Precursor Protein in Alzheimer's Disease. *Cold Spring Harb Perspect Med*. 2017;7(6):a024539. Published 2017 Jun 1.
- Teipel SJ, Fritz HC, Grothe MJ; Alzheimer's Disease Neuroimaging Initiative. Neuropathologic features associated with basal forebrain atrophy in Alzheimer disease. *Neurology*. 2020;95(10):e1301-e1311.
- Terry AV Jr, Buccafusco JJ. The cholinergic hypothesis of age and Alzheimer's disease-related cognitive deficits: recent challenges and their implications for novel drug development. *J Pharmacol Exp Ther*. 2003;306(3):821-827.
- Terry RD, Masliah E, Salmon DP, et al. Physical basis of cognitive alterations in Alzheimer's disease: synapse loss is the major correlate of cognitive impairment. *Ann Neurol*. 1991;30(4):572-580.
- Thal DR, Capetillo-Zarate E, Del Tredici K, Braak H. The development of amyloid beta protein deposits in the aged brain. *Sci Aging Knowledge Environ*. 2006;2006(6):re1.
- Thal DR, Del Tredici K, Ludolph AC, et al. Stages of granulovacuolar degeneration: their relation to Alzheimer's disease and chronic stress response. *Acta Neuropathol*. 2011;122(5):577-589.
- Thal DR, Ghebremedhin E, Rüb U, Yamaguchi H, Del Tredici K, Braak H. Two types of sporadic cerebral amyloid angiopathy. *J Neuropathol Exp Neurol*. 2002;61(3):282-293.
- Thal DR, Schultz C, Dehghani F, Yamaguchi H, Braak H, Braak E. Amyloid beta-protein (Abeta)-containing astrocytes are located preferentially near N-terminal-truncated Abeta deposits in the human entorhinal cortex. *Acta Neuropathol*. 2000;100(6):608-617.
- Thawkar BS, Kaur G. Inhibitors of NF- $\kappa$ B and P2X7/NLRP3/Caspase 1 pathway in microglia: Novel therapeutic opportunities in neuroinflammation induced early-stage Alzheimer's disease. *J Neuroimmunol*. 2019;326:62-74.
- Tomita S, Kirino Y, Suzuki T. Cleavage of Alzheimer's amyloid precursor protein (APP) by secretases occurs after O-glycosylation of APP in the protein secretory pathway. Identification of intracellular compartments in which APP cleavage occurs without using toxic agents that interfere with protein metabolism. *J Biol Chem*. 1998;273(11):6277-6284.
- Tran MH, Yamada K, Nabeshima T. Amyloid beta-peptide induces cholinergic dysfunction and cognitive deficits: a minireview. *Peptides*. 2002;23(7):1271-1283.

- Trojanowski JQ, Lee VM. The role of tau in Alzheimer's disease. *Med Clin North Am.* 2002;86(3):615-627.
- Troy CM, Rabacchi SA, Xu Z, et al. beta-Amyloid-induced neuronal apoptosis requires c-Jun N-terminal kinase activation. *J Neurochem.* 2001;77(1):157-164.
- Trzeciakiewicz H, Tseng JH, Wander CM, et al. A Dual Pathogenic Mechanism Links Tau Acetylation to Sporadic Tauopathy. *Sci Rep.* 2017;7:44102.
- Unichenko P, Dvorzhak A, Kirischuk S. Transporter-mediated replacement of extracellular glutamate for GABA in the developing murine neocortex. *Eur J Neurosci.* 2013;38(11):3580-3588.
- United Nations: World Population Prospects. The 2004 Revision. New York, Department of Economic and Social Affairs, Population Division, 2005.
- Varnum MM, Ikezu T. The classification of microglial activation phenotypes on neurodegeneration and regeneration in Alzheimer's disease brain. *Arch Immunol Ther Exp (Warsz).* 2012;60(4):251-266.
- Vedin I, Cederholm T, Freund Levi Y, et al. Effects of docosahexaenoic acid-rich n-3 fatty acid supplementation on cytokine release from blood mononuclear leukocytes: the OmegaAD study. *Am J Clin Nutr.* 2008;87(6):1616-1622.
- Veerhuis R, Nielsen HM, Tenner AJ. Complement in the brain. *Mol Immunol.* 2011;48(14):1592-1603.
- Vehmas AK, Kawas CH, Stewart WF, Troncoso JC. Immune reactive cells in senile plaques and cognitive decline in Alzheimer's disease. *Neurobiol Aging.* 2003;24(2):321-331.
- Venegas C, Heneka MT. Danger-associated molecular patterns in Alzheimer's disease. *J Leukoc Biol.* 2017;101(1):87-98.
- Venneti S, Lopresti BJ, Wiley CA. The peripheral benzodiazepine receptor (Translocator protein 18kDa) in microglia: from pathology to imaging. *Prog Neurobiol.* 2006;80(6):308-322.
- Verkhtsky A, Zorec R, Rodríguez JJ, Parpura V. Astroglia dynamics in ageing and Alzheimer's disease. *Curr Opin Pharmacol.* 2016;26:74-79.
- Verma M, Howard RJ. Semantic memory and language dysfunction in early Alzheimer's disease: a review. *Int J Geriatr Psychiatry.* 2012;27(12):1209-1217.
- Villegas-Llerena C, Phillips A, Garcia-Reitboeck P, Hardy J, Pocock JM. Microglial genes regulating neuroinflammation in the progression of Alzheimer's disease. *Curr Opin Neurobiol.* 2016;36:74-81.
- Voisin T, Vellas B. Diagnosis and treatment of patients with severe Alzheimer's disease. *Drugs Aging.* 2009;26(2):135-144.
- Wake H, Moorhouse AJ, Jinno S, Kohsaka S, Nabekura J. Resting microglia directly monitor the functional state of synapses in vivo and determine the fate of ischemic terminals. *J Neurosci.* 2009;29(13):3974-3980.
- Walker DG, Dalsing-Hernandez JE, Campbell NA, Lue LF. Decreased expression of CD200 and CD200 receptor in Alzheimer's disease: a potential mechanism leading to chronic inflammation. *Exp Neurol.* 2009;215(1):5-19.
- Walker DG, Lue LF. Immune phenotypes of microglia in human neurodegenerative disease: challenges to detecting microglial polarization in human brains. *Alzheimers Res Ther.* 2015;7(1):56.
- Walker LC. A $\beta$  Plaques. *Free Neuropathol.* 2020;1:31.
- Walsh DM, Selkoe DJ. Deciphering the molecular basis of memory failure in Alzheimer's disease. *Neuron.* 2004;44(1):181-193.
- Wang A, Das P, Switzer RC 3rd, Golde TE, Jankowsky JL. Robust amyloid clearance in a mouse model of Alzheimer's disease provides novel insights into the mechanism of amyloid-beta immunotherapy. *J Neurosci.* 2011;31(11):4124-4136.
- Weggen S, Eriksen JL, Das P, et al. A subset of NSAIDs lower amyloidogenic Abeta42 independently of cyclooxygenase activity. *Nature.* 2001;414(6860):212-216.

- Wennström M, Nielsen HM, Orhan F, Londos E, Minthon L, Erhardt S. Kynurenic Acid levels in cerebrospinal fluid from patients with Alzheimer's disease or dementia with lewy bodies. *Int J Tryptophan Res.* 2014;7:1-7.
- Westerman MA, Cooper-Blacketer D, Mariash A, et al. The relationship between Abeta and memory in the Tg2576 mouse model of Alzheimer's disease. *J Neurosci.* 2002;22(5):1858-1867.
- Wilcock GK, Esiri MM, Bowen DM, Smith CC. Alzheimer's disease. Correlation of cortical choline acetyltransferase activity with the severity of dementia and histological abnormalities. *J Neurol Sci.* 1982;57(2-3):407-417.
- Witkowska AM, Borawska MH. Soluble intercellular adhesion molecule-1 (sICAM-1): an overview. *Eur Cytokine Netw.* 2004;15(2):91-98.
- Wolf SA, Boddeke HW, Kettenmann H. Microglia in Physiology and Disease. *Annu Rev Physiol.* 2017;79:619-643.
- Wolfe MS, Xia W, Ostaszewski BL, Diehl TS, Kimberly WT, Selkoe DJ. Two transmembrane aspartates in presenilin-1 required for presenilin endoproteolysis and gamma-secretase activity. *Nature.* 1999;398(6727):513-517.
- WOODARD JS. Clinicopathologic significance of granulovacuolar degeneration in Alzheimer's disease. *J Neuropathol Exp Neurol.* 1962;21:85-91.
- Wyss-Coray T, Loike JD, Brionne TC, et al. Adult mouse astrocytes degrade amyloid-beta in vitro and in situ. *Nat Med.* 2003;9(4):453-457.
- Xia D, Watanabe H, Wu B, et al. Presenilin-1 knockin mice reveal loss-of-function mechanism for familial Alzheimer's disease. *Neuron.* 2015;85(5):967-981.
- Yamamoto M, Kiyota T, Walsh SM, Liu J, Kipnis J, Ikezu T. Cytokine-mediated inhibition of fibrillar amyloid-beta peptide degradation by human mononuclear phagocytes. *J Immunol.* 2008;181(6):3877-3886.
- Yang HD, Kim DH, Lee SB, Young LD. History of Alzheimer's Disease. *Dement Neurocogn Disord.* 2016;15(4):115-121.
- Yankner BA. The pathogenesis of Alzheimer's disease. Is amyloid beta-protein the beginning or the end?. *Ann N Y Acad Sci.* 2000;924:26-28.
- Yao Z, Macara AM, Lelito KR, Minosyan TY, Shafer OT. Analysis of functional neuronal connectivity in the Drosophila brain. *J Neurophysiol.* 2012;108(2):684-696.
- Yarza R, Vela S, Solas M, Ramirez MJ. c-Jun N-terminal Kinase (JNK) Signaling as a Therapeutic Target for Alzheimer's Disease. *Front Pharmacol.* 2016;6:321.
- Yasuhara O, Kawamata T, Aimi Y, McGeer EG, McGeer PL. Two types of dystrophic neurites in senile plaques of Alzheimer disease and elderly non-demented cases. *Neurosci Lett.* 1994;171(1-2):73-76.
- Yen K, Wan J, Mehta HH, et al. Humanin Prevents Age-Related Cognitive Decline in Mice and is Associated with Improved Cognitive Age in Humans. *Sci Rep.* 2018;8(1):14212.
- Yin KJ, Cirrito JR, Yan P, et al. Matrix metalloproteinases expressed by astrocytes mediate extracellular amyloid-beta peptide catabolism. *J Neurosci.* 2006;26(43):10939-10948.
- Yoshihara Y, Oka S, Nemoto Y, et al. An ICAM-related neuronal glycoprotein, telencephalin, with brain segment-specific expression. *Neuron.* 1994;12(3):541-553.
- Zhang B, Gaiteri C, Bodea LG, et al. Integrated systems approach identifies genetic nodes and networks in late-onset Alzheimer's disease. *Cell.* 2013;153(3):707-720.
- Zhao J, Liu X, Xia W, Zhang Y, Wang C. Targeting Amyloidogenic Processing of APP in Alzheimer's Disease. *Front Mol Neurosci.* 2020;13:137.
- Zhao J, O'Connor T, Vassar R. The contribution of activated astrocytes to Aβ production: implications for Alzheimer's disease pathogenesis. *J Neuroinflammation.* 2011;8:150. Published 2011 Nov 2. doi:10.1186/1742-2094-8-150

- Zheng X, Liu D, Roychaudhuri R, Teplow DB, Bowers MT. Amyloid  $\beta$ -Protein Assembly: Differential Effects of the Protective A2T Mutation and Recessive A2V Familial Alzheimer's Disease Mutation. *ACS Chem Neurosci*. 2015;6(10):1732-1740.
- Zhou B, Zuo YX, Jiang RT. Astrocyte morphology: Diversity, plasticity, and role in neurological diseases. *CNS Neurosci Ther*. 2019;25(6):665-673.
- Zhu X, Bergles DE, Nishiyama A. NG2 cells generate both oligodendrocytes and gray matter astrocytes. *Development*. 2008;135(1):145-157.
- Zorec R, Parpura V, Vardjan N, Verkhratsky A. Astrocytic face of Alzheimer's disease. *Behav Brain Res*. 2017;322(Pt B):250-257.

The background of the image is a light-colored, marbled paper with a complex, organic pattern of veins in shades of beige, cream, and light brown. In the center of the image, there is a dark blue rounded rectangle with a thin white border. Inside this rectangle, the words "CERTIFICATES AND PUBLICATIONS" are written in a white, bold, sans-serif font, arranged in three lines.

CERTIFICATES  
AND  
PUBLICATIONS

# Centre for Cellular and Molecular Biology

Hyderabad

(Council of Scientific & Industrial Research)



## Certificate

*This is to certify that Dr./Mr./Ms. **Subhalakshmi Guha** has participated/presented poster in the Brainstorming Meeting and Workshop on Proteomics : Present and Future field at Centre for Cellular and Molecular Biology, Hyderabad from 22<sup>nd</sup> November-1<sup>st</sup> December 2014.*

**Dr Ch Mohan Rao**  
Director, CCMB

  
**Dr Suman S Thakur**  
Convener

*Symposium on*  
**Neural Functions of the Aging Brain**

ON 27 - 28 SEPTEMBER 2016



ORGANISED BY  
**INTER UNIVERSITY CENTRE FOR BIOMEDICAL RESEARCH &  
SUPER SPECIALITY HOSPITAL**

THALAPPADY, KOTTAYAM-686009, KERALA, INDIA



SUPPORTED BY  
**RAJIV GANDHI CENTRE FOR BIOTECHNOLOGY**  
THIRUVANANTHAPURAM

# *Certificate*

*This is to Certify that*

*Prof./Dr./Mr./Ms.* ..... *Subhalakshmi Guha and*  
*was the 1<sup>st</sup> Prize.*

.....  
*has presented a paper (~~Keynote/Invited/Poster~~) / <sup>✓</sup> participated* in the  
*Symposium on Neural Functions of the Aging Brain (NFAB) held at*  
*Thiruvananthapuram, Kerala, India during 27<sup>th</sup> to 28<sup>th</sup> September 2016.*

THIRUVANANTHAPURAM  
28<sup>TH</sup> SEPTEMBER 2016

*Mohan K.P.*  
MOHANAKUMAR K.P.  
DIRECTOR



# XL All India Cell Biology Conference &



## International Symposium on *Functional Genomics and Epigenomics*

*Jiwaji University, Gwalior*

November 17-19, 2016

### Certificate

This is to certify that Dr./Mr./Ms. Subhalakshmi Ousha of  
CSIR- Indian Institute of Chemical Biology  
\_\_\_\_\_ has participated in the XL All India Cell Biology Conference.

He/She has presented a paper entitled "Role of astrocyte-secreted -----  
Alzheimer's disease" in the Oral/Poster session of the conference.

**Dr. H.S. Misra**  
Secretary, ISCB

**Prof. I.K. Patro**  
Convener

**Prof. P.K. Tiwari**  
Organizing Secretary



NDD-2017



International Conference  
on

“Neurodegenerative Disorders: Current and Future Perspective”

Hosted by

Centre with Potential for Excellence in Particular Area (CPEPA), University of Calcutta  
Institute of Neurosciences, Kolkata  
Institute of Neurosciences, Newcastle University, Newcastle, upon Tyne, UK



Held on

February 10-12, 2017

Venue: The Oberoi Grand, Kolkata, India

**Certificate of Excellence**

This is to certify that Dr./ Mr./ Ms. <sup>✓</sup> SUBHALAKSHMI GUHA has been awarded  
First/ Second/ Third <sup>✓</sup> position for best ‘short oral presentation’ / ‘poster <sup>✓</sup> presentation’ and in a tripartite  
International Conference, NDD-2017 held on February 10-12, 2017 at Kolkata, India.

Prof. David Burn  
University of New Castle,  
United Kingdom  
Chairperson

Prof. Robin Sengupta  
Institute of Neurosciences,  
Kolkata, India  
Chairperson

Prof. Pritha Mukhopadhyay  
University of Calcutta,  
Kolkata, India  
Convener

Prof. Sanjit Dey  
University of Calcutta,  
Kolkata, India  
Organizing Secretary



an international forum for cell biology

8120 woodmont avenue, suite 750 • bethesda, maryland 20814-2762, usa  
tel: 301-347-9300 • fax: 301-347-9310 • email: [ascbinfo@ascb.org](mailto:ascbinfo@ascb.org) • website: [www.ascb.org](http://www.ascb.org)

Thursday, December 13, 2018

To Whom It May Concern:

This confirms that Subhalakshmi Guha attended the ASCB|EMBO 2018 meeting held in San Diego, CA on December 8-12, 2018.

Sincerely,

Jodi Nunnari  
President of ASCB Board of Directors

This certificate of attendance was sent to:  
[subhalakshmi.guha@gmail.com](mailto:subhalakshmi.guha@gmail.com)

**OFFICERS**

JODI NUNNARI

*President*

PIETRO DE CAMILLI

*Past President*

ANDREW MURRAY

*President-Elect*

KERRY BLOOM

*Secretary*

GARY J. GORBSKY

*Treasurer*

ERIKA C. SHUGART

*Chief Executive Officer*

•

**COUNCIL**

ANGELIKA AMON

MIKE EHLERS

BOB GOLDSTEIN

JOHN K. HAYNES

REBECCA HEALD

ERIKA L. F. HOLZBAUR

JANET IWASA

GEORGE LANGFORD

WALLACE F. MARSHALL

ANNE SPANG

JULIE THERIOT

ORA A. WEISZ

•

**COMMITTEE CHAIRS**

ALYSSA LESKO

*Co-Chair*

COURTNEY SCHROEDER

*Co-Chair*

*Committee for Postdocs & Students*

ERIN DOLAN

*Co-Chair*

MELANIE STYERS

*Co-Chair*

*Education*

GARY J. GORBSKY

*Finance & Audit*

LAWRENCE M. BANKS

*Co-Chair*

XUBLAO YAO

*Co-Chair*

*International Affairs*

KERRY BLOOM

*Membership*

FRANKLIN CARRERO-MARTÍNEZ

*Co-Chair*

VERONICA SEGARRA

*Co-Chair*

*Minorities Affairs*

ARSHAD DESAI

*Nominating*

THOMAS LANGER

*Co-Chair*

SAMARA RECK-PETERSON

*Co-Chair*

*Program*

LEE LIGON

*Public Information*

CONNIE M. LEE

*Public Policy*

DIANE L. BARBER

*Women in Cell Biology*

•

**CBE—LIFE SCIENCES EDUCATION**

ERIN L. DOLAN

*Editor-in-Chief*

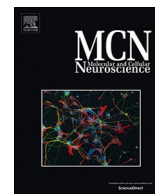
•

**MOLECULAR BIOLOGY**

**OF THE CELL**

DAVID G. DRUBIN

*Editor-in-Chief*



# P38K and JNK pathways are induced by amyloid- $\beta$ in astrocyte: Implication of MAPK pathways in astrogliosis in Alzheimer's disease

Pampa Saha<sup>1</sup>, Subhalakshmi Guha, Subhas Chandra Biswas\*

Cell Biology and Physiology Division, CSIR-Indian Institute of Chemical Biology, 4 Raja S. C. Mullick Road, Kolkata 700 032, India

## ARTICLE INFO

### Keywords:

Alzheimer's disease  
MAPK signalling  
Astrogliosis  
 $\beta$ -Amyloid  
p38K  
JNK

## ABSTRACT

Astrocyte activation is one of the crucial hallmarks of Alzheimer's disease (AD) along with amyloid- $\beta$  (A $\beta$ ) plaques, neurofibrillary tangles and neuron death. Glial scar and factors secreted from activated astrocytes have important contribution on neuronal health in AD. In this study, we investigated the mechanisms of astrocyte activation both in *in vitro* and *in vivo* models of AD. In this regard, mitogen activated protein kinase (MAPK) signalling cascades that control several fundamental and stress related cellular events, has been implicated in astrocyte activation in various neurological diseases. We checked activation of different MAPKs by western blot and immunocytochemistry and found that both JNK and p38K, but not ERK pathways are activated in A $\beta$ -treated astrocytes in culture and in A $\beta$ -infused rat brain cortex. Next, to investigate the downstream consequences of these two MAPKs (JNK and p38K) in A $\beta$ -induced astrocyte activation, we individually blocked these pathways by specific inhibitors in presence and absence of A $\beta$  and checked A $\beta$ -induced cellular proliferation, morphological changes and glial fibrillary acidic protein (GFAP) upregulation. We found that activation of both JNK and p38K signalling cascades are involved in astrocyte proliferation evoked by A $\beta$ , whereas only p38K pathway is implicated in morphological changes and GFAP upregulation in astrocytes exposed to A $\beta$ . To further validate the implication of p38K pathway in A $\beta$ -induced astrocyte activation, we also observed that transcription factor ATF2, a downstream phosphorylation substrate of p38, is phosphorylated upon A $\beta$  treatment. Taken together, our study indicates that p38K and JNK pathways mediate astrocyte activation and both the pathways are involved in cellular proliferation but only p38K pathway contributes in morphological changes triggered by A $\beta$ .

## 1. Introduction

Alzheimer's disease (AD) is a neurodegenerative disorder with no cure and most common form of dementia that occurs mostly in elderly. Extracellular amyloid- $\beta$  (A $\beta$ ) deposition in senile plaques (Hardy and Selkoe, 2002; Beyreuther et al., 1991; Moro et al., 2010; Villemagne et al., 2013) and intracellular neurofibrillary tangles formation due to hyperphosphorylation of tau (Hanger et al., 1998; Iqbal et al., 2002) are two important characteristic pathological features of the disease. In addition, reactive astrogliosis or astrocyte activation (Olabarria et al., 2010; Kraner and Norris, 2018) and neuron death underlie the pathology of the disease (Biswas et al., 2007; Hardy and Selkoe, 2002; LaFerla et al., 1995; Nakagawa et al., 2000; Selkoe, 2001). While A $\beta$  exposure to neuron results its death, astrocytes have been found to elicit

a different set of responses collectively known as astrocyte activation when exposed to A $\beta$  (Abeti et al., 2011; Abramov et al., 2004; Furman et al., 2012; Garwood et al., 2011; Hu et al., 1998; Paradisi et al., 2004; Ahmad et al., 2019). Astrocyte activation is characterized by cellular hypertrophy, cell proliferation and cytokine secretion (Garwood et al., 2011; Olabarria et al., 2010; Zhang et al., 2018). These events have immense effects on neuronal health in various neurodegenerative diseases including AD (Abeti et al., 2011; Abramov et al., 2004; Furman et al., 2012). However, the mechanism of astrocyte activation in response to A $\beta$  still remains elusive. During the course of inflammation, a number of signal transduction pathways are activated in astrocytes and in effect, neurons are affected through a number of neuroinflammatory molecules secreted by astrocytes (Gadea et al., 2008; Liu et al., 2014; McLennan et al., 2008; Xie et al., 2004; Allen and Eroglu, 2017).

**Abbreviation:** AD, Alzheimer's disease; A $\beta$ ,  $\beta$ -Amyloid; MAPK, Mitogen activated protein kinase; NFT, Neurofibrillary tangles; CNS, Central nervous system; JNK, c-Jun NH2 terminal kinase; ERK, extracellular signal related kinase; SAA, Serum Amyloid A; PI3K, Phosphatidylinositol 3-kinase; GFAP, Glial fibrillary acidic protein; SDF-1 $\alpha$ , stromal cell derived factor-1 $\alpha$ ; ET, Endothelin; TNF- $\alpha$ , tumour necrosis factor- $\alpha$ ; IL-6, Interleukin-6; IL-1 $\beta$ , Interleukin-1 $\beta$ ; IL- $\alpha$ , Interleukin- $\alpha$

\* Corresponding author.

E-mail address: [subhasbiswas@iicb.res.in](mailto:subhasbiswas@iicb.res.in) (S.C. Biswas).

<sup>1</sup> Current address: Department of Neurological Surgery, University of Pittsburgh, 200 Lothrop Street, Scaife Hall, Pittsburgh 15213, USA.

<https://doi.org/10.1016/j.mcn.2020.103551>

Received 25 April 2020; Received in revised form 28 August 2020; Accepted 31 August 2020

Available online 05 September 2020

1044-7431/ © 2020 Elsevier Inc. All rights reserved.

Although very little is known about the intricate mechanisms of astrocyte activation but mitogen activated protein kinase (MAPK) pathways have been found to be activated in astrocytes and in neurons in several neuropathological conditions (Bhat et al., 1998; Correa and Eales, 2012; Fields and Ghorpade, 2012; Gadea et al., 2008; Jin et al., 2005; Liu et al., 2014; McLennan et al., 2008; Morishima et al., 2001; Tang et al., 2008; Wang et al., 2002; Xie et al., 2004; Li et al., 2017). The role of these pathways has been strongly implicated in A $\beta$ -induced neuron death but how MAPK pathways are regulating A $\beta$ -induced astrocyte activation has not been fully elucidated (Jin et al., 2005; Kaminska, 2005).

MAPK signal transduction pathways are involved in many crucial cellular events including cell proliferation, differentiation, survival, apoptosis and transformation upon various stimuli (Kaminska, 2005; Plotnikov et al., 2011; Raman et al., 2007; Shaul and Seger, 2007; Morganti et al., 2019). There are three types of MAPKs in mammals namely, extracellular signal related kinase (ERK), p38, c-Jun NH2 terminal kinase (JNK; also known as stress related protein kinase or SAPK). ERK is further classified into ERK1 to ERK8 isotypes (Kaminska, 2005; Plotnikov et al., 2011; Raman et al., 2007; Shaul and Seger, 2007; Arkun and Yasemi, 2018). There are four isoforms of p38: p38- $\alpha$ , p38- $\beta$ , p38- $\gamma$  and p38- $\delta$  and three isoforms of JNK: JNK1, JNK2 and JNK3 are reported (Plotnikov et al., 2011; Raman et al., 2007; Shaul and Seger, 2007; Zarubin and Han, 2005).

Different MAPK pathways have been found to be activated in astrocytes under various pathological stimuli (Gorina et al., 2011; Lee and Kim, 2017; Li et al., 2017). It has been found that endothelin-1; a vasoactive peptide promotes a reactive phenotype in cultured astrocytes through ERK- and JNK-dependent pathways (Gadea et al., 2008). Whereas traumatic scratch injury triggers astrocyte activation through a calcium influx dependent activation of JNK/c-Jun/AP-1 pathway (Gao et al., 2013). The p38K pathway activation has been implicated in glial cells activation in several disease models (Bhat et al., 1998; Da Silva et al., 1997; Lee and Kim, 2017; Lee et al., 2000; Lo et al., 2014; Roy Choudhury et al., 2014). It has also been shown that activation of all three MAPK pathways is involved in lipopolysaccharides and thrombin induced astrocyte activation (Bhat et al., 1998; Gorina et al., 2011; Wang et al., 2002). Moreover, pro-inflammatory cytokine, IL-1 $\beta$  and brain injury can activate JNK, p38K and ERK pathways in astrocytes (Li et al., 2017). Although, A $\beta$  fibrils can activate p38K pathway in microglia (McDonald et al., 1998; Giovannini et al., 2002) but the role of MAPK pathways (JNK, p38K and ERK) in A $\beta$ -induced astrocyte activation, has not been fully established.

In this study, we investigated all three MAPK pathways and their specific roles in different functional and morphological characteristics that are found in activated astrocytes in response to A $\beta$  exposure. We observed that two MAPK pathways, JNK and p38K are activated in astrocytes upon A $\beta$  exposure *in vitro* and *in vivo*. Both of these pathways are involved in A $\beta$  mediated astrocyte cell proliferation, whereas only p38K pathway is required for characteristic morphological changes in astrocytes upon A $\beta$  exposure.

## 2. Materials and methods

### 2.1. Materials

DMEM, DMEM-F12, FBS, Penstrep, Goat serum, Alexafluor 546/488 – Thermo Fisher Scientific (Waltham, Massachusetts, USA)/Poly-D-Lysine, HFIP, DMSO, Paraformaldehyde, Triton-X-100, anti-rabbit GFAP antibody, Hoechst, Sucrose – Sigma (St. Louis, Missouri, United States)/ A $\beta$  – American peptide (Sunnyvale, CA, USA)/JNK inhibitor II, SB239063, U0126 – Calbiochem (Billerica, Massachusetts, USA)/anti-rabbit c-Jun antibody, anti-rabbit p38K antibody, anti-rabbit pATF2 antibody, anti-rabbit ERK antibody, anti-rabbit Ki67 antibody, anti-rabbit  $\beta$ -actin antibody, anti-rabbit vimentin antibody – Cell Signaling Technology (Danvers, Massachusetts, USA)/ Anti-rabbit S100B

antibody, anti-rabbit A $\beta$ <sub>1–42</sub> antibody -Abcam (Cambridge, UK).

### 2.2. Animals and ethics

All animal experiments were performed in accordance with the guidelines formulated by the Committee for the Purpose of Control and Supervision of Experiments on Animals (Animal Welfare Divisions, Ministry of Environment and Forests, Govt. of India), with approval from the Animal Ethics Committee of Indian Institute of Chemical Biology (IICB-AEC). Adult Sprague-Dawley rats, procured from the random bred colony of the animal house of our institute, were maintained under good husbandry conditions supported by diurnal cycles of 12 h light and 12 h darkness with lights on at 06.00 h daily.

### 2.3. Astrocyte primary culture

Astrocytes primary cultures were done from 0 to 1 day old Sprague-Dawley rat pups. First, whole brain was dissected out after removing the skin and skull. Very carefully meninges were removed. Neocortex parts from each hemisphere were isolated and cut into pieces. The small cortical pieces of tissues were minced and subjected to trypsinization for 30 min at 37 °C. Trypsinized brain tissue was then triturated in complete astrocyte medium [DMEM supplemented with 10% fetal bovine serum (FBS)] and to remove the remaining clumps, it was passed through nylon mesh. To remove neurons, the resultant single cell suspension was transferred onto PDL (Sigma-Aldrich, St. Louis, MO, USA) coated plate and incubated for 2–3 min for preferential sticking of neurons. The unattached cells in the suspension were collected and cells were harvested by centrifugation. Cell's pellet was resuspended in fresh astrocyte medium and seeded in a density of 1.2 million/35 mm plate or 0.4 million/well of 24-wells plate. Cells were maintained for 13 days *in vitro* (DIV) with medium change given every other day.

### 2.4. Oligomeric A $\beta$ preparation

A $\beta$ <sub>1–42</sub> lyophilized peptide (American peptide, Sunnyvale, CA, USA) was resuspended in 100% 1,1,1,3,3,3 hexafluoro-2-propanol (HFIP) (Sigma-Aldrich) to 1 mM concentration and centrifuged under vacuum condition in a speed vac (Eppendorf, Hamburg, Germany) until all the liquid HFIP get evaporated. The resultant peptide pellet was again dissolved in DMSO (Sigma-Aldrich) at 5 mM concentration and subjected to sonication in 37 °C water bath for 10 min. Then the solution was further diluted with phosphate buffer saline (PBS: NaCl 137mmole/L, KCL 2.7mmole/L, Na<sub>2</sub>HPO<sub>4</sub> 10mmole/L, KH<sub>2</sub>PO<sub>4</sub> 2mmole/L, pH 7.2) and SDS (0.2%) to a concentration of 400  $\mu$ M and incubated for 6–18 h at 37 °C. Finally PBS was added to a final concentration of 100  $\mu$ M and again incubated for 18–24 h at 37 °C.

### 2.5. A $\beta$ and MAPK inhibitors treatment to astrocytes

Mature astrocytes (13DIV) were kept for 24 h in sera free condition prior to treatment. Cells were then treated with 1.5 $\mu$ M A $\beta$  oligomers in the presence or absence of 10  $\mu$ M JNK inhibitor II or 100 nM p38K inhibitor (SB 239063) or 10  $\mu$ M ERK inhibitor (U0126) in the same sera free medium for different time points like 4 h, 8 h, 16 h and 24 h or for 24 h only at 37 °C or as mentioned in the figures. The concentration of inhibitors was used based on available literatures (Bennett et al., 2001; Roy Choudhury et al., 2014).

### 2.6. Immunocytochemistry

Both the control and treated cells on glass cover slips were fixed by 4% paraformaldehyde in PBS for 10 min at room temperature. For permeabilization and blocking, fixed cells were incubated with 3% goat serum, 0.3% Triton X-100 in PBS for 1–2 h. Cells were then incubated with anti-rabbit or anti-mouse GFAP (1:50), anti-rabbit total and

phospho-c-Jun, anti-rabbit total and phospho-p38K, anti-rabbit Ki67 (1:40) overnight at 4 °C. On the next day, cells were washed with PBST (0.3% Triton X-100 in PBS) to remove the excess antibodies. Then the cells were subjected to specific species matched secondary antibody, incubation with Alexafluor546/488 for 1–2 h at room temperature. Finally nuclei were stained with Hoechst 33342 at a concentration of 2 µg/ml in PBS for 30 min at room temperature. Images were taken under LeicaCTR4000 fluorescence microscope at ×20 or ×40 objectives as mentioned in the images. We calculated the corrected total cell fluorescence (CTCF) in ImageJ software by including integrated density of staining, area of the cell, and the background fluorescence of different experimental conditions.  $CTCF = \text{Integrated density} - (\text{area of selected cell} \times \text{mean fluorescence of background readings})$ . Data have been represented as the mean ± S.E.M. of ten astrocytes from three independent experiments. The morphological changes of reactivated astrocytes have been evaluated by sholl analysis using NIH-ImageJ software that has been previously described (Sholl, 1953; Cuesto et al., 2011; Sanphui and Biswas, 2013). GFAP stained primary cultures of astrocytes have been taken and imaging was performed at higher magnification. By using ImageJ plugin, the higher magnification images were traced and a number of concentric circles were drawn from the astrocytic soma with a 10 µm increasing radius. We performed a two-dimensional analysis on astrocyte primary culture where the number of intersecting points was calculated at each concentric circle. Data have been represented as the mean ± S.E.M. of five astrocytes from three independent experiments.

## 2.7. Aβ infusion in rat brain

Oligomeric preparation of Aβ was injected in male Sprague-Dawley rat brains following the method described previously (Sanphui and Biswas, 2013). Briefly, adult rats of 300–380 g were anesthetized with xylazine-ketamine mix and their head were fixed in a stereotaxic frame. Then a volume of 5 µl of 100 µM Aβ<sub>1–42</sub> in PBS was infused with the use of a 27-gauge Hamilton syringe, in right cerebral cortex at stereotaxic co-ordinates from bregma: AP: −4.1, L:2.5, DV:1.3 mm. In control animals, an equal volume and concentration of Aβ<sub>42–1</sub>-reverse peptide was infused. After at least 21 days of injection, animals were sacrificed through anesthetization and after cardiac perfusion; brains were dissected out and fixed in 4% PFA for 24 h. Both control and Aβ peptide treated brains were transferred to a 30% sucrose solution for another 24 h. Finally 20 µm sections were cut using a cryotome (Thermo Scientific).

## 2.8. Immunohistochemistry

Brain sections of both Aβ<sub>1–42</sub> (n = 3) and Aβ<sub>42–1</sub> (n = 3) infused adult rats were blocked with 3% goat serum, 0.3% Triton X-100 in PBS for 1 h. The sections were then incubated with primary antibody rabbit anti-GFAP with either anti-rabbit total/phospho-c-Jun or anti-rabbit total/phospho-p38K and anti-Aβ<sub>1–42</sub> antibody for overnight at 4 °C. On next day sections were washed thrice for 5 min with 0.3% Triton X-100 in PBS. Then species specific fluorescence-tagged secondary antibody was added and incubated for 1 h. After washing with the same solution for three times for 5 min each nuclei were stained with Hoechst33342 and mounted on glass slides. Pictures were taken under LeicaCTR4000 fluorescence microscope at ×20 magnification.

## 2.9. Preparation of cell lysate

All the treated cells along with the control were washed with PBS and collected by scraping in PBS. Cells were harvested by centrifugation at 1200 rpm at 4 °C for 5 min followed by lysis using lysis-buffer (10 mM Tris (pH.4), 150 mM NaCl, 1% Triton X-100, 0.5% NP-40, 1 mM EDTA, 1 mM EGTA, 20 mM NaF, 0.2 mM Orthovanadate, Protease Inhibitors) and incubation for 10 min in ice. The cell lysates were

centrifuged at 14000 rpm at 4 °C for 15 min. Supernatant was collected and proteins were estimated by Bradford method.

## 2.10. Western blotting

Lysates containing equal amount of protein of each condition were resolved in SDS-PAGE. The protein bands were transferred to PVDF membrane. After blocking with 5% non-fat dry milk for 1 h at room temperature, the membranes were incubated with primary antibodies using anti-rabbit GFAP (1:1000), anti-rabbit phospho- and total-ATF2 (1:1000), anti-rabbit phospho- and total-c-Jun (1:500), anti-rabbit phospho- and total-JNK (1:500), anti-rabbit phospho- and total-p38K (1:500), anti-rabbit phospho- and total-ERK1/2 (1:2000), anti-mouse β-Actin (1:2000) antibodies for overnight at 4 °C. Membranes were washed 3 times with TBST [1.5 M NaCl, 1 M Tris (pH 7.5), 0.1% Tween20] followed by HRP tagged secondary antibody incubation for 1–2 h at room temperature. Protein bands were detected on X-ray film by using ECL reagents after 3 times wash with TBST. Densitometric quantitation of each band was done by ImageJ software.

## 2.11. Cell survival assay

Cell survival assay of control and Aβ<sub>1–42</sub> treated astrocytes in presence or absence of different inhibitors [JNK inhibitor II, p38K inhibitor (SB 239063), ERK inhibitor (U0126)] was performed by a method that has been routinely used to assess viability of neuronal cells (Rukenstein et al., 1991; Sanphui et al., 2013; Troy et al., 2002). According to the method, cells were lysed in a detergent containing buffer that preferentially dissolves cell membrane leaving nuclear membrane intact. The absolute number of intact nuclei was then directly counted on a haemocytometer.

## 2.12. Statistical analysis

Data were analysed using student *t*-test and the differences were considered statistically significant when  $p \leq 0.05$ .

## 3. Results

### 3.1. Astrocytes are activated in response to Aβ exposure

Astrocyte activation is an integral part of pathophysiology and has an immense effect on neuronal health in AD. To study the mechanism of astrocyte activation in response to Aβ, we first checked whether upon Aβ treatment astrocytes get activated in culture or not. We considered morphological changes and GFAP, S100B and vimentin upregulation as markers for astrocyte activation. We exposed 14DIV mature astrocyte cultures to oligomeric Aβ for 24 h and performed immunocytochemistry with anti-GFAP, anti-S100B or anti-vimentin antibodies. We found a significant upregulation of GFAP (around 3 fold), S100B and vimentin, and characteristic morphological changes in terms of increase in perimeter (around 2 fold) from flat polygonal shapes to strong process bearing ones in response to Aβ treatment (Fig. 1A,B,C,E,F,  $p \leq 0.05$ ). We further evaluated the extension of reactivated astrocyte processes by sholl analysis and found a significant extension in strong processes of the activated astrocytes (Fig. 1D). Moreover, GFAP upregulation and hypertrophied strong process bearing astrocytes which is an indication of astrocyte activation, were also found in rat brain in the vicinity of Aβ infused sites when cortical sections of Aβ-infused rat brain were subjected to immunohistochemistry with anti-GFAP antibody (Fig. 1G,H,I,  $p \leq 0.05$ ). The deposition of Aβ<sub>1–42</sub> in the Aβ infused rat brain cortex has been confirmed (Supplementary Fig. 1). Finally, we performed western blot analysis to check GFAP levels at different time points (4 h, 8 h, 16 h and 24 h) of Aβ treatment on cultured astrocytes and found that the levels of GFAP were increased gradually starting from 8 h till 24 h after Aβ

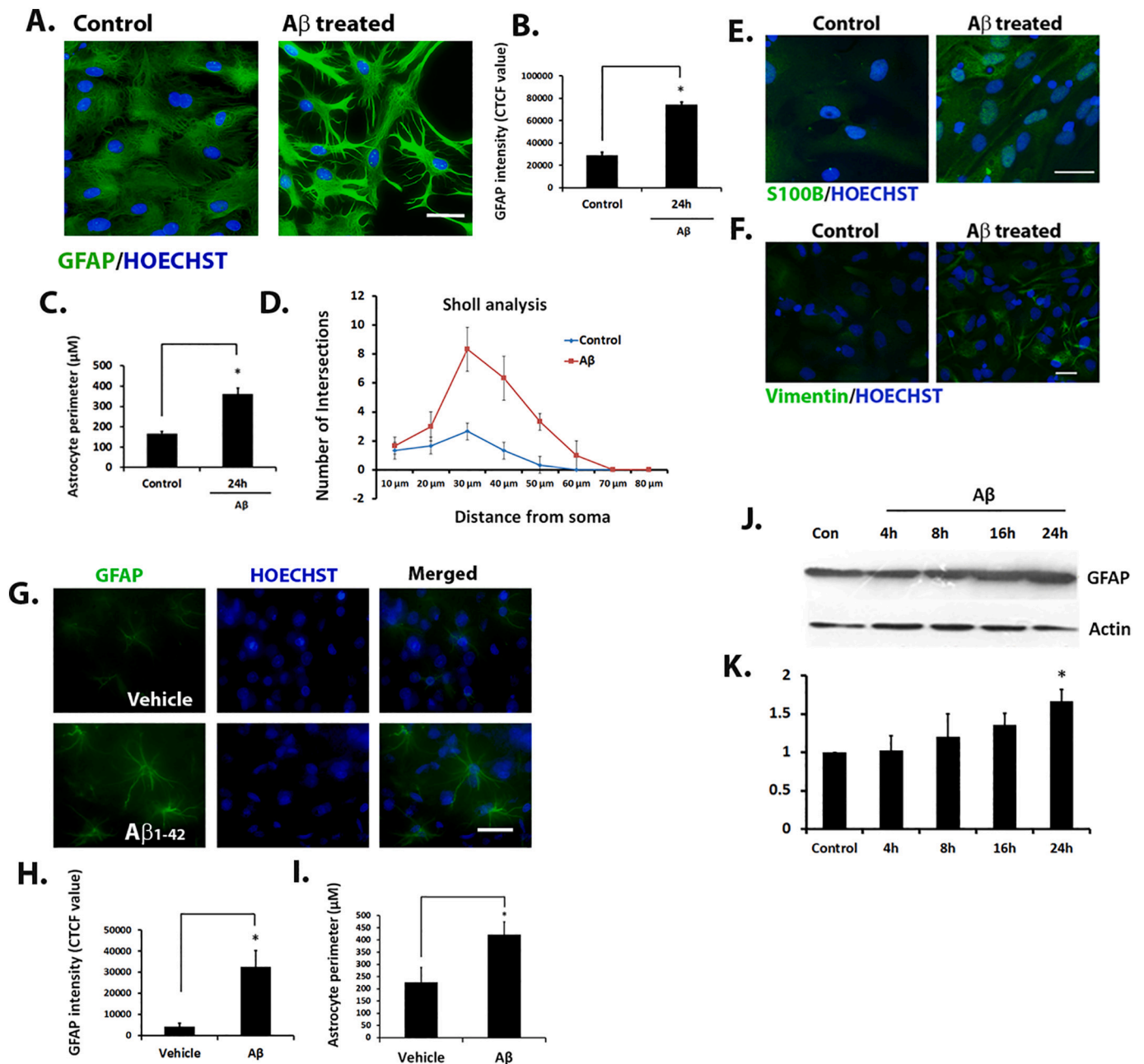


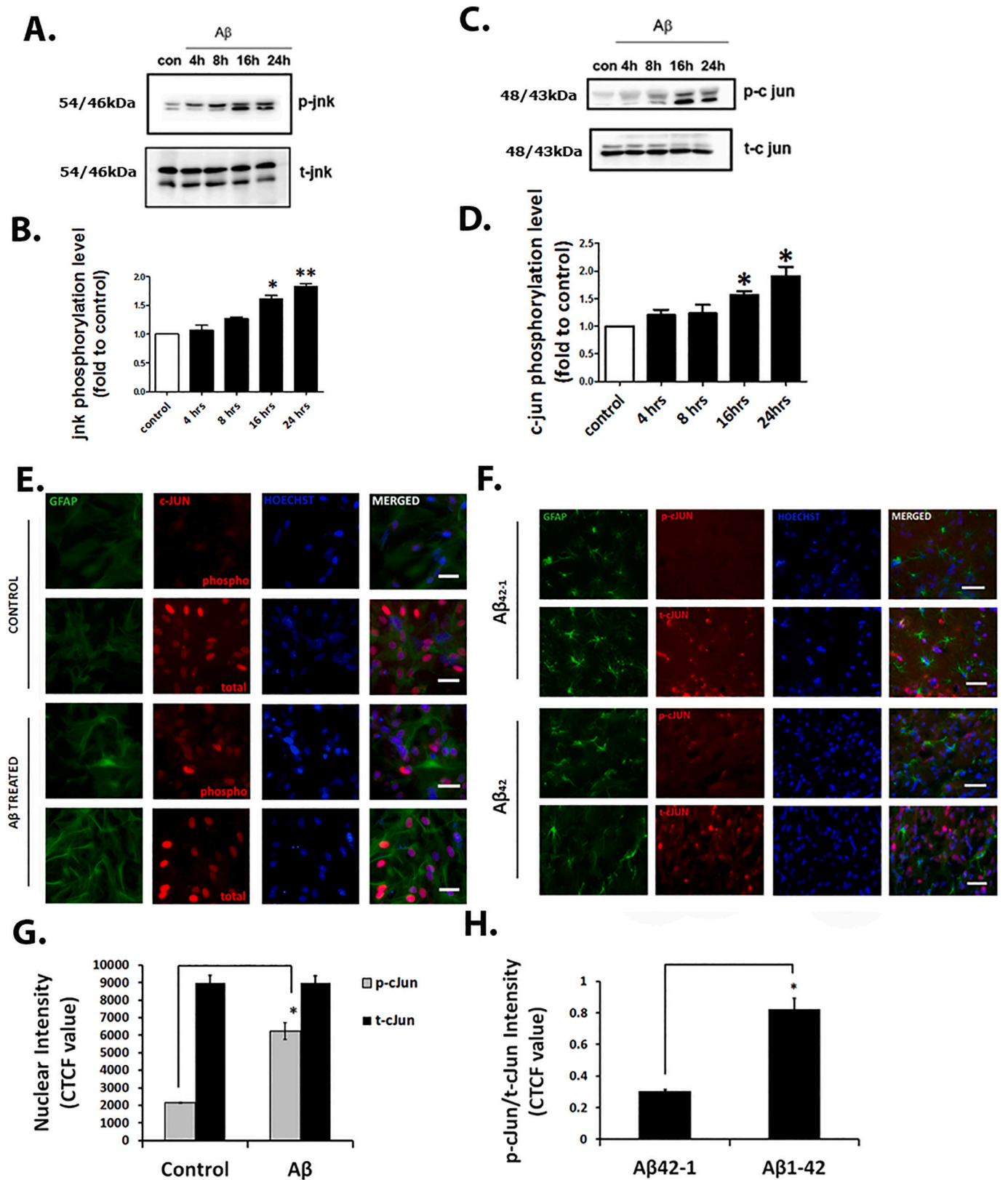
**Fig. 1.** Effect of Aβ on morphology and GFAP expression in astrocytes *in vitro* and *in vivo*. (A, E, F) Cultured astrocytes (14DIV) were treated with 1.5 μM Aβ. After 24 h, both control and treated cells were subjected to immunocytochemistry with anti-GFAP, S100B and Vimentin antibodies followed by nuclear Hoechst staining. Pictures were taken at ×40 magnification under a fluorescent microscope. Scale bar is indicating 50 μm. (B, C) Bar diagrams are representing the quantitative analysis of GFAP intensity (as CTCF value) and morphological change (as perimeter value) of control and Aβ treated astrocytes. (D) Sholl analysis of cultured astrocyte treated with Aβ. (G) Aβ<sub>1-42</sub> or vehicle (PBS) infused rat brains were fixed after cardiac perfusion. The cryosections of brains were subjected to immunohistochemistry using anti-GFAP antibody to stain astrocytes. Nuclei were stained with Hoechst. Pictures were taken at ×40 magnification under a fluorescent microscope. (H, I) Bar diagrams are showing the quantitative GFAP intensity through CTCF values and morphological changes in terms of perimeter. (J) Mature astrocyte cultures (14DIV) were treated with Aβ for different time points (4 h, 8 h, 16 h & 24 h). Equal amount of lysates from control and treated samples were subjected to SDS-PAGE followed by western blotting with GFAP antibody. Actin was used as loading control. (K) Bar diagram is representing the densitometry of the blots. Values are expressed as mean ± SEM; n = 3, \*p < 0.05.

exposure (Fig. 1J,K, p ≤ 0.05).

### 3.2. JNK and its downstream target c-Jun are activated in astrocytes both in vitro and in vivo in response to Aβ

Several signal transduction pathways including JNK have been reported to be implicated in astrocyte activation upon exposure to different stimuli (Gadea et al., 2008; Gao et al., 2013; Li et al., 2017). We

and other have shown the involvement of JNK and its downstream target c-Jun in Aβ-induced neuronal apoptosis (Akhter et al., 2015; Morishima et al., 2001; Troy et al., 2001; Yao et al., 2005). However, its specific role in Aβ mediated astrocyte activation is not clearly known. We checked this possibility by using 14DIV astrocyte primary cultures and treating them with oligomeric Aβ for different time points such as 4 h, 8 h, 16 h and 24 h. All treated samples along with control were subjected to western blot with phospho-JNK, total-JNK, phospho-c-Jun



(caption on next page)

and total-c-Jun antibodies. We found a significant increase of phospho-JNK levels at 16 h and at 24 h of Aβ treatment whereas the total JNK levels were remained unchanged (Fig. 2A,B,  $p \leq 0.05$ ). We further checked the activation of c-Jun, which is a downstream target of JNK.

Again we found a clear increase in phospho-c-Jun levels upon Aβ treatment at 16 h and at 24 h. But the total c-Jun levels were remained unaltered upon Aβ treatment at any time points (Fig. 2C,D,  $p \leq 0.05$ ). To further confirm, we checked the phospho- and total c-Jun levels in

**Fig. 2.** Activation of JNK/c-Jun in astrocytes *in vitro* and *in vivo* upon A $\beta$  exposure. Primary cultures of astrocyte (14DIV) were treated with A $\beta$  for 4 h, 8 h, 16 h & 24 h. After each time points cells were harvested and equal amount of lysates were analysed by SDS-PAGE and subsequent western blot analysis with anti-phospho-JNK (p-JNK), -total-JNK (t-JNK) and anti-phospho-c-Jun (p-c-Jun), anti-total-c-Jun (t-cJun) antibodies. (A, B) Representative western blots for phospho-JNK and total-JNK levels at different time points of A $\beta$  exposure are shown. Bar diagrams are representing the quantitative analysis of the blots. Values are expressed as mean  $\pm$  SEM: n = 3, \*p < 0.05. (C, D) Representative western blots for phospho-c-Jun and total-c-Jun levels at different time points of A $\beta$  exposure are shown. Lower panel: Densitometric analysis was performed by NIH ImageJ software. P-c-Jun values were normalized with t-c-Jun and are plotted as different time points of A $\beta$  treatment vs level of p-c-Jun values. Values are expressed as mean  $\pm$  SEM: n = 3, \*p < 0.05. (E, G) Cultured astrocytes were treated with A $\beta$  for 24 h, and then subjected to immunocytochemistry with GFAP, phospho- and total-c-Jun antibodies followed by nuclear staining with Hoechst. Images were taken at  $\times$ 40 magnification under a fluorescent microscope. Scale bar is indicating 50  $\mu$ m. Nuclear intensity of p-cJun and t-cJun was calculated and the CTCF values are represented as bar diagrams. (F, H) A $\beta$  infused rat brain sections were subjected to immunohistochemistry with GFAP, phospho- and total-c-Jun antibodies. Nuclei were stained with Hoechst. Images were taken at  $\times$ 40 magnification under a fluorescent microscope. Scale bar is indicating 50  $\mu$ m. Bar diagrams are showing the quantitative CTCF values of the ratio of p-cJun and t-cJun.

astrocytes by immunocytochemistry and found that upon A $\beta$  exposure, there was a significant nuclear upregulation (around 3 fold) of phospho-c-Jun in GFAP positive astroglial cells while the total-c-Jun levels did not show any changes (Fig. 2E,G, p  $\leq$  0.05). Next, we determined whether c-Jun is also activated in response to A $\beta$  *in vivo*. Cortical sections of A $\beta$ -infused rat brain were subjected to immunohistochemistry with phospho- and total-c-Jun antibodies along with astrocytic marker GFAP antibody. We found that there was a significant increase (around 3.5 fold) in phospho-c-Jun/total-c-Jun ratio in GFAP positive cortical astrocytes in A $\beta$ -infused brain tissue sections compared to that of control brain section where A $\beta$ 42-1 reverse peptide was injected (Fig. 2F,H, p  $\leq$  0.05).

### 3.3. A $\beta$ activates the p38K pathway in astrocytes both *in vitro* and *in vivo*

The p38K pathway is also implicated in astrocyte activation and its inhibition has been considered a promising therapeutic strategy for AD (Lee and Kim, 2017). Upon IL-1 $\beta$  exposure, activation of p38K pathway and its partial contribution to astrocyte activation have been reported (Fields and Ghorpade, 2012). Microglia is activated by A $\beta$  and cytokines (i.e., IL-1 $\beta$ ) secreted from activated microglia can activate astrocytes thereafter (Lee and Kim, 2017). So p38K pathway is presumed to be activated and have important roles to play in A $\beta$  induced astrocyte activation. In order to investigate the role of p38K pathway in A $\beta$ -induced astrocyte activation, we checked the phosphorylation level of p38K which is the indication of its activation, in cultured astrocytes of 14DIV, upon A $\beta$  treatment at different time points. A significant increase in p38K phosphorylation was found at 16h and 24 h of A $\beta$  treatment. The total p38K levels were remained unchanged at all the time points we checked (Fig. 3A,B, p  $\leq$  0.05). This observation was further validated by immunocytochemistry studies. Matured astrocyte cultures of 14DIV were subjected to immunocytochemistry after treatment with A $\beta$  for 24 h using phospho- and total-p38K antibodies. We found that there was a significant upregulation (around 2 fold) of phospho-p38K levels in A $\beta$ -treated astrocytes compared to that of control while changes in the total-p38K levels remain non-significant in both control and A $\beta$ -treated astrocytes (Fig. 3C,D, p  $\leq$  0.05). This *in vitro* finding was further strengthened by *in vivo* data where A $\beta$ -infused rat brain sections were shown to have elevated levels (around 6 fold) of phospho-p38K level which were localized in the GFAP positive cells compared to that of A $\beta$ 42-1 peptide infused-brain sections (Fig. 3E,F, p  $\leq$  0.05). The total p38K levels in both A $\beta$ 42-1 (control peptide) and A $\beta$ 1-42 infused brain cortex remained same.

ERK signalling which is a key regulator of cell proliferation and differentiation is another important member of MAPK pathway. Along with JNK, p38K, we also investigated the contribution of ERK pathway in A $\beta$  induced astrocyte activation. Again, 14DIV mature cultured astrocytes were treated with A $\beta$  for 4 h, 8 h, 16 h & 24 h and western blotting was performed with phospho- and total-ERK antibodies. Interestingly, we did not find any significant upregulation of phospho-ERK levels at any time points suggesting that, ERK pathway is not activated during the course of A $\beta$  treatment we tested (Fig. 3G,H). Collectively, we found that JNK and p38K but not ERK pathway are

activated in astrocytes in response to A $\beta$  both *in vitro* and *in vivo*.

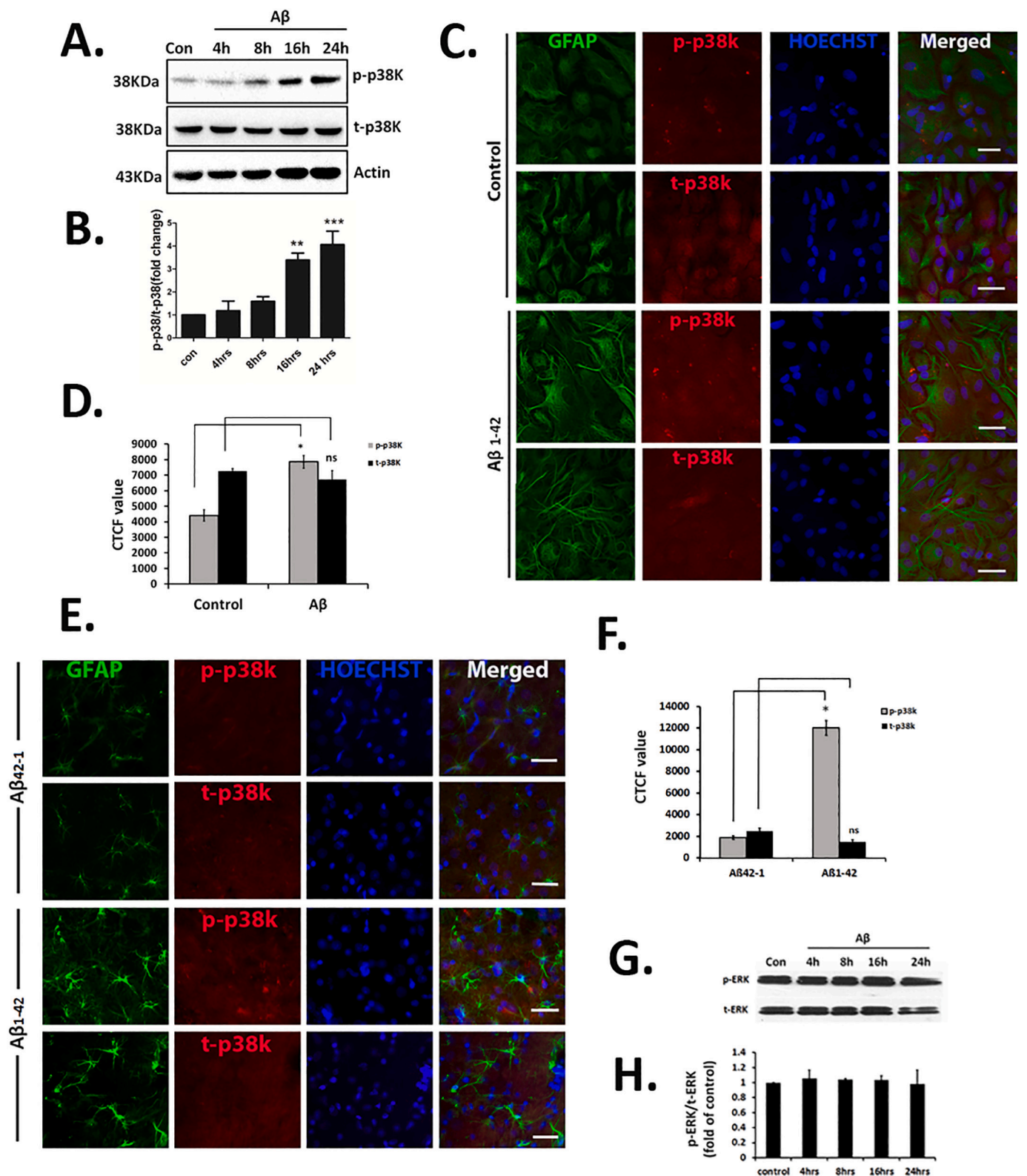
### 3.4. JNK and p38K pathways but not ERK pathway, are involved in A $\beta$ induced astrocyte proliferation

Astrocyte proliferation is one of the important changes that occur during the course of astrogliosis or astrocyte activation in AD (Bajetto et al., 2001; Gadea et al., 2008; McLennan et al., 2008; Olabarria et al., 2010; Sorensen et al., 2003; Wang et al., 2002). So next we checked whether A $\beta$  induces astrocyte proliferation and if so which MAPK pathways are involved therein. We found that, A $\beta$  at low dose (1.5  $\mu$ M) triggers significant proliferation (2 to 2.5 fold) of cultured astrocytes within 24 h (Fig. 4A,C, p  $\leq$  0.05). To check which pathways are involved in astrocyte proliferation, we treated mature astrocyte cultures of 14DIV with A $\beta$  in presence and absence of specific inhibitors of JNK (JNK inhibitor II), p38K (SB 239063) or ERK (U0126). After 24 h of incubation, cells were counted by nuclei counting method and we found that A $\beta$  caused around 2-fold increase in the number of astrocytes compared to control. Interestingly, when cells were treated with JNK or p38K inhibitors in the presence of A $\beta$ , a clear and significant inhibition of cell proliferation was observed suggesting that JNK & p38K are involved in A $\beta$  mediated astrocyte proliferation. But we failed to find any involvement of ERK pathway in A $\beta$  induced cell proliferation as there was no significant reduction of cell numbers when astrocytes were treated with A $\beta$  along with ERK inhibitor (Fig. 4A, p  $\leq$  0.05). To further strengthen this observation, we performed immunocytochemistry with an antibody Ki67 which is a cell proliferation marker with A $\beta$  treated astrocytes along with inhibitors of all three MAPK pathways. Similar results were found where A $\beta$  triggered 2.5 fold increase in Ki67 positive cells compared to the control (Fig. 4B,C, p  $\leq$  0.05). And in accordance with earlier results, JNK and p38K inhibitors showed a significant reduction of Ki67 positive cell numbers that was otherwise increased significantly in the presence of A $\beta$ . Whereas, as seen by nuclei counting method earlier, the ERK inhibitor could not show any significant reduction of Ki67 positive cell numbers in presence of A $\beta$  (Fig. 4B,C, p  $\leq$  0.05). To further confirm the involvement of the p38K and JNK pathways in A $\beta$  mediated astrocyte proliferation, we have checked the active phosphorylated status of both these MAPKs after treating the cells with corresponding inhibitors in the presence and absence of A $\beta$  (Fig. 4D,E, p  $\leq$  0.05). We found that, inhibiting both of these pathways could significantly reduce the phosphorylation levels of them even in the presence of A $\beta$  further suggesting that phosphorylated active forms of p38K and JNK are involved in A $\beta$  induced astrocyte proliferation.

### 3.5. p38K is required for morphological changes of astrocyte in response to A $\beta$

As shown in Fig. 1, we found a clear morphological change and time dependent upregulation of GFAP levels in cultured astrocytes upon A $\beta$  treatment. Along with these observations, we found that A $\beta$  could cause activation of both JNK and p38K pathways in astrocytes. We presumed that this A $\beta$  induced morphological changes and GFAP upregulation





(caption on next page)

can be regulated by any of the activated MAPK pathways. So, we first checked whether JNK pathway has any roles in astrocyte morphological changes in response to Aβ. Astrocyte primary cultures were treated with Aβ along with or without JNK inhibitor (JNK inhibitor II) and were subjected to immunocytochemistry using GFAP antibody. Interestingly, we failed to find the restoration of morphological changes

induced by Aβ in presence of JNK inhibitor (Fig. 5A).

Next, we checked whether p38K pathway has any contribution in astrocyte morphological changes induced by Aβ. To do this, mature astrocyte cultures of 14DIV were treated with Aβ in the presence or absence of p38K inhibitor (SB 239063). After 24 h of incubation, immunocytochemistry was done with GFAP antibody to check astrocyte

**Fig. 3.** Activation of p38K in astrocytes *in vitro* and *in vivo* in response to A $\beta$ . Cultured astrocytes were treated with A $\beta$  for 4 h, 8 h, 16 h and 24 h. Equal amount of cell lysates were subjected to western blot analysis with phospho- and total-p38K or phospho- and total-ERK antibody. (A, B) Representative western blots are showing phospho-p38K (p-p38K) and total-p38K (t-p38K) levels at different time points of A $\beta$  treatment. Densitometric analysis was performed by NIH ImageJ software and p-p38K values were normalized with t-p38K values. Lower panel: Graphical representation of densitometric analysis of fold changes of phospho-p38K levels in the indicated conditions. Values are expressed as mean  $\pm$  SEM; n = 3, \*p < 0.05. (C, D) Cultured astrocytes were treated with A $\beta$  for 24 h and subjected to immunocytochemistry with GFAP and phospho-ortotal-p38K antibodies followed by nuclei staining with Hoechst. Pictures were taken at  $\times$ 40 magnification under a fluorescent microscope. Scale bar is indicating 50  $\mu$ m. Bar diagrams are showing the quantitative CTCF value of p-p38K and t-p38K. (E, F) Brain sections of both A $\beta$ <sub>1-42</sub> and A $\beta$ <sub>42-1</sub> (reverse peptide) infused rats were subjected to immunohistochemistry with GFAP and phospho- or total-p38K antibodies. Nuclei were stained with Hoechst. Pictures were taken at  $\times$ 40 magnification under an inverted fluorescent microscope. Scale bar is indicating 50  $\mu$ m. Bar diagrams are representations of quantitative analysis of p-p38K. (G, H) Representative blots are showing levels of phospho- and total-ERK at different time points of A $\beta$  treatment. Lower panel: Graphical representation of densitometric analysis of fold change of phospho-ERK levels in the indicated conditions.

morphology by measuring perimeter. We found that, when astrocytes were treated with A $\beta$ , they changed their morphology from flat polygonal to strong process bearing cells. But when A $\beta$  along with a p38K inhibitor were used to treat astrocytes, a clear restoration of morphological changes was observed (Fig. 5B,D, p  $\leq$  0.05). To further check whether this morphological change by p38K requires GFAP upregulation, we determined the GFAP intensity of immunostained astrocytes and protein level of GFAP in astrocytes those were treated with A $\beta$  in presence and absence of p38K inhibitor by western blot using GFAP antibody. We found that A $\beta$  caused upregulation of GFAP levels significantly (around 2 fold) in astrocytes whereas this upregulation was completely blocked when astrocytes were treated with specific p38K inhibitor (Fig. 5C,E,F, p  $\leq$  0.05). Interestingly, we also found that phosphorylation of transcription factor ATF2, a target of p38K pathway was increased in time dependent manner in response to A $\beta$  treatment (Fig. 5G,H, p  $\leq$  0.05). These results suggest that, A $\beta$  triggers morphological changes in astrocytes by activating p38K pathway and its target ATF2 which might upregulate GFAP expression thereafter. Taken together, our findings indicate that two MAPK pathways, JNK and p38K are activated in astrocytes upon A $\beta$  exposure *in vitro* and *in vivo*, both of these pathways are involved in A $\beta$  mediated proliferation of astrocytes, whereas only p38K pathway is required for characteristic morphological changes in astrocytes upon A $\beta$  exposure.

#### 4. Discussion

Recently, we have shown that cortical astrocytes are activated in response to very low dose (1.5  $\mu$ M) (Saha and Biswas, 2015) and within very short period of time (6 h) following A $\beta$  exposure (Saha et al., 2020). In this study, we investigated the molecular mechanisms involved in astrocyte activation in response to A $\beta$  exposure. We focused our study on MAPK pathways, the evolutionarily conserved signalling pathways that control a myriad of fundamental cellular events like growth, survival, apoptosis, differentiation, transformation, motility, stress in response to various extracellular stimuli (Kaminska, 2005; Plotnikov et al., 2011; Raman et al., 2007; Shaul and Seger, 2007). The MAPK pathways are also shown to be involved in astrocyte activation in various brain inflammatory conditions (Bhat et al., 1998; Fields and Ghorpade, 2012; Gadea et al., 2008; Kaminska, 2005; Liu et al., 2014; Wang et al., 2002). However, how MAPK pathways instigate phenotypes of astrocyte activation in response to A $\beta$  stimuli has not been delineated.

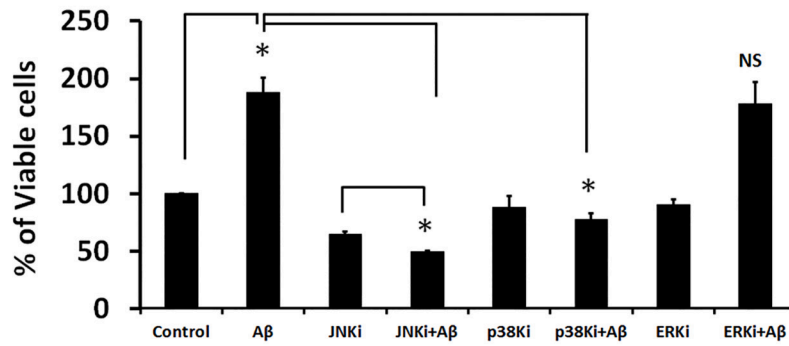
Upregulation of intermediate filament protein, GFAP and characteristic morphological changes are widely accepted and reliable signs of astrocyte transformation from quiescent to activated one (Furman et al., 2012; Gadea et al., 2008; Garwood et al., 2011; Hu et al., 1998; Kamphuis et al., 2012; Kamphuis et al., 2014; Olabarria et al., 2010; Paradisi et al., 2004; Pekny and Nilsson, 2005; Placone et al., 2015; Gomes et al., 1999). First, we checked the astrocyte activation both *in vitro* and *in vivo* by exposing cultured astrocytes to A $\beta$  and infusing A $\beta$  in rat brain respectively. We observed characteristic morphological changes with strong processes and hypertrophy of astrocytes. As morphological changes are associated with upregulation of GFAP in astrocytes, we also checked the levels of GFAP in A $\beta$  treated astrocytes and

found a significant and gradual upregulation of this protein over time. Moreover, other important astrocyte activation markers such as S100B and vimentin were also found to be upregulated in A $\beta$  treated astrocytes. Previously we and others have shown that, both in cultured and *in vivo* conditions, astrocytes get activated upon A $\beta$  exposure (Saha and Biswas, 2015; Olabarria et al., 2010; Rodriguez et al., 2009; Saha et al., 2020). Thus, our results corroborated with previous findings and further indicate that astrocyte activation is associated with GFAP upregulation. In contrast, reports are there that claim during astrocyte activation, GFAP reorganization and condensation might take place without upregulation of its mRNA or protein levels (Hu et al., 1998).

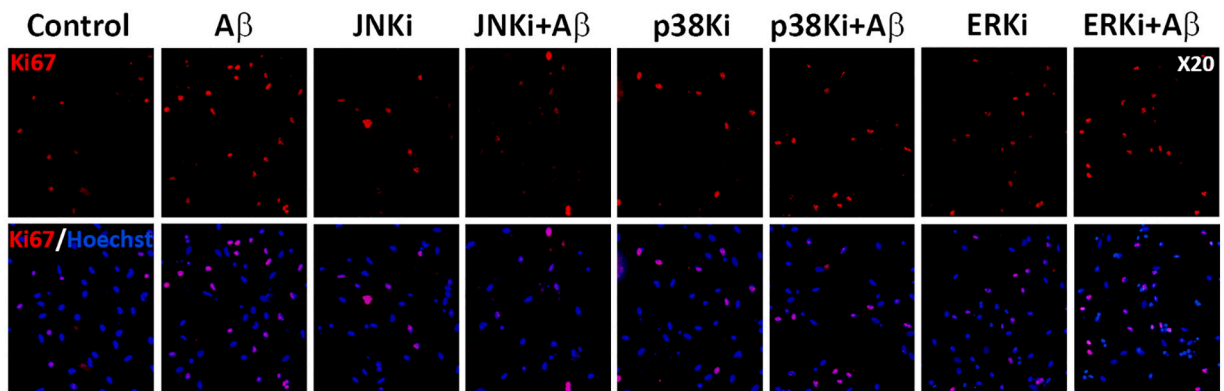
Next we checked MAPK pathways that are activated in astrocytes both *in vitro* and *in vivo* model of AD. JNK/c-Jun pathway gets activated in astrocytes under adverse and pathological conditions like ischemia, scratch induced astrocyte activation, amyotrophic lateral sclerosis (Dong et al., 2009; Gao et al., 2013; Migheli et al., 1997). We found that, both JNK and its downstream target c-Jun are activated in cultured astrocytes in response to A $\beta$  treatment. The immunocytochemical analysis shows a high nuclear expression of p-c-Jun in A $\beta$  treated astrocytes. Our *in vivo* data also shows the similar effect of A $\beta$  in astrocytes in rat brain cortex where a higher number of GFAP positive astrocytes are having nuclear p-c-Jun stain. Interestingly, c-Jun has been mainly implicated in A $\beta$  induced death of neurons (Morishima et al., 2001; Troy et al., 2001). Here we show that it is also involved in astrocyte activation and proliferation upon A $\beta$  exposure. Recently we have reported that astrocyte proliferation takes place at lower A $\beta$  dose (1.5  $\mu$ M), however, at high A $\beta$  dose (4  $\mu$ M), astrocyte death occurs (Saha and Biswas, 2015). Therefore, it would be interesting to know whether c-Jun is involved in astrocyte death in response to high dose of A $\beta$  as well. In fact a recent investigation reveals this possibility where it has been shown that A $\beta$ <sub>1-42</sub> can induce astrocyte cell death through JNK and c-JUN pathway (Li et al., 2018).

Another well-known MAPK, p38K which is conventionally known as stress kinase, involved in various cellular functions including apoptosis, survival and immunological effects, and it considerably shares a wide array of JNK downstream components (Kyriakis and Avruch, 2001; Zarubin and Han, 2005; Santos-Carvalho et al., 2013; Xie et al., 2004; Luft et al., 2004; Correa and Eales, 2012). Most importantly, p38K cascade has long been implicated in neuroinflammation and neurodegeneration especially in AD (Correa and Eales, 2012; Xie et al., 2004). One of the very first evidences that p38K pathway is involved in astrocyte mediated neuroinflammation comes from the study where it has been shown that the involvement of p38K pathway in iNOS and TNF $\alpha$  gene expression in response to LPS endotoxins in primary culture (Bhat et al., 1998). It has been reported that, p38K can hyper-phosphorylate tau protein and through other downstream target proteins, it also induce the release of pro-inflammatory cytokines like TNF- $\alpha$ , IL-6, IL-1 $\beta$ , IL- $\alpha$ , eventually culminating neuronal death (Correa and Eales, 2012). In addition, this pathway is also involved in IL-1 $\beta$  mediated astrocyte activation that finally causes the COX-2 upregulation through C/EBP $\beta$  transcription modulator and thereby implicated in AD (Fields and Ghorpade, 2012). So far A $\beta$  mediated direct activation of microglia through p38K pathway has been better understood (Lee et al., 2000; McDonald et al., 1998). Here we show that A $\beta$  oligomers can stimulate

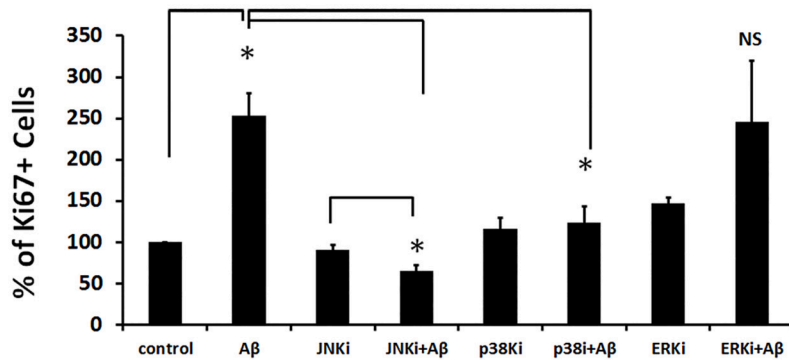
**A.**



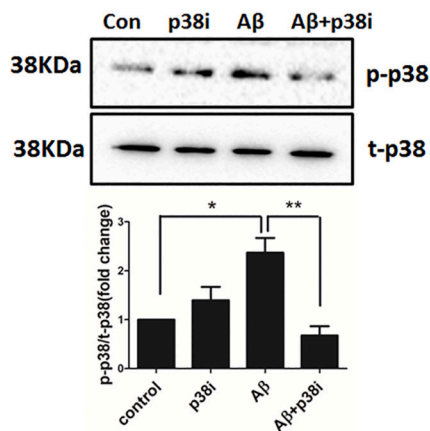
**B.**



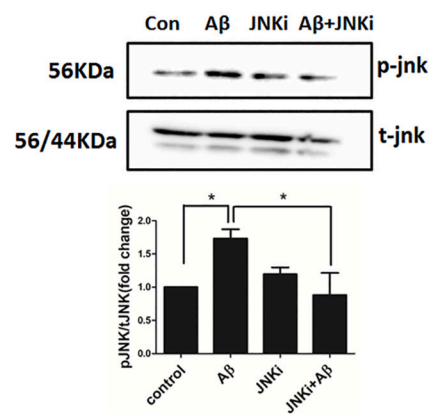
**C.**



**D.**



**E.**



(caption on next page)

**Fig. 4.** JNK and p38K pathways are implicated in Aβ induced astrocyte cell proliferation. Mature astrocyte cultures (14DIV) were treated with three MAPK inhibitors: JNK inhibitor II, p38K inhibitor (SB 239063), ERK inhibitor (U0126) for 24 h in presence and absence of Aβ. (A) Cells were lysed with nuclei counting buffer that dissolve plasma membrane but not nuclear membrane. Nuclei were counted under phase contrast microscope with the help of haemocytometer. Percent of intact nuclei (represent viable cells) are plotted against different treatment conditions. Values are expressed as mean ± SEM; n = 3, \*p < 0.05. (B) Astrocytes were treated with indicated conditions and then were fixed and subjected to immunocytochemistry with anti-Ki67 antibody followed by nuclei stain by Hoechst. Pictures were taken at ×20 magnification under an inverted fluorescent microscope. (C) Number of Ki67 positive cells and total number of Hoechst stained nuclei were enumerated and the percentage of Ki67 positive cells were plotted against different treatment conditions. Bar diagram is showing the percentage of Ki67 positive cells vs different treatment condition. Values are expressed as mean ± SEM; n = 3, \*p < 0.05. (D,E) Cultured astrocytes were treated with either p38K or JNK inhibitors with or without Aβ for 24 h. Equal amount of cell lysates were subjected to western blot analysis with phospho- and total-p38K or phospho- and total-JNK antibodies. Densitometric analysis was performed by NIH ImageJ software and p-p38K and p-JNK values were normalized with t-p38K and t-JNK values respectively. Lower panel: Graphical representation of densitometric analysis of fold changes of p-p38K and p-JNK levels in the indicated conditions. Values are expressed as mean ± SEM; n = 3, \*p < 0.05.

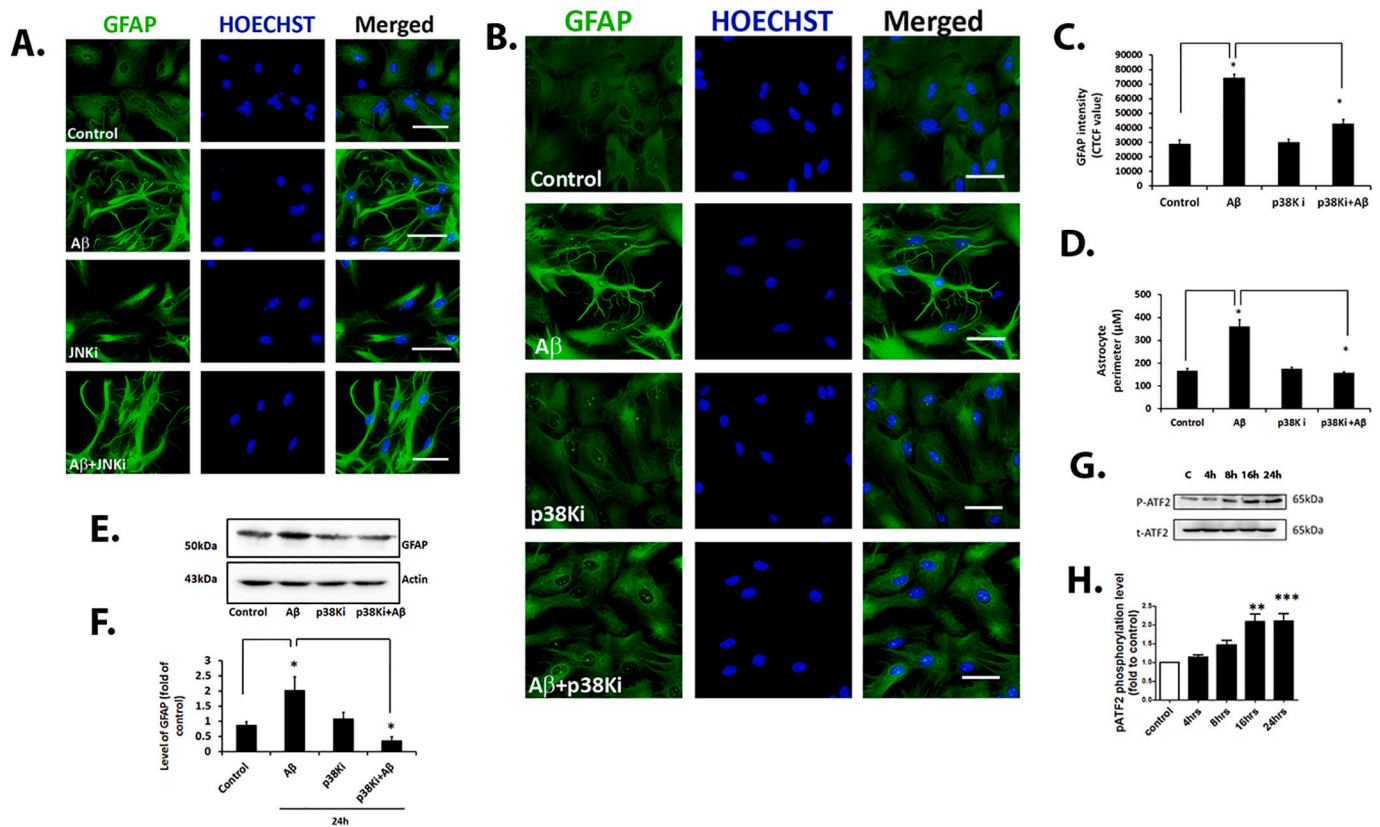


**Fig. 5.** Role of p38K and JNK pathways in astrocyte morphological changes and GFAP upregulation induced by Aβ. Mature astrocyte cultures were treated with Aβ for 24 h in presence and absence of either JNK inhibitor II (JNKi) (A) or p38K inhibitor, SB 239063 (p38Ki) (B). After 24 h, cells were fixed and subjected to immunocytochemistry with anti-GFAP antibody followed by nuclei staining with Hoechst. Pictures were taken at ×40 magnification under an inverted fluorescence microscope. Scale bar is indicating 50 µm. (C, D) Bar diagrams are showing the quantitative GFAP intensity through CTCF values and morphological changes in terms of perimeter. (E, F) Equal amount of cell lysates from treated astrocytes (Aβ, p38K inhibitor and Aβ + p38K inhibitor) along with controls were subjected to western blot with anti-GFAP antibody. Actin was taken as internal loading control. Graphical representation of densitometric analysis of fold change of GFAP levels in the indicated conditions. Bar diagram is representing the quantitative ImageJ analysis of the blots. Values are expressed as mean ± SEM; n = 3, \*p < 0.05. (G, H) 4 h, 8 h, 16 h and 24 h Aβ treated astrocyte samples were subjected to western blot analysis with p-ATF2 and t-ATF2 antibodies. p-ATF2 values were normalized with t-ATF2 values and bar diagram are showing the quantitative analysis of band intensities at different time points. Values are expressed as mean ± SEM; n = 3, \*p < 0.05.

the phosphorylation and hence the activation of p38K in astrocytes in both the *in vitro* and *in vivo* models of AD. The distribution of p38K has been found to be both in cytosol and nuclei where the cytosolic distribution was higher than nuclei with a relatively higher proportion in the cytosol. This is again in agreement with the previous reports that suggest p38K has both cytosolic and nuclear downstream substrates (Ben-Levy et al., 1998; Correa and Eales, 2012). Surprisingly, although activation of ERK pathway has been reported in activated astrocytes in various neurodegenerative models (Bajetto et al., 2001; Biesiada et al., 1996; Wang et al., 2002), but we were unable to find activation of ERK pathway in cultured astrocytes upon Aβ treatment.

Astrocyte proliferation is considered as one of the important

characteristics of astrogliosis upon external stimuli (Garwood et al., 2011; Olabarria et al., 2010). Recently we have reported that astrocytes undergo rapid proliferation upon oligomeric Aβ treatment at a comparatively lower dose (1.5 µM) compared to the doses reported previously (Garwood et al., 2011; Olabarria et al., 2010; Rodriguez et al., 2009; Saha and Biswas, 2015). In this study, we found that, out of three MAPK pathways tested, JNK/c-Jun and p38K cascades induce astrocyte proliferation, as specific inhibitor could block the astrocyte proliferation in response to Aβ treatment. It has been reported that Endothelin-1 which is implicated in many CNS pathologies that involve reactive gliosis, causes astrocyte proliferation via both JNK and ERK pathways (Gadea et al., 2008). There are other inducers of astrocyte proliferation

like thrombin, stromal cell derived factor-1 $\alpha$  (SDF-1 $\alpha$ ) and ET-3 (Bajetto et al., 2001; Biesiada et al., 1996; Wang et al., 2002). Interestingly, in most of these cases, ERK pathway gets activated and in few cases JNK pathway was also activated. In an ischemic stroke model it has been shown that permanent MCAO mediated astrogliosis could be blocked in a p38K KO mouse (Roy Choudhury et al., 2014). Here, we clearly show that, A $\beta$  can cause a rapid increase in astrocyte proliferation within 24 h of treatment and both the JNK and p38K (but not ERK) pathways are activated and play a crucial role in astrocyte proliferation. Hence, the type of stimulus is important determinative factor for MAPK pathways activation and their involvement in astrocyte proliferation.

Finally and interestingly, we found that inhibition of p38K could block the activation specific morphological changes in astrocytes evoked by A $\beta$ . Not only that, A $\beta$  induced upregulation of GFAP also get reduced when astrocytes are treated with specific inhibitor of p38K pathway. Although it has been reported that accumulation of mutant GFAP in astrocytes in Alexander disease is enhanced when p38K is inhibited, but a direct role of p38K on GFAP upregulation is novel (Tang et al., 2008). So, this might be the first instance where we show that p38K activation upregulates the expression of GFAP and thereby induce morphological changes in astrocytes upon A $\beta$  exposure. p38K has a wide array of both cytosolic and nuclear substrates (Plotnikov et al., 2011; Raman et al., 2007). We investigated the levels of a well-known transcription factor, ATF2 which is the downstream substrate of p38 signalling pathway (Watson et al., 2017) and found its upregulation in response to A $\beta$  treatment. In addition, it will be worth investigating if ATF-2 binding motif is present in GFAP promoter as inhibiting p38K, restores GFAP level in A $\beta$  treated astrocytes. In this regard, there is no report that suggests any ATF-2 binding motif in GFAP promoter. But existing report indicate that ATF-2 can also recognize activator protein-1 (AP-1) and GFAP promoter has intrinsic AP-1 binding sequence (Bachetti et al., 2010). A current report is suggesting that p38K pathway activation is strongly correlated with the immunological response and thereafter the release of several inflammatory chemokines and cytokines from activated astrocytes due to LPS incorporation (Lo et al., 2014). So it will be further worth studying the altered profile of different cytokines and chemokines those can be secreted from astrocytes upon A $\beta$  exposure specifically through p38K pathway. In conclusion, this work on the role of MAPK pathways on astrocyte activation in an AD model reveals that although both JNK/c-Jun and p38K pathways are activated but they are differentially involved in eliciting different phenotypical and functional changes of astrocyte activation, whereby both the pathways are involved in cellular proliferation but only p38K pathway contributes in morphological changes in astrocytes triggered by A $\beta$ .

Supplementary data to this article can be found online at <https://doi.org/10.1016/j.mcn.2020.103551>.

#### Acknowledgement and conflict of interest disclosure

The work was supported in part by one of the 12th Five Year Plan Projects, miND (BSC0115) of CSIR, Govt. of India and by the Department of Biotechnology, Govt. of India, Project BT/PR14383/MED/12/475/2010. The authors would like to thank Dr. P. K. Sarkar for critical reading of this manuscript and helpful discussions. The authors would also like to thank Ms. Poulomi Bhadra for her assistance in preliminary works.

The authors have no conflict of interest.

#### CRediT authorship contribution statement

**Subhas Chandra Biswas:** Conceptualization, Supervision, Reviewing and Editing.

**Pampa Saha:** Conceptualization, Experimentation, Writing-Original draft preparation and Reviewing.

**Subhalakshmi Guha:** Experimentation, Reviewing and Revising.

#### References

- Abeti, R., Abramov, A.Y., Duchen, M.R., 2011. Beta-amyloid activates PARP causing astrocytic metabolic failure and neuronal death. *Brain* 134, 1658–1672.
- Abramov, A.Y., Canevari, L., Duchen, M.R., 2004. Beta-amyloid peptides induce mitochondrial dysfunction and oxidative stress in astrocytes and death of neurons through activation of NADPH oxidase. *J. Neurosci.* 24, 565–575.
- Ahmad, M.H., Fatima, M., Mondal, A.C., 2019. Influence of microglia and astrocyte activation in the neuroinflammatory pathogenesis of Alzheimer's disease: rational insights for the therapeutic approaches. *J. Clin. Neurosci.* 59, 6–11.
- Akhter, R., Sanphui, P., Das, H., Saha, P., Biswas, S.C., 2015. The regulation of p53 up-regulated modulator of apoptosis by JNK/c-Jun pathway in beta-amyloid-induced neuron death. *J. Neurochem.* 134, 1091–1103.
- Allen, N.J., Eroglu, C., 2017. Cell biology of astrocyte-synapse interactions. *Neuron* 96, 697–708.
- Arkun, Y., Yasemi, M., 2018. Dynamics and control of the ERK signaling pathway: sensitivity, bistability, and oscillations. *PLoS One* 13, e0195513.
- Bachetti, T., Di Zanni, E., Lantieri, F., et al., 2010. A novel polymorphic AP-1 binding element of the GFAP promoter is associated with different allelic transcriptional activities. *Ann. Hum. Genet.* 74, 506–515.
- Bajetto, A., Barbero, S., Bonavia, R., Piccioli, P., Pirani, P., Florio, T., Schettini, G., 2001. Stromal cell-derived factor-1 $\alpha$  induces astrocyte proliferation through the activation of extracellular signal-regulated kinases 1/2 pathway. *J. Neurochem.* 77, 1226–1236.
- Ben-Lvy, R., Hooper, S., Wilson, R., Paterson, H.F., Marshall, C.J., 1998. Nuclear export of the stress-activated protein kinase p38 mediated by its substrate MAPKAP kinase-2. *Curr. Biol.* 8, 1049–1057.
- Bennett, B.L., Sasaki, D.T., Murray, B.W., et al., 2001. SP600125, an anthranyprazolone inhibitor of Jun N-terminal kinase. *Proc. Natl. Acad. Sci. U. S. A.* 98, 13681–13686.
- Beyreuther, K., Bush, A.L., Dyrks, T., et al., 1991. Mechanisms of amyloid deposition in Alzheimer's disease. *Ann. N. Y. Acad. Sci.* 640, 129–139.
- Bhat, N.R., Zhang, P., Lee, J.C., Hogan, E.L., 1998. Extracellular signal-regulated kinase and p38 subgroups of mitogen-activated protein kinases regulate inducible nitric oxide synthase and tumor necrosis factor- $\alpha$  gene expression in endotoxin-stimulated primary glial cultures. *J. Neurosci.* 18, 1633–1641.
- Biesiada, E., Razandi, M., Levin, E.R., 1996. Egr-1 activates basic fibroblast growth factor transcription. Mechanistic implications for astrocyte proliferation. *J. Biol. Chem.* 271, 18576–18581.
- Biswas, S.C., Shi, Y., Vonsattel, J.P., Leung, C.L., Troy, C.M., Greene, L.A., 2007. Bim is elevated in Alzheimer's disease neurons and is required for beta-amyloid-induced neuronal apoptosis. *J. Neurosci.* 27, 893–900.
- Correa, S.A., Eales, K.L., 2012. The role of p38 MAPK and its substrates in neuronal plasticity and neurodegenerative disease. *J. Signal Transduct.* 2012, 649079.
- Cuesto, G., Enriquez-Barreto, L., Carames, C., Cantarero, M., Gasull, X., Sandi, C., Ferrus, A., Acebes, A., Morales, M., 2011. Phosphoinositide-3-kinase activation controls synaptogenesis and spinogenesis in hippocampal neurons. *J. Neurosci.* 31, 2721–2733.
- Da Silva, J., Pierrat, B., Mary, J.L., Lesslauer, W., 1997. Blockade of p38 mitogen-activated protein kinase pathway inhibits inducible nitric-oxide synthase expression in mouse astrocytes. *J. Biol. Chem.* 272, 28373–28380.
- Dong, Y., Liu, H.D., Zhao, R., Yang, C.Z., Chen, X.Q., Wang, X.H., Lau, L.T., Chen, J., Yu, A.C., 2009. Ischemia activates JNK/c-Jun/AP-1 pathway to up-regulate 14-3-3 $\gamma$  in astrocyte. *J. Neurochem.* 109 (Suppl. 1), 182–188.
- Fields, J., Ghorpade, A., 2012. C/EBP $\beta$  regulates multiple IL-1 $\beta$ -induced human astrocyte inflammatory genes. *J. Neuroinflammation* 9, 177.
- Furman, J.L., Sama, D.M., Gant, J.C., Beckett, T.L., Murphy, M.P., Bachstetter, A.D., Van Eldik, L.J., Norris, C.M., 2012. Targeting astrocytes ameliorates neurologic changes in a mouse model of Alzheimer's disease. *J. Neurosci.* 32, 16129–16140.
- Gadea, A., Schinelli, S., Gallo, V., 2008. Endothelin-1 regulates astrocyte proliferation and reactive gliosis via a JNK/c-Jun signaling pathway. *J. Neurosci.* 28, 2394–2408.
- Gao, K., Wang, C.R., Jiang, F., et al., 2013. Traumatic scratch injury in astrocytes triggers calcium influx to activate the JNK/c-Jun/AP-1 pathway and switch on GFAP expression. *Glia* 61, 2063–2077.
- Garwood, C.J., Pooler, A.M., Atherton, J., Hanger, D.P., Noble, W., 2011. Astrocytes are important mediators of Abeta-induced neurotoxicity and tau phosphorylation in primary culture. *Cell Death Dis.* 2, e167.
- Giovannini, M.G., Scali, C., Prosperi, C., Bellucci, A., Vannucchi, M.G., Rosi, S., Pepeu, G., Casamenti, F., 2002. Beta-amyloid-induced inflammation and cholinergic hypofunction in the rat brain in vivo: involvement of the p38MAPK pathway. *Neurobiol. Dis.* 11, 257–274.
- Gomes, F.C., Paulin, D., Moura Neto, V., 1999. Glial fibrillary acidic protein (GFAP): modulation by growth factors and its implication in astrocyte differentiation. *Braz. J. Med. Biol. Res.* 32, 619–631.
- Gorina, R., Font-Nieves, M., Marquez-Kisinousky, L., Santalucia, T., Planas, A.M., 2011. Astrocyte TLR4 activation induces a proinflammatory environment through the interplay between MyD88-dependent NF $\kappa$ B signaling, MAPK, and Jak1/Stat1 pathways. *Glia* 59, 242–255.
- Hanger, D.P., Betts, J.C., Loviny, T.L., Blackstock, W.P., Anderton, B.H., 1998. New phosphorylation sites identified in hyperphosphorylated tau (paired helical filament-tau) from Alzheimer's disease brain using nano-electrospray mass spectrometry. *J. Neurochem.* 71, 2465–2476.
- Hardy, J., Selkoe, D.J., 2002. The amyloid hypothesis of Alzheimer's disease: progress and problems on the road to therapeutics. *Science* 297, 353–356.
- Hu, J., Akama, K.T., Krafft, G.A., Chromy, B.A., Van Eldik, L.J., 1998. Amyloid-beta

- peptide activates cultured astrocytes: morphological alterations, cytokine induction and nitric oxide release. *Brain Res.* 785, 195–206.
- Iqbal, K., Alonso Adel, C., El-Akkad, E., et al., 2002. Significance and mechanism of Alzheimer neurofibrillary degeneration and therapeutic targets to inhibit this lesion. *J. Mol. Neurosci.* 19, 95–99.
- Jin, Y., Yan, E.Z., Fan, Y., Zong, Z.H., Qi, Z.M., Li, Z., 2005. Sodium ferulate prevents amyloid-beta-induced neurotoxicity through suppression of p38 MAPK and upregulation of ERK-1/2 and Akt/protein kinase B in rat hippocampus. *Acta Pharmacol. Sin.* 26, 943–951.
- Kaminska, B., 2005. MAPK signalling pathways as molecular targets for anti-inflammatory therapy—from molecular mechanisms to therapeutic benefits. *Biochim. Biophys. Acta* 1754, 253–262.
- Kamphuis, W., Mamber, C., Moeton, M., et al., 2012. GFAP isoforms in adult mouse brain with a focus on neurogenic astrocytes and reactive astrogliosis in mouse models of Alzheimer disease. *PLoS One* 7, e42823.
- Kamphuis, W., Middeldorp, J., Kooijman, L., Sluijs, J.A., Kooij, E.J., Moeton, M., Freriks, M., Mizee, M.R., Hol, E.M., 2014. Glial fibrillary acidic protein isoform expression in plaque related astrogliosis in Alzheimer's disease. *Neurobiol. Aging* 35, 492–510.
- Kraner, S.D., Norris, C.M., 2018. Astrocyte activation and the calcineurin/NFAT pathway in cerebrovascular disease. *Front. Aging Neurosci.* 10, 287.
- Kyriakis, J.M., Avruch, J., 2001. Mammalian mitogen-activated protein kinase signal transduction pathways activated by stress and inflammation. *Physiol. Rev.* 81, 807–869.
- LaFerla, F.M., Tinkle, B.T., Bieberich, C.J., Haudenschild, C.C., Jay, G., 1995. The Alzheimer's A beta peptide induces neurodegeneration and apoptotic cell death in transgenic mice. *Nat. Genet.* 9, 21–30.
- Lee, J.K., Kim, N.J., 2017. Recent advances in the inhibition of p38 MAPK as a potential strategy for the treatment of Alzheimer's disease. *Molecules* 22.
- Lee, Y.B., Schrader, J.W., Kim, S.U., 2000. p38 map kinase regulates TNF-alpha production in human astrocytes and microglia by multiple mechanisms. *Cytokine* 12, 874–880.
- Li, D., Liu, N., Zhao, H.H., Zhang, X., Kawano, H., Liu, L., Zhao, L., Li, H.P., 2017. Interactions between Sirt1 and MAPKs regulate astrocyte activation induced by brain injury in vitro and in vivo. *J. Neuroinflammation* 14, 67.
- Li, G.Q., Cong, D.W., Sun, P., Meng, X., 2018. Abeta1-42 regulates astrocytes through JNK/AP-1 pathway. *Eur. Rev. Med. Pharmacol. Sci.* 22, 2015–2021.
- Liu, X., Shah, A., Gangwani, M.R., Silverstein, P.S., Fu, M., Kumar, A., 2014. HIV-1 Nef induces CCL5 production in astrocytes through p38-MAPK and PI3K/Akt pathway and utilizes NF-kB, CEBP and AP-1 transcription factors. *Sci. Rep.* 4, 4450.
- Lo, U., Selvaraj, V., Plane, J.M., Chechneva, O.V., Otsu, K., Deng, W., 2014. p38alpha (MAPK14) critically regulates the immunological response and the production of specific cytokines and chemokines in astrocytes. *Sci. Rep.* 4, 7405.
- Luft, T., Maraskovsky, E., Schnurr, M., et al., 2004. Tuning the volume of the immune response: strength and persistence of stimulation determine migration and cytokine secretion of dendritic cells. *Blood* 104, 1066–1074.
- McDonald, D.R., Bamberger, M.E., Combs, C.K., Landreth, G.E., 1998. beta-Amyloid fibrils activate parallel mitogen-activated protein kinase pathways in microglia and THP1 monocytes. *J. Neurosci.* 18, 4451–4460.
- McLennan, G.P., Kiss, A., Miyatake, M., et al., 2008. Kappa opioids promote the proliferation of astrocytes via Gbetagamma and beta-arrestin 2-dependent MAPK-mediated pathways. *J. Neurochem.* 107, 1753–1765.
- Migheli, A., Piva, R., Atzori, C., Troost, D., Schiffer, D., 1997. c-Jun, JNK/SAPK kinases and transcription factor NF-kappa B are selectively activated in astrocytes, but not motor neurons, in amyotrophic lateral sclerosis. *J. Neuropathol Exp Neurol* 56, 1314–1322.
- Morganti, J.M., Goulding, D.S., Van Eldik, L.J., 2019. Deletion of p38alpha MAPK in microglia blunts trauma-induced inflammatory responses in mice. *J. Neuroinflammation* 16, 98.
- Morishima, Y., Gotoh, Y., Zieg, J., Barrett, T., Takano, H., Flavell, R., Davis, R.J., Shirasaki, Y., Greenberg, M.E., 2001. Beta-amyloid induces neuronal apoptosis via a mechanism that involves the c-Jun N-terminal kinase pathway and the induction of Fas ligand. *J. Neurosci.* 21, 7551–7560.
- Moro, M.L., Collins, M.J., Cappellini, E., 2010. Alzheimer's disease and amyloid beta-peptide deposition in the brain: a matter of 'aging'? *Biochem. Soc. Trans.* 38, 539–544.
- Nakagawa, T., Zhu, H., Morishima, N., Li, E., Xu, J., Yankner, B.A., Yuan, J., 2000. Caspase-12 mediates endoplasmic-reticulum-specific apoptosis and cytotoxicity by amyloid-beta. *Nature* 403, 98–103.
- Olabarria, M., Noristani, H.N., Verkhratsky, A., Rodriguez, J.J., 2010. Concomitant astroglial atrophy and astrogliosis in a triple transgenic animal model of Alzheimer's disease. *Glia* 58, 831–838.
- Paradisi, S., Sacchetti, B., Balduzzi, M., Gaudi, S., Malchiodi-Albedi, F., 2004. Astrocyte modulation of in vitro beta-amyloid neurotoxicity. *Glia* 46, 252–260.
- Pekny, M., Nilsson, M., 2005. Astrocyte activation and reactive gliosis. *Glia* 50, 427–434.
- Placone, A.L., McGuigan, P.M., Bergles, D.E., Guerrero-Cazares, H., Quinones-Hinojosa, A., Searson, P.C., 2015. Human astrocytes develop physiological morphology and remain quiescent in a novel 3D matrix. *Biomaterials* 42, 134–143.
- Plotnikov, A., Zehorai, E., Procaccia, S., Seger, R., 2011. The MAPK cascades: signaling components, nuclear roles and mechanisms of nuclear translocation. *Biochim. Biophys. Acta* 1813, 1619–1633.
- Raman, M., Chen, W., Cobb, M.H., 2007. Differential regulation and properties of MAPKs. *Oncogene* 26, 3100–3112.
- Rodriguez, J.J., Olabarria, M., Chvatal, A., Verkhratsky, A., 2009. Astroglia in dementia and Alzheimer's disease. *Cell Death Differ.* 16, 378–385.
- Roy Choudhury, G., Ryou, M.G., Poteet, E., Wen, Y., He, R., Sun, F., Yuan, F., Jin, K., Yang, S.H., 2014. Involvement of p38 MAPK in reactive astrogliosis induced by ischemic stroke. *Brain Res.* 1551, 45–58.
- Rukenstein, A., Rydel, R.E., Greene, L.A., 1991. Multiple agents rescue PC12 cells from serum-free cell death by translation- and transcription-independent mechanisms. *J. Neurosci.* 11, 2552–2563.
- Saha, P., Biswas, S.C., 2015. Amyloid-beta induced astrocytosis and astrocyte death: implication of FoxO3a-Bim-caspase3 death signaling. *Mol. Cell. Neurosci.* 68, 203–211.
- Saha, P., Sarkar, S., Paidi, R.K., Biswas, S.C., 2020. TIMP-1: a key cytokine released from activated astrocytes protects neurons and ameliorates cognitive behaviours in a rodent model of Alzheimer's disease. *Brain Behav. Immun.* 87, 804–819.
- Sanphui, P., Biswas, S.C., 2013. FoxO3a is activated and executes neuron death via Bim in response to beta-amyloid. *Cell Death Dis.* 4, e625.
- Sanphui, P., Pramanik, S.K., Chatterjee, N., Moorthi, P., Banerji, B., Biswas, S.C., 2013. Efficacy of cyclin dependent kinase 4 inhibitors as potent neuroprotective agents against insults relevant to Alzheimer's disease. *PLoS One* 8, e78842.
- Santos-Carvalho, A., Elvas, F., Alvaro, A.R., Ambrosio, A.F., Cavadas, C., 2013. Neuropeptide Y receptors activation protects rat retinal neural cells against necrotic and apoptotic cell death induced by glutamate. *Cell Death Dis.* 4, e636.
- Selkoe, D.J., 2001. Alzheimer's disease results from the cerebral accumulation and cytotoxicity of amyloid beta-protein. *J. Alzheimers Dis.* 3, 75–80.
- Shaul, Y.D., Seger, R., 2007. The MEK/ERK cascade: from signaling specificity to diverse functions. *Biochim. Biophys. Acta* 1773, 1213–1226.
- Sholl, D.A., 1953. Dendritic organization in the neurons of the visual and motor cortices of the cat. *J. Anat.* 87, 387–406.
- Sorensen, S.D., Nicole, O., Peavy, R.D., Montoya, L.M., Lee, C.J., Murphy, T.J., Traynelis, S.F., Hepler, J.R., 2003. Common signaling pathways link activation of murine PAR-1, LPA, and S1P receptors to proliferation of astrocytes. *Mol. Pharmacol.* 64, 1199–1209.
- Tang, G., Yue, Z., Tallocczy, Z., Hagemann, T., Cho, W., Messing, A., Sulzer, D.L., Goldman, J.E., 2008. Autophagy induced by Alexander disease-mutant GFAP accumulation is regulated by p38/MAPK and mTOR signaling pathways. *Hum. Mol. Genet.* 17, 1540–1555.
- Troy, C.M., Rabacchi, S.A., Xu, Z., Maroney, A.C., Connors, T.J., Shelanski, M.L., Greene, L.A., 2001. beta-Amyloid-induced neuronal apoptosis requires c-Jun N-terminal kinase activation. *J. Neurochem.* 77, 157–164.
- Troy, C.M., Friedman, J.E., Friedman, W.J., 2002. Mechanisms of p75-mediated death of hippocampal neurons. Role of caspases. *J Biol Chem* 277, 34295–34302.
- Villemagne, V.L., Burnham, S., Bourgeat, P., et al., 2013. Amyloid beta deposition, neurodegeneration, and cognitive decline in sporadic Alzheimer's disease: a prospective cohort study. *Lancet Neurol.* 12, 357–367.
- Wang, H., Ubl, J.J., Stricker, R., Reiser, G., 2002. Thrombin (PAR-1)-induced proliferation in astrocytes via MAPK involves multiple signaling pathways. *Am. J. Physiol. Cell Physiol.* 283, C1351–C1364.
- Watson, G., Ronai, Z.A., Lau, E., 2017. ATF2, a paradigm of the multifaceted regulation of transcription factors in biology and disease. *Pharmacol. Res.* 119, 347–357.
- Xie, Z., Smith, C.J., Van Eldik, L.J., 2004. Activated glia induce neuron death via MAP kinase signaling pathways involving JNK and p38. *Glia* 45, 170–179.
- Yao, M., Nguyen, T.V., Pike, C.J., 2005. Beta-amyloid-induced neuronal apoptosis involves c-Jun N-terminal kinase-dependent downregulation of Bcl-w. *J. Neurosci.* 25, 1149–1158.
- Zarubin, T., Han, J., 2005. Activation and signaling of the p38 MAP kinase pathway. *Cell Res.* 15, 11–18.
- Zhang, L., Xie, H., Cui, L., 2018. Activation of astrocytes and expression of inflammatory cytokines in rats with experimental autoimmune encephalomyelitis. *Exp Ther Med* 16, 4401–4406.

# Rheb-mTOR activation rescues A $\beta$ -induced cognitive impairment and memory function by restoring miR-146 activity in glial cells

Dipayan De,<sup>1</sup> Ishita Mukherjee,<sup>2</sup> Subhalakshmi Guha,<sup>3</sup> Ramesh Kumar Paidi,<sup>3</sup> Saikat Chakrabarti,<sup>2</sup> Subhas C. Biswas,<sup>3</sup> and Suvendra N. Bhattacharyya<sup>1</sup>

<sup>1</sup>RNA Biology Research Laboratory, Molecular Genetics Division, CSIR-Indian Institute of Chemical Biology, Kolkata 700032, India; <sup>2</sup>Structural Biology and Bio-informatics Division, CSIR-Indian Institute of Chemical Biology, Kolkata 700032, India; <sup>3</sup>Cell Biology and Physiology Division, CSIR-Indian Institute of Chemical Biology, Kolkata 700032, India

**Deposition of amyloid beta plaques in adult rat or human brain is associated with increased production of proinflammatory cytokines by associated glial cells that are responsible for degeneration of the diseased tissue. The expression of these cytokines is usually under check and is controlled at the post-transcriptional level via several microRNAs. Computational analysis of gene expression profiles of cortical regions of Alzheimer's disease patients' brain suggests ineffective target cytokine mRNA suppression by existing micro-ribonucleoproteins (miRNPs) in diseased brain. Exploring the mechanism of amyloid beta-induced cytokine expression, we have identified how the inactivation of the repressive miR-146 miRNPs causes increased production of cytokines in amyloid beta-exposed glial cells. In exploration of the cause of miRNP inactivation, we have noted amyloid beta oligomer-induced sequestration of the mTORC1 complex to early endosomes that results in decreased Ago2 phosphorylation, limited Ago2-miRNA uncoupling, and retarded Ago2-cytokine mRNA interaction in rat astrocytes. Interestingly, constitutive activation of mTORC1 by Rheb activator restricts proinflammatory cytokine production by reactivating miR-146 miRNPs in amyloid beta-exposed glial cells to rescue the disease phenotype in the *in vivo* rat model of Alzheimer's disease.**

## INTRODUCTION

MicroRNAs (miRNAs) are 20- to 22-nt-long non-coding RNAs that can fine-tune the expression of their target mRNAs post-transcriptionally in metazoan cells by imperfect base pairing.<sup>1,2</sup> As in other tissues, miRNAs are important gene regulators in the mammalian brain, where hundreds of miRNAs are known to control thousands of transcripts encoding important proteins that affect several physiological processes and events in the mammalian brain.<sup>3</sup> Differentiation of embryonic stem cells to neuronal cells is also controlled by specific miRNAs such as miR-9,<sup>4</sup> while miR-128 regulates the growth of the dendrites.<sup>5</sup> There is also evidence of miRNA playing a significant role in neurodegenerative diseases (NDDs) such as in Alzheimer's disease (AD), Parkinson's disease (PD), Huntington's disease (HD), or in amyotrophic lateral sclerosis (ALS).<sup>6</sup> There have been reports

that show the effect of conditional knockout of Dicer, an essential enzyme for miRNA biogenesis, on neuronal death.<sup>7</sup> Additionally, differential miRNA expression profiles from postmortem brains of patients who died of AD have shown the possible importance of miRNA expression in the pathophysiology of this disease.<sup>8,9</sup>

Astrocytes are the most abundant cells in the mammalian brain. The increases in the number and complexity of this glial cell population during brain development support their possible role in regulating complex traits such as human cognition and behavior.<sup>10</sup> Astrocytes provide support to the neuronal function by regulating ion homeostasis,<sup>11</sup> or by controlling CNS blood flow,<sup>12</sup> and they also play a crucial role in synaptic transmission by forming tripartite synapse.<sup>13,14</sup> Apart from their supportive role, astrocytes are also immunomodulatory cells known to secrete various cytokines and chemokines, which play an important role in the pathophysiology of different diseases, including AD.<sup>15</sup> In AD, increased production of inflammatory cytokines may lead to death of the neighboring neurons and is considered as the major path that amyloid beta (A $\beta$ ) oligomers activate in the glial cell population, leading to neuronal death.<sup>16</sup> However, the exact mechanism of the excess cytokine production in glial cells by A $\beta$  exposure is not clear. miRNAs are important regulators of the immune response, and they can control hyperresponsiveness of immune cells by reversibly regulating miRNA activity in activated macrophage cells.<sup>17-19</sup> Thus, the expression and activity of miRNAs in astroglia, the major immune cells in brain context, are likely to have a role in controlling neuroinflammation during neurodegenerative diseases.

Argonaute (Ago) proteins play a crucial role in post-transcriptional gene silencing in eukaryotic cells. According to published reports, Ago proteins are responsible for the regulation of expression of

Received 16 September 2020; accepted 9 April 2021;  
<https://doi.org/10.1016/j.omtn.2021.04.008>.

**Correspondence:** Suvendra N. Bhattacharyya, RNA Biology Research Laboratory, Molecular Genetics Division, CSIR-Indian Institute of Chemical Biology, Kolkata 700032, India.

**E-mail:** [suvendra@iicb.res.in](mailto:suvendra@iicb.res.in)



most protein-coding genes primarily by associating with specific miRNAs having complementarities with those protein-coding genes.<sup>20,21</sup> In mammals, there are four Ago proteins (Ago1–Ago4), and Ago2 is the major and most widely expressed Ago in different tissues, including the brain.<sup>22</sup> Upon its association with miRNAs, it can cleave the target mRNAs, having perfect complementarities with bound miRNAs.<sup>23</sup> Post-translational modification of Ago protein can also determine its function. Increased Ago stability and catalytic activity are associated with modifications such as hydroxylation and methylation of Ago.<sup>24,25</sup> Among all of the modifications, phosphorylation at different positions may play a significant role in miRNA binding of Ago2 and its subcellular localization.<sup>26–28</sup>

Mammalian target of rapamycin (mTOR), a master regulator of cell growth, is comprised of mTORC1 and mTORC2, which are different forms of structural and functional complexes involving mTOR protein. Raptor and mLST8, along with mTOR, are the major subunits of mTORC1, which regulates cell growth, protein homeostasis and synthesis, and autophagy.<sup>29</sup> mTORC2 constitutes mTOR, Rictor, mSin1, and mLST8. The major function of this complex includes lipogenic regulation and that of the cytoskeletal structure.<sup>30</sup> The mTOR pathway specializes in sensing multiple external stimuli such as growth factors and oxygen level, and it is known to respond by sensing amino acid and glucose concentrations as well. Important neuronal physiological phenomena such as synaptic plasticity, memory, and learning are often maintained by mTOR.<sup>31</sup> Faulty mTORC1 signaling has been linked with AD previously, and TREM2-deficient microglial cells were shown to have a decrease in mTORC1 activity that contributed to high autophagic flux, leading to weakened microglial fitness.<sup>32</sup> Studies have shown that in spite of known upstream and downstream regulatory factors, the major key to the mTOR-associated signaling lies in the compartmentalization of the mTORC1 to specific cellular sites.<sup>33,34</sup> How disease conditions influence mTOR localization and whether mTOR localization plays a role in the pathophysiology of a disease are unresolved questions in the field.

In this study, we report how the exposure of an A $\beta$  oligomer (A $\beta$ <sub>1–42</sub>) in rat astrocytes decreases cellular mTORC1 activity by enhancing the sequestration of mTORC1 complexes to the early endosome. A $\beta$ <sub>1–42</sub> also restricts translocation of mTORC1 to the lysosome, which is found to be important for mTORC1 activation. mTOR inactivation reduces miRNA activity due to a decrease in Ago2 phosphorylation. Interestingly, reactivation of mTORC1 through the expression of the constitutive activator Rheb reverses both A $\beta$ <sub>1–42</sub>-mediated pro-inflammatory cytokine production and restores behavioral abnormalities in animals along with a rescue of miRNA function, suggesting a pivotal role of miRNA activity modulation by mTORC1 in AD.

## RESULTS

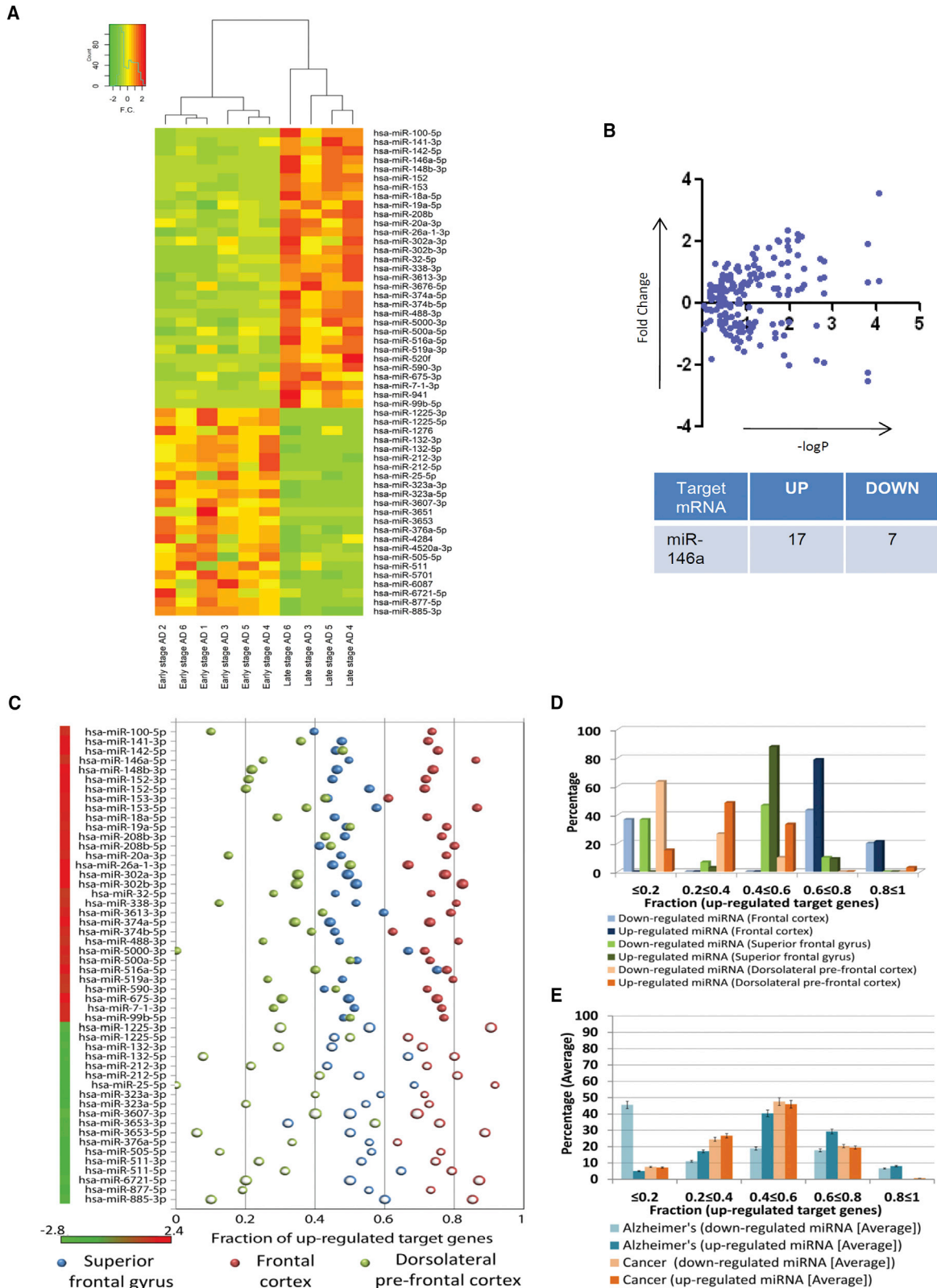
### Exposure to A $\beta$ <sub>1–42</sub> oligomer causes miRNA upregulation in human and adult rat brain

miRNAs are important regulators of most metazoan genes that are supposed to be upregulated and expressed profoundly upon inactivation or downregulation of cognate miRNAs. To obtain an insight into

whether the miRNA and mRNA profiles get altered in the disease process, we analyzed the “regulator(s)-to-target(s)” (miRNA/mRNA) expression profiles in different brain regions of AD patients. The relationship between the differentially expressed miRNAs and their corresponding target genes were studied. A set of 30 miRNAs were found to be upregulated whereas 23 miRNAs were found to be downregulated in the prefrontal cortex of AD patients (Figure 1A; Table S1), and these miRNAs are likely to be related to AD etiology or progression. Clustering has been done for the analyzed miRNAs. Analysis of miRNA expression profiles in the prefrontal cortex of AD patients was performed by considering the samples provided in a GEO dataset (GEO: GSE48552).<sup>35</sup> Based on clinical presentation and stage of the disease, the samples had been grouped into early stage and late-stage AD. Differentially expressed miRNA between these stages were determined by using the DESeq package in R. Normalized counts of the differentially expressed miRNAs identified when considering these samples have been depicted in a heatmap (Figure 1A).<sup>36</sup> Furthermore, when considering mRNA expression profiling data, 2,092, 2,166, and 292 mRNAs were found to be upregulated while 1,253, 699, and 676 genes were found to be downregulated within the superior frontal gyrus, frontal cortex, and dorsolateral prefrontal cortex, respectively. Moreover, 271 genes (mRNAs) were found to be commonly upregulated among two or more of the different brain cortical regions considered herein for the analysis. The corresponding fraction of upregulated target mRNAs of each of the differentially expressed miRNAs was determined in different cortical regions (frontal cortex, superior frontal gyrus, and dorsolateral prefrontal cortex) of the human brain. Herein, we observed that in comparison to the downregulated miRNAs, nearly 79% of the upregulated miRNAs had a substantial fraction (0.6–0.8) of their target mRNAs also upregulated as in the frontal cortex (Figures 1C and 1D). Furthermore, the observation that in comparison to the downregulated miRNAs, a higher percentage of the upregulated miRNAs had a substantial fraction of their target mRNAs as upregulated is consistent within the other cortical regions considered in this study. Herein, in comparison to the downregulated miRNAs, 88% and 48% of the upregulated miRNAs had between 0.4 and 0.6 or between 0.2 and 0.4 fractions of their target mRNAs as upregulated within the superior frontal gyrus and dorsolateral prefrontal cortex, respectively (Figures 1C and 1D).

In order to determine whether similar regulator(s)-to-target(s) relationship patterns could be prevalent in other diseases or cell types, we determined whether these deregulated mRNAs could be related to any other disease condition as well by performing a disease enrichment analysis that considered the set of commonly upregulated mRNAs. With the help of disease enrichment analysis, we found that these genes are also associated with cancer (Figures S1A and S1B). Therefore, subsequently we analyzed regulator(s)-to-target(s) (miRNA/mRNA) expression profiles in different cancer tissues. A substantial fraction of upregulated miRNAs had their target mRNAs as upregulated in oral squamous cell carcinoma, colorectal cancer, and breast cancer (Figures S1C–S1E). In this scenario, we observed that similar percentages of downregulated miRNAs and upregulated miRNAs have their target mRNA fractions as upregulated (Figure S1 In





(legend on next page)

particular, the upregulated miRNAs (65%) and downregulated miRNAs (67%) have similar fraction (between 0.4 and 0.6 or between 0.2 and 0.4) of their corresponding target mRNAs as upregulated in the cancer case studies considered herein (Figures 1E and S1F).

Importantly, we have considered multiple datasets to identify a common trend in the deregulated miRNA-mRNA interaction network by considering target mRNAs that are commonly differentially expressed in two or more of the different brain cortical regions. However, during the analysis we considered all of the target mRNAs that were significantly differentially expressed in each dataset to study the regulator(s)-to-target(s) (miRNA/mRNA) expression profile patterns in AD patients and compared the same. miR-146a-5p has consistently been found to exhibit this phenomenon across all of the conditions analyzed in the present study. Furthermore, miR-146a, which is known to regulate expression of a number of cytokines, was found to be upregulated.<sup>37</sup> Expression of all of the probable miR-146a targets was also analyzed. Interestingly, most miR-146a targets were found to be upregulated in AD brain, indicating a possible loss of function of miR-146a on its target in the AD brain (Figure 1B; Table S2).

In the AD datasets considered herein for analysis, a substantial percentage of upregulated miRNAs have a large fraction of their corresponding target genes as upregulated. This is contrary to the general regulatory relationship between miRNAs and their target genes wherein the target genes of upregulated miRNAs are downregulated, as expected.<sup>2,38</sup> However, this inverse relationship between the target genes and upregulated miRNAs has also been noted in other cell types other than those in the degenerative brain. In cancer cells, the trend of target gene upregulation in the backdrop of upregulated cognate miRNA expression has also been noted (Figure S1F). However, the upregulation of a target gene with an increase in cognate miRNAs has been more prominent in AD than in cancer (Figures 1D and 1E). Thus, we observed trends that in comparison to the downregulated miRNA, target mRNAs of upregulated miRNAs are mainly upregulated, and this phenomenon is more prominent in the AD condition than in cancer. Therefore, in the AD brain there is a possibility of the existence of a mechanism for gross inactivation of micro-ribonucleoproteins (miRNPs) that may make them ineffective to suppress their targets.

We wanted to explore the effect of the A $\beta$ <sub>1-42</sub> oligomer, the suspected causative link between amyloid plaque and the disease phenotype in AD patients, on cellular miRNA levels in rat brain. The preformed A $\beta$ <sub>1-42</sub> oligomer was stereotactically injected in the adult rat brain

hippocampal region and animals were kept for 21 days, which is known to cause deposition of A $\beta$  plaques in and around the injection area (Figures 2A and 2B).<sup>39</sup> A deposition of A $\beta$  plaques also resulted in glial fibrillary acidic protein (GFAP) activation, which is a marker for astrocyte proliferation as well as immune activation in rat brain (Figure 2B).<sup>40</sup> Now there are several miRNAs present in rat brain that can regulate the expression profile of these cytokine mRNAs either directly or indirectly. For example, interleukin (IL)-6 is a direct target of let-7a, and miR-146a fine-tunes cytokine production by repressing the nuclear factor  $\kappa$ B (NF- $\kappa$ B) pathway.<sup>41,42</sup> Therefore, we wanted to check what are the expression patterns of those miRNAs that directly and indirectly regulate expression of pro-inflammatory cytokines in both rat brain as well as in primary rat astrocytes. mRNA levels of different proinflammatory cytokines, such as IL-1 $\beta$  and IL-6, were increased several fold when oligomeric A $\beta$ <sub>1-42</sub> was stereotactically infused in the hippocampus of adult rat brain, supporting an already reported A $\beta$ <sub>1-42</sub>-induced immunoactivation reaction in affected brain (Figure 2C). Interestingly, as observed in human patient samples, expression profiles of several miRNAs, including the immunogenic miRNAs miR-21, miR-146a, and miR-155, also showed upregulation in adult rat brain injected with A $\beta$ <sub>1-42</sub> (Figure 2D). To identify the contribution of astrocytes in cytokine production in rat brain upon activation with the A $\beta$ <sub>1-42</sub> oligomer, we treated the primary rat astrocytes with A $\beta$ <sub>1-42</sub> oligomer *ex vivo*. The activation of the cells was scored by excess production of GFAP in rat primary astrocyte on A $\beta$ <sub>1-42</sub> oligomer exposure (Figures 2E and 2F). It was found that A $\beta$  can activate astrocytes where mRNA levels of different cytokines were found to be increased several fold (Figures 2E and 2F). We noted a global increase in miRNA levels in A $\beta$ <sub>1-42</sub>-treated astrocytes where 65%–70% of the miRNAs were found to be upregulated, including miR-146a, miR-155, miR-21, and let-7a. These miRNAs are direct and indirect regulators of IL-1 $\beta$ . IL-6 was also noted to have increased in treated astrocytes (Figure 2G). Interestingly, we found increases in several other miRNAs, such as miR-16, miR-29a, and miR-145, in both brain tissue as well as in primary glial cells upon amyloid exposure (Figures 2D and 2G). These miRNAs are not known to affect cytokine expression in mammalian cells, indicating the possibility that the phenomena we observed could have broader implications and affect several different types of miRNAs.

#### mTOR-mediated Ago2 phosphorylation is required for miRNA-mediated repression of targets

To uncover the mechanism of non-functional miRNP accumulation in A $\beta$ <sub>1-42</sub>-treated cells, we used C6 glioblastoma cells to treat with

#### Figure 1. Possible miRNA-to-mRNA expression relationships in Alzheimer's disease (AD) and cancer

(A) Heatmap of differentially expressed miRNAs in prefrontal cortex of AD patients. The significance threshold for selection of differentially expressed miRNAs was considered as fold change of  $\pm 1.25$  and a p value of  $\leq 0.05$ . (B) Graphs showing expression levels of miR-146a targets in the prefrontal cortex of Alzheimer's disease patients. The y axis represents fold change of individual mRNAs, and the x axis represents the  $-\log_{10}$  p value. The table represents the number of miR-146a targets having at least 1.5-fold changes. (C) The probable relationship between differentially expressed miRNAs and mRNAs in AD considering the possible fraction of upregulated target mRNAs of each of the miRNAs as studied in different cortical regions (frontal cortex, superior frontal gyrus, and dorsolateral prefrontal cortex) is depicted here. (D) Percentages of upregulated or downregulated miRNAs that possibly have a fraction of their target genes as upregulated within the frontal cortex, superior frontal gyrus, and dorsolateral prefrontal cortex are shown here. (E) Comparison among the percentages of differentially expressed miRNAs that have different subsets or fractions of their target mRNAs as upregulated in degenerative tissues (AD) as opposed to highly proliferative tissues (cancer) was performed.

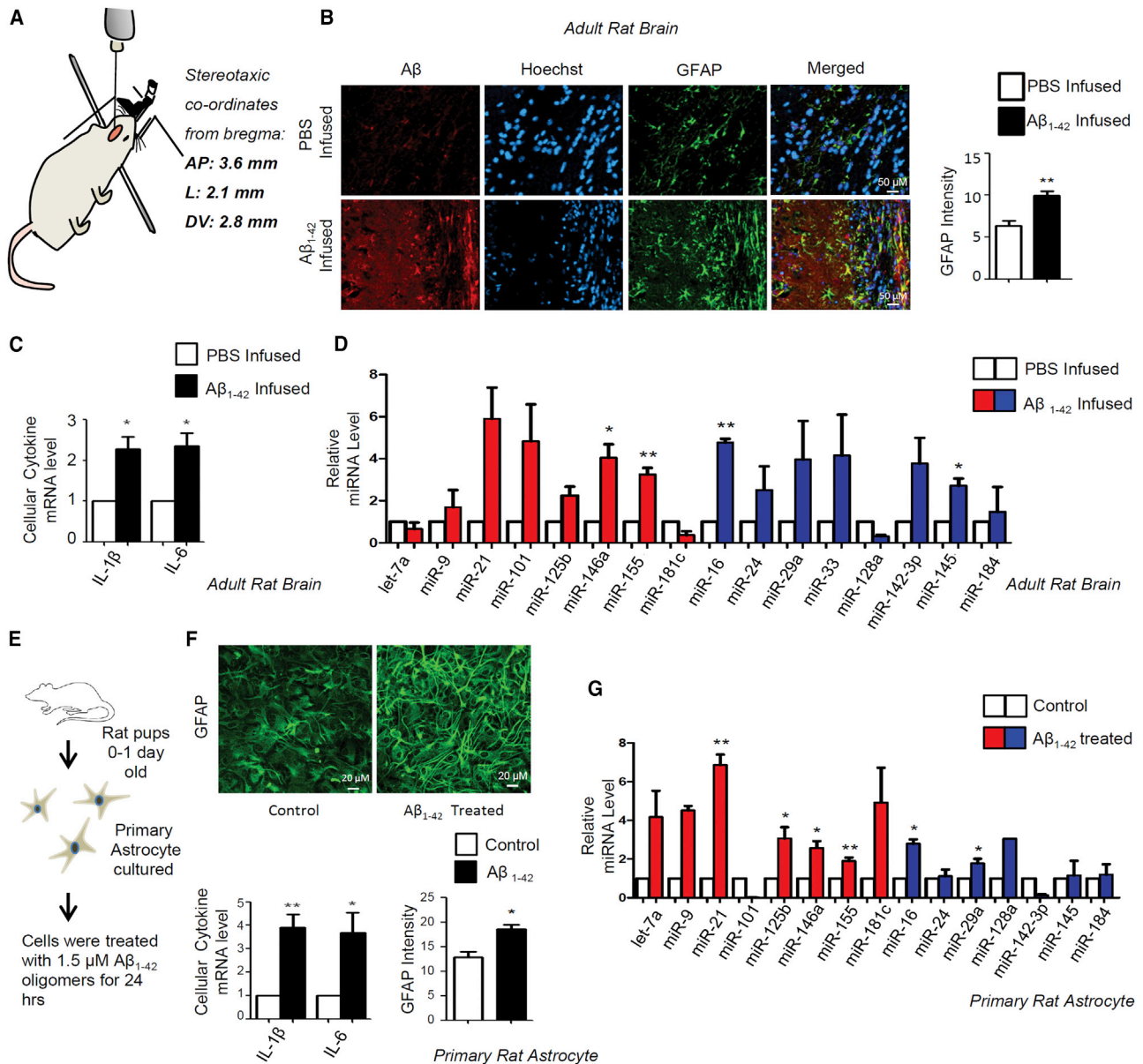


**Figure 2. Aβ<sub>1-42</sub> induces an inflammatory response and increases miRNA levels in astrocytes**

(A) Preformed Aβ<sub>1-42</sub> oligomers in PBS were infused in the hippocampus at stereotaxic coordinates from bregma (AP, 3.6 mm; L, 2.1 mm; DV, 2.8 mm) in adult rat brain. PBS without Aβ<sub>1-42</sub> was used for control injection. Animals were kept 21 days for plaque formation. (B) Cryosections of Aβ<sub>1-42</sub>-infused and PBS-infused control rat brain hippocampus were subjected to immunohistochemistry (IHC) analysis. Astrocytes were immunostained for GFAP (green), whereas Aβ was visualized in red and the nucleus was stained with Hoechst (blue). Relative intensities of the GFAP signals were measured by ImageJ software, and quantification is shown in the right panel. (C) qPCR-based quantification of total mRNA levels of IL-1β and IL-6 in PBS and Aβ<sub>1-42</sub>-infused adult rat hippocampus. The data were normalized against GAPDH mRNA levels. (D) Cellular miRNA levels in PBS- and Aβ<sub>1-42</sub>-infused adult rat brain hippocampus. TaqMan-based miRNA level quantification was done. Values were normalized with U6 snRNA level. Red represents the miRNAs that are known to regulate cytokine mRNAs, and blue represents miRNAs that are not known to regulate cytokine mRNAs. (E and F) Experimental strategy of isolation of rat primary astrocytes from 0- to 1-day-old rat pup brain followed by treatment of the primary cells with 1.5 μM Aβ<sub>1-42</sub> oligomers *ex vivo* (E). Microscopic images showing effect of Aβ<sub>1-42</sub> on primary cortical astrocytes stained with GFAP (green, F, upper panel). The intensity levels of the GFAP in both conditions were calculated by ImageJ software and plotted (F, bottom right panel). Graphs depict levels of cellular IL-1β and IL-6 mRNA levels in Aβ<sub>1-42</sub>-treated primary cortical astrocytes. The data were normalized against GAPDH mRNA level (F, lower left panel). (G) Cellular miRNA levels in Aβ<sub>1-42</sub>-treated primary cortical astrocytes. TaqMan-based miRNA level quantifications were done. Values were normalized with U6 snRNA. Red represents the miRNAs that are known to regulate cytokine mRNAs, and blue represents miRNAs that are not known to regulate cytokine mRNAs. For statistical significance, a minimum of three independent experiments were considered in each case unless otherwise mentioned, and error bars represent means ± SEM. p values were calculated with a Student's t test. \*p < 0.05, \*\*p < 0.01, \*\*\*p < 0.0001. ns, not significant.

the  $A\beta_{1-42}$  oligomer before the biochemical analysis was done for the treated and control cells. To confirm the accumulation of nonfunctional miRNPs with the increase in total cellular miRNP levels observed in  $A\beta_{1-42}$  oligomer-treated cells, C6 glioma cells were transfected with Renilla luciferase (RL) reporter having the 3' UTR of IRAK1 mRNA with two miR-146a binding sites (Figure 3A). A reduction in miR-146a activity was observed in  $A\beta_{1-42}$ -treated cells compared to the DMSO-treated control cells (Figure 3B). The most probable cause of reduced miRNA activity could be the unbinding of miRNA with Ago2 proteins, which is known to happen in the mammalian macrophage during its activation phase and also in neuronal cells during the nerve growth factor-induced differentiation process.<sup>19,26</sup> To check whether similar effects on Ago2 by  $A\beta_{1-42}$  may cause the downregulation of miRNA-Ago2 binding in  $A\beta_{1-42}$ -treated astrocytes, we cultured primary astrocytes from rat pups and treated them with DMSO or  $A\beta_{1-42}$  for 24 h. Ago2 was immunoprecipitated (IP) followed by qPCR-based measurement of bound miRNAs. The RNA amount was normalized with the quantity of Ago2 protein recovered during the IP process. The quantification revealed, in  $A\beta_{1-42}$ -treated cells, that there was an increased association of Ago2 with miR-146a and miR-155 compared to the control cells (Figure 3C). We also found an increase in both Ago2-associated miR-16 and miR-29a level upon  $A\beta_{1-42}$  treatment (Figure S2A). We performed similar experiments with primary neurons cultured *ex vivo*, where we could not detect a significant effect of  $A\beta_{1-42}$  oligomers on neuronal miRNA levels or Ago2-associated miRNA levels, suggesting an astrocyte-specific effect of  $A\beta_{1-42}$  on cellular miRNPs (Figures 3D and 3E). To check the possible role of any post-translational modification affecting miRNA activity in the  $A\beta$  treatment context, we measured phosphorylated Ago2 levels in  $A\beta_{1-42}$ -treated cells. The reduced phosphorylated Ago2 level in  $A\beta_{1-42}$ -treated cells was detected and compared to the control cells, and the results correlated with reduced interaction between Ago2 and mTOR after  $A\beta_{1-42}$  treatment (Figures 3F and 3G), indicating a possible role of mTOR in miRNA activity regulation via controlling Ago phosphorylation. This was suggestive from the earlier experiments in which an  $A\beta_{1-42}$ -mediated decrease in Ago2 phosphorylation might hinder dissociation of miRNA from Ago2 protein but reduce miRNA activity. Therefore, we hypothesized that lack of Ago2 phosphorylation might perturb the repression of target mRNA in mammalian cells. Ago2 proteins have a MID domain that is found to be important for binding with the 5' phosphate group of small RNAs.<sup>28</sup> A phosphorylation at the Y529 position in the MID domain imparts a negative charge that dissociates miRNAs from Ago2 protein. The Ago2Y529F mutant, which cannot be phosphorylated at the Tyr529 position, remains bound to miRNA.<sup>19,28</sup> C6 glioblastoma cells were transiently transfected with the Ago2-wild-type (WT) and Ago2-Y529F protein in the absence and presence of  $A\beta_{1-42}$  oligomers, and qPCR was performed to check the cellular mRNA levels of IL-1 $\beta$  and IL-6. We found a higher expression of both IL-1 $\beta$  and IL-6 mRNA levels in Ago2-Y529F-expressing cells even without  $A\beta_{1-42}$  exposure, which suggests the importance of Ago2 phosphorylation in cytokine mRNA expression (Figure 3H). However, the effect of  $A\beta_{1-42}$  on cytokine expression was absent in cells expressing Ago2-

Y529E. This further suggests that cytokine expression is regulated primarily via Ago2 phosphorylation in glial cells. To confirm the involvement of mTORC1 in the miRNA activity regulation process possibly via Ago2 phosphorylation, cells were exposed to rapamycin, a known mTORC1 blocker.<sup>43</sup> We found a significant decrease in miR-146a activity when treated with rapamycin (Figure 3I). We also found reduced amounts of Ago2 phosphorylation and an increase in Ago2-bound miR-146a levels upon rapamycin treatment (Figure 3J and 3K). These data signify the effects of mTORC1 inhibition in controlling miRNA activity and Ago2 phosphorylation that are also observed in astrocytes exposed to  $A\beta_{1-42}$ . Experiments were also done in a heterogeneous context using HEK293 cells depleted for Raptor, an integral protein of the mTORC1 complex, and expressing exogenously a liver-specific miR-122 there.<sup>44</sup> This was done to recheck the interlinking of mTOR inactivation with Ago2 phosphorylation and miRNA activity regulation even in non-astroglial cells. In HEK293 cells treated with siRaptor, we documented reduced miRNA activity and, as in  $A\beta_{1-42}$  treated cells, a reduction in Ago2 phosphorylation, confirming mTORC1 involvement in miRNA activity regulation in general in mammalian cells by targeting Ago2 phosphorylation (Figures S2B and S2C).

#### Sequestration of mTORC1 to early endosome causes miRNA inactivation and increased miRNP formation in glial cells

We found a decrease in phosphorylated p70-S6 kinase along with active phosphorylated mTOR levels in  $A\beta_{1-42}$ -treated astrocytes (Figures 4A and 4B). The expression of mTOR is tightly regulated in mammalian cells where different nutrients and growth factor-like glucose, amino acids, and insulin can activate mTORC1 depending on the metabolic state of the cell.<sup>45</sup> Interestingly, it is not only the presence of upstream signals, but mTORC1 also shows localization-based activation. It was reported earlier that translocation of mTOR to the lysosomal membrane is important for mTORC1 activation, where it can be activated by the GTPase Rheb.<sup>34</sup> Thus, to check for the possibility that  $A\beta_{1-42}$ -mediated mTORC1 deactivation may happen because of the reduced mTORC1 localization to the lysosomal membrane, we microscopically looked at the localization of mTOR in control and treated cell. Confocal images were taken from both control and  $A\beta_{1-42}$ -treated C6 glioblastoma cells, where lysosomes were stained with LysoTracker (red) and mTOR (green) was visualized by indirect immunofluorescence (Figure 4C). There was a decrease in colocalization between mTOR and lysosomes indicating a faulty translocation of mTOR in amyloid-treated cells (Figure 4D). Since mTOR was not translocating at the lysosomal surface, it was important to find out the altered localization of mTOR upon  $A\beta_{1-42}$  exposure. We found a significant increase in colocalization between mTOR and early endosomes (Figures 4E and 4F). Cells were transiently transfected with yellow fluorescent protein (YFP)-Endo, which marks early endosomes, and then activated with oligomeric  $A\beta_{1-42}$  for 24h. Higher colocalization between early endosomes and mTOR suggests that  $A\beta_{1-42}$  restricts mTOR to the early endosomes, which retards its translocation to the lysosomal surfaces to get activated. To determine whether mTOR sequestration in early endosome can affect miRNA activity or miRNP formation, we expressed a

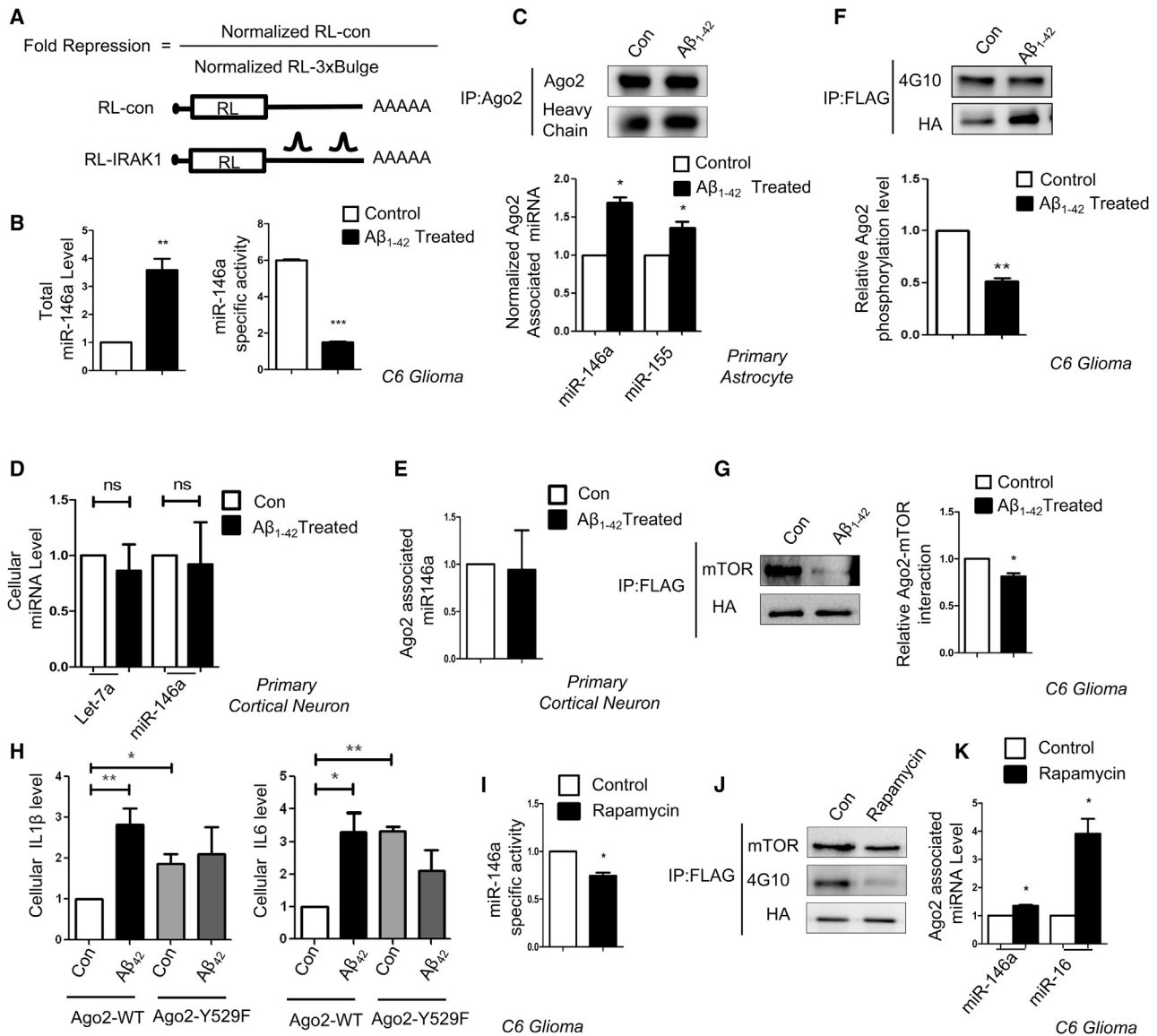


**Figure 3. mTOR-mediated Ago2 phosphorylation is required for miRNA activity**

(A) Schematic design of different Renilla luciferase (RL) reporters used for scoring miRNA activity. The 3' UTR of IRAK1 mRNA with two miR-146a binding sites was cloned on the 3' UTR of the Renilla mRNA. (B) Effect of Aβ<sub>1-42</sub> treatment on cellular miR-146a activity and level. Specific activity of miR-146a was calculated by normalizing the fold repression of target reporter mRNA against the corresponding miRNA expression level. An increased cellular miR-146a level in C6 glioblastoma cells upon Aβ<sub>1-42</sub> treatment is shown. The data were obtained by qRT-PCR-based quantification and were normalized against the expression of U6 snRNA. (C) Increase in Ago2-miRNA association in rat primary astrocytes upon Aβ<sub>1-42</sub> treatment. Endogenous Ago2 from control- and 1.5 μM Aβ<sub>1-42</sub>-treated primary rat astrocytes was immunoprecipitated and the levels of Ago2-associated miR-146a and miR-155 were estimated by qRT-PCR. Values were normalized against the amount of Ago2 obtained in each immunoprecipitation reaction. (D and E) No change in miRNP levels in rat cortical neurons exposed to 1.5 μM Aβ<sub>1-42</sub>. Primary neuronal cells were treated with Aβ<sub>1-42</sub> oligomers for 24 h, and the amounts of endogenous miRNAs and miRNAs associated with immunoprecipitated Ago2 were estimated and plotted after normalization against U6 snRNA and Ago2 levels, respectively. (F and G) Reduced mTOR-Ago2 interaction and Ago2 phosphorylation in Aβ<sub>1-42</sub> oligomer-treated C6 glioblastoma cells. Western blot data show the amount of Ago2 phosphorylation (F) and the amount of mTOR pulled down with Ago2 (G). C6 glioblastoma cells were transiently transfected with FH-Ago2 and then treated with 2.5 μM Aβ<sub>1-42</sub> for 24 h. Immunoseparation of FH-Ago2 was done with FLAG beads. The amount of Ago2 pulled down was detected by anti-HA antibody, and levels of phosphorylated Ago2 (Tyr phosphorylation) were detected by anti-phosphorylated (p-)Tyr antibody 4G10. (H) Effect of expression of Y529F mutant of Ago2 on cellular IL-1β and IL-6 mRNA levels on C6 cells. The qPCR data were normalized against GAPDH mRNA level. (I) Graph representing miR-146a-specific activity upon rapamycin (100 nM) treatment in C6 glioblastoma cells. The fold repression of miR-146a was normalized with the miR-146a expression level. (J) Western blot data showing level of Ago2 phosphorylation and Ago2-mTOR interaction upon rapamycin (100 nM) treatment. (K) qPCR data showing Ago2-associated miR-146a and miR-16 levels upon rapamycin (100 nM) treatment. qPCR data were normalized with the amount of Ago2 pulled down from the immunoprecipitation reaction. For statistical significance, a minimum of three independent experiments were considered in each case unless otherwise mentioned, and error bars represent means ± SEM. p values were calculated by utilizing a Student's t test. \*p < 0.05, \*\*p < 0.01, \*\*\*p < 0.0001.

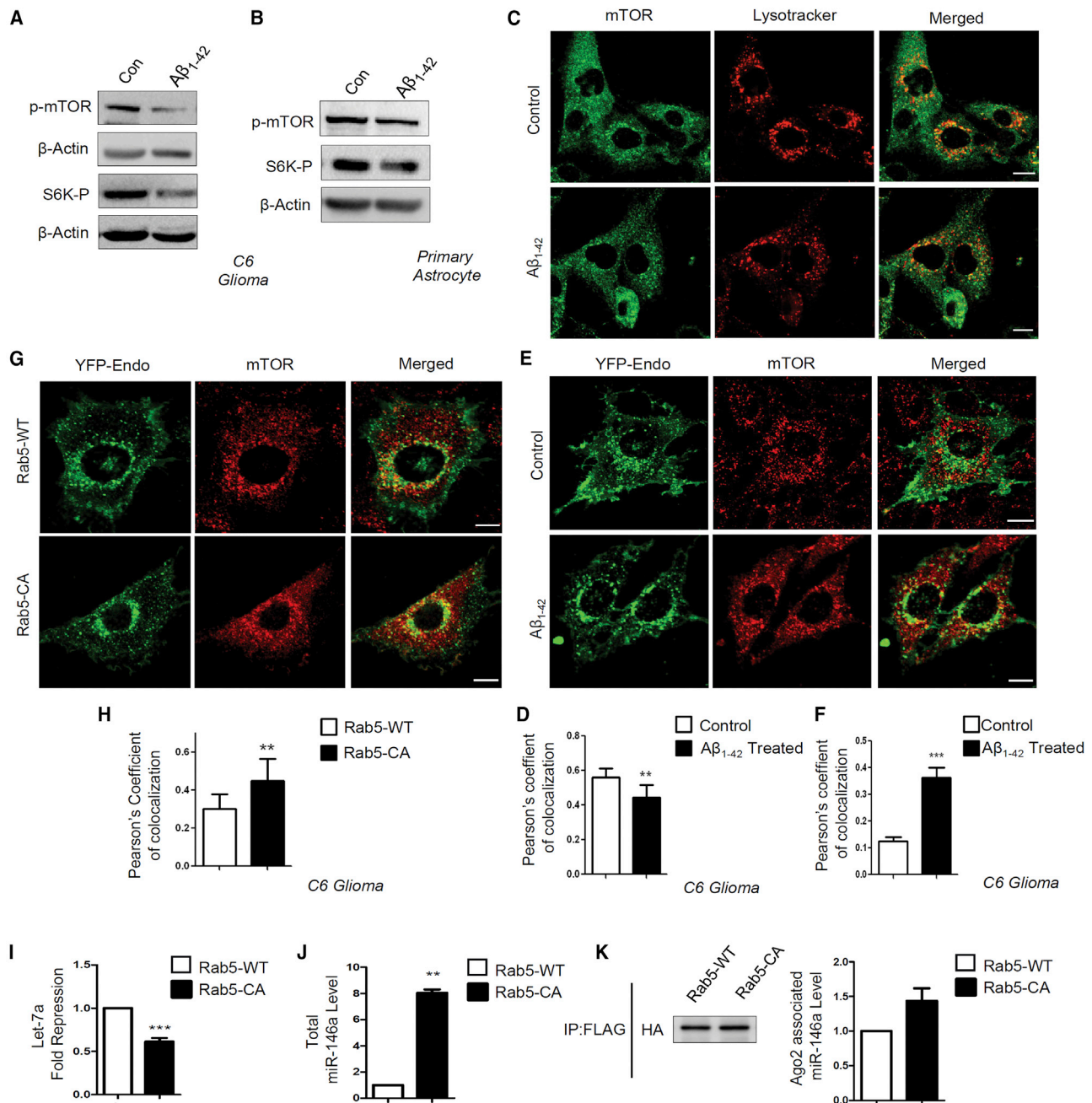


**Figure 4. Sequestration to endosome causes mTORC1 inactivation linked with increased miRNA-Ago2 interaction in glial cells**

(A and B) Lowering of p-mTOR in  $A\beta_{1-42}$  oligomer-treated C6 glioblastoma cells. Western blot data showing the levels of cellular p-mTOR levels along with downstream substrate of mTOR p-S6K levels in C6 glioblastoma cells (A) and in primary astrocytes (B) treated with  $A\beta_{1-42}$ . (C and D) Decreased lysosome targeting of mTOR after  $A\beta_{1-42}$  oligomer treatment. Confocal images depicting localization of mTOR to lysosome in control and treated cells are shown in (C). Endogenous mTOR was visualized indirectly with immunofluorescence (green), and lysosomes are labeled with LysoTracker (red) in C6 glioblastoma cells. A Pearson's coefficient of colocalization was used to measure the amount of mTOR translocating to lysosomes in control and  $A\beta_{1-42}$ -treated C6 glioblastoma cells (D). (E and F) Increased endosome-mTOR localization after  $A\beta_{1-42}$  oligomer treatment. Confocal images show localization of endosomes and mTOR. Endosomes were tagged with YFP-Endo (green), and endogenous mTOR (red) was detected by indirect immunofluorescence. Colocalization between endosomes and mTOR was visualized as yellow (E). A Pearson's coefficient of colocalization of early endosomes and mTOR in  $A\beta_{1-42}$  oligomer-treated C6 glioblastoma cells is shown in (F). (G and H) Effect of Rab5-CA on mTOR localization in C6 glioblastoma cells. Colocalization of mTOR in C6 cells expressing YFP-Endo upon Rab5-CA expression was done. The cells with YFP-Endo (green) and mTOR (red) were visualized in control and Rab5-CA-expressing cells (G). A Pearson's coefficient of colocalization of mTOR and early endosome is shown in (H). (I) Alteration of miRNA activity and levels in mammalian

(legend continued on next page)

constitutively active GTPase-deficient Rab5 mutant, Rab5Q79C (Rab5-CA), that is known to cause mTOR sequestration in early endosomes (Figures 4G and 4H).<sup>46</sup> With overexpression of the Rab5-CA mutant, we observed a decrease in specific activity of let-7a (Figure 4I) and an increase in both cellular and Ago2-associated miR-146a (Figures 4J and 4K). These results connect the mTOR compartmentalization defects in A $\beta$ <sub>1-42</sub>-treated cells to functional inactivation of increased miRNPs observed.

#### mTORC1 activation rescues cytokine repression by targeting the miRNP reactivation pathway

Based on the results described so far, mTOR translocation to lysosome could be important for Ago2 phosphorylation leading to sustained miRNP recycling and activity in astrocytes. To confirm this mode of action of mTOR in glial cells, C6 cells were transfected with plasmids encoding Rheb-Myc before the A $\beta$ <sub>1-42</sub> oligomer treatment. Rheb is a constitutive activator of mTOR that can activate mTOR independently of growth factor or amino acid stimulation.<sup>47,48</sup> Results from Rheb-expressing cells suggest rescue of mTOR localization upon A $\beta$ <sub>1-42</sub> treatment in Rheb-Myc-expressing cells (Figure 5A). We observed about a 1.6-fold reduction in mTOR sequestration in endosomes, suggesting that there was mobilization of mTOR from endosomal compartments (Figures 5A and 5B). To investigate a possible role of mTOR reactivation in miRNA activity, we checked the status of Ago2-positive bodies in A $\beta$ <sub>1-42</sub>-treated cells expressing Rheb-Myc (Figure 5C). Interestingly, in Rheb-expressing cells, we found that fewer Ago2-positive bodies colocalized with processing bodies or PBs compared to that in A $\beta$ <sub>1-42</sub>-treated cells (Figure 5D). These data clearly suggest a role of mTOR signaling in mobilizing the Ago2 from an otherwise inactive compartment into an active compartment where it could repress the target cytokines. Activation of mTOR upon Rheb-Myc expression was confirmed by measuring the levels of phosphorylated mTOR and S6 kinase in untreated and A $\beta$ <sub>1-42</sub>-treated cells before transfection with control or Rheb-Myc expression plasmids (Figure 5E). To get further evidence whether this process restores miRNA activity per se, we checked the different cytokine levels. Quantitative estimation revealed that there has been a 2.7-fold decrease in IL-1 $\beta$  mRNA level and about a 1.5-fold decrease in IL-6 mRNA level compared to the A $\beta$ <sub>1-42</sub>-treated cells upon Rheb-Myc expression (Figure 5F). Again, Rheb-Myc-expressing cells showed a decrease in cellular miR-146a and miR-155 levels compared to the only A $\beta$ <sub>1-42</sub>-treated cells (Figure 5G). Rheb-mediated mTOR reactivation also increases Ago2 phosphorylation in A $\beta$ <sub>1-42</sub>-treated cells, reducing the Ago2-associated miR-146a and miR-155 levels (Figures 5H and 5I). We also observed a similar effect in cellular and Ago2-associated miR-16 and miR-29a levels

when cells were expressing Rheb-Myc (Figures S3A–S3C). Since miR-16 and miR-29a do not directly regulate expression of any proinflammatory cytokines, there is a possibility that the A $\beta$ <sub>1-42</sub>-mediated mTOR inactivation mechanism may affect the function of quite a few miRNAs.

Rheb-Myc expression has also increased the fraction of IL-1 $\beta$  and IL-6 mRNA bound to Ago2 in A $\beta$ <sub>1-42</sub>-treated cells, confirming the availability of active miRNPs for repression of target messages (Figure 5J). miR-146 and miR-155 are the two major miRNAs reported as primary controllers of cytokine expression, and by trying the inactivation of both of these miRNAs with inhibitory antisense oligomers, we can expect to find the reduced response of Rheb-Myc expression in A $\beta$ <sub>1-42</sub>-treated cells. We found a drop in the IL-1 $\beta$  level when A $\beta$ <sub>1-42</sub>-exposed cells expressed Rheb-Myc (Figure 5F). Now, we wanted to check whether Rheb-Myc-mediated rescue in the cytokine mRNA repression depends on the repressive activity of the miRNAs. In the experiment shown in Figure 5K, all of the C6 glioblastoma cells were treated with A $\beta$ <sub>1-42</sub>. Cells expressing control vector, control anti-miR-122, and exposed to 2.5  $\mu$ M A $\beta$ <sub>1-42</sub> were taken as the control set. Cellular cytokine mRNA levels of the control set were taken as 1, and the rest of the experimental samples were plotted against it. Supporting the notion that the response of Rheb-Myc expression on cytokine expression is through reactivation of miR-155 and miR-146 in A $\beta$ <sub>1-42</sub>-exposed cells, we have noted no significant reduction in cytokine production upon Rheb-Myc expression when the same cells were transfected with anti-miR-146 and anti-miR-155 oligomers in combination (Figure 5K). This is expected as, due to the lack of functional miR-146 and miR-155, the cytokines become non-responsive to mTOR activation, and thus mTOR must have an affect primarily through these miRNAs on expression of the cytokines in glial cells. These results suggest that activation of mTOR signaling causes miRNP activity restoration in A $\beta$ <sub>1-42</sub>-treated glial cells.

#### Rescue of cognitive function in A $\beta$ <sub>1-42</sub> oligomer-infused adult rat brain upon Rheb-Myc expression

Inactivation of the mTORC1 pathway has been reported in AD brain.<sup>32,49</sup> In the *in vitro* cell culture, we have documented restoration of mTORC1 activation to rescue cytokine repression by miRNPs. We checked whether overexpression of Rheb-Myc in an A $\beta$ <sub>1-42</sub> oligomer-induced AD model of the disease can result in reduction of proinflammatory cytokine expression to cause improvement in cognitive function of treated animal against the control group of animals. It has been shown before that A $\beta$ <sub>1-42</sub> oligomer infusion in the brain resulted in neuronal death and deposition of A $\beta$  plaque in the vicinity of the infusion site with defective cognitive functions.<sup>39</sup> To check the

---

cells defective for endosome maturation due to expression of the constitutively active form of Rab5 protein. A drop in cellular activity of let-7a miRNA in C6 cells upon expression of constitutively activated Rab5 mutant Rab5-CA is shown. The RL reporter with three let-7a miRNA binding sites was used to score the effect of Rab5-CA expression on miRNA repressive activity. (J and K) Levels of cellular and Ago2-associated miR-146a upon Rab5-CA expression in C6 glioblastoma cells. The cellular miR-146 level was normalized against the U6 snRNA level (J). The amount of Ago2 immunoprecipitated from control and Rab5-CA-expressing cells were used for normalization of the amount of miRNAs associated with Ago2 (K). For statistical significance, a minimum of three independent experiments were considered in each case unless otherwise mentioned, and error bars represent means  $\pm$  SEM. p values were calculated by utilizing a Student's t test. \*p < 0.05, \*\*p < 0.01, \*\*\*p < 0.0001. Scale bar represents 10 $\mu$ m in panels C, G, E.

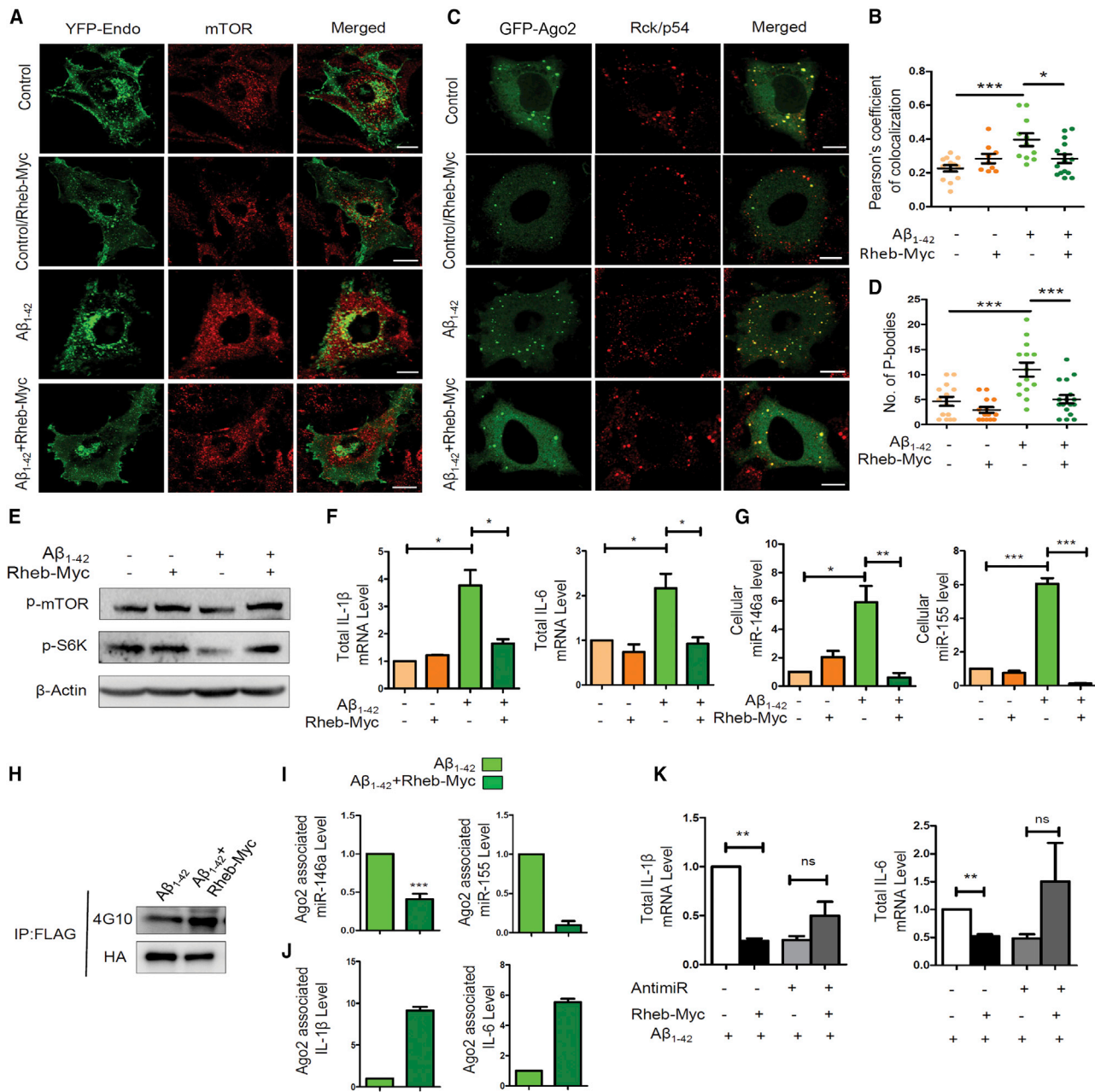


**Figure 5. Reactivation of mTOR by Rheb-Myc mobilizes mTOR from endosomes and reduces cytokine production by targeting the miRNA pathway**

(A and B) Altered mTOR localization upon expression of Rheb-Myc in A $\beta_{1-42}$  oligomer-treated C6 glioblastoma cells. Confocal images showing colocalization of endosomes and mTOR. The C6 glioblastoma cells expressing YFP-Endo and thus having endosomes tagged with YFP-Endo (green). Endogenous mTOR was stained by indirect immunofluorescence (red). Yellow is used to show the extent of colocalization between endosomes and mTOR (A). A plot is shown depicting the amount of colocalization between mTOR and endosomes in control and A $\beta_{1-42}$  oligomer-treated C6 glioblastoma cells transfected rather with control vector or with Rheb-Myc expression plasmid. The amount of colocalization was measured with a Pearson's coefficient of colocalization (B). (C and D) Ago2 localization to PBs gets affected in cells expressing Rheb-Myc. Confocal microscopic images of Ago2 bodies stained with GFP-Ago2 (green) co-stained for endogenous Rck/p54 (red) are shown. Colocalized Ago2 and Rck/p54 bodies were considered as PBs (yellow) (C). Plots depicting number of PBs per cell in C6 glioblastoma cells that were untreated or treated with A $\beta_{1-42}$ . In both conditions, the effect of expression of Rheb-Myc was scored (D). (E) Effect of Rheb-Myc expression on mTOR activation in control and A $\beta_{1-42}$  oligomer-treated C6 glioblastoma cells. Western blot data show the levels of cellular p-mTOR and p-S6K levels in untreated and cells expressing either control or Rheb-Myc expression vectors. (F and G) Expression of Rheb-Myc restores cytokine and miRNA expression to control untreated levels in A $\beta_{1-42}$  oligomers exposed to C6 glioblastoma cells. Quantitative data show the effect of Rheb-Myc expression on cellular IL-1 $\beta$  and IL-6 mRNA levels in both control- and A $\beta_{1-42}$ -treated C6 glioblastoma cells. The cytokine mRNA levels were normalized against the GAPDH

(legend continued on next page)



effect of Rheb-Myc on  $A\beta_{1-42}$ -induced neuroinflammation and cognitive functions, we injected  $A\beta_{1-42}$  oligomers along with the Rheb-Myc expression cassette or control vector bilaterally in the hippocampal area of the brain of adult rats and kept them for 15 days. Following this infusion, several memory function tests were performed to assess cognitive functions in the experimental group of animals (Figure 6A).

We performed the passive avoidance test, which is used to understand learning and memory defects of rodents. This test showed that intra-hippocampal  $A\beta_{1-42}$  infusion significantly reduced wait latency compared to that in the control group of animals. Wait latency represents the time each animal spends in the light chamber before entering into the dark chamber where they experience a shock upon entering (experimental details are described in Materials and methods) during the 300-s period following 5-min habituation (Figure 6B). The probe test was performed 24 h after the training test. Compared to the control group, injection of  $A\beta_{1-42}$  markedly reduced the retention of fear memory, as they showed lower wait latency on the probe test as they moved to a dark chamber within a few seconds. However, rats having Rheb-Myc plasmid infused in the hippocampus along with  $A\beta_{1-42}$  oligomer showed higher wait latency on the probe stage as compared to the animals having only  $A\beta_{1-42}$  infused (Figures 6C and 6D). After behavioral studies, the animals were sacrificed. Brain tissues were fixed, and immunohistochemistry was done to check the expression of both Rheb-Myc and ZsGreen (ZsGreen-encoding plasmid was co-injected with Rheb-Myc encoding plasmid) at the infusion site. We found colocalization between both ZsGreen and Rheb-Myc at the infection site, confirming their expression (Figures S4A and S4B). This result indicates that Rheb-Myc could reverse the declining cognitive function in  $A\beta_{1-42}$ -infused rats.

Next, we performed the novel object recognition test and observed that  $A\beta_{1-42}$ -infused animals had no preference toward the novel object as compared to control group. In contrast, this short-term memory recognition capability in  $A\beta_{1-42}$  co-infused animals was significantly improved upon Rheb-Myc expression. The Rheb-Myc- $A\beta$ -infused animals also showed an increased preferential index and discrimination index as compared to those in the  $A\beta_{1-42}$ -infused group of animals (Figures 6E–6H). Additionally, the elevated plus maze (EPM) analysis showed improvement in cognitive ability in the above-mentioned group of animals. In Figure 6I, latency was the measure of the time taken by the animal to move from the open to the closed arm in the EPM. In the  $A\beta$ -infused group, retention transfer latency (RTL) was higher than initial transfer latency (ITL), which was significantly

reduced in other groups. The difference between ITL and RTL (ITL – RTL) was used to assess memory and learning in the EPM test. Notably, a negative difference was obtained in the  $A\beta_{1-42}$ -infused animals (Figure 6I). However,  $A\beta_{1-42}$ -infused rats injected with Rheb-Myc plasmid showed a positive difference between ITL and RTL compared to the  $A\beta$ -infused group (Figures 6I and 6J).

The immunohistochemistry of  $A\beta_{1-42}$ -infused adult rat brains showed astrogliosis, depicting an increase in GFAP in astrocytes, but in Rheb-Myc plasmid and  $A\beta$  co-infused rat brain, enhanced GFAP was found to decrease as compared to the  $A\beta_{1-42}$  oligomer-infused rat brain. However, no decrease in  $A\beta$  accumulation was found in Rheb-expressed,  $A\beta_{1-42}$ -infused brains, suggesting that the effect of Rheb-Myc was on glial cell response and cytokine production rather than an effect on  $A\beta$  deposition (Figures 7A and 7B). These results indicate that ectopic expression of Rheb protein in  $A\beta_{1-42}$ -infused rat brain causes improvement in cognitive behavior and spatial memory. While checking the differential expression status of cytokine mRNA levels in the infused rat brains, an almost 2-fold decrease in proinflammatory IL-6 and IL-1 $\beta$  was observed in the Rheb-Myc- $A\beta_{1-42}$  co-infused rats as compared to the  $A\beta_{1-42}$ -only infused rats (Figures 7C and 7D). Rheb-Myc-expressed animals showed a decrease in both the cellular and Ago2-associated miR-146a levels compared to the only  $A\beta_{1-42}$ -injected animal tissue (Figures 7E and 7F). Therefore, by activating mTOR and miRNP, recycling the cytokine expression could be controlled to rescue the memory loss and the related phenotype in the AD model by expressing Rheb (Figure 7G).

## DISCUSSION

Several miRNAs are expressed in brain and thought to regulate thousands of transcripts within the brain.<sup>3</sup> In the present analysis, we could identify deregulated miRNA and mRNA within the cortical regions of AD patients, which may be associated with AD development or progression. Interestingly, in our analysis, a substantial percentage of upregulated miRNAs had a higher fraction of their corresponding target mRNAs as upregulated. This trend was consistently observed in late-stage AD cases considered from multiple studies. These observations suggest that contrary to the general regulatory relationship between miRNAs and their target mRNAs wherein miRNAs mainly downregulate mRNAs, other regulator-to-target relationships might also exist in tissues under disease conditions. In particular, miR-146a-5p is one such miRNA that exhibited this phenomenon wherein increased production of miR-146a-5p resulted in the upregulation of multiple target mRNAs.

---

mRNA level (F). The effect of Rheb-Myc expression on cellular miR-146a and miR-155 levels in both control- and  $A\beta_{1-42}$ -treated C6 glioblastoma cells is shown (G). The data were normalized against U6 snRNA level. (H–J) Reversal of Ago2-miRNA and Ago2-cytokine mRNA interaction upon Rheb-Myc expression. Ago2-associated miR-146a and miR-155 levels and IL-1 $\beta$  and IL-6 mRNA levels were measured in C6 glioblastoma cells pre-treated with  $A\beta_{1-42}$  oligomers (I and J). The RNA level was normalized by the amount of Ago2 pulled down in the immunoprecipitation reaction (H). (K) Effect of Rheb-Myc expression on IL-1 $\beta$  and IL-6 mRNA levels when the cells were pre-treated either with control or by miR-146a- and miR-155-specific antagomiRs. In all of the sets, C6 glioblastoma cells were activated with 2.5  $\mu$ M  $A\beta_{1-42}$  after 48 h of Rheb-Myc and anti-miR transfection. The data were normalized against GAPDH mRNA level. For statistical significance, a minimum of three independent experiments were considered in each case unless otherwise mentioned, and error bars represent means  $\pm$  SEM. p values were calculated with a Student's t test. \*p < 0.05, \*\*p < 0.01, \*\*\*p < 0.0001. Scale bar represents 10 $\mu$ m in panel A and C.

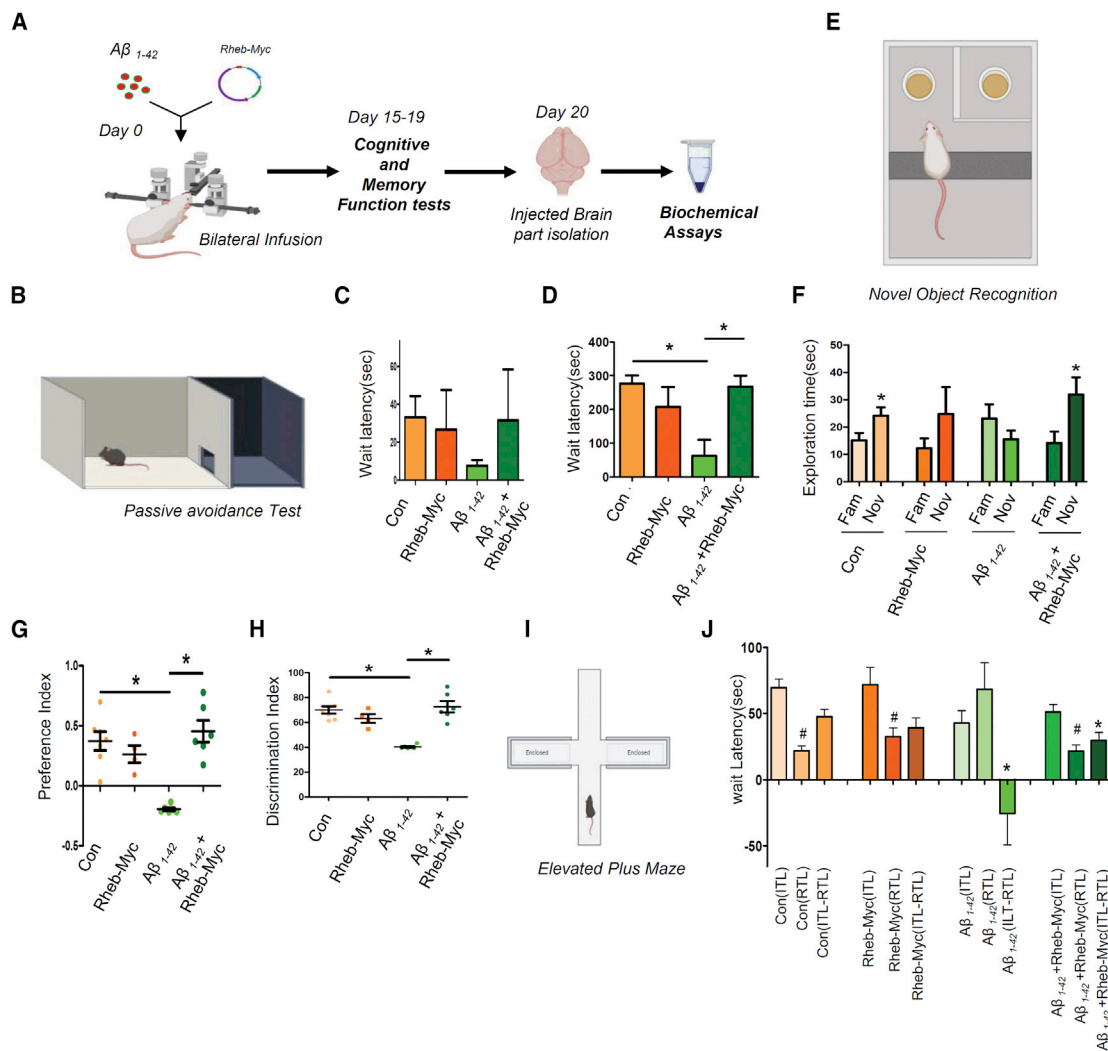
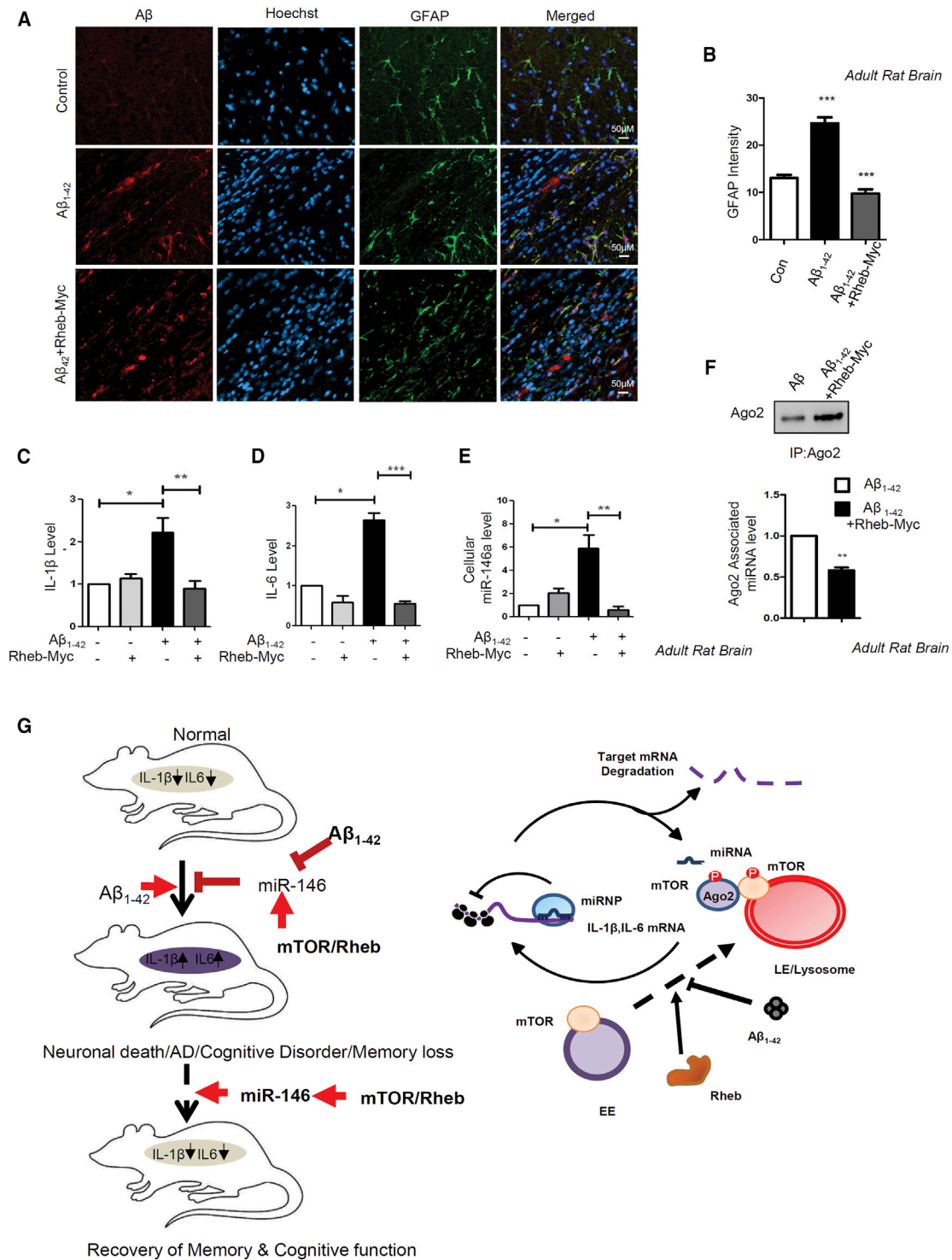


**Figure 6. Rescue of cognitive function in Aβ<sub>1-42</sub>-infused adult rat brain upon Rheb-Myc expression**

(A) Experimental flowchart shows a bilateral infusion of Aβ<sub>1-42</sub> oligomers and Rheb-Myc plasmid that was done in adult rat hippocampus. After 15 days of incubation, different behavioral assays were carried out followed by sacrificing the animals. (B–D) Rescue of wait latency in Aβ<sub>1-42</sub>-infused adult rat brain upon Rheb-Myc expression. Passive avoidance assessment of memory performance was done, and the graph shows the acquisition process of experimental subjects. The rats that were able to enter the dark chamber within 300 s were selected as eligible for testing. The bar diagram reveals the wait latency in different experimental sets of rats. Rats having Rheb-Myc plasmid infused along with Aβ<sub>1-42</sub> showed higher wait latency on the probing day, as compared to the animals having only Aβ<sub>1-42</sub> infusion (D) (n = 7). (E–H) Novel object recognition test to show that the short-term memory recognition capability has been restored by Rheb-Myc expression in Aβ<sub>1-42</sub>-injected animals. Aβ<sub>1-42</sub> and Rheb-Myc expression plasmid co-infused animals showed improvement in novel object identification capacity as compared to the Aβ<sub>1-42</sub>-infused rodents (F). The Rheb-Myc-Aβ<sub>1-42</sub> co-infused animals also showed an increased preferential index and discrimination index as compared to the Aβ<sub>1-42</sub>-infused group of animals, indicating improvement in learning and memory function (G and H) (n = 7). (I and J) The elevated plus maze analysis showed improvement in cognitive ability in Rheb-Myc-expressing animals. The retention transfer latency (RTL) was measured in all control and Aβ<sub>1-42</sub>-infused groups, and the difference of initial transfer latency (ITL) and RTL was plotted along with the ITL and RTL separately (n = 7). For statistical significance, a minimum of three independent experiments were considered in each case unless otherwise mentioned. Animal data are represented as means ± SEM and analyzed by one-way ANOVA followed by Bonferroni’s test. p value <0.05 corresponds to \*. In EPM data in panel J, # stands for significance between all the RTL data between all the animal groups, \* denotes significance between (ITL-RTL) data between all the animal groups.

Therefore, any change in the activity of the miRNA pathway could play a significant role during development or during any pathological condition. Also, the molecular mechanism behind Aβ-mediated neuronal death is still elusive, and an interplay between cellular structure, molecular biological processes, and the resulting immune

response of the disease could contribute to the reason why AD is so difficult to treat. Another important aspect was to look at the involvement of glial cells in the buildup and disease progression, as glial cells easily outnumber neurons in the brain.<sup>50</sup> Thus, in the early stage of the disease, glial cells might be involved in rectifying the problems



of the neurons due to  $A\beta_{1-42}$  oligomer deposition, but they eventually contribute to the prognosis of the disease.

We found that mTOR sequesters into early endosome with exposure to  $A\beta_{1-42}$  in glial cells. mTORC1 is a very important protein complex that can regulate neuronal differentiation and brain activity. Depletion of an essential mTORC1 component, Raptor, is known to reduce the brain size considerably.<sup>51</sup> mTORC1 signaling can also play a role in phosphorylation of Ago2 protein, which eventually can affect the miRNP function. Rheb, which is a GTPase and an activator of mTORC1, can reverse this process and results in a decrease in Ago2 miRNP content. mTORC1 activity-driven pathways may regulate the miRNA maturation process as well. The tuberous sclerosis complex (TSC) is an autosomal-dominant disorder and is caused by mutations in TSC1 or TSC2 that are connected with mTOR hyperactivity. TSC knockout cells, which have increased mTORC1 activity, have a reduced mature miRNA level.<sup>52</sup> Accordingly, mTOR activation by Rheb can bring down the maturation process and also recycle existing miRNPs, and both of these pathways may contribute to the miRNA activity rescue process. Rheb knockout animals are embryonic lethal.<sup>53,54</sup> Also, conditional Rheb knockout adult mice have a limited lifespan, indicating that Rheb is an essential protein factor that could play a major role in brain development and function. In the present study, by injecting Rheb-expressing plasmid into animal brain, we could improve motor function as well as memory of the AD animals. Similarly, researchers have shown that Rheb expression in brain of HD mouse model resulted in improved motor function.<sup>55</sup> Also in PD, Rheb expression in dopaminergic neurons promoted axonal regrowth.<sup>56</sup> Therefore, Rheb can affect brain function at multiple points. For example, mTOR-mediated translation, a Rheb-dependent process, is important at synapse for maintaining synaptic plasticity and at the cell body for maintaining memory.<sup>57,58</sup> Also, Rheb expression can increase the acetyl choline level in the brain that can improve brain cognitive functions.<sup>59</sup> Although all of these factors may play a role, our data suggest that miRNA activity regained by Rheb expression may be the most important factor in the recovery of behavioral, cognitive, and memory function in AD.

We have stereotactically injected  $A\beta_{1-42}$  oligomers in adult rat brain to produce amyloid plaques in the brain. This model has several advantages, as we can monitor the early cellular events during plaque formation and the effects it has on the miRNA machinery during the early phase of the disease. Also, oligomers can be taken up by glial cells in both the *in vivo* and *in vitro* cell culture system, which can have additional physiological effects on the cellular structure and ma-

chinery. This allows the limited and spatiotemporal-specific exposure of brain cells to  $A\beta_{1-42}$  and thus is advantageous over the transgenic mouse models that have a mutated  $A\beta$  gene (APP) or related protease gene, which may have some compensatory effect on both structure and physiology in the adult brain. Additionally, the transgene is expressed at a very early stage and in all of the cells of the brain. Importantly, the number of AD cases reported with genetic mutations in APP gene is very limited compared to the higher number of cases noted with sporadic  $A\beta$  expression.<sup>60</sup> We have also injected Rheb expression vector with  $A\beta_{1-42}$  oligomer in brain hippocampus. This is to ensure only that a portion of the brain that is exposed to  $A\beta_{1-42}$  oligomer only takes up the Rheb-expressing plasmid and not the entire brain, which could complicate the analysis. This method can be useful in introducing specific miRNA or antisense RNA in a specific part of the brain with the help of co-injected  $A\beta_{1-42}$  oligomer.

Although we have only observed the effect that  $A\beta_{1-42}$  oligomer has on miRNA machinery on astroglial cells, it would be interesting to see what effect it may have on the miRNAs in other glial cells. Glial cells outnumber neurons at a 10:1 ratio, and among them almost 40% of cells are astrocytes, making them one of the most abundant cells of the brain. Also,  $A\beta_{1-42}$  oligomer-injected brain tissues showed considerable astrocyte activation along  $A\beta$  deposition. Primary astrocytes show elevated cytokine mRNA levels when exposed to  $A\beta_{1-42}$  oligomer. We did find some changes in the neuronal miRNA expression level, but a drop in miRNA activity resulting in cytokine overproduction was found to be specific for astroglial cells and not for neurons. In LPS-activated macrophages, miRNAs play a significant role in reducing pro-inflammatory cytokines such as tumor necrosis factor (TNF)- $\alpha$ , IL-1 $\beta$ , or IL-6 so that anti-inflammatory IL-10 production can be initiated.<sup>19</sup> This is a very important step in the inflammation process where miRNA fine-tunes the balance between pro-inflammatory and anti-inflammatory cytokine levels to maintain homeostasis of the process. The astrocytes exposed to  $A\beta_{1-42}$  oligomer show a loss in miRNA activity whereas loss of Ago2 phosphorylation leads to building up inactive miRNPs in astrocytes that restrict their encounter with the target mRNA. This leads to uncontrolled production of pro-inflammatory cytokines that eventually create neuroinflammation, leading to the loss of neurons.

If the mechanism is happening through Ago2 phosphorylation, then this mechanism should affect other miRNAs as well. We found that the patterns of data of miR-16 and miR-29a are very similar to what we also got for miR-146a and miR-155. Since miR-16 and miR-29a do not directly regulate expression of pro-inflammatory cytokines, we think that there is a possibility that this mechanism affects

---

levels in the infused rat brains. The values were obtained by qRT-PCR and normalized against the U6 snRNA level. (F) Levels of Ago2-associated miR-146a are restored by Rheb-Myc in  $A\beta_{1-42}$ -infused rat hippocampus tissue. Immunoprecipitation was done for endogenous Ago2, and associated miRNA was measured with qRT-PCR. The value was normalized against Ago2 band intensity as measured from the western blot. (G) The model depicts how  $A\beta$  exposure causes mTOR entrapment with endosomes restricting miRNP target RNA interaction. This causes inactivation of miRNPs to elevate proinflammatory cytokine production in glial cells. Interestingly, ectopic activation of mTOR by Rheb restores miRNP function in diseased brain, rescuing the cognitive function in adult rat brain. The mechanism of action of  $A\beta_{1-42}$  on miRNA via mTOR is shown in the right panel. For statistical significance, a minimum of three independent experiments were considered in each case unless otherwise mentioned, and error bars represent means  $\pm$  SEM. p values were calculated with a Student's t test. \*p < 0.05, \*\*p < 0.01, \*\*\*p < 0.0001.

the functions of other miRNAs as well. In this context, we note that in primary astrocytes and rat brain (also in AD patient brain data) we have documented increased expression of many miRNAs that are not even astrocyte specific or not a known regulator of cytokines. This also signifies that the common pathway of miRNA activity modulation by mTORC1 has been targeted by  $A\beta_{1-42}$  oligomers. However, there are miRNAs that may be regulated at the transcriptional level in a significant way, while there could be a subset of miRNAs that also have regulated export and turnover in  $A\beta_{1-42}$ -treated cells, and thus these factors may contribute significantly to the overall cellular levels of those miRNAs to show a reduction in the overall expression level.

The identification of important miRNAs in the gene regulation process in AD brain was initially a challenge, and thus we studied tissue-specific miRNA expression patterns in different parts of the brain tissue, with the help of TissueAtlas.<sup>61</sup> Interestingly, in comparison to basal levels, miR-146a expression in the cortical part is preferentially enriched in AD brain. Subsequently, we wanted to focus on miRNAs specifically associated with the effect of  $A\beta$  oligomers in neural cell subsets. Correspondingly, with the help of a previous study, we determined that miRNA expression patterns can vary substantially across cell types, such as neurons and astrocytes. In particular, miR-146a and miR-21 are highly enriched in astrocytes in comparison to neurons in primary cultures from the rat cortex.<sup>62</sup> Furthermore, based on our previous computational analysis and the miRNA distribution patterns in different human brain regions we selected miRNAs for our further analyses.

How does astrocyte activation affect neuronal health? We observed that rat primary astrocytes cultured in the *in vitro* condition secrete extra-cellular vesicles 70–100 nm in size known as the exosomes. These exosomes carry miRNAs and different RNA-binding proteins from astrocytes to recipient neuronal cells (D.D, unpublished data). Functional assays carried out in recipient cells showed that these exported miRNAs are stable and functional in neuronal cells, where they can regulate the gene expression of recipient cells. Exposure to  $A\beta_{1-42}$  increases miR-146a secretion through exosomes along with other RNA-binding proteins such as Ago2 and GW182 (D.D, unpublished data). We think that these exosomes could play an important role in both normal physiology and in pathological conditions such as AD, where astrocytes can regulate gene expression of neighboring neuronal cells and through these also fine-tune complex physiological processes such as learning and memory formation.

Several reports suggest the role of astroglia in improving cognition and memory by demonstrating that the reduction in their activity leads to memory impairment.<sup>63</sup> Interestingly, human astrocyte grafting in immunodeficient mice improved memory in these cognition-deficient animals.<sup>64</sup> Studies have also featured the necessity of astrocyte activation in maintaining synaptic plasticity and causing *N*-methyl-D-aspartate (NMDA)-mediated long-term potentiation and memory development in the hippocampus.<sup>65</sup>

Is astroglia the primary contributor in the high cytokine profile observed in AD? In the AD condition,  $A\beta$  is known to cause disrup-

tion in gliotransmission by elevating the calcium signaling levels in astrocytes.<sup>66</sup> Besides during AD, interrupted glutamate uptake capacity and astrocytic calcium signaling can be disrupted by  $A\beta$  as well.<sup>67,68</sup> Also, hippocampal astrocytes exposed to  $A\beta$  helped in improving the frequency of NMDA receptor-mediated slow inward currents, along with calcium elevations.<sup>69</sup> Precisely, due to this wide array of functional properties, we thought of astrocytes as an interesting target for studying brain pathologies such as AD, where miRNA dysregulation in astrocytes may play a significant role in both neuroinflammation and cognition of the animal.

Postmortem neuropathological studies have shown that the number of reactive astrocytes in the vicinity of amyloid plaques increases as the disease advances.<sup>70</sup> We also found astrogliosis at the amyloid deposition site in adult rat brain hippocampus (Figure 2B). Interestingly, microglial cells are also found in amyloid deposition sites along with astrocytes, and in APP/PS1: GFAP/vimentin double knockout mice where astrocyte activation is attenuated had increased numbers of microglial cells found around plaques.<sup>70</sup> Also, microglia secrete inflammatory cytokines, which can convert the neuroprotective resting astrocytes into neurotoxic cells. Conversely, astrocytes secrete C3 complement fraction via NF- $\kappa$ B in oligomeric  $A\beta$  treatment, and C3 can in turn activate microglia through its C3R receptor.<sup>71</sup> Studies also reported that astrocytes appear to influence the degree of microglial reactivity in mouse models of brain  $\beta$ -amyloidosis.<sup>72</sup>

Our findings suggest that restoring mTOR activity in the glial cells can rescue the disease phenotype and also cognition and memory in adult animals. Previous studies in the field of neurodegenerative diseases suggest maintenance of homeostasis of mTOR activity could be beneficial for disease management. For example, in the case of autism, inactivation of mTOR is found to be beneficial, as in autism patient hyperactivation of mTOR is common. Again, in ALS, where mTOR activity is reduced, restoring the activity is found to be advantageous in disease prognosis.<sup>73,74</sup> In a nutshell, our study emphasizes the complex circuit between metabolic pathways, with gene expression regulation having an effect on disease pathology. An intervention with gene therapy or with small molecules to sustain normal miRNA metabolic pathways in brain will have a therapeutic value in a complex disease such as AD.

## MATERIALS AND METHODS

### Expression profile analysis of miRNAs and their corresponding target mRNAs in AD and cancer

Expression profiles of miRNAs and mRNAs were utilized to study the possible regulatory relationships between miRNAs and their corresponding target mRNAs in multiple cortical regions of AD patients as opposed to normal deceased individuals. With the help of R packages (R Core Team, 2017),<sup>75</sup> differentially expressed (fold change of  $\pm 1.25$  and *p* value of  $\leq 0.05$ ) miRNAs within the pre-frontal cortex and mRNA within different regions of the frontal cortex were determined in the brains of AD patients. The differentially expressed miRNAs and mRNAs identified in this manner considering patient samples are likely to be associated with the development or progression

of AD (GEO: GSE48552, GSE5281, GSE53697, and GSE15222).<sup>35,76–80</sup> Utilizing miRNA-target regulatory information from TarBase and miRTarBase databases, regulator(s)-to-target(s) (miRNA/mRNA) maps for the differentially expressed miRNAs and mRNAs were determined.<sup>81,82</sup> Subsequently, we have compared the fractions of target mRNAs of each differentially expressed miRNA that are significantly upregulated or downregulated. Additionally, to ascertain whether such regulator(s)-to-target(s) patterns could be occurring in other disease conditions, we performed a disease enrichment analysis considering only the genes that were commonly upregulated among the AD datasets considered.<sup>83</sup>

In order to study regulator(s)-to-target(s) patterns in cancer, we have analyzed miRNA and mRNA expression profiling data from different cancer tissue samples. With the help of R packages, differentially expressed (fold change of  $\pm 1.25$  and  $p$  value of  $\leq 0.05$ ) miRNAs and mRNAs were determined in breast cancer, colorectal cancer, and oral squamous cell carcinoma by considering relevant GEO datasets (GEO: GSE40056/GSE40057, GSE35982, and GSE70664/GSE70665).<sup>75,84–86</sup> Subsequently, the fractions of significantly upregulated or downregulated target mRNAs of each of the differentially expressed miRNAs under each condition were compared.

#### siRNA and plasmid constructs

Plasmid information about pRL-con, pRL-3XBulge-let7a, pRL-3XBulge-miR-122, and firefly (FF) plasmids were previously explained in Pillai et al. and were a kind gift from Witold Filipowicz. miR-122 was expressed from pmiR-122 plasmid, which was previously described.<sup>87</sup> FLAG-hemagglutinin (HA)-Ago2 and FLAG-HA-Ago2-Y529F were obtained as a kind gift from Gunter Meister. The plasmids Rab5-CA and Rheb-Myc were previously used and were a kind gift from J.M. Backer.<sup>88</sup> All small interfering RNAs (siRNAs) were purchased from Dharmacon (ON-TARGETplus siRNA).

#### Cell culture and reagents

HEK293 and C6 glioblastoma cells were grown in Dulbecco's modified Eagle's medium (DMEM, Gibco) supplemented with 2 mM L-glutamine and 10% heat-inactivated fetal bovine serum (FBS).

Primary astrocytes were cultured from 0-1 day-old Sprague-Dawley rat pups. The whole brain was dissected out and meninges were removed carefully. The neocortex parts were isolated and cut into pieces. The small cortical tissue pieces were minced and subjected to trypsinization for 30 min. Trypsinized brain tissue was triturated in DMEM (Gibco) medium supplemented with 10% FBS (Gibco) and passed through nylon mesh to avoid clumps. This single-cell suspension was then added onto a poly-D-lysine (PDL)-coated plate (Sigma-Aldrich, St. Louis, MO, USA) and incubated for 2–3 min for preferential sticking of neurons. Next, the unattached cells were collected and harvested by centrifugation. Cells were resuspended in a fresh medium and seeded at a density of 1.2 million/35-mm plate or 0.4 million/well of a 24-well plate. Cells were maintained for 13 days *in vitro* (DIV) with a medium change given every alternate day.

Plasmid and siRNAs were transfected with Lipofectamine 2000 (Invitrogen) and RNAiMAX (Invitrogen), respectively, following the manufacturer's protocol. All of the siRNA and plasmid co-transfection was done using Lipofectamine 2000. For activation of primary rat astrocytes or neurons 1.5  $\mu\text{M}$   $\text{A}\beta_{1-42}$  was used, whereas 2.5  $\mu\text{M}$   $\text{A}\beta_{1-42}$  was used for activating C6 glioblastoma cells. 100 nM rapamycin (Sigma) was used for blocking mTORC1.

#### Preparation of $\text{A}\beta$

High-pressure liquid chromatography (HPLC)-purified  $\text{A}\beta_{1-42}$  was purchased from American Peptide (Sunnyvale, CA, USA), and oligomeric  $\text{A}\beta_{1-42}$  was prepared as described previously.<sup>39</sup> Briefly, lyophilized  $\text{A}\beta_{1-42}$  was reconstituted in 100% 1,1,1,3,3,3 hexafluoro-2-propanol (HFIP) to 1 mM. HFIP was removed by evaporation in a SpeedVac (Eppendorf, Hamburg, Germany), then resuspended in 5 mM anhydrous DMSO. This stock was then stored at 80°C. The stock was diluted with PBS to a final concentration of 400 mM, and SDS was added to a final concentration of 0.2%. The resulting solution was incubated at 37°C for 18–24 h. The preparation was diluted again with PBS to a final concentration of 100 mM and incubated at 37°C for 18–24 h before use.

#### Brain stereotaxic surgery

Adult male Sprague Dawley rats weighing 270g–330g were kept in a room controlled around 25°C and humidity 65%, providing food and water to ad-libitum. A 12h light-dark cycle was provided in the animal house of CSIR-Indian Institute of Chemical Biology, Kolkata. All the studies were performed with guidelines provided by the Committee for the Purpose of Control and Supervision of Experiments on Animals (Animal Welfare Divisions, Ministry of Environments and Forests, Govt. of India) along with the approval from the Institutional Animal Ethics Committee (IAEC). Male Sprague-Dawley rats (280–320 g) were anesthetized by injecting 50 mg/kg thiopentone (thiosol sodium, Neon Laboratories, Mumbai, India) and placing them on a stereotaxic frame (Stoelting, USA). Injection was done by using a 27G Hamilton syringe. A volume of 5  $\mu\text{L}$  of 100  $\mu\text{M}$   $\text{A}\beta$  in PBS and 3  $\mu\text{g}$  (4  $\mu\text{L}$ ) of plasmid was infused at a flow rate of 0.5  $\mu\text{L}/\text{min}$  in the hippocampus at stereotaxic coordinates from bregma (AP, 3.6 mm; L, 2.1 mm; DV, 2.8 mm) according to the rat brain atlas. An equal volume of PBS was injected in control animals. Proper post-operative care was taken to maintain proper health conditions of the animal. Behavioral tests were performed 14 days after stereotaxic surgery of the animal. Animals were sacrificed on 20th days after behavioral analysis. The brains were dissected out, following cardiac perfusion, and fixed in 4% paraformaldehyde (PFA) for 24 h. They were then incubated in a 30% sucrose solution for another 24 h before proceeding for cryosectioning. Cryosections of the brain were done in a cryotome (Thermo Shandon, Pittsburgh, PA, USA).

#### Immunohistochemistry of brain slices

20- $\mu\text{m}$  coronal cryosections of the brain from  $\text{A}\beta$ -infused or PBS-infused rats were blocked with 4% BSA in PBS containing 0.43% Triton X-100 for 1 h 20 min at room temperature. Brain slices were incubated in primary antibody in a blocking solution overnight at

4°C. Sections were washed three times with PBST and incubated with a fluorescence-tagged secondary antibody for 2 h at room temperature. Following three washes with PBS and Hoechst staining for the nucleus, the sections were mounted with Dibutylphthalate Polyesterene Xylene (DPX) and observed in a confocal microscope.

### RNA isolation and qPCR

Total RNA was isolated by using TRIzol or TRIzol LS reagent (Invitrogen) according to the manufacturer's protocol. miRNA assays by real-time PCR were performed using specific TaqMan primers (Invitrogen). U6 small nuclear RNA (snRNA) was used as an endogenous control. Real-time analyses by two-step RT-PCR were performed for quantification of miRNA levels on a Bio-Rad CFX96 real-time system using an Applied Biosystems TaqMan chemistry-based miRNA assay system. One third of the reverse transcription mix was subjected to PCR amplification with TaqMan universal PCR master mix, no AmpErase (Applied Biosystems) and the respective TaqMan reagents for target miRNAs. Samples were analyzed in triplicates. The comparative Ct method, which included normalization by the U6 snRNA, was used for relative quantification. For quantification of mRNA levels, 200 ng of total cellular RNA was subjected to cDNA preparation followed by qPCR by the SYBR Green method. Each sample was analyzed in triplicates using the comparative Ct method. mRNA levels were normalized with GAPDH as the loading control.

### IP assay

For IP of Ago2, cells were either transfected with FLAG-HA-tagged Ago2 or endogenous Ago2 and were pulled down from primary cells and tissue samples. For IP reactions, cells were lysed in lysis buffer (20 mM Tris-HCl [pH 7.5], 150 mM KCl, 5 mM MgCl<sub>2</sub>, 1 mM DTT, 10 mM sodium orthovanadate, 15 mM NaF), 0.5% Triton X-100, 0.5% sodium deoxycholate, and 1× EDTA-free protease inhibitor cocktail (Roche) for 30 min at 4°C, followed by three sonication pulses of 10 s each. The lysates, clarified by centrifugation, were incubated with HA antibody (at a concentration of 1:100) pre-bound protein G agarose beads (Invitrogen) or with pre-blocked anti-FLAG M2 beads and rotated overnight at 4°C. Subsequently, the beads were washed three times with IP buffer (20 mM Tris-HCl [pH 7.5], 150 mM KCl, 5 mM MgCl<sub>2</sub>, 1 mM DTT, 10 mM sodium orthovanadate, 15 mM NaF). Washed beads were divided into two equal parts, and each part was analyzed for bound proteins and RNAs by western blot and qPCR, respectively.

### Luciferase assay

miRNA repression was observed by performing a dual-luciferase assay. 10 ng of RL-con and RL-3xB-let-7a, RL-3xB-122, or RL-IRAK1 encoding plasmids was co-transfected with 100 ng of firefly encoding plasmid per well of a 24-well plate to study endogenous let-7a or exogenous miR-122 repression. Cells were lysed with 1× passive lysis buffer (PLB, Promega) before being subjected to a dual-luciferase assay (Promega, Madison, WI, USA) following the supplier's protocol on a VICTOR X3 plate reader with injector (PerkinElmer, Waltham, MA, USA). RL expression levels for control and

reporter were normalized with the firefly expression level for each reaction. All samples were done in triplicates.

### Immunoblotting

SDS-polyacrylamide gel electrophoresis was performed with the samples, which included cell lysates, membrane fractions, and IP proteins, followed by transfer of the same to polyvinylidene fluoride (PVDF) nylon membranes. Specific required antibodies were used to probe the blot for at least 16 h at 4°C. This antibody-associated overnight incubation was followed by three washes with TBST (Tris buffered saline with Tween 20), after which at room temperature the membranes were incubated for 1 h with horseradish peroxidase-conjugated secondary antibodies (1:8,000 dilutions). Images of developed western blots were taken using an UVP BioImager 600 system equipped with VisionWorks Life Science software (UVP) v6.80.

### Immunofluorescence and confocal imaging

For immunofluorescence studies, primary and C6 glioblastoma cells were grown on 18-mm coverslips coated with PDL and gelatin, respectively. Cells were transfected on the coverslips as discussed previously and fixed for 30 min in the dark with 4% PFA solution after 48 h of transfection. Cells were blocked and permeabilized with 3% BSA containing 0.1% Triton X-100 for 30 min, followed by overnight incubation with specific primary antibodies at 4°C. After the incubation, cells were washed three times with PBS and probed with respective secondary antibodies (Life Technologies) attached with specific fluorophores for 1 h at room temperature. For detection of lysosomes, 100 nM of LysoTracker Red DND-99 was added in the growing cells for 1 h before fixation. Images were captured using a Zeiss LSM800 confocal microscope and analyzed with Imaris7 software. All of the interactions between organelles were measured by calculating Pearson's and Mander's coefficient of colocalization using the colocalization plug-in of Imaris7 software.

### Passive avoidance test

First, the rats were subjected to passive avoidance (shuttle box) training. Rodents have a natural tendency to move toward dark. The passive avoidance device had two identical compartments comprising 25 × 25 × 20 cm, which were divided by a guillotine door. One of the chambers was lighted and the other was dark. Electric shocks were conveyed to the grid floor by an isolated stimulator. At the beginning of the experiment rats were habituated in the device for 5 min in the lighted chamber facing away from the entrance to the dark side. On acquisition day the guillotine door was raised, and the latency to enter the dark chamber was recorded. When the animals did not enter the dark compartment within 5 min, they were eliminated from the experiment. Once they entered the dark chamber, they received a foot shock of 0.8 mA, which forced them to return to the light chamber. On the next day, defined as the probe day, the same rats were kept in the light chamber and time taken by them to enter the dark chamber was noted as the latency time. When the rats did not enter the dark chamber by 300 s, the successful acquisition of passive avoidance response was said to occur. The

experimental work and data recording was performed by SHUTA-VOID software by Panlab.

### Novel object recognition (NOR)

The NOR task evaluates the rodents' ability to recognize a novel object in the environment. The task procedure consists of three phases: habituation, familiarization, and test phase. In the habituation phase, each animal is allowed to freely explore the open-field arena in the absence of any objects. After the familiarization phase, a single animal is placed in the open-field arena containing two identical sample objects (A & A), for 5 min. After 24 h, the animal was returned to the open-field arena with two objects, one of which was identical to the sample and the other one was novel (A & B). The test was performed for 5 min. During both the familiarization and the test phase, objects were located in the opposite and symmetrical corners of the arena, and location of the novel versus familiar object was counterbalanced. The wait latency of the animals observed in each of the objects on probe day was calculated and designated as TN and TF for the novel and familiar objects, respectively. The discrimination index (DI) and preference index (PI) were derived according to the following formulae:  $DI = (TN - TF) / (TN + TF)$  and  $PI = [TN / (TN + TF)] \times 100$ .

### Elevated Plus Maze (EPM) test

The EPM was used for the assessment of memory processes in the animals on the 15th day following the method of that used in rats.<sup>89</sup> The apparatus was made of a wooden plus-shaped maze elevated 60 cm from the floor having two open arms measuring 50 × 10 cm, crossed at right angles by two arms of the same dimensions enclosed by 50-cm-high walls. A 1-cm-high plywood edge surrounding the open arms was added to prevent the animals from falling off the maze. A rat was placed on the open arm facing away from the center and the transfer latency (TL; time in which the rat moves from the open arm to closed arms) was recorded on the day 1 and again on the following day. The time taken by the animal on day 1 to move from open arm to the closed arm was recorded as ITL, and that on day 2 was recorded as RTL. A duration of 5 min was used for each subject to record the data.

### Statistical analysis

GraphPad Prism 5.00 (GraphPad, San Diego, CA, USA) was used to analyze the experiments performed in triplicate unless mentioned otherwise. The p values were obtained with the help of a non-parametric Student's t test. Animal data are represented as means ± SEM and analyzed by one-way ANOVA followed by a Bonferroni's test.

### Data availability

Information related to antibodies, primers, and miRNA assays are available as Tables S3–S5.

### SUPPLEMENTAL INFORMATION

Supplemental information can be found online at <https://doi.org/10.1016/j.omtn.2021.04.008>.

### ACKNOWLEDGMENTS

We acknowledge Witold Filipowicz, Gunter Meister, and J.M. Backer for different plasmid constructs. S.N.B. is supported by The Swarnajayanti Fellowship (DST/SJF/LSA-03/2014-15) from the Department of Science and Technology, Government of India, while D.D., S.G., and I.M. received support from CSIR, India. This work was supported by funds from a High Risk High Reward Project Grant (HRR/2016/000093) from the Department of Science and Technology, Government of India, and by CEFIPRA fund 6003-J.

### AUTHOR CONTRIBUTIONS

S.N.B. conceptualized the project, designed research, and analyzed data; D.D., I.M., S.G., and R.K.P. performed research and conducted animal experiments. S.N.B., D.D., and I.M., along with S.C.B. and S.C., analyzed data; and S.N.B., D.D., S.C.B., S.C., and I.M. wrote the paper.

### DECLARATION OF INTERESTS

The authors declare no competing interests.

### REFERENCES

- Bartel, D.P. (2018). Metazoan microRNAs. *Cell* 173, 20–51.
- Filipowicz, W., Bhattacharyya, S.N., and Sonenberg, N. (2008). Mechanisms of post-transcriptional regulation by microRNAs: Are the answers in sight? *Nat. Rev. Genet.* 9, 102–114.
- Petri, G., Expert, P., Turkheimer, F., Carhart-Harris, R., Nutt, D., Hellyer, P.J., and Vaccarino, F. (2014). Homological scaffolds of brain functional networks. *J. R. Soc. Interface* 11, 20140873.
- Li, Y., Wang, F., Lee, J.A., and Gao, F.B. (2006). *MicroRNA-9a* ensures the precise specification of sensory organ precursors in *Drosophila*. *Genes Dev.* 20, 2793–2805.
- Bruno, I.G., Karam, R., Huang, L., Bhardwaj, A., Lou, C.H., Shum, E.Y., Song, H.W., Corbett, M.A., Gifford, W.D., Gecz, J., et al. (2011). Identification of a microRNA that activates gene expression by repressing nonsense-mediated RNA decay. *Mol. Cell* 42, 500–510.
- Maciotta, S., Meregalli, M., and Torrente, Y. (2013). The involvement of microRNAs in neurodegenerative diseases. *Front. Cell. Neurosci.* 7, 265.
- Kawase-Koga, Y., Otaegi, G., and Sun, T. (2009). Different timings of dicer deletion affect neurogenesis and gliogenesis in the developing mouse central nervous system. *Dev. Dyn.* 238, 2800–2812.
- Lukiw, W.J., Zhao, Y., and Cui, J.G. (2008). An NF-κB-sensitive micro RNA-146a-mediated inflammatory circuit in Alzheimer disease and in stressed human brain cells. *J. Biol. Chem.* 283, 31315–31322.
- Sethi, P., and Lukiw, W.J. (2009). Micro-RNA abundance and stability in human brain: Specific alterations in Alzheimer's disease temporal lobe neocortex. *Neurosci. Lett.* 459, 100–104.
- Molofsky, A.V., Krencik, R., Ullian, E.M., Tsai, H.H., Deneen, B., Richardson, W.D., Barres, B.A., and Rowitch, D.H. (2012). Astrocytes and disease: A neurodevelopmental perspective. *Genes Dev.* 26, 891–907.
- Mazzanti, M., Sul, J.Y., and Haydon, P.G. (2001). Glutamate on demand: Astrocytes as a ready source. *Neuroscientist* 7, 396–405.
- Koehler, R.C., Roman, R.J., and Harder, D.R. (2009). Astrocytes and the regulation of cerebral blood flow. *Trends Neurosci.* 32, 160–169.
- Araque, A., Parpura, V., Sanzgiri, R.P., and Haydon, P.G. (1999). Tripartite synapses: Glia, the unacknowledged partner. *Trends Neurosci.* 22, 208–215.
- Perea, G., Navarrete, M., and Araque, A. (2009). Tripartite synapses: Astrocytes process and control synaptic information. *Trends Neurosci.* 32, 421–431.
- Cordiglieri, C., Odoardi, F., Zhang, B., Nebel, M., Kawakami, N., Klunkert, W.E., Lodygin, D., Lühder, F., Breunig, E., Schild, D., et al. (2010). Nicotinic acid adenine



- dinucleotide phosphate-mediated calcium signalling in effector T cells regulates autoimmunity of the central nervous system. *Brain* 133, 1930–1943.
16. Kinney, J.W., Bemiller, S.M., Murtishaw, A.S., Leisgang, A.M., Salazar, A.M., and Lamb, B.T. (2018). Inflammation as a central mechanism in Alzheimer's disease. *Alzheimers Dement.* (N. Y.) 4, 575–590.
  17. O'Neill, L.A., Sheedy, F.J., and McCoy, C.E. (2011). MicroRNAs: The fine-tuners of Toll-like receptor signalling. *Nat. Rev. Immunol.* 11, 163–175.
  18. Goswami, A., Mukherjee, K., Mazumder, A., Ganguly, S., Mukherjee, I., Chakrabarti, S., Roy, S., Sundar, S., Chattopadhyay, K., and Bhattacharyya, S.N. (2020). MicroRNA exporter HuR clears the internalized pathogens by promoting pro-inflammatory response in infected macrophages. *EMBO Mol. Med.* 12, e11011.
  19. Mazumder, A., Bose, M., Chakraborty, A., Chakrabarti, S., and Bhattacharyya, S.N. (2013). A transient reversal of miRNA-mediated repression controls macrophage activation. *EMBO Rep.* 14, 1008–1016.
  20. Fabian, M.R., Sonenberg, N., and Filipowicz, W. (2010). Regulation of mRNA translation and stability by microRNAs. *Annu. Rev. Biochem.* 79, 351–379.
  21. Friedman, R.C., Farh, K.K., Burge, C.B., and Bartel, D.P. (2009). Most mammalian mRNAs are conserved targets of microRNAs. *Genome Res.* 19, 92–105.
  22. Dueck, A., Ziegler, C., Eichner, A., Berezikov, E., and Meister, G. (2012). MicroRNAs associated with the different human Argonaute proteins. *Nucleic Acids Res.* 40, 9850–9862.
  23. Liu, C.G., Calin, G.A., Meloon, B., Gamlie, N., Sevignani, C., Ferracin, M., Dumitru, C.D., Shimizu, M., Zupo, S., Dono, M., et al. (2004). An oligonucleotide microchip for genome-wide microRNA profiling in human and mouse tissues. *Proc. Natl. Acad. Sci. USA* 101, 9740–9744.
  24. Qi, H.H., Ongusaha, P.P., Myllyharju, J., Cheng, D., Pakkanen, O., Shi, Y., Lee, S.W., Peng, J., and Shi, Y. (2008). Prolif 4-hydroxylation regulates Argonaute 2 stability. *Nature* 455, 421–424.
  25. Kirino, Y., and Mourelatos, Z. (2007). Mouse Piwi-interacting RNAs are 2'-O-methylated at their 3' termini. *Nat. Struct. Mol. Biol.* 14, 347–348.
  26. Patrabis, S., and Bhattacharyya, S.N. (2016). Phosphorylation of Ago2 and subsequent inactivation of let-7a RNP-specific microRNAs control differentiation of mammalian sympathetic neurons. *Mol. Cell. Biol.* 36, 1260–1271.
  27. Zheng, D., Ezzeddine, N., Chen, C.Y., Zhu, W., He, X., and Shyu, A.B. (2008). Deadenylation is prerequisite for P-body formation and mRNA decay in mammalian cells. *J. Cell Biol.* 182, 89–101.
  28. Rüdell, S., and Meister, G. (2008). Phosphorylation of Argonaute proteins: Regulating gene regulators. *Biochem. J.* 413, e7–e9.
  29. Ma, X.M., and Blenis, J. (2009). Molecular mechanisms of mTOR-mediated translational control. *Nat. Rev. Mol. Cell Biol.* 10, 307–318.
  30. Cybulski, N., and Hall, M.N. (2009). TOR complex 2: A signaling pathway of its own. *Trends Biochem. Sci.* 34, 620–627.
  31. Casadio, A., Martin, K.C., Giustetto, M., Zhu, H., Chen, M., Bartsch, D., Bailey, C.H., and Kandel, E.R. (1999). A transient, neuron-wide form of CREB-mediated long-term facilitation can be stabilized at specific synapses by local protein synthesis. *Cell* 99, 221–237.
  32. Iland, T.K., Song, W.M., Huang, S.C., Ulrich, J.D., Sergushichev, A., Beatty, W.L., Loboda, A.A., Zhou, Y., Cairns, N.J., Kambal, A., et al. (2017). TREM2 maintains microglial metabolic fitness in Alzheimer's disease. *Cell* 170, 649–663.e13.
  33. Saito, K., Araki, Y., Kontani, K., Nishina, H., and Katada, T. (2005). Novel role of the small GTPase Rheb: Its implication in endocytic pathway independent of the activation of mammalian target of rapamycin. *J. Biochem.* 137, 423–430.
  34. Sancak, Y., Peterson, T.R., Shaul, Y.D., Lindquist, R.A., Thoreen, C.C., Bar-Peled, L., and Sabatini, D.M. (2008). The Rag GTPases bind raptor and mediate amino acid signaling to mTORC1. *Science* 320, 1496–1501.
  35. Lau, P., Bossers, K., Janky, R., Salta, E., Frigerio, C.S., Barbash, S., Rothman, R., Sierksma, A.S., Thathiah, A., Greenberg, D., et al. (2013). Alteration of the microRNA network during the progression of Alzheimer's disease. *EMBO Mol. Med.* 5, 1613–1634.
  36. Love, M.I., Huber, W., and Anders, S. (2014). Moderated estimation of fold change and dispersion for RNA-seq data with DESeq2. *Genome Biol.* 15, 550.
  37. Tahamtan, A., Teymoori-Rad, M., Nakstad, B., and Salimi, V. (2018). Anti-inflammatory microRNAs and their potential for inflammatory diseases treatment. *Front. Immunol.* 9, 1377.
  38. Vasudevan, S. (2012). Posttranscriptional upregulation by microRNAs. *Wiley Interdiscip. Rev. RNA* 3, 311–330.
  39. Sanphui, P., and Biswas, S.C. (2013). FoxO3a is activated and executes neuron death via Bim in response to  $\beta$ -amyloid. *Cell Death Dis.* 4, e625.
  40. Frost, G.R., and Li, Y.M. (2017). The role of astrocytes in amyloid production and Alzheimer's disease. *Open Biol.* 7, 170228.
  41. Iliopoulos, D., Hirsch, H.A., and Struhl, K. (2009). An epigenetic switch involving NF- $\kappa$ B, Lin28, Let-7 microRNA, and IL6 links inflammation to cell transformation. *Cell* 139, 693–706.
  42. Boldin, M.P., Taganov, K.D., Rao, D.S., Yang, L., Zhao, J.L., Kalwani, M., Garcia-Flores, Y., Luong, M., Devrekanli, A., Xu, J., et al. (2011). miR-146a is a significant brake on autoimmunity, myeloproliferation, and cancer in mice. *J. Exp. Med.* 208, 1189–1201.
  43. Tsang, C.K., Qi, H., Liu, L.F., and Zheng, X.F. (2007). Targeting mammalian target of rapamycin (mTOR) for health and diseases. *Drug Discov. Today* 12, 112–124.
  44. Sabatini, D.M. (2017). Twenty-five years of mTOR: Uncovering the link from nutrients to growth. *Proc. Natl. Acad. Sci. USA* 114, 11818–11825.
  45. Hay, N., and Sonenberg, N. (2004). Upstream and downstream of mTOR. *Genes Dev.* 18, 1926–1945.
  46. Flinn, R.J., and Backer, J.M. (2010). mTORC1 signals from late endosomes: Taking a TOR of the endocytic system. *Cell Cycle* 9, 1869–1870.
  47. Long, X., Lin, Y., Ortiz-Vega, S., Yonezawa, K., and Avruch, J. (2005). Rheb binds and regulates the mTOR kinase. *Curr. Biol.* 15, 702–713.
  48. Long, X., Ortiz-Vega, S., Lin, Y., and Avruch, J. (2005). Rheb binding to mammalian target of rapamycin (mTOR) is regulated by amino acid sufficiency. *J. Biol. Chem.* 280, 23433–23436.
  49. Lafay-Chebassier, C., Paccalin, M., Page, G., Barc-Pain, S., Perault-Pochat, M.C., Gil, R., Pradier, L., and Hugon, J. (2005). mTOR/p70S6k signalling alteration by A $\beta$  exposure as well as in APP-PS1 transgenic models and in patients with Alzheimer's disease. *J. Neurochem.* 94, 215–225.
  50. von Bartheld, C.S., Bahney, J., and Herculano-Houzel, S. (2016). The search for true numbers of neurons and glial cells in the human brain: A review of 150 years of cell counting. *J. Comp. Neurol.* 524, 3865–3895.
  51. Cloëtta, D., Thomanetz, V., Baranek, C., Lustenberger, R.M., Lin, S., Oliveri, F., Atanasoski, S., and Rüegg, M.A. (2013). Inactivation of mTORC1 in the developing brain causes microcephaly and affects gliogenesis. *J. Neurosci.* 33, 7799–7810.
  52. Ye, P., Liu, Y., Chen, C., Tang, F., Wu, Q., Wang, X., Liu, C.G., Liu, X., Liu, R., Liu, Y., and Zheng, P. (2015). An mTORC1-Mdm2-Drosha axis for miRNA biogenesis in response to glucose- and amino acid-deprivation. *Mol. Cell* 57, 708–720.
  53. Goorden, S.M., Hoogveen-Westerveld, M., Cheng, C., van Woerden, G.M., Mozaffari, M., Post, L., Duckers, H.J., Nellist, M., and Elgersma, Y. (2011). Rheb is essential for murine development. *Mol. Cell. Biol.* 31, 1672–1678.
  54. Goorden, S.M., Abs, E., Bruinsma, C.F., Riemsdijk, F.W., van Woerden, G.M., and Elgersma, Y. (2015). Intact neuronal function in Rheb1 mutant mice: Implications for TORC1-based treatments. *Hum. Mol. Genet.* 24, 3390–3398.
  55. Lee, J.H., Tecedor, L., Chen, Y.H., Monteys, A.M., Sowada, M.J., Thompson, L.M., Davidson, B.L., and Ruegg, M.A. (2015). Reinstating aberrant mTORC1 activity in Huntington's disease mice improves disease phenotypes. *Neuron* 85, 303–315.
  56. Kim, S.R., Kareva, T., Yarygina, O., Kholodilov, N., and Burke, R.E. (2012). AAV transduction of dopamine neurons with constitutively active Rheb protects from neurodegeneration and mediates axon regrowth. *Mol. Ther.* 20, 275–286.
  57. Swiech, L., Perycz, M., Malik, A., and Jaworski, J. (2008). Role of mTOR in physiology and pathology of the nervous system. *Biochim. Biophys. Acta* 1784, 116–132.
  58. Gkogkas, C., Sonenberg, N., and Costa-Mattioli, M. (2010). Translational control mechanisms in long-lasting synaptic plasticity and memory. *J. Biol. Chem.* 285, 31913–31917.
  59. Jeon, M.T., Nam, J.H., Shin, W.H., Leem, E., Jeong, K.H., Jung, U.J., Bae, Y.S., Jin, Y.H., Kholodilov, N., Burke, R.E., et al. (2015). In vivo AAV1 transduction with

- hRheb(S16H) protects hippocampal neurons by BDNF production. *Mol. Ther.* 23, 445–455.
60. Barykin, E.P., Mitkevich, V.A., Kozin, S.A., and Makarov, A.A. (2017). Amyloid  $\beta$  modification: A key to the sporadic Alzheimer's disease? *Front. Genet.* 8, 58.
  61. Ludwig, N., Leidinger, P., Becker, K., Backes, C., Fehlmann, T., Pallasch, C., Rheinheimer, S., Meder, B., Stähler, C., Meese, E., and Keller, A. (2016). Distribution of miRNA expression across human tissues. *Nucleic Acids Res.* 44, 3865–3877.
  62. Jovičić, A., Roshan, R., Moiso, N., Pradervand, S., Moser, R., Pillai, B., and Luthi-Carter, R. (2013). Comprehensive expression analyses of neural cell-type-specific miRNAs identify new determinants of the specification and maintenance of neuronal phenotypes. *J. Neurosci.* 33, 5127–5137.
  63. Gao, V., Suzuki, A., Magistretti, P.J., Lengacher, S., Pollonini, G., Steinman, M.Q., and Alberini, C.M. (2016). Astrocytic  $\beta$ 2-adrenergic receptors mediate hippocampal long-term memory consolidation. *Proc. Natl. Acad. Sci. USA* 113, 8526–8531.
  64. Han, X., Chen, M., Wang, F., Windrem, M., Wang, S., Shanz, S., Xu, Q., Oberheim, N.A., Bekar, L., Betstadt, S., et al. (2013). Forebrain engraftment by human glial progenitor cells enhances synaptic plasticity and learning in adult mice. *Cell Stem Cell* 12, 342–353.
  65. Adamsky, A., Kol, A., Kreisel, T., Doron, A., Ozeri-Engelhard, N., Melcer, T., Refaeli, R., Horn, H., Regev, L., Groysman, M., et al. (2018). Astrocytic activation generates de novo neuronal potentiation and memory enhancement. *Cell* 174, 59–71.e14.
  66. Lee, L., Kosuri, P., and Arancio, O. (2014). Picomolar amyloid- $\beta$  peptides enhance spontaneous astrocyte calcium transients. *J. Alzheimers Dis.* 38, 49–62.
  67. Vincent, A.J., Gasperini, R., Foa, L., and Small, D.H. (2010). Astrocytes in Alzheimer's disease: Emerging roles in calcium dysregulation and synaptic plasticity. *J. Alzheimers Dis.* 22, 699–714.
  68. Matos, M., Augusto, E., Machado, N.J., dos Santos-Rodrigues, A., Cunha, R.A., and Agostinho, P. (2012). Astrocytic adenosine A2A receptors control the amyloid- $\beta$  peptide-induced decrease of glutamate uptake. *J. Alzheimers Dis.* 31, 555–567.
  69. Pirttimaki, T.M., Codadu, N.K., Awni, A., Pratik, P., Nagel, D.A., Hill, E.J., Dineley, K.T., and Parri, H.R. (2013).  $\alpha$ 7 Nicotinic receptor-mediated astrocytic gliotransmitter release: A $\beta$  effects in a preclinical Alzheimer's mouse model. *PLoS ONE* 8, e81828.
  70. Vehmas, A.K., Kawas, C.H., Stewart, W.F., and Troncoso, J.C. (2003). Immune reactive cells in senile plaques and cognitive decline in Alzheimer's disease. *Neurobiol. Aging* 24, 321–331.
  71. Lian, H., Litvinchuk, A., Chiang, A.C., Aithmitti, N., Jankowsky, J.L., and Zheng, H. (2016). Astrocyte-microglia cross talk through complement activation modulates amyloid pathology in mouse models of Alzheimer's disease. *J. Neurosci.* 36, 577–589.
  72. Rodriguez, G.A., Tai, L.M., LaDu, M.J., and Rebeck, G.W. (2014). Human APOE4 increases microglia reactivity at A $\beta$  plaques in a mouse model of A $\beta$  deposition. *J. Neuroinflammation* 11, 111.
  73. Tsai, P.T., Hull, C., Chu, Y., Greene-Colozzi, E., Sadowski, A.R., Leech, J.M., Steinberg, J., Crawley, J.N., Regehr, W.G., and Sahin, M. (2012). Autistic-like behaviour and cerebellar dysfunction in Purkinje cell *Tsc1* mutant mice. *Nature* 488, 647–651.
  74. Saxena, S., Roselli, F., Singh, K., Leptien, K., Julien, J.P., Gros-Louis, F., and Caroni, P. (2013). Neuroprotection through excitability and mTOR required in ALS motoneurons to delay disease and extend survival. *Neuron* 80, 80–96.
  75. Ritchie, M.E., Phipson, B., Wu, D., Hu, Y., Law, C.W., Shi, W., and Smyth, G.K. (2015). limma powers differential expression analyses for RNA-sequencing and microarray studies. *Nucleic Acids Res.* 43, e47.
  76. Liang, W.S., Reiman, E.M., Valla, J., Dunckley, T., Beach, T.G., Grover, A., Niedzielko, T.L., Schneider, L.E., Mastroeni, D., Caselli, R., et al. (2008). Alzheimer's disease is associated with reduced expression of energy metabolism genes in posterior cingulate neurons. *Proc. Natl. Acad. Sci. USA* 105, 4441–4446.
  77. Liang, W.S., Dunckley, T., Beach, T.G., Grover, A., Mastroeni, D., Walker, D.G., Caselli, R.J., Kukull, W.A., McKeel, D., Morris, J.C., et al. (2007). Gene expression profiles in anatomically and functionally distinct regions of the normal aged human brain. *Physiol. Genomics* 28, 311–322.
  78. Readhead, B., Haure-Mirande, J.-V., Funk, C.C., Richards, M.A., Shannon, P., Haroutunian, V., Sano, M., Liang, W.S., Beckmann, N.D., Price, N.D., et al. (2018). Multiscale analysis of independent Alzheimer's cohorts finds disruption of molecular, genetic, and clinical networks by human herpesvirus. *Neuron* 99, 64–82.e7.
  79. Scheckel, C., Drapeau, E., Frias, M.A., Park, C.Y., Fak, J., Zucker-Scharff, I., Kou, Y., Haroutunian, V., Ma'ayan, A., Buxbaum, J.D., and Darnell, R.B. (2016). Regulatory consequences of neuronal ELAV-like protein binding to coding and non-coding RNAs in human brain. *Elife* 5, e10421.
  80. Webster, J.A., Gibbs, J.R., Clarke, J., Ray, M., Zhang, W., Holmans, P., Rohrer, K., Zhao, A., Marlowe, L., Kaleem, M., et al.; NACC-Neuropathology Group (2009). Genetic control of human brain transcript expression in Alzheimer disease. *Am. J. Hum. Genet.* 84, 445–458.
  81. Vlachos, I.S., Paraskevopoulou, M.D., Karagkouni, D., Georgakilas, G., Vergoulis, T., Kanellos, I., Anastasopoulos, I.L., Maniou, S., Karathanou, K., Kalfakakou, D., et al. (2015). DIANA-TarBase v7.0: Indexing more than half a million experimentally supported miRNA:mRNA interactions. *Nucleic Acids Res.* 43, D153–D159.
  82. Chou, C.H., Chang, N.W., Shrestha, S., Hsu, S.D., Lin, Y.L., Lee, W.H., Yang, C.D., Hong, H.C., Wei, T.Y., Tu, S.J., et al. (2016). miRTarBase 2016: Updates to the experimentally validated miRNA-target interactions database. *Nucleic Acids Res.* 44 (D1), D239–D247.
  83. Yu, Y., and Ye, R.D. (2015). Microglial A $\beta$  receptors in Alzheimer's disease. *Cell. Mol. Neurobiol.* 35, 71–83.
  84. Luo, D., Wilson, J.M., Harvel, N., Liu, J., Pei, L., Huang, S., Hawthorn, L., and Shi, H. (2013). A systematic evaluation of miRNA:mRNA interactions involved in the migration and invasion of breast cancer cells. *J. Transl. Med.* 11, 57.
  85. Fu, J., Tang, W., Du, P., Wang, G., Chen, W., Li, J., Zhu, Y., Gao, J., and Cui, L. (2012). Identifying microRNA-mRNA regulatory network in colorectal cancer by a combination of expression profile and bioinformatics analysis. *BMC Syst. Biol.* 6, 68.
  86. Shi, W., Yang, J., Li, S., Shan, X., Liu, X., Hua, H., Zhao, C., Feng, Z., Cai, Z., Zhang, L., and Zhou, D. (2015). Potential involvement of miR-375 in the premalignant progression of oral squamous cell carcinoma mediated via transcription factor KLF5. *Oncotarget* 6, 40172–40185.
  87. Chang, J., Nicolas, E., Marks, D., Sander, C., Lerro, A., Buendia, M.A., Xu, C., Mason, W.S., Moloshok, T., Bort, R., et al. (2004). miR-122, a mammalian liver-specific microRNA, is processed from hcr mRNA and may downregulate the high affinity cationic amino acid transporter CAT-1. *RNA Biol.* 1, 106–113.
  88. Flinn, R.J., Yan, Y., Goswami, S., Parker, P.J., and Backer, J.M. (2010). The late endosome is essential for mTORC1 signaling. *Mol. Biol. Cell* 21, 833–841.
  89. Itoh, J., Nabeshima, T., and Kameyama, T. (1990). Utility of an elevated plus-maze for the evaluation of memory in mice: Effects of nootropics, scopolamine and electroconvulsive shock. *Psychopharmacology (Berl.)* 101, 27–33.